PB84-196740

Evaluation of Chemical Reaction Mechanisms for Photochemical Smog. Part 2. Quantitative Evaluation of the Mechanisms

California Inst. of Tech., Pasadena

Prepared for

Environmental Sciences Research Lab.
Research Triangle Park, NC

May 84

U.S. Department of Commerce
National Technical Information Service
NTIS

PB84-196740

EPA-600/3-84-063
May 1984

EVALUATION OF CHEMICAL REACTION MECHANISMS FOR PHOTOCHEMICAL SMOG

PART II. QUANTITATIVE EVALUATION OF THE MECHANISMS

by

Joseph A. Leone
and
John H. Seinfeld

California Institute of Technology
Pasadena, California 91125

Cooperative Agreement 810184

Project Officer

Marcia C. Dodge

Gas Kinetics and Photochemistry Branch
Environmental Sciences Research Laboratories
Research Triangle Park, North Carolina 27711

ENVIRONMENTAL SCIENCES RESEARCH LABORATORY
OFFICE OF RESEARCH AND DEVELOPMENT
U.S. ENVIRONMENTAL PROTECTION AGENCY
RESEARCH TRIANGLE PARK, NORTH CAROLINA 27711

REPRODUCED BY
NATIONAL TECHNICAL
INFORMATION SERVICE
U.S. DEPARTMENT OF COMMERCE
SPRINGFIELD, VA. 22161

TECHNICAL REPORT DATA
(Please read Instructions on the reverse before completing)

1. REPORT NO. EPA-600/3-84-063	**2.**	**3. RECIPIENT'S ACCESSION NO.** PB84 196740
4. TITLE AND SUBTITLE EVALUATION OF CHEMICAL REACTION MECHANISMS FOR PHOTOCHEMICAL SMOG. PART II. QUANTITATIVE EVALUATION OF THE MECHANISMS		**5. REPORT DATE** May 1984 **6. PERFORMING ORGANIZATION CODE**
7. AUTHOR(S) J. A. Leone and J. H. Seinfeld		**8. PERFORMING ORGANIZATION REPORT NO.**
9. PERFORMING ORGANIZATION NAME AND ADDRESS California Institute of Technology Pasadena, CA 91125		**10. PROGRAM ELEMENT NO.** CDWA1A/01-2048 (FY-84) **11. CONTRACT/GRANT NO.** Cooperative Agreement 810184
12. SPONSORING AGENCY NAME AND ADDRESS Environmental Sciences Research Laboratory-RTP,NC Office of Research and Development U.S. Environmental Protection Agency Research Triangle Park, North Carolina 27711		**13. TYPE OF REPORT AND PERIOD COVERED** Interim (4/83-2/84) **14. SPONSORING AGENCY CODE** EPA/600/09

15. SUPPLEMENTARY NOTES

16. ABSTRACT

Six chemical reaction mechanisms for photochemical smog were analyzed to determine why, under identical conditions, they predict different maximum ozone concentrations. To perform the analysis, a counter species technique was used to determine the contributions of individual reactions or sets of reactions to the overall behavior of the chemical reaction mechanism. Using this technique, answers were obtained to previously inaccessible questions such as what is the relative contribution of individual organic species to photochemical ozone formation. Based on the results of the counter species analysis specific aspects of each mechanism were identified that are responsible for the discrepancies with other mechanisms. For each mechanism, parameters were identified that when altered brought the predictions of the various mechanisms into much closer agreement.

17. KEY WORDS AND DOCUMENT ANALYSIS

a. DESCRIPTORS	b. IDENTIFIERS/OPEN ENDED TERMS	c. COSATI Field/Group

18. DISTRIBUTION STATEMENT RELEASE TO PUBLIC	**19. SECURITY CLASS** *(This Report)* UNCLASSIFIED	**21. NO. OF PAGES** 212
	20. SECURITY CLASS *(This page)* UNCLASSIFIED	**22. PRICE**

EPA Form 2220-1 (Rev. 4-77) PREVIOUS EDITION IS OBSOLETE

NOTICE

This document has been reviewed in accordance with U.S. Environmental Protection Agency policy and approved for publication. Mention of trade names or commercial products does not constitute endorsement or recommendation for use.

ABSTRACT

The six chemical reaction mechanisms for photochemical smog described in Part I are analyzed to determine why, under identical conditions, they predict different maximum ozone concentrations. To perform the analysis, a counter species analysis technique is used to determine the contributions of individual reactions or sets of reactions to the overall behavior of a chemical reaction mechanism. Using this technique, we can obtain answers to previously inaccessible questions such as the relative contributions of individual organic species to photochemical ozone formation. Based on the results of the analysis we have identified specific aspects of each mechanism that are responsible for the discrepancies with other mechanisms and with a master mechanism based on the latest understanding of atmospheric chemistry. For each mechanism critical areas are identified that when altered bring the predictions of the various mechanisms into much closer agreement. Thus, we have been able to identify why the predictions of the mechanisms are different, and have recommended research efforts that are needed to eliminate many of the discrepancies.

TABLE OF CONTENTS

ABSTRACT iii

LIST OF FIGURES vii

LIST OF TABLES viv

ACKNOWLEDGEMENT xi

CHAPTER 1 INTRODUCTION 1

CHAPTER 2 METHOD OF ANALYSIS 4

- 2.1 Introduction 4
- 2.2 Counter Species Analysis 5
- 2.3 Master Mechanism 11
- 2.4 Details of the Master Mechanism 11
- 2.5 Verification of the Master Mechanism 15
- 2.6 Chamber Effects 16
- 2.7 Initial Reactant Conditions 17
- 2.8 NO_2 Photolysis Rate Profile 17

CHAPTER 3 RESULTS AND DISCUSSION 21

- 3.1 Introduction 21
- 3.2 Counter Species Results 21
- 3.3 NO to NO_2 Conversions vs. O_3 Yield 38
- 3.4 The Atkinson et al. (1982) Mechanism 39
  - 3.4.1 Description of the Mechanism 39
  - 3.4.2 NO to NO_2 Conversion Results 43
  - 3.4.3 Possible Modifications to the Atkinson et al. (1982) Mechanism 46
- 3.5 The Killus and Whitten (1982) Mechanism 47
  - 3.5.1 Description of the Mechanism 47
  - 3.5.2 No to NO_2 Conversion Results 48
  - 3.5.3 Possible Modifications to the Killus and Whitten (1982) Mechanism 57

3.6 The Demerjian (1982) Mechanism 59

3.6.1 Description of the Mechanism 59

3.6.2 NO to NO$_2$ Conversion Results 61

3.6.3 Possible Modifications to the Demerjian (1982) Mechanism 66

3.7 The McRae and Seinfeld (1983) Mechanism 66

3.7.1 Description of the Mechanism 66

3.7.2 NO to NO$_2$ Conversion Results 67

3.7.3 Possible Modifications to the McRae and Seinfeld (1982) Mechanism 71

3.8 The Penner and Walton (1982) Mechanism 71

3.8.1 Description of the Mechanism 71

3.8.2 NO to NO$_2$ Conversion Results 74

3.8.3 Possible Modifications to the Penner and Walton (1982) Mechanism 79

3.9 The Dodge (1977) Mechanism 79

3.9.1 Description of the Mechanism 79

3.9.2 NO to NO$_2$ Conversion Results 80

3.10 Discussion of Results 82

3.11 Conclusions 83

CHAPTER 4 CONCLUSIONS AND RECOMMENDATIONS 93

REFERENCES 95

APPENDIX 99

FIGURE CAPTIONS

		PAGE
Figure 1.	Counter Species Results Obtained Using Initial Condition Set 1. Amount of NO to NO_2 Conversions Attributable to Each of the Initially Present Organics	32
Figure 2.	Counter Species Results Obtained Using Initial Condition Set 2. Amount of NO to NO_2 Conversions Attributable to Each of the Initially Present Organics	33
Figure 3.	Counter Species Results Obtained Using Initial Condition Set 3. Amount of NO to NO_2 Conversions Attributable to Each of the Initially Present Organics	34
Figure 4.	Percent of the Total NO to NO_2 Conversions Due to Each Class of Organic for the Simulation Using Initial Condition Set 1.	35
Figure 5.	Percent of the Total NO to NO_2 Conversions Due to Each Class of Organic for the Simulation Using Initial Condition Set 2.	36
Figure 6.	Percent of the Total NO to NO_2 Conversions Due to Each Class of Organic for the Simulation Using Initial Condition Set 3	37
Figure 7.	O_3 Yield (shaded) vs. Total Amount of NO to NO_2 Conversions (unshaded) for Each Mechanism Obtained with Initial Condition Set 1 ($[RHC)_o/[NO_x]_o = 7.14$).	40
Figure 8.	O_3 Yield (shaded) vs. Total Amount of NO to NO_2 Conversions (unshaded) for Each Mechanism Obtained with Initial Condition Set 2 ($[RHC]_o/[NO_x]_o = 28.6$).	41
Figure 9.	O_3 Yield (shaded) vs. Total Amount of NO to NO_2 Conversions (unshaded) for Each Mechanism Obtained with Initial Condition Set 3 ($[RHC]_o/[NO_x]_o = 1.79$).	42
Figure 10.	A Comparison of the Total Amount of NO to NO_2 Conversions Predicted by the Original (unshaded) and Modified (shaded) Versions of Five Lumped Mechanisms Using Initial Condition Set 1 ($[RHC]_o/[NO_x]_o = 7.14$)	87
Figure 11.	A Comparison of the Total Amount of NO to NO_2 Conversions Predicted by the Original (unshaded) and Modified (shaded) Versions of Five Lumped Mechanisms Using Initial Condition Set 2 ($[RHC]_o/[NO_x]_o = 28.6$).	88
Figure 12.	A Comparison of the Total Amount of NO to NO_2 Conversions Predicted by the Original (unshaded and Modified (shaded) Versions of Five Lumped Mechanisms Using Initial Condition Set 3 ($[RHC]_o/[NO_x]_o = 1.79$).	89

Figure 13. A Comparison of the O_3 Yield After 360 minues of Simulation Predicted by the Original (unshaded) and Modified (shaded) Versions of Five Lumped Mechanisms Using Initial Condition Set 1 90

Figure 14. A Comparison of the O_3 Yield After 150 minues of Simulation Predicted by the Original (unshaded) and Modified (shaded) Versions of Five Lumped Mechanisms Using Initial Condition Set 2 91

Figure 15. A Comparison of the O_3 Yield After 360 minutes of Simulation Predicted by the Original (unshaded) and Modified (shaded) Versions of Five Lumped Mechanisms Using Initial Condition Set 3. 92

Figure A1. Observed and Calculated Concentration-Time Profiles for 7-Hydrocarbon-NO_x Experiment EC-237 141

Figure A2. Observed and Calculated Concentration-Time Profiles for 7-Hydrocarbon-NO_x Experiment EC-238 146

Figure A3. Observed and Calculated Concentration-Time Profiles for 7-Hydrocarbon-NO_x Experiment EC-231 151

Figure A4. Observed and Calculated Concentration-Time Profiles for 7-Hydrocarbon-NO_x Experiment EC-233 159

Figure A5. Observed and Calculated Concentration-Time Profiles for 7-Hydrocarbon-NO_x Experiment EC-241 166

Figure A6. Observed and Calculated Concentration-Time Profiles for 7-Hydrocarbon-NO_x Experiment EC-242 173

Figure A7. Observed and Calculated Concentration-Time Profiles for 7-Hydrocarbon-NO_x Experiment EC-243. 180

Figure A8. Observed and Calculated Concentration-Time Profiles for 7-Hydrocarbon-NO_x Experiment EC-245 186

Figure A9. Observed and Calculated Concentration-Time Profiles for 7-Hydrocarbon-NO_x Experiment EC-246 193

LIST OF TABLES

PAGE

Table 1. Composition of Smog Chamber Experiment SUR-119J (Pitts et al., 1976) 12

Table 2. Initial Conditions and Other Important Parameters for Test Cases 1, 2, and 3 18

Table 3. NO_2 Photolysis Rate Profile Used in Each of the Test Cases 20

Table 4. Counter Species Results Obtained with Initial Condition Set 1 ($[RHC]_o/[NO_x]_o = 7.14$) 23

Table 5. Counter Species Results Obtained with Initial Condition Set 2 ($[RHC]_o/[NO_x]_o = 28.6$) 26

Table 6. Counter Species Results Obtained with Initial Condition Set 3 ($[RHC]_o/[NO_x]_o = 1.79$) 29

Table 7. Counter Species Results for the Original and Modified Versions of the Killus and Whitten (1982) Mechanism Using Initial Condition Set 1 ($[RHC]_o/[NO_x]_o = 7.14$) 51

Table 8. Counter Species Results for the Original and Modified Versions of the Killus and Whitten (1982) Mechanism Using Initial Condition Set 1 ($[RHC]_o/[NO_x]_o = 7.14$) 58

Table 9. Results of Separating Ethylene from the Remaining Olefins in the Demerjian (1982) Mechanism 62

Table 10. Result of Updating the Aldehyde Photolysis Rates in the McRae and Seinfeld (1983) Mechanism 69

Table 11. Result of Replacing the Aromatic Reaction and Updating the Aldehyde Photolysis Rates in the McRae and Seinfeld (1983) Mechanism 72

Table 12. Results Obtained by Updating the Methyl Glyoxal and Aldehyde Photolysis Rates in the Penner and Walton (1982) Mechanism 76

Table 13. Summary of our Possible Modifications for all but the Dodge (1977) Mechanism 85

Table 14. Comparison of the Counter Species Results for the Orinal and Modified (in parenthesis) Versions of 5 Lumped Mechanisms 86

PAGE

Table A.1 "Master" Reaction Mechanism 99

Table A.2 The Atkinson et al. (1982) Reaction Mechanism as Used in this Study 116

Table A.3 Species Used in the Atkinson et al. (1982) Reaction Mechanism 119

Table A.4 The Killus and Whitten (1982a) Reaction Mechanism as Used in this Study 121

Table A.5 Species Used in the Killus and Whitten (1982a) Reaction Mechanism 124

Table A.6 The Demerjian (1982) Reaction Mechanism as Used in this Study 126

Table A.7 Species Used in the Demerjian (1982) Reaction Mechanism 128

Table A.8 The McRae and Seinfeld (1983) Reaction Mechanism as Used in this Study 129

Table A.9 Species Used in the McRae and Seinfeld (1983) Reaction Mechanism 132

Table A.10 The Penner and Walton (1982) Reaction Mechanism as Used in this Study 133

Table A.11 Species Used in the Penner and Walton (1982) Reaction Mechanism 136

Table A.12 The Dodge (1977) Reaction Mechanism as Used in this Study 137

Table A.13 Species Used in the Dodge (1977) Reaction Mechanism 139

Table A.14 Explanation of Rate Constant Format 140

ACKNOWLEDGEMENT

We wish to acknowledge the assistance of: Alan C. Lloyd, Fred Lurmann, Marcia Dodge, Kenneth Demerjian, Kenneth Schere, Gary Whitten, Jim Killus and Joyce Penner for providing computer codes and documentation of their mechanisms. Appreciation is extended to Gregory J. McRae for his assistance.

CHAPTER 1

INTRODUCTION

In determining emission control levels, one must be able to predict how changes in emission levels will affect ambient air quality. An important component of such an approach is a description of atmospheric organic chemistry. Unfortunately, the development of a chemical reaction mechanism that accurately describes atmospheric chemistry and, at the same time, is computationally tractable, is a difficult undertaking. Since typical urban atmospheres contain hundreds of different organic species, it is not feasible to write a mechanism that includes each individual species. Thus, these reaction mechanisms must maintain a balance between the level of chemical detail and, for numerical reasons, the number of species and reaction pathways.

Currently, several chemical reaction mechanisms exist that describe the organic chemistry of the urban atmosphere and that attempt to maintain a balance between chemical detail and mechanism length (McRae et al., 1983). These mechanisms are all based on the same body of experimental rate constant data, and each mechanism has been evaluated against data from various smog chamber facilities. In each mechanism, the detailed atmospheric chemistry has been greatly simplified by a process referred to as lumping (McRae et al., 1983). However, because this simplification, or lumping process, has been carried out in different ways, no two mechanisms are the same. The differences among mechanisms would not be of any concern if each of the mechanisms gave similar predictions over a range of atmospheric conditions. However, several recent investigations have shown that different mechanisms predict substantially different degrees of emission controls to achieve the same desired air quality under identical conditions (Jeffries et al., 1981;

Whitten, 1981; Carter et al., 1982a). Since tremendous expenses are involved in implementing hydrocarbon and NO_x emission controls predicted by such mechanisms, there is an urgent need to understand the fundamental reasons for these discrepancies.

Analyzing the behavior of these atmospheric reaction mechanisms is a demanding task because of the large number of species and reactions that each contains, and because of the interwoven nature of the free radical chain reactions characterizing each mechanism. We make use of a method termed counter species analysis that enables one to account for the influence of individual reactions or reaction networks on the predictions of a mechanism. Using this technique one can assess the differences among the available photochemical smog mechanisms and, where appropriate, point out areas where improvements in our understanding of atmospheric chemistry are needed.

This report represents the second part of a three-part study of lumped reaction mechanisms for photochemical smog. Part I (McRae et al., 1983) contains information concerning the various approaches to lumping, and how the particular mechanisms chosen for this study were selected. Also included in Part I is a detailed description of each lumped mechanism.

Part II of our study contains the quantitative analysis of the six lumped mechanisms selected for study. In the next chapter we describe "counter species analysis" and the "master" mechanism, both of which play an important role in our comparison of the lumped mechanisms. Also included in Chapter 2 is a summary of the initial conditions and NO_2 photolysis rate profile used in our tests. The bulk of this report is contained in Chapter 3, which presents and discusses all the major results for each of the mechanisms. Chapter 4 summarizes the key findings of this study.

In Part III we will extend the analysis contained in Part II to conditions approximating the real atmosphere. The emission control requirements predicted by the various mechanisms will be examined. In Part III we will also consider the effects of atmospheric hydrocarbon makeup, continous dilution, and the presence of background pollutant concentrations.

CHAPTER 2

METHOD OF ANALYSIS

2.1 Introduction

In this three-part study we want to determine why the various photochemical smog mechanisms predict different emission control requirements to reach the same desired air quality (specifically, the same maximum ozone concentration). The goal of Part II of this study is to understand why these mechanisms, under identical conditions, predict that substantially different levels of O_3 will be reached. In order to answer this question, we would like to determine how much of the total O_3 production can be attributed to each of the initially present organic species in each mechanism. With this information, we could determine the relative contributions of individual organics (or reactions, reaction pathways, etc.) to overall behavior of each mechanism.

Unfortunately, because of the interwoven nature of the free radical chemistry, there is no direct way of calculating the relative amounts of O_3 that each organic species is responsible for producing in a mechanism. We can, however, using a method described below, keep track of the number of NO to NO_2 conversions that arise as a result of the presence of each organic species. The amount of O_3 attributable to a given organic species is well established to be directly proportional to the amount of NO oxidation affected by the species.

The technique we use to determine the number of NO to NO_2 conversions attributable to individual species is called *counter species analysis*. The idea of counter species has been used previously by several investigators (Calvert et al. 1978; Graedel 1977; Whitten, 1983), and the technique used here is described in detail elsewhere (Leone and Seinfeld, 1983a). However, for completeness, we include in the next section an example illustrating its use.

2.2 Counter Species Analysis

Let us consider one of the simplest atmospheric reaction mechanisms - the photooxidation of the three aldehydes, formaldehyde, acetaldehyde, and propionaldehyde, in the presence of NO and NO_2. For the purpose of illustrating the technique, assume that we wish to limit the number of species appearing in our mechanism by lumping propionaldehyde together with acetaldehyde. A typical reaction mechanism for this situation might contain the following reactions:

$$NO_2 + h\nu \xrightarrow[O_2]{1} NO + O_3$$

$$NO + O_3 \xrightarrow{2} NO_2 + O_2$$

$$HO_2\cdot + NO \xrightarrow{3} NO_2 + OH\cdot$$

$$HCHO + h\nu \xrightarrow[2O_2]{4} 2HO_2\cdot + CO$$

$$HCHO + h\nu \xrightarrow{5} H_2 + CO$$

$$HCHO + OH\cdot \xrightarrow[O_2]{6} HO_2\cdot + CO + H_2O$$

$$CH_3CHO + h\nu \xrightarrow[2O_2]{7} CH_3O_2\cdot + HO_2\cdot + CO$$

$$CH_3CHO + OH\cdot \xrightarrow[O_2]{8} CH_3C(O)O_2\cdot + H_2O$$

$$CH_3C(O)O_2\cdot + NO \xrightarrow[O_2]{9} NO_2 + CH_3O_2\cdot + CO_2$$

$$CH_3C(O)O_2\cdot + NO_2 \xrightarrow{10} CH_3C(O)O_2NO_2(PAN)$$

$$PAN \xrightarrow{11} CH_3C(O)O_2\cdot + NO_2$$

$$CH_3O_2\cdot + NO \xrightarrow{12} CH_3O\cdot + NO_2$$

$$CH_3O\cdot + O_2 \rightarrow HCHO + HO_2\cdot$$

$$NO_2 + OH\cdot \xrightarrow{14} HNO_3$$

In the atmosphere these aldehydes react to produce HO_2, CH_3O_2, and $CH_3C(O)O_2$ radicals that can convert NO to NO_2, and thus cause $[NO_2]/[NO]$, and consequently O_3, to increase. Ozone formation will continue as long as aldehydes and NO_x are both present. NO_x is consumed via reactions 10 and 14, so ultimate O_3 yields are limited by NO_x availability as well as by how fast the aldehydes lead to O_3 formation through the conversion of NO to NO_2. In the reaction mechanism shown above, NO to NO_2 conversions occur via reactions 3, 9, and 12. We seek to know the number of these NO to NO_2 conversions attributable to formaldehyde, acetaldehyde, and propionaldehyde, and, within each of these, the number due to photolysis and OH reaction. In order to obtain this information, we first rewrite the mechanism as:

$$NO_2 + h\nu \xrightarrow[O_2]{1} NO + O_3$$

$$NO + O_3 \xrightarrow{2} NO_2 + O_2$$

$$HO_2\cdot + NO \xrightarrow{3} NO_2 + OH\cdot + C3$$

$$HCHO + h\nu \xrightarrow[2O_2]{4} 2HO_2\cdot + CO + C4$$

$$HCHO + h\nu \xrightarrow{5} H_2 + CO$$

$$HCHO + OH\cdot \xrightarrow[O_2]{6} HO_2\cdot + CO + H_2O + C6$$

$$CH_3CHO(a) + h\nu \xrightarrow[2O_2]{7} CH_3O_2\cdot + HO_2\cdot + CO + C7$$

$$CH_3CHO(a) + OH\cdot \xrightarrow[O_2]{8} CH_3C(O)O_2\cdot + H_2O + C8$$

$$CH_3C(O)O_2\cdot + NO \xrightarrow[O_2]{9} NO_2 + CH_3O_2\cdot + CO_2 + C9$$

$$CH_3C(O)O_2\cdot + NO_2 \xrightarrow{10} CH_3C(O)O_2NO_2(PAN)$$

$$PAN \xrightarrow{11} CH_3C(O)O_2\cdot + NO_2$$

$$CH_3O_2\cdot + NO \xrightarrow{12} CH_3O\cdot + NO_2 + C12$$

$$CH_3O\cdot + O_2 \xrightarrow{13} HCHO + HO_2\cdot + C13$$

$$NO_2 + OH\cdot \xrightarrow{14} HNO_3$$

$$HCHI + h\nu \xrightarrow[2O_2]{15} 2HO_2\cdot + CO + C15$$

$$HCHI + h\nu \xrightarrow{16} H_2 + CO$$

$$HCHI + OH\cdot \xrightarrow[O_2]{17} HO_2\cdot + CO + H_2O + C17$$

$$CH_3CHO(b) + h\nu \xrightarrow[2O_2]{18} CH_3O_2\cdot + HO_2\cdot + CO + C18$$

$$CH_3CHO(b) + OH\cdot \xrightarrow[O_2]{19} CH_3C(O)O_2\cdot + H_2O + C19$$

Three changes have been made from the original mechanism. First, for reasons that will be made clear shortly, reactions 15, 16, and 17 have been added to the mechanism. For now, we note that whenever a species that is present initially is also formed as a product in the reaction mechanism, we represent this species by two separate species. Thus, we now have photolysis and OH reactions for both HCHO (formaldehyde formed as a product) and HCHI (initially present formaldehyde). If there were initially 30 ppb of formaldehyde present, we would specify 30 ppb as the initial concentration of HCHI.

The second change from the original mechanism is the addition of reactions 18 and 19. Because we wish to distinguish the NO to NO_2 conversions due to the initial acetaldehyde from those due to the initial propionaldehyde, we include reactions for both $CH_3CHO(a)$ (acetaldehyde) and $CH_3CHO(b)$ (propionaldehyde). If there were initially 20 ppb of acetaldehyde and 5 ppb of propionaldehyde, we would specify 20 ppb of $CH_3CHO(a)$ and 5 ppb of $CH_3CHO(b)$ as initial conditions.

The third change from the original mechanism is the addition of fictitious products, Ci, to some of the reactions. These products are produced only in one reaction and are not consumed. For instance, one "molecule" of C9 is formed for each molecule of NO converted to NO_2 by reaction 9. Since Ci counts the number of times reaction i has occurred, Ci is called a counter species, and the analysis using the Ci is termed a counter species analysis.

The next step in the counter species analysis is to determine the fraction of the molecules of any product species S that have led to NO to NO_2 conversions up until any time t,

$$F_S = \frac{\text{Number of NO/NO}_2\text{ conversions due to produced species S, up to time t}}{\text{Number of molecules of S formed up to time t}}$$

Using this definition and the mechanism shown above, we find that:

$$F_{HO_2} = \frac{C3}{2C4+C6+C7+C13+2C15+C17+C18}$$

$$F_{HCHO} = \frac{(2C4+C6)F_{HO_2\cdot}}{C13}$$

$$F_{CH_3O} = \frac{C13(F_{HO_2}+F_{HCHO})}{C12}$$

$$F_{CH_3O_2} = \frac{C12(1+F_{CH_3O\cdot})}{C7+C9+C18}$$

$$F_{CH_3C(O)O_2} = \frac{C9(1+F_{CH_3O_2})}{C8+C19}$$

The desired quantities are then expressed in terms of these fractional relations,

Number of NO to NO_2 conversions due to:

photolysis of initial formaldehyde = $2C15\ F_{HO_2}$

photolysis of initial acetaldehyde = $C7(F_{CH_3O_2} + F_{HO_2})$

photolysis of initial propionaldehyde = $C18(F_{CH_3O_2} + F_{HO_2})$

OH reaction of initial formaldehyde = $C17\ F_{HO_2}$

OH reaction of initial acetaldehyde = $C8\ F_{CH_3C(O)O_2}$

OH reaction of initial propionaldehyde = $C19\ F_{CH_3C(O)O_2}$

If desired, we can gain additional information from the conter species analysis. For example,

NO to NO_2 conversions due to:

photolysis of produced HCHO = $2C4\ F_{HO_2}$

OH reaction of produced HCHO = $C6\ F_{HO_2}$

radical initiation due to the photolysis of:

initial formaldehyde = 2C15

acetaldehyde = 2C7

propionaldehyde = 2C18

radical termination to:

PAN = [PAN]

$HNO_3 = [HNO_3]$

The reason for dividing formaldehyde into two species, HCHI(representing the initially present formaldehyde) and HCHO (representing formaldehyde produced by reaction 13), can now be fully explained. We need to form F_{HCHO}, which represents the fraction of all *produced* formaldehyde molecules that lead to NO to NO_2 conversions. By definition this fraction does not involve any of the initially present HCHO. Thus, we must separate the two types of formaldehyde in order to properly calculate the relation F_{HCHO}.

The mechanisms to be evaluated shortly are considerably more complicated than the simple aldehyde mechanism described above. However, no matter how complex the mechanism, the counter species analysis proceeds exactly as illustrated above, even though the expressions are more complicated. As a means of ensuring the accuracy of the analysis, we can count the actual number of NO to NO_2 conversions, and compare this to the total obtained via the counter species analysis. For instance, in our simple example above, the actual number of NO to NO_2 conversions that have occurred up to any time is given by C3+C9+C12. This same result must be obtained when we total the NO oxidations attributed to the three aldehydes (calculated from the relations on page 9). All of the results given in Chapter 3 have been confirmed in this way.

In summary, the counter species analysis enables one to assess quantitatively the importance of individual reactions and reaction sub-networks to the overall behavior of a complex mechanism. By using the counter species analysis on the six lumped mechanisms considered in this study, we can compare individual portions of these mechanisms to each other. These individual comparisons are then used to determine the reasons for the observed differences in overall behavior.

2.3 Master Mechanism

Each of the lumped mechanisms represents an attempt to simplify the detailed chemistry of the atmospheric organic/NO_x system. The lumped mechanisms are, it is important to stress, derived from known detailed, explicit chemistry and are not simply empirical curve fits of data. For this reason, it is appropriate to compare the structure and behavior of each mechanism to a fully explicit, detailed mechanism containing as many of the important organic species as possible. In doing so, we can assess the degree to which each of the lumped mechanisms represents the explicit chemistry of the organic constituents that are included in the lumped classes in the mechanisms.

Table 1 gives the initial composition of smog chamber experiment SUR-119J performed at the Statewide Air Pollution Research Center (SAPRC), University of California at Riverside (Pitts et al., 1976). The individual species concentrations for this experiment were chosen to represent the 6-9 AM ambient pollutant burden in the Los Angeles atmosphere. If we exclude the first three hydrocarbons (methane, acetylene, and ethane) because of their low reactivity, we see that the remainder of the list is dominated by the presence of about 10-12 organic species. A great deal of kinetic and mechanistic data dealing with the atmospheric chemistry of these species has been obtained over the past decade or so. These data have been analyzed and summarized by Atkinson and Lloyd (1984). Thus, with this information, we feel that a realistic, explicit reaction mechanism can be formulated for the key species in Table 1. We call this the "master mechanism."

2.4 Details of the Master Mechanism

A listing of the master mechanism is given in Table A.1 of the Appendix. The primary organics whose explicit chemistry is contained in the

TABLE 1

Composition of Smog Chamber Experiment SUR-119J
(Pitts et al., 1976)

SPECIES	CONCENTRATION	
	ppbV	ppbC
Methane (CH_4)	2740.0	2740.0
Acetylene (C_2H_2)	46.4	92.8
Ethane (C_2H_6)	76.8	153.6
Propane (C_3H_8)	17.0	51.0
Acetone (CH_3COCH_3)	35.2	105.6
Isobutane (C_4H_{10})	0.2	0.8
n-butane	166.0	664.0
2,3-Dimethyl Butane ($C_4H_8-(CH_3)_2$)	97.6	585.6
Ethene (C_2H_4)	43.2	86.4
Propene (C_2H_4)	10.6	31.8
Trans-2-Butene (C_4H_8)	0.7	2.8
Cis-2-Butene (C_4H_8)	13.0	52.0
2-methyl Butene-2 ($C_4H_7-CH_3$)	14.8	74.0
Benzene (C_6H_6)	1.6	9.6
Toluene ($C_6H_5-CH_3$)	16.8	117.6
Ethyl Benzene ($C_6H_5-C_2H_5$)	6.4	51.2
Meta-xylene ($C_6H_4-(CH_3)_2$)	42.4	339.2
Isopropyl Benzene ($C_6H_5-C_3H_7$)	0.4	3.6
n-Propyl Benzene ($(C_6H_4-C_3H_7)_n$)	0.1	0.9
Meta-Ethyl Toluene ($C_6H_4-CH_3-C_2H_5$)	1.0	9.0
1,2,3 Trimethyl Benzene ($C_6H_3-(CH_3)_3$)	1.6	14.4

Table 1 (Continued)

SPECIES	CONCENTRATION ppbV	ppbC
Formaldehyde (HCHO)	38.0	38.0
Acetaldehyde (CH_3CHO)	20.0	40.0
Propionaldehyde (C_2H_5CHO)	3.2	9.6
Nitric Oxide (NO)	301.0	
Nitrogen Dioxide (NO_2)	41.0	
Nitrous Acid (HONO)	12.0	
Carbon Monoxide (CO)	7450.0	
Water (H_2O) (ppm)	15500.0	
Oxygen (O_2) (ppm)	210,000.0	
M (ppm)	1,000,000.0	
TOTALS FOR MIXTURE		
Nitrogen oxides (ppbV)	354.0	
THC (ppbV)	3393.0	
THC (ppbC)	5274.0	

master mechanism are:

propane
n-butane
2,3-dimethylbutane
} alkanes

toluene
m-xylene
} aromatics

ethene
propene
trans-2-butene
} alkenes

formaldehyde
acetaldehyde
propionaldehyde
acetone
} aldehydes and ketones

These species were chosen from the list of compounds contained in experiment SUR-119J. The reasoning behind this choice was as follows. Propene was selected because it is treated explicitly in some of the lumped mechanisms. Acetone is included because it is present at significant concentrations and is also formed from alkane photooxidation. Of the four alkanes included in SUR-119J, we include the chemistry of propane, n-butane, and 2,3-dimethylbutane in the master mechanism. Isobutane is ignored because of its low concentration. Three alkenes are included in the master mechanism, ethene, propene, and 2-butene (included as trans-2-butene). We have chosen to ignore 2-methyl-2-butene. Two aromatic hydrocarbons are included, toluene and m-xylene. These are the two most abundant, and best understood atmospheric aromatics. Benzene is not important because of its low concentration and reactivity. The remainder of the aromatics are present in small amounts, and is therefore ignored.

Excluding methane, acetylene, and ethane, 529.8 ppbv of initial organics are present in SUR-119J. Of these, 503.7 ppbv or 95 percent is represented by the 12 organics included in the master mechanism. Thus, to the extent that the mixture studied in experiment SUR-119J is representative, we feel that the master mechanism provides a reasonable description of the chemistry occurring in typical urban atmospheres.

The reactions and rate constants comprising the master mechanism were taken almost exclusively from three sources. The inorganic reactions were compiled using the recent reviews of Baulch et al. (1982), Demore et al. (1982), and Atkinson and Lloyd (1984). The vast majority of the organic reactions was taken from the review of Atkinson and Lloyd (1984).

2.5 Verification of the Master Mechanism

The evaluation of mechanisms with smog chamber data is not the object of this report. In fact, it is our feeling that with the current controversy regarding the magnitude of chamber radical sources (see section 2.6), it is difficult to consider any mechanism validated simply because it can simulate chamber data. However, because the master mechanism plays an important role in this study, we feel it is useful to include the results of simulating a series of experiments performed in the evacuable chamber at SAPRC.

The particular experiments simulated here are EC-231, EC-232, EC-233, EC-237, EC-238, EC-241, EC-242, EC-243, EC-245, EC-246, and SUR-119J. The series of "EC" experiments are hydrocarbon-NO_x experiments in which both the initial hydrocarbon distribution and the $[RHC]_o/[NO_x]_o$ are varied. The initial conditions for experiment SUR-119J are shown in Table 1. The chamber dependent reactions added to the master mechanism to adopt it for modeling chamber experiments are (Carter et al., 1982b):

O_3 wall loss: $k = 1.65\times10^{-3}\ \text{min}^{-1}$

NO wall source: $k = 1.0\times10^{-4}\ \text{min}^{-1}$

OH radical source: $k = k_{NO_2}(0.39 + 1.37[NO_2])\ \text{ppb-min}^{-1}$

heterogeneous HNO_3 formation $k = 4.4\times10^{-6}\ \text{ppm}^{-1} - \text{min}^{-1}$

It is important to note at this point that the evaluation of the master mechanism is the only place in this report where chamber effects are included in the simulations.

The results of simulating most of the above experiments with the master mechanism are shown in the Appendix (Figures A1-A9). In nearly every case the agreement among experiment and mechanism predictions is excellent. One should keep in mind that the master mechanism contains no adjustable parameters. Similarly, the chamber dependent terms are held constant and not varied as the initial conditions of the experiments change.

2.6 Chamber Effects

The question of smog chamber radical sources has proven to be one of the most perplexing problems in the study of photochemical smog chemistry. Because our concern in the present study is with atmospheric application of the mechanisms, and not with the modeling of smog chamber experiments, we do not consider chamber effects here (except in the evaluation of the master mechanism in section 2.5). Consequently, all of the results shown in Chapter 3 are obtained with mechanisms that contained no chamber dependent reactions.

The Carter et al. (1982b) study of chamber dependent radical sources provides strong evidence that chamber radical sources exist in the evacuable chamber at SAPRC. However, there is still considerable controversy over the magnitude of these radical sources. In fact, the magnitude of the radical source term varies substantially between the mechanisms considered in this study. Since each mechanism in its original form can simulate experimental data, it is obvious that the predicted reactivity will differ between the mechanisms once the chamber radical source terms are removed. This result is also evident from the analysis presented in Chapter 3. The point we wish to make here is that this disagreement in predicted reactivity will continue to exist until the chamber radical source issue is understood, and agreed upon by all investigators.

2.7 Initial Reactant Conditions

The performance of lumped mechanisms is, because of their very nature, sensitive to the initially assumed organic species distributions. Ideally, one would like to test each mechanism using a wide variety of initial hydrocarbon distributions and $[RHC]/[NO_x]$ ratios. To keep the results presented to a manageable level, we have chosen to compare the mechanisms using three related sets of initial conditions, hereafter denoted initial condition sets 1, 2, and 3. Initial condition set 1, which is loosely based on smog chamber experiment SUR-119J, is given in Table 2. These conditions were chosen to represent the early morning pollutant levels found in a typical urban atmosphere. Initial condition set 2 is obtained from set 1 by doubling the initial loadings of all hydrocarbons and halving the initial NO and NO_2 concentrations. This modification changes the $[RHC]_o/[NO_x]_o$ ratio from 7.14 to 28.6. Initial condition set 3 has $[RHC]_o/[NO_x]_o = 1.79$, which is obtained by doubling the NO and NO_2 loadings while halving the hydrocarbon concentrations from set 1. The three sets of initial conditions thus span a range of initial $[RHC]_o/[NO_x]_o$ ratios, which is acknowledged to be one of the key parameters influencing O_3 formation.

2.8 NO_2 Photolysis Rate Profile

Each of our simultations is carried out for a total of seven hours. The NO_2 photolysis rate profile used over this time period is shown in Table 3. This profile approximately corresponds to the NO_2 photolysis profile from 8 AM to 3 PM on a clear September day in Los Angeles.

TABLE 2

Initial Conditions and Other Important Parameters for Test Cases 1, 2, and 3

SPECIES	CONCENTRATION (ppbV)		
	CASE 1	CASE 2	CASE 3
NO	300	150	600
NO_2	50	25	100
Propane	20	40	10
n-Butane	190	380	95
2,3-Dimethylbutane	110	220	55
Ethene	50	100	25
Propene	15	30	7.5
tr-2-butene	30	60	15
Toluene	20	40	10
m-Xylene	50	100	25
Formaldehyde	45	90	22.5
Acetaldehyde	25	50	12.5
Propionaldehyde	5	10	2.5
Acetone	35	70	17.5
CO	7450	7450	7450
H_2O	15,500	15,500	15,500
HONO	12	12	12

Table 2 (Continued)

ADDITIONAL PARAMETERS:

Temperature (K)	298	298	298
Pressure (atm)	1.0	1.0	1.0
Dilution	0	0	0
$[RHC]_o/[NO_x]_o$ (ppmC/ppm)	7.14	28.6	1.79

TABLE 3

NO_2 Photolysis Rate Profile Used in Each of the Test Cases

TIME (MINUTES)	NO_2 PHOTOLYSIS RATE (min^{-1})
0	0.30
60	0.39
120	0.44
180	0.46
240	0.47
300	0.46
360	0.41
420	0.34

CHAPTER 3

RESULTS AND DISCUSSION

3.1 Introduction

In this chapter we present and discuss the detailed analysis of the relative behavior of the six lumped mechanisms under consideration. We first present the complete results in both tabular and graphical form, and then consider each mechanism individually. These individual discussions are divided into two parts. First, a very brief discussion of the mechanism itself is presented, primarily to note any changes from the listings included in Part I. Second, the counter species results for NO to NO_2 conversions are compared to those for both the master mechanism and the other lumped mechanisms. In the final section of this chapter we re-examine the predictions of each mechanism after they have been modified to reflect the results of the analysis.

3.2 Counter Species Results

The counter species results obtained using initial condition sets 1, 2, and 3 are presented in Tables 4, 5, and 6, respectively. The amount of NO to NO_2 conversions attributable to the various reaction pathways is listed for each of the seven mechanisms in this study. The results obtained with initial condition sets 1 and 3 correspond to an analysis time of 360 minutes, i.e. the end of a six-hour simulation. With initial condition set 2 each mechanism predicted the time of the O_3 peak to be less than 150 minutes. For this reason an analysis time of 150 minutes was chosen with this set of conditions. These same results are presented graphically in Figures 1-3. In addition, Figures 4, 5, and 6 present the results in a different form. There, the percentage of the total NO to NO_2 conversions due to each of four organic classes is shown.

Note that each of the initially present organic species contributes to the total amount of NO to NO_2 conversions predicted by each mechanism. For example, even though the Dodge mechanism does not include aromatic hydrocarbons, the initially present toluene and m-xylene are represented as 75 percent butane and 25 percent propene. Thus, these initially present aromatics do lead to NO to NO_2 conversions.

TABLE 4

Counter Species Results Obtained with Initial Condition Set 1
$([RHC]_o/[NO_x]_o = 7.14)$

The Amount of NO to NO_2 Conversions Attributable to Various Species and Reaction Pathways is Shown.
The Time of Analysis is After 360 Minutes of Simulation.

	NO TO NO_2 CONVERSIONS (ppb)[a]						
	Master	Killus & Whitten	Atkinson & Lloyd	Penner & Walton	Demerjian	McRae & Seinfeld	Dodge
I) AROMATICS							
Toluene abstraction	1	4	1	22	68	72	48
Toluene addition	14	82	17				
m-Xylene + OH	170	228	128	195	171	181	138
Methyl glyoxal + hv	73	143[b]	62	90	---	---	---
Methyl glyoxal + OH	11	4[b]	2	---	---	---	---
Glyoxal	1	---	1	---	---	---	---
Benzaldehyde	0	---	0	---	---	---	---
o-Cresol	1	14	6	---	---	---	---
Dimethyl phenols	9			---	---	---	---
cis-2-butene-1,4-dial	4	93	30	---	---	---	---
2-Pentene-1,4-dial	18			---	---	---	---
Other -dicarbonyls	25			---	---	---	---
Pyruvic acid	1	---	NI	---	---	---	---
TOTAL AROMATIC	185	314	146	217	239	253	186
II) ALKANES							
Propane + OH	3	7	3	6	15	16	21
Propane + $O(^3P)$	NI	NI	NI	NI	NI	0	
Butane + $O(^3P)$	0	NI	NI	0	NI	1	263
Butane + OH	68	168	112	88	142	154	
2,3-Dimethylbutane + $O(^3P)$	1	NI	NI	0	NI	0	228
2,3-Dimethylbutane + OH	85	146	65	124	82	89	
TOTAL ALKANE	157	321	180	218	239	260	512

Table 4 (Continued)

	NO TO NO_2 CONVERSIONS (ppb)[a]						
	Master	Killus & Whitten	Atkinson & Lloyd	Penner & Walton	Demerjian	McRae & Seinfeld	Dodge
III) ALKENES							
Ethene + OH	47	81	48	41	105	70	35
Ethene + $O(^3P)$	NI	1	NI	1	3	1	
Ethene + O_3	4	13	6	5	74	NI	
Propene + OH	36	39	31	38	31	33	16
Propene + $O(^3P)$	NI	0	NI	1	1	1	
Propene + O_3	5	9	9	5	22	10	
Butene + OH	66	81	69	206	63	66	41
Butene + $O(^3P)$	NI		NI	4	2	2	
Butene + O_3	23		28	25	45	19	
Ethene + NO_3	NI	NI	NI	0	NI	NI	NI
Propene + NO_3	NI	NI	NI	0	NI	NI	NI
Butene + NO_3	NI	NI	NI	1	NI	NI	NI
CH_2OO	3	9	4	---	---	---	---
CH_3CHOO	7	4	8	---	---	---	---
TOTAL ALKENE	181	221	191	327	346	202	92
IV) ALDEHYDES AND KETONES							
Initial HCHO	32	51	35	42	43	33	44
Initial CH_3CHO	23	34	28	34	24	53	50
Initial CH_3CH_2CHO	8	8	7	8	5	11	5
Initial $CH_3C(O)CH_3$ + OH	2	55	NI	0	26	---	36
Initial $CH_3C(O)CH_3$ + hv	3		4[d]	0	NI	---	
Initial HCHO + NO_3	NI	NI	NI	0	NI	NI	NI
Initial CH_3CHO + NO_3	NI	NI	NI	0	NI	NI	NI
Initial CH_3CH_2CHO + NO_3	NI	NI	NI	0	NI	NI	NI
Initial $CH_3C(O)CH_3$ + NO_3	NI	NI	NI	0	NI	NI	NI
Created HCHO	43	360[c]	58	282[e]	384[f]	88	128
Created CH_3CHO	61		73			345[g]	130
Created CH_3CH_2CHO	1		5[d]				37
Created $CH_3CH_2CH_2CHO$	3						59
Created $CH_3C(O)CH_3$ + OH	2		NI				---
Created $CH_3C(O)CH_3$ + hv	3		1				---
Created MEK + OH	1		15				---
Created MEK + hv	8		6				---
TOTAL ALDEHYDE	68	148	74	84	98	97	135

GRAND TOTAL	591	1007	591	846	922	812	925
ACTUAL NUMBER OF NO/NO_2 CONVERSIONS[h]	597	1005	587	847	923	813	927

Footnotes for Table 4:

a NI stands for not included
b The number shown is for the lumped group DCRB
c The number shown is for the lumped group CARB
d Number of conversions due to created RCHO species
e Number of conversions due to created HC4 species
f Number of conversions due to created HC3 species
g Number of conversions due to created RCHO species
h This is the actual number of NO to NO_2 conversions which have taken place. The grand total predicted by the counter species analysis should approximately equal this number.

TABLE 5

Counter Species Results Obtained with Initial Condition Set 2
($[RHC]_o/[NO_x]_o = 28.6$)

The Amount of NO to NO_2 Conversions Attributable to Various Species and Reaction Pathways is Shown.
The Time of Analysis is After 150 Minutes of Simulation.

	NO TO NO_2 CONVERSIONS (ppb)[a]						
	Master	Killus & Whitten	Atkinson & Lloyd	Penner & Walton	Demerjian	McRae & Seinfeld	Dodge
I) AROMATICS							
Toluene abstraction	1	3	2	} 19	} 66	} 64	} 37
Toluene addition	15	65	15				
m-Xylene + OH	159	178	125	169	165	160	105
Methyl glyoxal + hv	47	104[b]	48	87	---	---	---
Methyl glyoxal + OH	7	2[b]	1	---	---	---	---
Glyoxal	1	---	0	---	---	---	---
Benzaldehyde	0	---	0	---	---	---	---
o-Cresol	0			---	---	---	---
Dimethyl phenols	5	7	3	---	---	---	---
cis-2-butene-1,4-dial	1	} 81	} 10	---	---	---	---
2-Pentene-1,4-dial	10			---	---	---	---
Other -dicarbonyls	11			---	---	---	---
Pyruvic acid	0	---	NI	---	---	---	---
TOTAL AROMATIC	175	246	142	188	231	224	142
II) ALKANES							
Propane + OH	4	5	4	5	14	14	} 16
Propane + $O(^3P)$	NI	NI	NI	0	NI	0	
Butane + $O(^3P)$	0	NI	NI	0	NI	0	}200
Butane + OH	77	117	129	72	128	137	
2,3-Dimethylbutane + $O(^3P)$	0	NI	NI	0	NI	0	}174
2,3-Dimethylbutane + OH	116	101	74	102	74	79	
TOTAL ALKANE	197	223	207	179	216	230	390

Table 5 (Continued)

	NO TO NO_2 CONVERSIONS (ppb)[a]						
	Master	Killus & Whitten	Atkinson & Lloyd	Penner & Walton	Demerjian	McRae & Seinfeld	Dodge
III) ALKENES							
Ethene + OH	58	61	57	43	122	66	26
Ethene + $O(^3P)$	NI	0	NI	0	1	0	
Ethene + O_3	5	6	5	7	126	NI	
Propene + OH	42	34	37	40	37	41	12
Propene + $O(^3P)$	NI	0	NI	0	0	0	
Propene + O_3	8	11	10	6	38	18	
Butene + OH	71	63	72	215	73	81	32
Butene + $O(^3P)$	NI		NI	1	1	1	
Butene + O_3	48		48	34	76	36	
Ethene + NO_3	NI	NI	NI	0	NI	NI	NI
Propene + NO_3	NI	NI	NI	0	NI	NI	NI
Butene + NO_3	NI	NI	NI	3	NI	NI	NI
CH_2OO	3	5	3	---	---	---	---
CH_3CHOO	10	6	10	---	---	---	---
TOTAL ALKENE	232	175	229	349	474	243	70
IV) ALDEHYDES AND KETONES							
Initial HCHO	39	41	41	34	40	45	46
Initial CH_3CHO	12	26	16	29	22	39	36
Initial CH_3CH_2CHO	5	6	5	7	4	8	4
Initial $CH_3C(O)CH_3$ + OH	2	42	NI	0	24	---	28
Initial $CH_3C(O)CH_3$ + hv	2		2[d]	0	NI	---	
Initial HCHO + NO_3	NI	NI	NI	0	NI	NI	NI
Initial CH_3CHO + NO_3	NI	NI	NI	0	NI	NI	NI
Initial CH_3CH_2CHO + NO_3	NI	NI	NI	0	NI	NI	NI
Initial $CH_3C(O)CH_3$ + NO_3	NI	NI	NI	0	NI	NI	NI
Created HCHO	28	122[c]	37	135[e]	259 259[f]	66	65
Created CH_3CHO	27		34			155[g]	51
Created CH_3CH_2CHO	0		2[d]				11
Created $CH_3CH_2CH_2CHO$	1						34
Created $CH_3C(O)CH_3$ + OH	1		NI				---
Created $CH_3C(O)CH_3$ + hv	1		0				---
Created MEK + OH	0		3				---
Created MEK + hv	3		5				---
TOTAL ALDEHYDE	60	115	64	70	90	92	114

GRAND TOTAL	664	759	642	786	1011	789	716
ACTUAL NUMBER OF NO/NO_2 CONVERSIONS[h]	668	759	637	787	1010	789	715

Footnotes for Table 5:

a NI stands for not included
b The number shown is for the lumped group DCRB
c The number shown is for the lumped group CARB
d Number of conversions due to created RCHO species
e Number of conversions due to created HC4 species
f Number of conversions due to created HC3 species
g Number of conversions due to created RCHO species
h This is the actual number of NO to NO_2 conversions which have taken place. The grand total predicted by the counter species analysis should approximately equal this number.

TABLE 6

Counter Species Results Obtained with Initial Condition Set 3
$([RHC]_o/[NO_x]_o = 1.79)$

The Amount of NO to NO_2 Conversions Attributable to Various Species and Reaction Pathways is Shown.
The Results are Calculated at a Simulation Time of 360 Minutes.

	NO TO NO_2 CONVERSIONS (ppb)[a]						
	Master	Killus & Whitten	Atkinson & Lloyd	Penner & Walton	Demerjian	McRae & Seinfeld	Dodge
I) AROMATICS							
Toluene abstraction	0	1	0	} 5	} 17	} 26	} 18
Toluene addition	4	36	7				
m-Xylene + OH	65	96	61	48	42	69	51
Methyl glyoxal + hv	35	71[b]	35	31	---	---	---
Methyl glyoxal + OH	4	2[b]	1	---	---	---	---
Glyoxal	0	---	0	---	---	---	---
Benzaldehyde	0	---	0	---	---	---	---
o-Cresol	0	} 10	} 4	---	---	---	---
Dimethyl phenols	4			---	---	---	---
cis-2-butene-1,4-dial	1	} 44	} 17	---	---	---	---
2-Pentene-1,4-dial	6			---	---	---	---
Other -dicarbonyls	10			---	---	---	---
Pyruvic acid	1	---	NI	---	---	---	---
TOTAL AROMATIC	69	133	68	53	59	95	69
II) ALKANES							
Propane + OH	1	2	1	1	3	5	} 8
Propane + $O(^3P)$	NI	NI	NI	0	NI	0	
Butane + $O(^3P)$	0	NI	NI	0	NI	0	} 96
Butane + OH	18	46	34	13	26	45	
2,3-Dimethylbutane + $O(^3P)$	0	NI	NI	0	NI	0	} 88
2,3-Dimethylbutane + OH	23	40	19	18	15	26	
TOTAL ALKANE	41	88	54	32	44	76	187

Table 6 (Continued)

	NO TO NO_2 CONVERSIONS (ppb)[a]						
	Master	Killus & Whitten	Atkinson & Lloyd	Penner & Walton	Demerjian	McRae & Seinfeld	Dodge
III) ALKENES							
Ethene + OH	12	26	14	12	45	21	13
Ethene + $O(^3P)$	NI	1	NI	1	5	1	
Ethene + O_3	0	1	0	0	13	NI	
Propene + OH	10	18	12	11	14	19	6
Propene + $O(^3P)$	NI	1	NI	1	1	3	
Propene + O_3	1	1	1	0	4	3	
Butene + OH	34	47	37	58	27	37	15
Butene + $O(^3P)$	NI		NI	5	3	5	
Butene + O_3	8		10	1	8	6	
Ethene + NO_3	NI	NI	NI	0	NI	NI	NI
Propene + NO_3	NI	NI	NI	0	NI	NI	NI
Butene + NO_3	NI	NI	NI	0	NI	NI	NI
CH_2OO	0	1	0	---	---	---	---
CH_3CHOO	2	0	3	---	---	---	---
TOTAL ALKENE	65	95	74	89	120	96	34
IV) ALDEHYDES AND KETONES							
Initial $HCHO$	14	32	16	21	21	15	20
Initial CH_3CHO	13	20	16	18	11	39	31
Initial CH_3CH_2CHO	4	4	5	4	2	8	2
Initial $CH_3C(O)CH_3$ + OH	1	29	NI	0	5	---	13
Initial $CH_3C(O)CH_3$ + hv	2		3[d]	0	NI	---	
Initial $HCHO + NO_3$	NI	NI	NI	0	NI	NI	NI
Initial $CH_3CHO + NO_3$	NI	NI	NI	0	NI	NI	NI
Initial $CH_3CH_2CHO + NO_3$	NI	NI	NI	0	NI	NI	NI
Initial $CH_3C(O)CH_3 + NO_3$	NI	NI	NI	0	NI	NI	NI
Created $HCHO$	13	146[c]	20	61[e]	93[f]	31	40
Created CH_3CHO	23		31			162[g]	56
Created CH_3CH_2CHO	0		2[d]				24
Created $CH_3CH_2CH_2CHO$	1		NI				31
Created $CH_3C(O)CH_3$ + OH	0		1				---
Created $CH_3C(O)CH_3$ + hv	1		1				---
Created MEK + OH	0		1				---
Created MEK + hv	3		6				---

TOTAL ALDEHYDE	34	85	40	43	39	62	66
GRAND TOTAL	209	401	236	217	262	329	356
ACTUAL NUMBER OF NO/NO$_2$ CONVERSIONS[h]	214	398	236	217	260	330	355

Footnotes for Table 6:

[a] NI stands for not included

[b] The number shown is for the lumped group DCRB

[c] The number shown is for the lumped group CARB

[d] Number of conversions due to created RCHO species

[e] Number of conversions due to created HC4 species

[f] Number of conversions due to created HC3 species

[g] Number of conversions due to created RCHO species

[h] This is the actual number of NO to NO$_2$ conversions which have taken place. The grand total predicted by the counter species analysis should approximately equal this number.

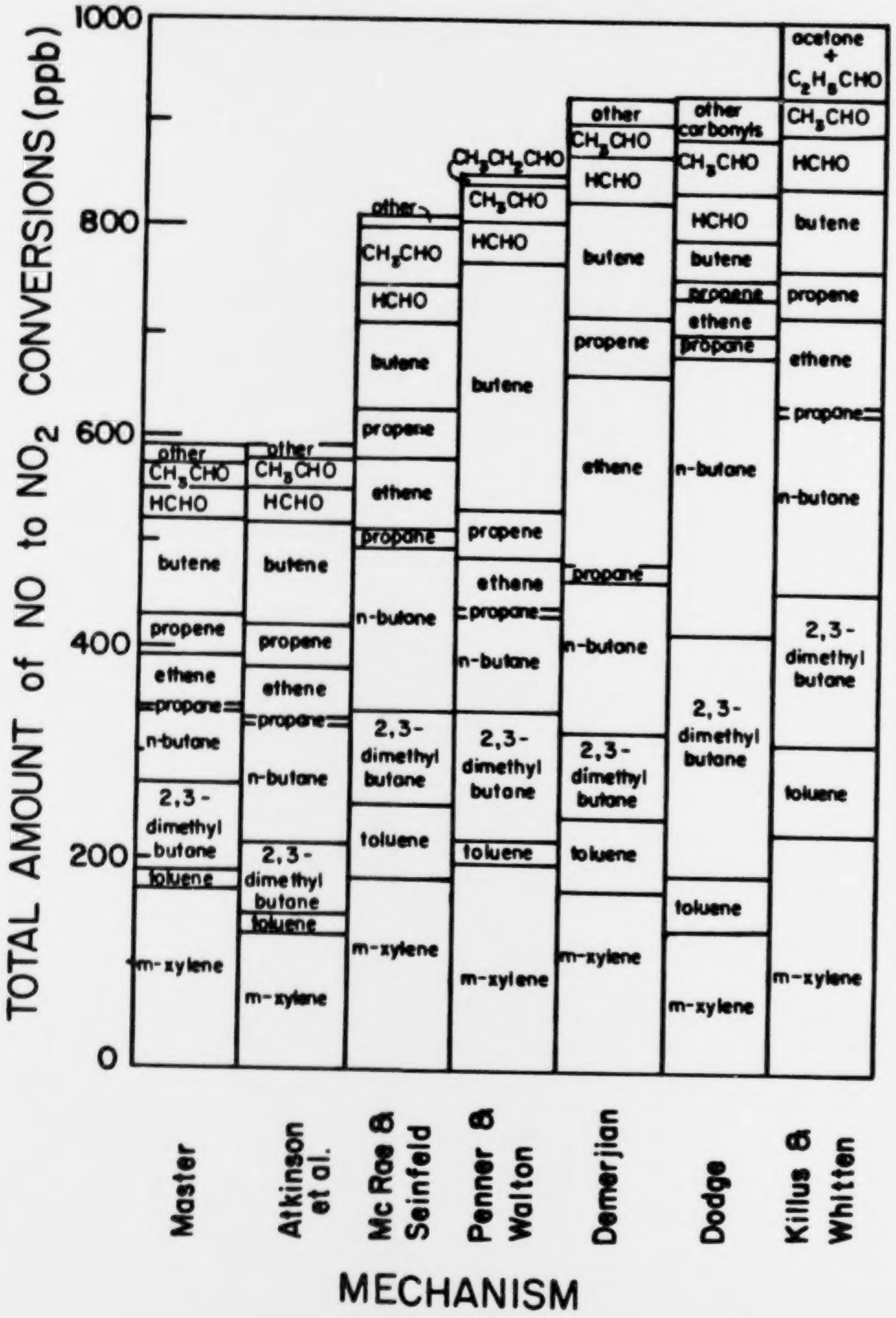

Figure 1. Counter Species Results Obtained Using Initial Condition Set 1. Amount of NO to NO$_2$ Conversions Attributable to Each of the Initially Present Organics.

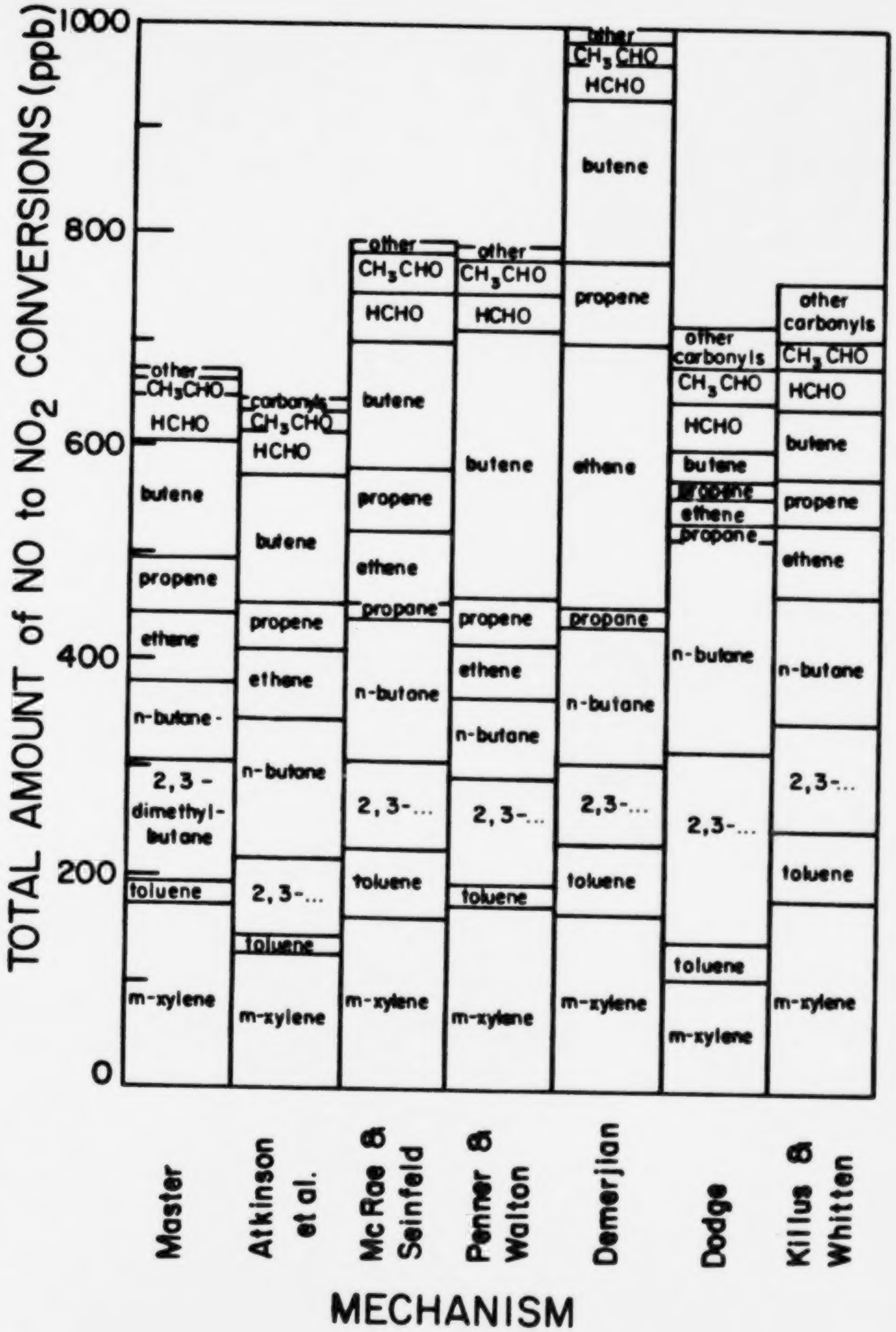

Figure 2. Counter Species Results Obtained Using Initial Condition Set 2. Amount of NO to NO_2 Conversions Attributable to Each of the Initially Present Organics.

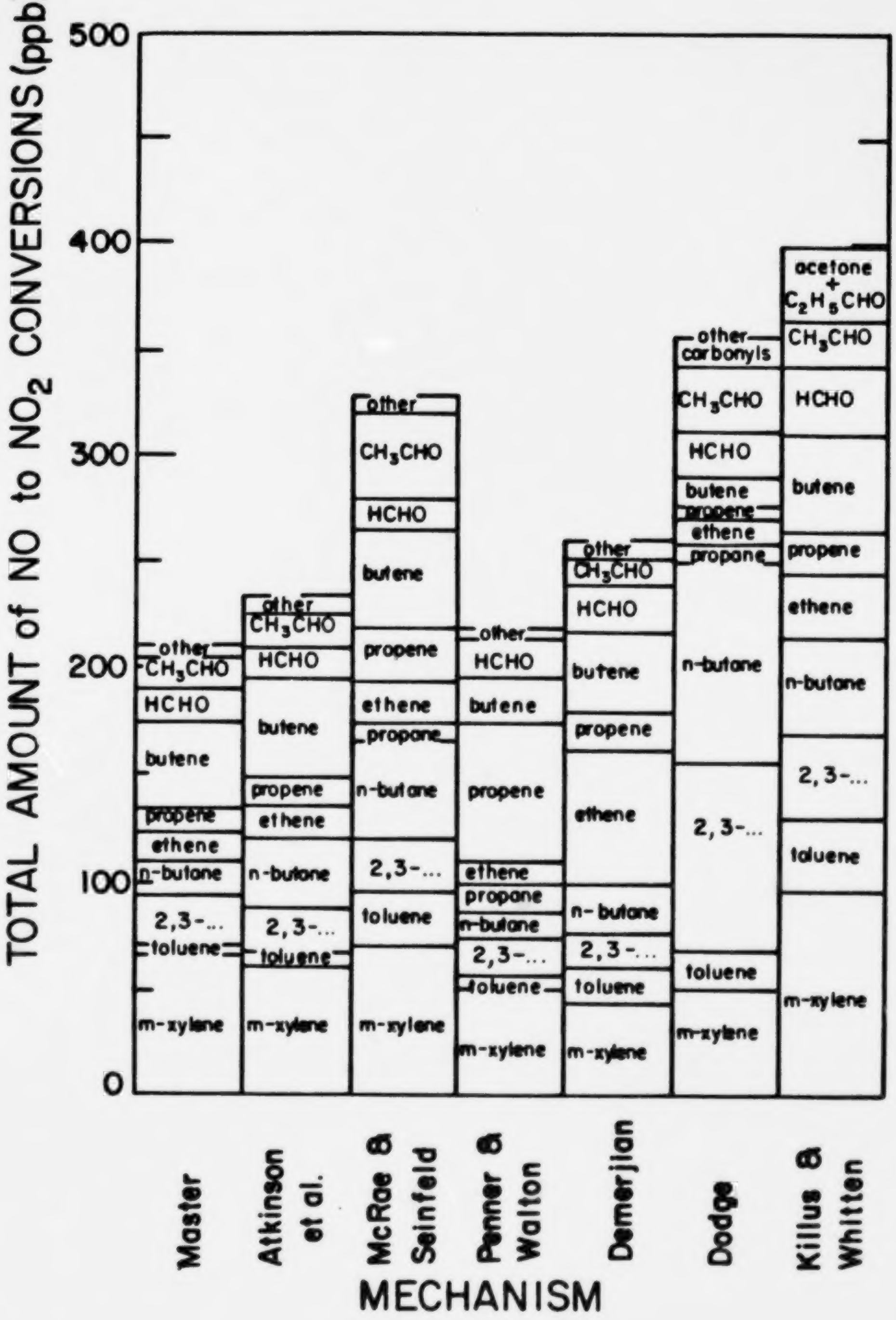

Figure 3. Counter Species Results Obtained Using Initial Condition Set 3. Amount of NO to NO_2 Conversions Attributable to Each of the Initially Present Organics.

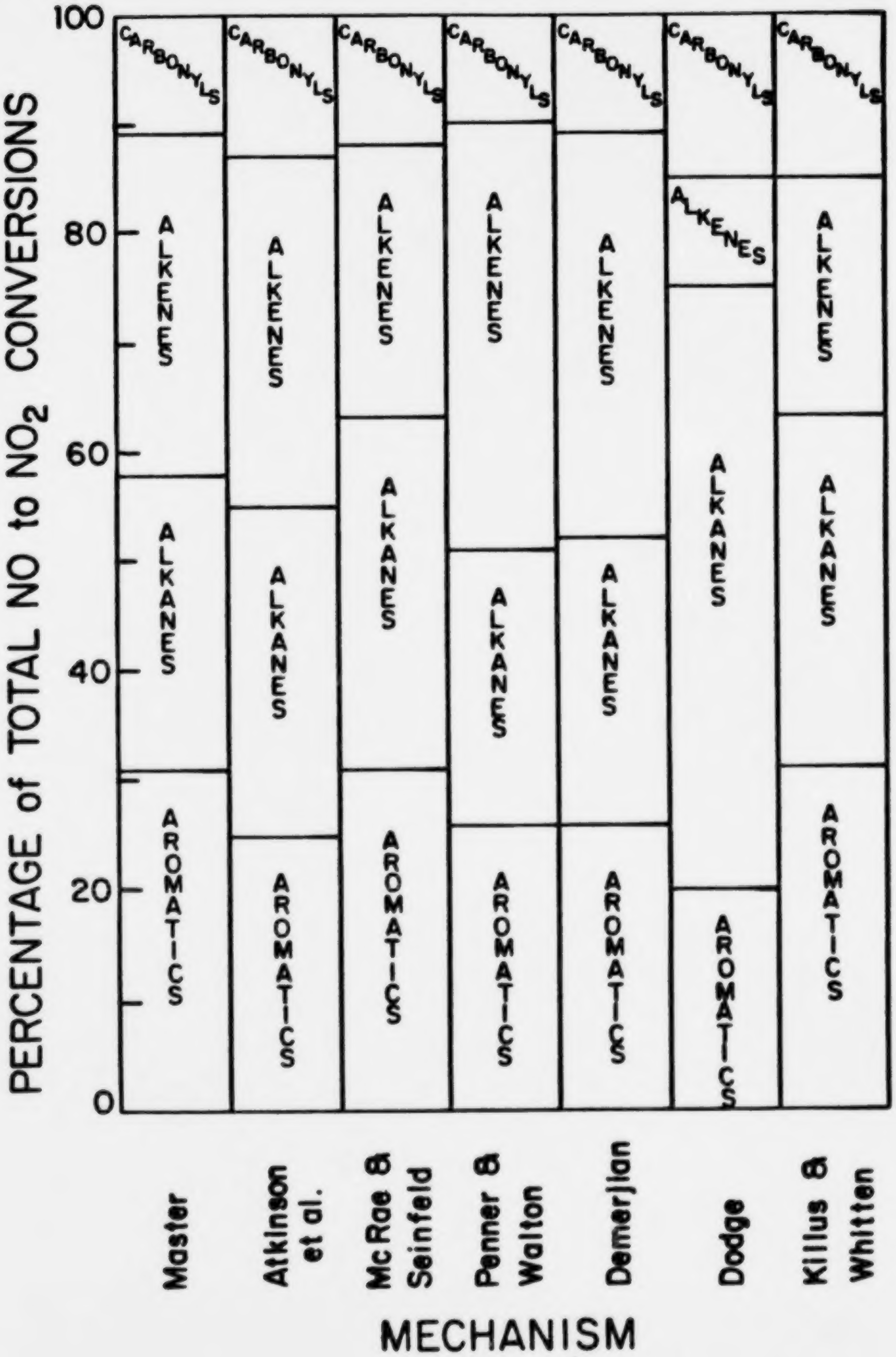

Figure 4. Percent of the Total NO to NO_2 Conversions Due to Each Class of Organic for the Simulation Using Initial Condition Set 1.

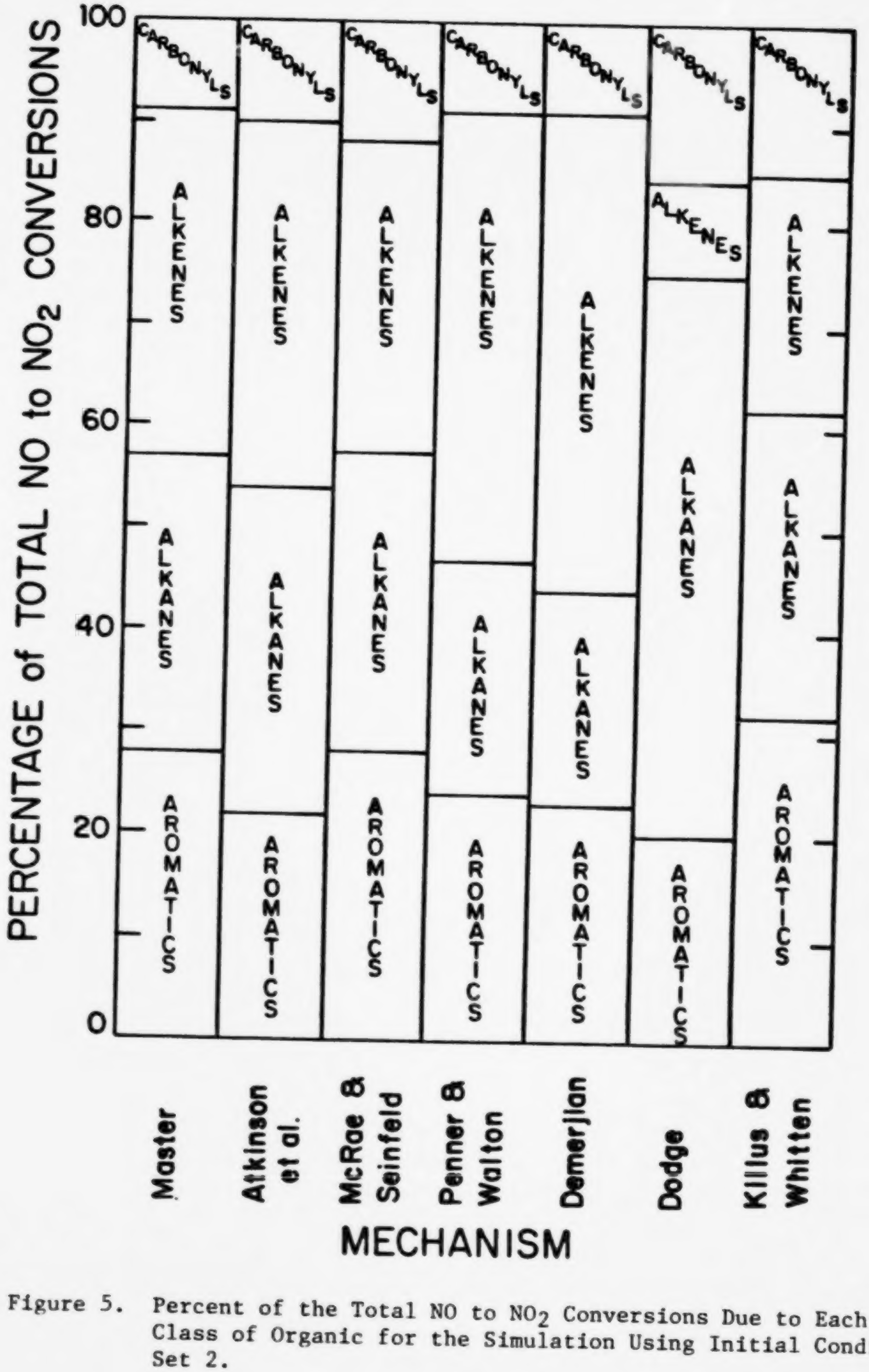

Figure 5. Percent of the Total NO to NO_2 Conversions Due to Each Class of Organic for the Simulation Using Initial Condition Set 2.

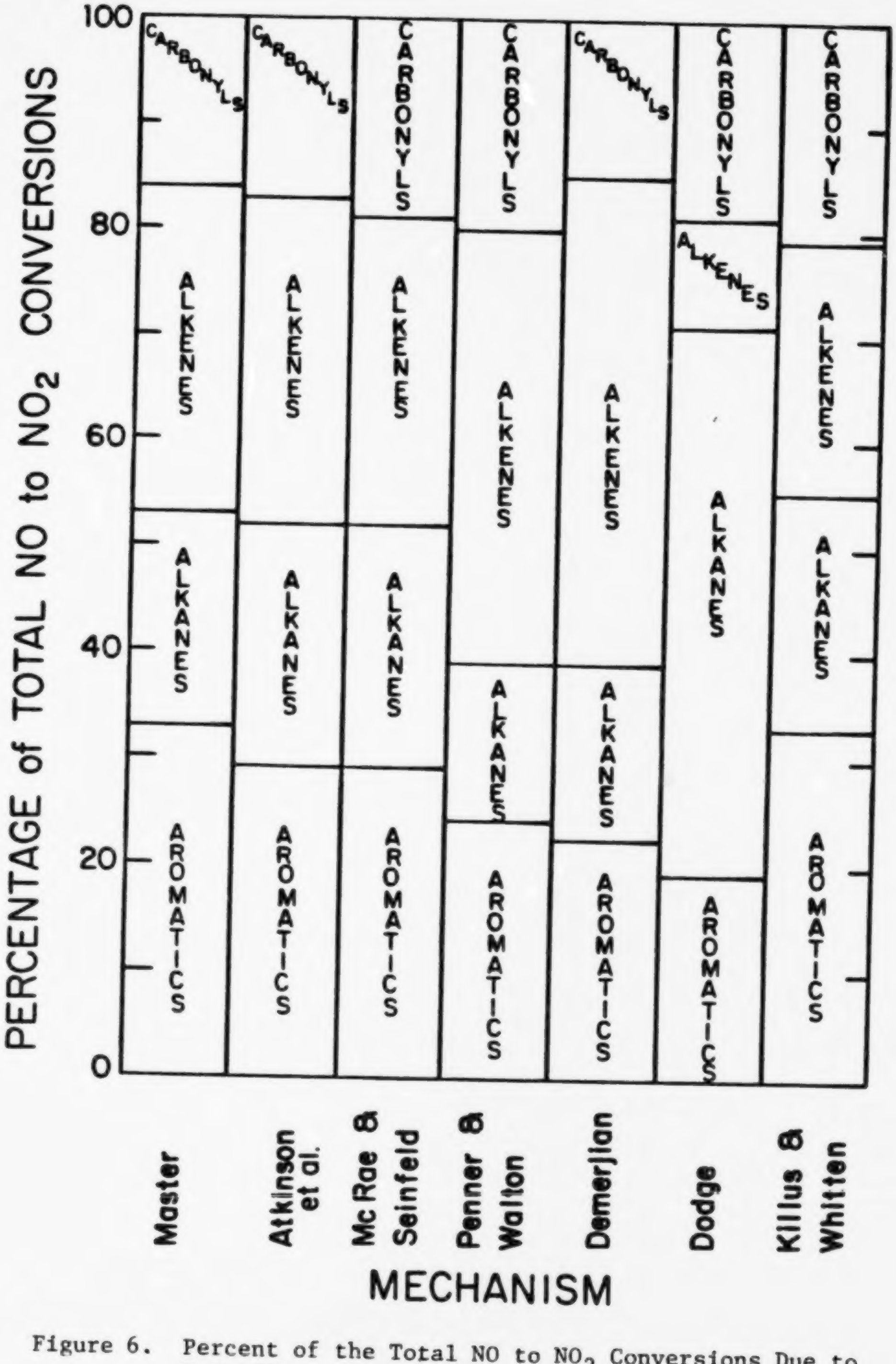

Figure 6. Percent of the Total NO to NO_2 Conversions Due to Each Class of Organic for the Simulation Using Initial Condition Set 3.

Although we will shortly discuss these results in detail for each mechanism, a few of the salient features are noted here. First, note that, except for the Atkinson et al. (1982) mechanism (which bears the closest resemblance to the master mechanism) each of the lumped mechanisms consistently predicts more NO to NO_2 conversions than does the master mechanism. Also, note the differences in the bar graph patterns found between Figures 1, 2, and 3. For instance, in Figure 2 ($[RHC]_o/[NO_x]_o = 28.6$, high O_3) the Demerjian (1982) mechanism predicts many more NO to NO_2 conversions than does the Killus and Whitten (1982) mechanism. However, in Figure 3 ($[RHC]_o/[NO_x]_o = 1.79$, low O_3) the opposite is true. Examination of Figures 4 to 6 shows that the percentage of the total NO to NO_2 conversions attributable to each class of organic varies substantially between the mechanisms.

3.3 NO to NO_2 Conversions vs. O_3 Yield

Before we discuss the counter species results in detail, it is interesting to examine, for each mechanism, the relationship between the total number of NO to NO_2 conversions and the maximum predicted O_3 concentration. Although the amount of O_3 for which a given reaction is responsible is proportional to the number of NO to NO_2 conversions attributable to that reaction, the overall yield of O_3 depends not only on the number of NO molecules converted to NO_2, but also on the NO and NO_2 removal mechanisms. Thus, if two mechanisms predict a similar number of NO to NO_2 conversions but have vastly different NO_x removal mechanisms, they will not agree on the resulting O_3 concentrations. By and large, the differences among the NO_x removal steps in the lumped mechanisms are not substantial. The one exception is the Dodge (1977) mechanism. For example, the PAN reactions in the Dodge (1977) mechanism differ significantly from the corresponding reactions in the other lumped mechanisms. We might therefore expect that the relationship between [O_3] and the number of NO to NO_2 conversions in the Dodge (1977) mechanism will be somewhat different from those in the other lumped mechanisms.

Figures 7, 8, and 9 depict the relationship between the number of NO to NO_2 conversions and the maximum O_3 concentration for each lumped mechanism. We see that for the most part, as we proceed horizontally across the various mechanisms, the O_3 concentrations (shaded) follow the pattern of the NO to NO_2 conversions (unshaded). As we noted, the exception is the Dodge (1977) mechanism, which predicts a much smaller O_3 concentration per NO to NO_2 conversion than the others. This difference must be taken into account in our subsequent discussions concerning the Dodge (1977) mechanism.

3.4 The Atkinson et al. (1982) Mechanism

3.4.1 Description of the Mechanism:

The Atkinson et al. (1982) mechanism as used in this study appears in Table A2 of the Appendix. The only differences between the mechanism used here and that shown in Table 22 of Part I of this report (McRae et al. 1983) are the following:

(1) The chamber-dependent reactions have been removed (reactions 18, 80, and 81 of Table 22, Part I).

(2) The rate constant used for reaction 59 is the value recommended by Atkinson et al. (1982) for m-xylene ($k_{59} = 1.05 \times 10^7 T^{-1}$), not the value for a lumped xylene ($k = 7.9 \times 10^6 T^{-1}$).

(3) Since there is no benzene present in our initial hydrocarbon mix, and we have only m-xylene (no other isomers), the expression for B01

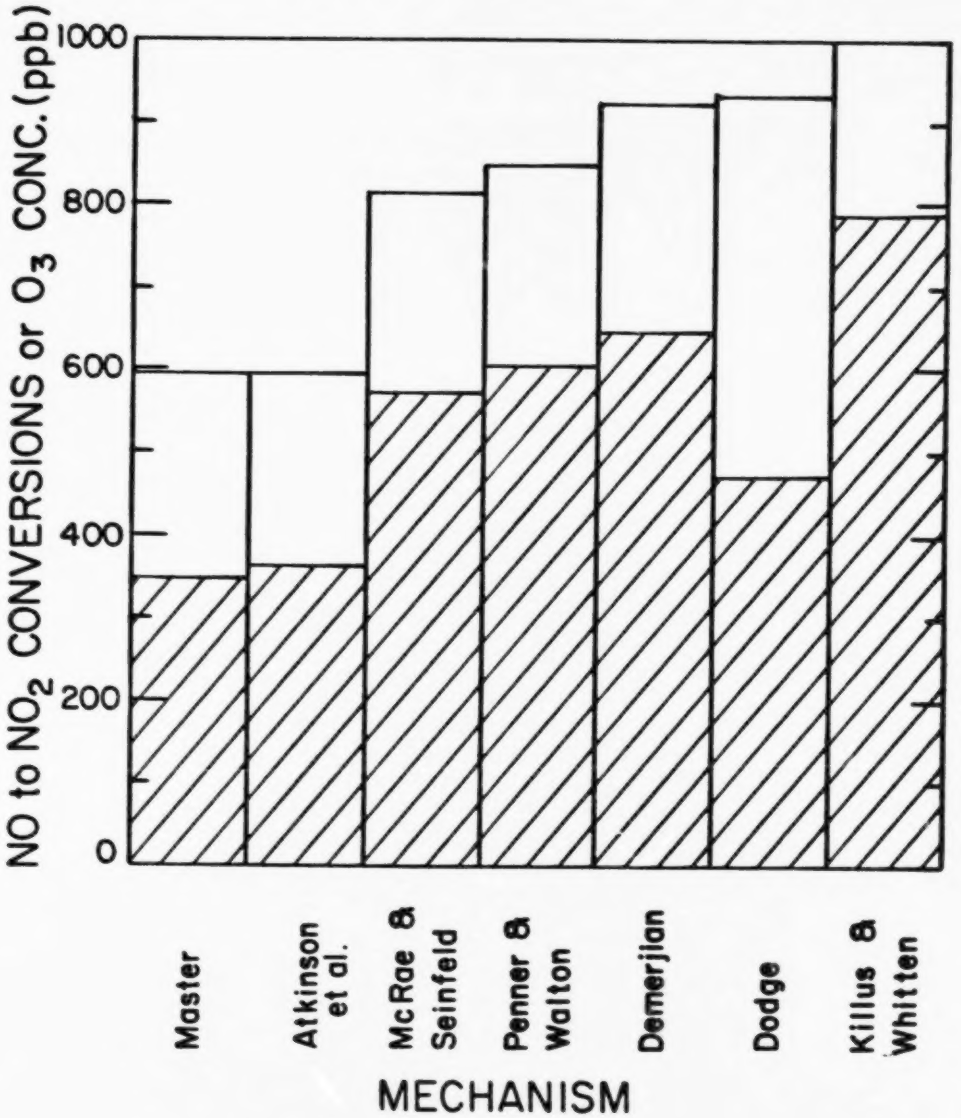

Figure 7. O_3 Yield (shaded) vs. Total Amount of NO to NO_2 Conversions (unshaded) for Each Mechanism Obtained with Initial Condition Set 1 ($[RHC]_o/[NO_x]_o = 7.14$).

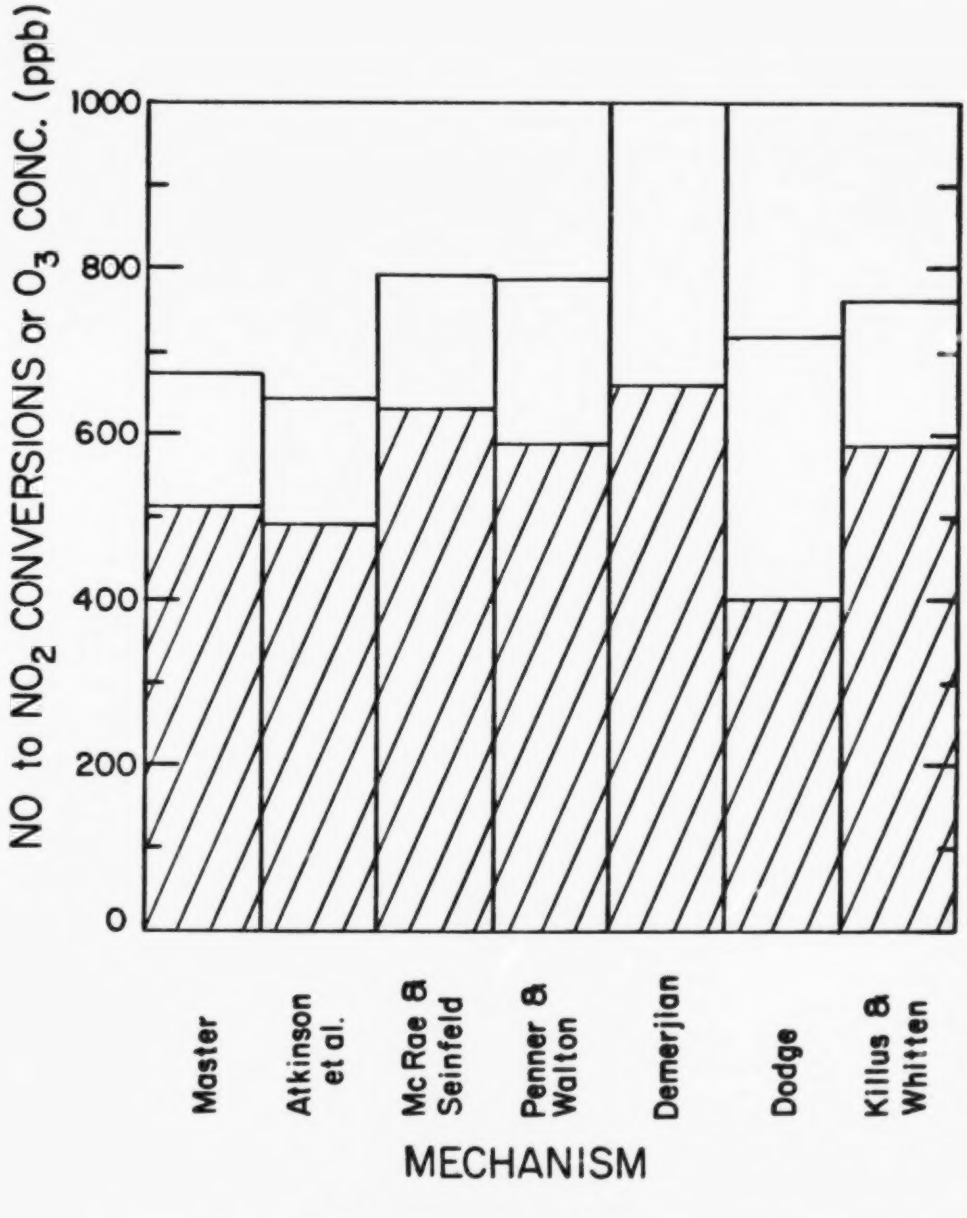

Figure 8. O_3 Yield (shaded) vs. Total Amount of NO to NO_2 Conversions (unshaded) for Each Mechanism Obtained with Initial Condition Set 2 ($[RHC]_o/[NO_x]_o = 28.6$)

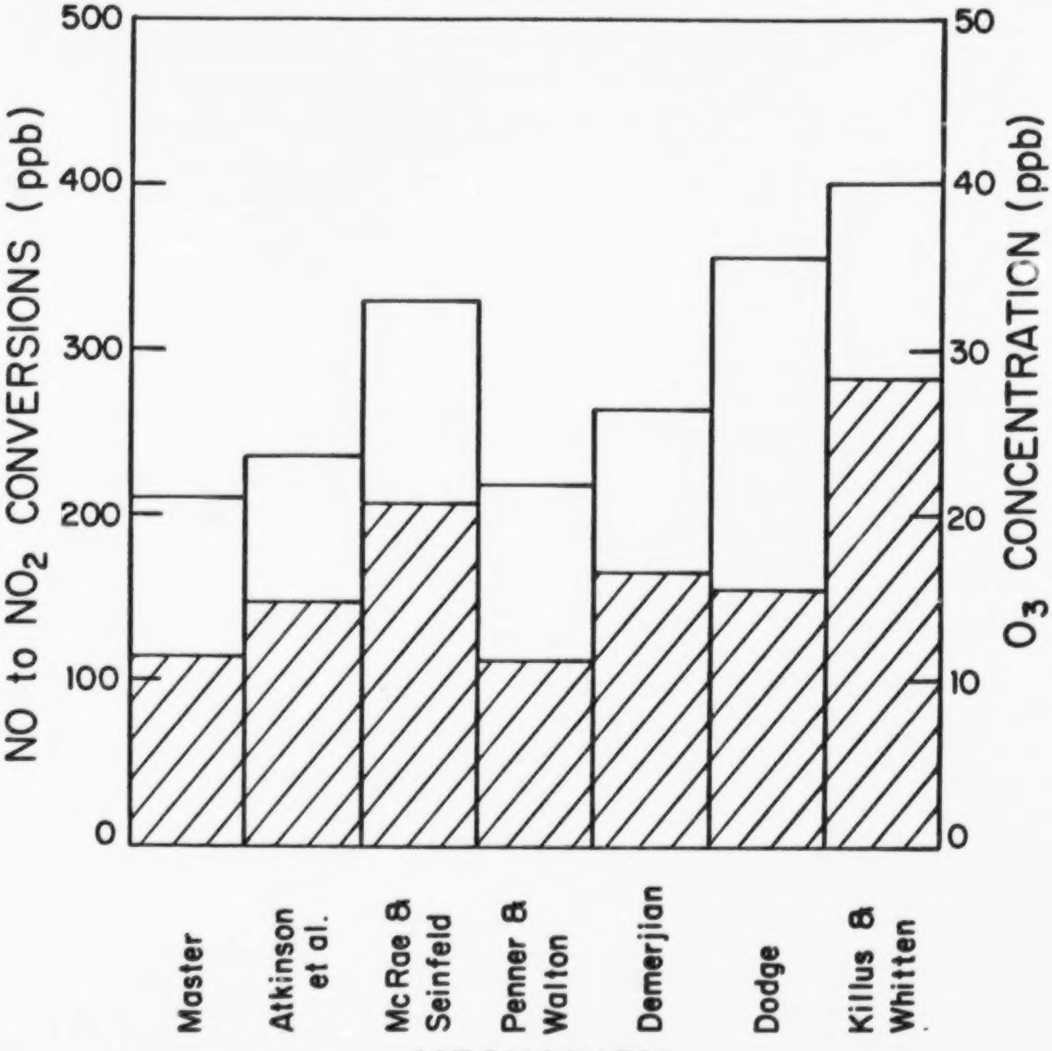

Figure 9 . O_3 Yield (shaded) vs. Total Amount of NO to NO_2 Conversions (unshaded) for Each Mechanism Obtained with Initial Condition Set 3 ($[RHC]_o/[NO_x]_o$ = 1.79).

given on page 15 of Part I becomes

$$B01 = \frac{0.75\ k_{57}[\text{benzene}]}{k_{57}[\text{benzene}]+k_{58}[\text{toluene}]+k_{59}[\text{m-xylene}]} = 0$$

$$B02 = 0.75 - B01 = 0.75$$

(4) The variable stoichiometric coefficients appearing in reaction 64 were held constant throughout the course of our simulations. The value for B03 was chosen by first setting B03 = 0.55, its value at the beginning of the simulation. Next, a simulation was performed using $[B03]_i = 0.55$, during which the actual values of B03 were calculated at constant time intervals. Using these values, an average B03 was then calculated and the simulations repeated using this average value. Although this is an approximation, we feel that using an average value for B03 has only a minor effect on the reported results. For instance, the average value for B03 in the simulation with initial condition set 1 was 0.58, as compared with the initial value of 0.55.

PHOTOLYSIS RATES: The photolysis rates for reactions 3, 31, 22, and 24 were obtained by averaging over a zenith angle ranging from 30° to 60°. This was done because the NO_2 photolysis profile used in our simulations approximately represents a zenith angle distribution of 30°-60°. The data needed to calculate these averages were obtained from Table 23 of Part I. Rates for the remaining photolysis reactions were taken directly from Table 22 of Part I.

3.4.2 NO to NO_2 Conversion Results

As can be seen from Tables 4-6, the Atkinson et al. (1982) mechanism consistently predicts fewer overall NO to NO_2 conversions than the other lumped mechanisms. Notice also that the Atkinson et al. (1982)

results are very similar to those found by using the master mechanism. This is true for each of the three $[RHC]_o/[NO_x]_o$ ratios and is not unexpected since this mechanism bears the closest resemblance to the master mechanism. In particular, the numbers of NO to NO_2 conversions due to the alkanes, alkenes, and carbonyl compounds in this mechanism are very close to the values obtained with the master mechanism. The majority of the discrepancy between the two mechanisms involves the aromatic hydrocarbons. It can be seen from Tables 4-6 that the Atkinson et al (1982) mechanism consistently predicts fewer NO to NO_2 conversions due to the initial m-xylene than the master mechanism. The reasons for this discrepancy are:

(1) The Atkinson et al. (1982) mechanism assumes that 25 percent of the aromatic-OH-O_2 adducts react with NO to yield stable (?) nitrates. Based on the work of Atkinson et al. (1980) with toluene and the cresols, this 25 percent aromatic nitrate formation was the prevailing opinion at the time when this lumped mechanism was formulated. More recent investigations have led us to conclude that this nitrate formation probably does not occur to any significant extent (Leone and Seinfeld, 1983b). Thus, since the master mechanism does not include any nitrate formation, all of the aromatic-OH-O_2 adducts lead to ring opening, and therefore give rise to more NO to NO_2 conversions. When the assumed 25 percent nitrate formation is removed from the Atkinson et al. (1982) mechanism, the number of NO to NO_2 conversions attributed to m-xylene (using initial condition set 1) increases from 128 ppb to 172 ppb, much closer to the 170 ppb predicted by the master mechanism.

(2) By necessity, the representation of the chemistry of the conjugated-γ-dicarbonyls in the Atkinson et al. (1982) mechanism is considerably simplified relative to that in the explicit mechanism. In the course of condensing this chemistry a number of NO to NO_2 conversions are not accounted for. However, since the detailed chemistry of these compounds is not well understood, changes in the current version of the Atkinson et al. (1982) mechanism in this aspect of the chemistry can not really be justified at this time.

(3) At the time the Atkinson et al. (1982) mechanism was formulated, the photolysis rate of methyl glyoxal was estimated to be approximately, $k_{MGLY} \approx 0.15\ k_{NO_2}$. Recently, experimental data have indicated that the earlier estimates were about eight times too large (Plum et al., 1983), i.e. $k_{MGLY} \approx 0.019\ k_{NO_2}$. Since methyl glyoxal is an efficient source of radicals, this would indicate that the Atkinson et al. (1982) mechanism actually over-estimates the number of NO to NO_2 conversions attributable to methyl glyoxal. However, there is another difference between the methyl glyoxal chemistry contained in these two mechanisms. The Atkinson et al. (1982) mechanism assumes that the only methyl glyoxal photolysis pathway leads to $CH_3C(O)O_2\cdot$ and $HO_2\cdot$ radicals, while the master mechanism, based on Leone and Seinfeld (1983b),
contains two photolysis pathways,

$$\begin{aligned} CH_3C(O)CHO + h\nu &\xrightarrow{O_2} CH_3C(O)O_2\cdot + HO_2\cdot + CO && (65\%) \\ &\xrightarrow{O_2} CH_3O_2\cdot + HO_2\cdot + 2CO && (35\%) \end{aligned}$$

with their approximate percentages of occurrence indicated. Because a fraction of the peroxyacetyl radicals ($CH_3C(O)O_2\cdot$) lead to PAN, they do not effect as many NO to NO_2 conversions as do methoxy radicals ($CH_3O_2\cdot$). As an example, at a simulation time of 360 minutes using initial condition set 1, the fraction of these species leading to NO to NO_2 conversions are,

$$F_{CH_3O_2} = 2.52$$

$$F_{CH_3C(O)O_2} = 1.77$$

This difference somewhat counteracts the overestimated rate of methyl glyoxal photolysis.

The formaldehyde and acetaldehyde photolysis rates used in the Atkinson et al. (1982) mechanism are also out of date. Horowitz and Calvert (1982) have recently measured quantum yields for acetaldehyde, and have proposed updated values for formaldehyde photolysis. These latest recommendations lead to significantly different rates for the aldehyde photolysis steps. For example, when these updated aldehyde photolysis rates are substituted into the Atkinson et al. (1982) mechanism the amount of NO to NO_2 oxidations attributable to these aldehydes is reduced by about 10 percent. This results in even closer agreement with the master mechanism.

3.4.3 Possible Modifications to the Atkinson et al. (1982) Mechanism

Based on our analysis we would recommend the following modifications for the Atkinson et al. mechanism be considered.

(1) The 25 percent nitrate formation from the aromatic-OH-O_2 adduct reaction with NO be removed.

(2) The photolysis rate of methyl glyoxal be updated to the currently accepted value.

(3) The photolysis rates of formaldehyde and acetaldehyde be updated to reflect the quantum yields of Horowitz and Calvert (1982).

The results in Tables 5-7 support the view expressed by Atkinson et al. that a number of species can be eliminated from this mechanism without significantly affecting its ozone predictions. Our results show that eliminating propane, acetone, the two Criegee intermediates, glyoxal, and benzaldehyde and its oxidation products ($ARCO_3$, PBZN, and PHO_2) will have an almost imperceptable affect on the simulations. Additional species, such as benzene, can be eliminated with only very minor effects. This will bring the size of the mechanism more in line with those used in complex transport models. It should be noted however that small differences in ozone predictions can sometimes lead to relatively large differences in emission control estimates.

3.5 The Killus and Whitten (1982) Mechanism

3.5.1 Description of the Mechanism

The Killus and Whitten mechanism as used in this study, is shown in Table A.4 of the Appendix. The only change from the mechanism as listed in Table 8 of Part I is that the four chamber dependent reactions (reactions 76-79) have been removed.

PHOTOLYSIS RATES: The photolysis rates relative to NO_2 for each photolysis step (reactions 37, 38, 67, 71, and 73) were taken from Table 24 of Part I.

3.5.2 NO to NO_2 Conversion Results

Examination of Tables 4 to 6 shows that the Killus and Whitten mechanism (also known as the Carbon Bond Mechanism) always predicts more NO to NO_2 conversions than does the master mechanism. In most cases, the Killus and Whitten mechanism also predicts more NO to NO_2 conversions than do the other lumped mechanisms considered in this study. The counter species results also show that the greater "reactivity" of the Killus and Whitten mechanism is present in each of the organic classes. In our attempt to pinpoint the reasons for these differences, we first examine the treatment of aromatic hydrocarbon photooxidation in the Killus and Whitten mechanism.

The aromatic portion of the Killus and Whitten mechanism reflects much of what has been learned over the past five years regarding the photooxidation of aromatic hydrocarbons. However, one reason for the discrepancy between the predictions of this mechanism and those of the master mechanism is the new photolysis rate of methyl glyoxal. In the Killus and Whitten mechanism, methyl glyoxal and biacetyl are lumped together into the group DCRB. The photolysis rate assigned to DCRB is that of biacetyl, $k_{DCRB} = 0.04\ k_{NO_2}$. This rate is about twice as large as the recently measured value for methyl glyoxal, $k_{MGLY} = 0.019\ k_{NO_2}$.

Only methyl glyoxal is formed from the aromatic hydrocarbons appearing in initial condition sets 1-3. Thus, to investigate the effect of the photolysis rate of DCRB, we first modify the Killus and Whitten mechanism by reducing the photolysis rate of DCRB from $0.04\ k_{NO_2}$ to $0.019\ k_{NO_2}$. This change reduces the total number of NO to NO_2 conversions, in case 1, from 1007 ppb to 949 ppb.

Even after updating the DCRB photolysis rate, the aromatic portion of the Killus and Whitten mechanism still predicts significantly more NO to NO_2 conversions than does the master mechanism. Killus and Whitten use the species APRC to represent the remainder of the aromatic-OH-O_2 adduct after an α-dicarbonyl has been subtracted. In the master mechanism this species is assumed to be a stable conjugated-γ-dicarbonyl, such as cis-2-butene-1,4-dial, which can undergo reaction with OH radicals. In the Killus and Whitten mechanism, however, APRC is assumed to be a free radical intermediate that falls apart to yield two α-dicarbonyls:

$$\text{APRC} \rightarrow \text{DCRB} + \text{GLY} + \text{X}$$

$$\text{APRC} \rightarrow 2\text{GLY},$$

where DCRB is a methyl-substituted dicarbonyl, GLY is glyoxal, and X is a fictitious species used to maintain carbon-mass balance. Killus and Whitten then make the further assumption that the oxidation of GLY is similar to the oxidation of HCHO (represented as CARB in their mechanism) except that GLY produces an extra molecule of CO. Killus and Whitten, therefore, assume that GLY is equivalent to CARB + CO and the reactions of APRC then become:

$$\text{APRC} \xrightarrow{60} \text{DCRB} + \text{CARB} + \text{CO} + \text{X} \qquad k_{60} = 1\text{x}10^4 \ \text{min}^{-1}$$

$$\text{APRC} \xrightarrow{61} 2\text{CARB} + 2\text{CO} \qquad k_{61} = 1\text{x}10^4 \ \text{min}^{-1}$$

The authors state that experiments containing equal amounts of toluene and xylene are best modeled by assigning equal rates for the above pathways. We find that by representing APRC as a free radical rather than as a stable conjugated-γ-dicarbonyl, leads to a substantially more reactive system. Examination of Tables 4 to 6 shows that the number of NO to NO_2 conversions due to the APRC species in the Killus and Whitten mechanism is very high as compared to the number due to the conjugated-γ-dicarbonyls in the master mechanism. For example, in case 1, these species account for 93 ppb of NO to NO_2 conversions in the Killus and Whitten mechanism, while the master mechanism attributes only 47 ppb of conversions to these compounds.

If we modify the Killus and Whitten mechanism and treat APRC as a conjugated-γ-dicarbonyl instead of a free radical, the predictions of this mechanism are in much better agreement with those of the master mechanism. For instance, Atkinson et al. (1982) have condensed the chemistry of APRC into the four reaction steps shown below:

$$\mathrm{APRC + OH} \xrightarrow{61} \mathrm{EL} \qquad k_{61} = 4.4\mathrm{x}10^{4}\ \mathrm{ppm}^{-1}\text{-}\mathrm{min}^{-1}$$

$$\mathrm{EL + NO_2} \xrightarrow{62} \mathrm{LNO_2} \qquad k_{62} = 7.1\mathrm{x}10^{3}\ \mathrm{ppm}^{-1}\text{-}\mathrm{min}^{-1}$$

$$\mathrm{LNO_2} \xrightarrow{63} \mathrm{EL + NO_2} \qquad k_{63} = 2.2\mathrm{x}10^{-2}\ \mathrm{min}^{-1}$$

$$\mathrm{EL + NO} \xrightarrow{64} 3\mathrm{NO_2} - 2\mathrm{NO} + \alpha_3\mathrm{HO_2}\cdot + \alpha_3(\mathrm{CHO})_2 + \alpha_4\,\mathrm{CH_3CO_3}\cdot + \alpha_4\mathrm{CH_3C(O)CHO} + \alpha_3\mathrm{CO} \qquad k_{64} = 1.04\mathrm{x}10^{4}\ \mathrm{ppm}^{-1}\text{-}\mathrm{min}^{-1}$$

For the initial conditions used in our study, $\alpha_3 \approx \alpha_4 \approx 0.5$. Also, since the Killus and Whitten mechanism represents glyoxal ($(\mathrm{CHO})_2$) as GLY = HCHO + CO, reaction 64 shown above becomes, in carbon-bond form,

$$\mathrm{EL + NO} \xrightarrow{64} 3\mathrm{NO_2} - 2\mathrm{NO} + 0.5\ \mathrm{HO_2}\cdot + 0.5\ \mathrm{HCHO} + \mathrm{CO} + 0.5\ \mathrm{ACO3} + 0.5\ \mathrm{DCRB}$$

Substituting this reaction sequence for APRC into the Killus and Whitten mechanism, along with the updated DCRB photolysis rate, leads to the results shown in Table 7. By making these two changes, the overall reactivity of the system decreases appreciably, in that the total number of

TABLE 7

Counter Species Results for the Original and Modified Versions of the Killus and Whitten (1982) Mechanism Using Initial Condition Set 1 ($[RHC]_o/[NO_x]_o = 7.14$)

The Modifications Involved in These Results Deal with the DCRB Photolysis Rate, and the Reactions of the Lumped Group APRC.

	NO TO NO_2 CONVERSIONS (ppb)		
ORGANIC CLASS	MASTER MECHANISM	ORIGINAL KILLUS AND WHITTEN	MODIFIED KILLUS AND WHITTEN
Aromatics	185	314	222
Alkanes	157	321	257
Alkenes	181	224	208
Aldehydes and Ketones	68	148	147
TOTAL	591	1007	834

NO to NO_2 conversions has been reduced from 1007 ppb to 834 ppb, which is substantially closer to the 591 ppb predicted by the master mechanism. Although these changes primarily affect the aromatic hydrocarbon results, better agreement also results with the alkane and alkene portions.

One caveat should be made before we end our discussion of the Killus and Whitten treatment of aromatics chemistry. We are not suggesting that the Atkinson et al. treatment of the aromatic-OH-O_2 adduct be used in the Killus and Whitten mechanism. The fate of this adduct is unknown. It may react to form an α-dicarbonyl and a conjugated-γ-dicarbonyl as suggested by Atkinson et al., or it may cleave to form three α-dicarbonyls as suggested by Killus and Whitten. Thus, attempting to modify the chemistry of aromatics in the Killus and Whitten mechanism may not be justifiable. What is needed at this time is a better understanding of the atmospheric fate of aromatic hydrocarbons.

Even after the above two changes are made, the Killus and Whitten mechanism still predicts considerably more NO to NO_2 conversions than does the master mechanism. Examining the counter species results shown in Tables 4 to 7 shows that the carbonyl compounds in the Killus and Whitten mechanism are attributed many more conversions than in the master mechanism. There are a number of possible explanations for this behavior:

(1) The Killus and Whitten mechanism contains an inconsistency in the product stoichiometry for the radical producing photolysis pathway from the carbonyls (McRae et al., 1983). Without going into details, the Killus and Whitten mechanism uses the following expression for this reaction:

$$\text{CARB} + h\nu \xrightarrow{\frac{a+1}{2} k_f} (1+a)\ \text{HO}_2\cdot + (1-a)\text{MEO}_2 + \text{CO}$$

where

$$a = \frac{[\text{HCHO}]+[\text{ketones}]}{[\text{total carbonyls}]}$$

k_f = photolysis rate of formaldehyde to molecular products

As derived in Part I, this expression should read:

$$\text{CARB} = + h\nu \xrightarrow{\frac{a+1}{2} k_f} \frac{3a+1}{a+1}\ \text{HO}_2\cdot + \frac{1-a}{1+a}\ \text{MEO}_2 + \text{CO}$$

(2) In each of the mechanism listings sent to us by Killus and Whitten, the product stoichiometry for reaction 37 indicated that the parameter "a" (defined above) was assigned a value of 0.33, independent of the initial conditions. Apparently then, 0.33 is the default value for this parameter. However, if we calculate this parameter based on the initial conditions of our study, we find that $a \simeq 0.75$. Making this adjustment may be important in applying the Killus and Whitten mechanism to the conditions of our study.

(3) In formulating the carbonyl photolysis reaction mechanisms appearing in the Carbon Bond Mechanism, Killus and Whitten assumed that the two formaldehyde photolysis pathways proceed at equal rates, and that acetaldehyde photolyzes at about one-half of this rate. In other words, Killus and Whitten assume:

$$HCHO + h\nu \xrightarrow{k_a} H_2 + CO \tag{a}$$

$$HCHO + h\nu \xrightarrow[O_2]{k_b} 2HO_2\cdot + CO \tag{b}$$

$$CH_3CHO + h\nu \xrightarrow[O_2]{k_c} CH_3CO_3\cdot + HO_2\cdot \tag{c}$$

$$k_a = k_b = k_f$$

$$k_c = \frac{k_f}{2}$$

If we take the recent recommendations of Horowitz and Calvert (1982), and average these over a zenith angle range of 30° - 60°, we obtain the following approximate rates,

$$k_a \simeq 3.3x10^{-3}\ k_{NO_2}$$

$$k_b \approx 2.3x10^{-3}\ k_{NO_2}$$

$$k_c \approx 3x10^{-4}\ k_{NO_2}$$

Thus, a more accurate description of carbonyl photolysis in the Killus and Whitten mechanism might be obtained by choosing,

$$k_a = k_f = 3.3x10^{-3}\ min^{-1}$$

$$k_b = \frac{2}{3}\ k_f$$

$$k_c = \frac{1}{10}\ k_f$$

(4) The Killus and Whitten mechanism treats acetone as part paraffin and part carbonyl, i.e.,

acetone = 2PAR + 1CARB

Since acetone leads to very few NO to NO_2 conversions, we would suggest treating it as being unreactive, or as 3PAR.

We now examine the effect on the Killus and Whitten mechanism of adopting each of the above modifications. In each of the tests described below, the Killus and Whitten mechanism has been modified to include our first two suggestions concerning the DCRB photolysis rate and the reactions of APRC.

Correcting the Killus and Whitten treatment of CARB photolysis changes the radical producing pathway from,

$$\text{CARB} + h\nu \xrightarrow{0.67k_f} 1.33\ \text{HO}_2\cdot + 0.67\ \text{MEO}_2 + \text{CO} + 0.67\text{X}$$

to

$$\text{CARB} + h\nu \xrightarrow{0.67k_f} 1.5\ \text{HO}_2\cdot + 0.5\ \text{MEO}_2 + \text{CO} + 0.5\text{X}$$

Making this change in the Killus and Whitten mechanism reduces the total number of NO to NO_2 conversions by about 30 ppb, from 834 ppb to 802 ppb. Thus, at least for a = 0.33, this change has only a minor effect.

If we change the parameter "a" from its default value of 0.33 to its value at the beginning of our simulations, 0.75, the carbonyl photolysis pathways change from

$$\text{CARB} + h\nu \xrightarrow{0.33k_f} \text{H}_2 + \text{CO}$$

$$\xrightarrow{0.67k_f} 1.5\ \text{HO}_2\cdot + 0.5\ \text{MEO}_2 + \text{CO} + 0.5\text{X}$$

to

$$\text{CARB} + h\nu \xrightarrow{0.75k_f} \text{H}_2 + \text{CO}$$

$$\xrightarrow{0.875k_f} 1.86\ \text{HO}_2\cdot + 0.14\ \text{MEO}_2 + \text{CO} + 0.14\text{X}$$

The stoichiometric coefficients shown above are calculated using the corrected expression shown on page 53. Modifying the Killus and Whitten mechanism in this manner actually increases the number of NO to NO_2 conversions from 802 ppb to 847 ppb. This change does not reflect a problem with the Killus and Whitten (1982) mechanism, but merely represents the adaptation of the mechanism to the conditions of our study.

Choosing $k_a = \frac{3}{2} k_b = 10k_c$ and assuming a = 0.75 results in,

$$\mathrm{CARB} + h\nu \xrightarrow{0.75k_f} H_2 + CO$$

$$\xrightarrow{0.525k_f} 1.95\ HO_2\cdot + 0.048\ MEO_2 + CO + 0.048X$$

In contrast, using the modified expression on page 53 with a = 0.75 and Killus and Whitten's relations $k_a = k_b = 2k_c$ gives rise to,

$$\mathrm{CARB} + h\nu \xrightarrow{0.75k_f} H_2 + CO$$

$$\xrightarrow{0.875k_f} 1.86\ HO_2\cdot + 0.14\ MEO_2 + CO + 0.14X$$

Also, we now use $k_f = 3.3\mathrm{x}10^{-3}\ k_{NO_2}$ instead of the Killus and Whitten value of $k_f = 3.0\mathrm{x}10^{-3}\ k_{NO_2}$. This new photolysis rate is consistent with the assumption of $k_a = \frac{3}{2} k_b = 10k_c = k_f$.

Making the above modifications to the Killus and Whitten mechanism has a marked affect on its predictions. The total number of NO to NO_2 conversions is reduced from 847 ppb to 659 ppb, which is much closer to the 591 ppb predicted by the master mechanism. Thus, we feel that updating the current treatment of carbonyl photolysis in the Killus and Whitten mechanism should be considered in future versions of that mechanism.

The fourth and final possible modification listed above is to treat acetone as an unreactive species, rather than as part paraffin and part carbonyl. Examination of the counter species results in Tables 4 to 6 shows that acetone accounts for very few NO to NO_2 conversions in the master mechanisms. For example, with initial condition set 1, the master mechanism attributes only five conversions to the initial acetone. In contrast, the Killus and Whitten mechanism derives 55 ppb of conversions from the initially present acetone, in this same case. If, in addition to the modifications described above, we treat acetone as an unreactive species, the counter species results for the Killus and Whitten mechanism agree very well with those of the master mechanism. These results are shown in Table 8.

3.5.3 Possible Modifications to the Killus and Whitten (1982) Mechanism

Based on our analysis we recommend the following modifications in future versions of the Killus and Whitten mechanism be considered:

(1) The photolysis rates of the DCRB and CARB species be updated to reflect the currently accepted values.

(2) Alternative reaction sequences be developed for the lumped group APRC.

(3) Acetone be classified as an unreactive compound.

TABLE 8

Counter Species Results for the Original and Modified Versions of the Killus and Whitten (1982) Mechanism Using Initial Condition Set 1 ($[RHC]_o/[NO_x]_o = 7.14$)

The Modified Results were Obtained by Employing all of the Changes Discussed in Section 3.5.2

	NO TO NO_2 CONVERSIONS (ppb)		
ORGANIC CLASS	MASTER MECHANISM	ORIGINAL KILLUS AND WHITTEN	MODIFIED KILLUS AND WHITTEN
Aromatics	185	314	201
Alkanes	157	321	187
Alkenes	181	224	146
Aldehydes and Ketones	68	148	64
TOTAL	591	1007	598

3.6 The Demerjian (1982) Mechanism

3.6.1 Description of the Mechanism

A listing of the Demerjian (1982) mechanism as used in this study can be found in Table A6 of the Appendix. A number of lumped rate constants have been updated from the values listed in Table 4 of Part I (McRae et al., 1983). The reactions involved are numbers 26 through 31, 39, 44, and 45. These changes were made in response to our conversation with Ken Demerjian.

This mechanism uses molar weighted averaging to determine the lumped rate constants. For instance, initial condition set 1 contains 20 ppb of initial toluene and 50 ppb of initial m-xylene, and no other aromatics. In this case the rate constant employed in the Demerjian mechanism for the aromatic (HC4) plus OH reaction is

$$k_{HC4+OH} = \frac{20\, k_{toluene\ +\ OH} + 50\, k_{m\text{-}xylene\ +\ OH}}{20 + 50}$$

Since the initial conditions are specified for a given simulation, the only information needed to calculate the lumped rate constants is the rates for the individual hydrocarbon reactions. Demerjian indicated to us that he wanted the most up-to-date rates used in these calculations. Thus, the rates for reactions 26 through 29, 31, 39, and 45 were calculated using the individual hydrocarbon reaction rate constants recommended by Atkinson and Lloyd (1983). These are the same rates employed in the master mechanism. We note that substituting these updated rate constants could effect the original evaluation of the Demerjian mechanism using smog chamber data.

PHOTOLYSIS RATES: Rates for the photolysis reactions of O_3, HONO, and H_2O_2 (reactions 5, 12, and 25, respectively) were obtained in the same manner as with the Atkinson et al. (1982) mechanism. That is, these rates were obtained by averaging over a zenith angle range of 30° to 60°. The data needed to calculate these averages were obtained from Demerjian et al. (1980). There are two additional photolysis reactions included in the Demerjian mechanism, reactions 30 and 44. Reaction 44 represents the photolysis of formaldehyde to stable products, and reaction 30 describes the photolysis of both formaldehyde and acetaldehyde to radical products,

$$\mathrm{HC3} + h\nu \xrightarrow{k_{30}} 0.5\ \mathrm{RO_2} + 1.5\ \mathrm{HO_2}\cdot + \mathrm{CO}$$

$$\xrightarrow{k_{44}} \mathrm{CO} + \mathrm{H_2}$$

The photolysis rates for these reactions were calculated as follows. First, the rates for the three explicit photolysis reactions were calculated by averaging over zenith angles as described above. Next, a correction factor was used to take into account the more recent quantum yields of Horowitz and Calvert (1982). These correction factors are shown below:

$$\mathrm{HCHO} + h\nu \xrightarrow{k_1} \mathrm{H}\cdot + \mathrm{H\dot{C}O} \qquad k_A = 0.714\ k_1$$

$$\mathrm{HCHO} + h\nu \xrightarrow{k_2} \mathrm{H_2} + \mathrm{CO} \qquad k_B = 0.676\ k_2$$

$$\mathrm{CH_3CHO} + h\nu \xrightarrow{k_3} \cdot\mathrm{CH_3} + \mathrm{H\dot{C}O} \qquad k_C = 0.444\ k_3$$

Finally, mole-weighted rate constants are calculated using the above rates and the initial amounts of formaldehyde and acetaldehyde,

$$k_{30} = \frac{k_A[\mathrm{HCHO}]_o + k_C[\mathrm{CH_3CHO}]_o}{[\mathrm{HCHO}]_o + [\mathrm{CH_3CHO}]_o}$$

$$k_{44} = \frac{[\mathrm{HCHO}]_o}{[\mathrm{HCHO}]_o + [\mathrm{CH_3CHO}]_o}\ k_B$$

3.6.2 NO to NO_2 Conversion Results

The Demerjian mechanism consistently predicts a greater number of NO to NO_2 conversions than does the master mechanism. Although the discrepancies between the Demerjian and master mechanisms occur in all four organic classes, the greatest differences occur with the alkenes. For example, with initial condition set 1 the Demerjian mechanism predicts that the alkenes will lead to 346 ppb of NO to NO_2 conversions, 165 ppb more than predicted by the master mechanism. In the Demerjian treatment of alkene mechanisms ethene is not treated separately from the other olefins. Ethene reacts at a significantly slower rate than the higher alkenes, and in addition, its reaction products do not lead to as many NO to NO_2 conversions as do those from the higher alkenes. The lower reactivity of ethene is partially taken into account by the molar weighting used to obtain the lumped rate constants. However, this weighting is most effective early in the simulation. At later times the alkene distribution is much different from its initial form.

If we modify the Demerjian mechanism by simply separating ethene from the remaining alkenes, the results are in much better agreement with those of the master mechanism. In performing this test only the rate constants were changed, the reactants and products remained the same. The ethene reactions were assigned rates specific for ethene, while the lumped group HC1 (alkenes) was given rates determined by molar weighted averaging with propene and tr-2-butene. The results obtained with this modified Demerjian mechanism are shown in Table 9. Using initial condition set 1,

TABLE 9

Results of Separating Ethylene from the Remaining Olefins in the Demerjian (1982) Mechanism

These Results were Obtained Using Initial Condition Set 1
($[RHC]_o/[NO_x]_o = 7.14$)

	NO TO NO_2 CONVERSIONS (ppb)		
ORGANIC CLASS	MASTER MECHANISM	ORIGINAL DEMERJIAN	MODIFIED DEMERJIAN
Aromatics	185	239	206
Alkanes	157	239	177
Alkenes	181	346	254
Aldehydes and Ketones	68	98	85
TOTAL	591	922	722

we find that the number of NO to NO_2 conversions attributable to ethene is reduced from 182 ppb to 88 ppb. At the same time, the number of conversions due to propene and tr-2-butene remains virtually unchanged. Separating ethene from the remaining olefins also has a substantial effect on the number of NO to NO_2 conversions due to the alkanes and aromatics. In fact, the total number of NO to NO_2 conversions is reduced from 922 ppb to 722 ppb. These differences can be explained by examining the radical concentrations present in each simulation. The rate of radical production is much slower in the case where ethene is treated explicitly.

Even after ethene is separated from the remaining olefins, the modified Demerjian mechanism still predicts 131 ppb, or 22 percent more NO to NO_2 conversions than does the master mechanism. This represents, in our view, a difference that is large enough to warrant investigation. It is important to remember that these discrepancies occur even though the same individual hydrocarbon rate constants have been used in both mechanisms. That leaves two possible explanations for the greater reactivity of the Demerjian mechanism:

(1) The molar weighted averaging technique gives rise to lumped rate constants that are too large. We expect that this is true since the more reactive species are depleted faster. Thus, the species with the larger rate constants are weighted too heavily at all times except at the beginning of the simulations. The fact that the Demerjian and master mechanisms are in much closer agreement when initial condition set 3 is used also indicates that this may be the problem. In that case ($[RHC]_o/[NO_x]_o = 1.79$), a much smaller amount of the initial hydrocarbons is consumed over the course of the

photooxidation. Thus, the lumped rate constants based on initial conditions apply for a much longer period of the simulation than for initial condition set 1.

(2) The actual mechanism is incorrect. For example, Killus and Whitten (1983) have found that assuming a yield of two peroxy radicals for the olefin plus ozone reaction introduces significant error into the Demerjian mechanism.

In order to determine which explanation is more responsible for the observed behavior, the Demerjian mechanism was modified as follows. First, remember that as part of the counter species analysis, each initially present hydrocarbon has a specific reaction written for itself. For example, we have two reactions for HC4 + OH present in the Demerjian mechanism used in the counter species analysis:

$$\mathrm{HC41 + OH \xrightarrow{k} R2O2 + 2HC3 + CO} \qquad k = 2.7\times10^{4}\ \mathrm{ppm}^{-1}\ \mathrm{min}^{-1}$$

$$\mathrm{HC42 + OH \xrightarrow{k} R2O2 + 2HC3 + CO} \qquad k = 2.7\times10^{4}\ \mathrm{ppm}^{-1}\ \mathrm{min}^{-1}$$

The first reaction represents toluene chemistry, and the second m-xylene chemistry. Similarly, there are three HC1 + O_3 reactions, one each for ethene, propene, and tr-2-butene. Thus, we can easily substitute the individual rate constants for each hydrocarbon. In this way, we are eliminating the problem of specifying a lumped rate constant.

The results obtained with this twice-modified Demerjian mechanism show that about one-half of the 131 ppb difference from the master mechanism is eliminated. The total number of predicted NO to NO_2 conversions is reduced from 722 ppb to 663 ppb, in better agreement with the 591 ppb predicted by the master mechanism. The largest area of improvement is with the aromatic hydrocarbons. Thus, in this case, molar-weighted averaging with initial conditions is responsible for a significant fraction of the observed difference in reactivity between the Demerjian and master mechanisms.

Before summarizing our results concerning the Demerjian mechanism, we would like to discuss one additional aspect. We feel that it is important to note that the lumped group representing the carbonyls HC3, is present as a product in a large number of reactions. Since HC3 is a source of radicals, we might expect that the predictions of this mechanism would be especially sensitive to any inaccuracies in the photolysis rates of formaldehyde and acetaldehyde. To test this assumption, we modified the Demerjian mechanism as follows:

(1) Ethene was treated separately from the other olefins.

(2) The rate constants for the two HC3 photolysis steps were calculated using the Demerjian et al. (1980) rates for formaldehyde and acetaldehyde. In each of the earlier tests, these values were modified based on the work of Horowitz and Calvert (1982).

We can compare the results obtained with this mechanism to those obtained with the Demerjian mechanism in which the only modification is an explicit treatment of ethene chemistry. This comparison shows that the old photolysis rates lead to a 17 percent increase (722 ppb to 842 ppb) in the predicted number of NO to NO_2 conversions when initial conditions set 1 is used. In contrast, the Atkinson et al. (1982) "semi-lumped" mechanism, which contains more species, shows only a 10 percent difference when the same photolysis rate changes are made. We note that this sensitivity to the aldehyde photolysis rates is not peculiar to the Demerjian mechanism, but is also present in some of the other lumped mechanisms in this study.

3.6.3 Possible Modifications to the Demerjian (1982) Mechanism

In summary, we recommend the following modifications in future versions of the Demerjian mechanism be considered:

(1) Ethene be treated separately from the other alkenes.

(2) The use of molar weighted averages based on initial conditions be thoroughly investigated with an aim toward possible modification.

(3) An improved treatment of aromatic chemistry be tested when future versions of this mechanism are developed. A great deal has been learned about aromatic hydrocarbon photooxidation since this mechanism was first formulated and this information can be incorporated.

(4) Acetone be treated as an unreactive species instead of as an alkane.

3.7 The McRae and Seinfeld (1983) Mechanism

3.7.1 Description of the Mechanism

The McRae and Seinfeld (1983) Mechanism as used in this study is shown in Table A.8 of the Appendix. A number of changes have been made from the mechanism shown in Table 10 of Part I (McRae et al., 1983). First, reaction 49, the O_3 wall loss term, has been eliminated. Also, the rate constant for reaction 50 has been changed from 8.28×10^3 to 7.45×10^3. This new value applies at an H_2O concentration of 15,500 ppm, the amount of water vapor present in our simulations. Rate constants for reactions involving the lumped species were calculated using molar-weighted averaging based on the initial hydrocarbon distribution, as in the Demerjian (1982) mechanism. The individual rate constants used in this calculation were taken from McRae et al. (1982a). These explicit rates are close to those contained in the master mechanism. The reactions whose rate constants were calculated in this fashion are reactions 25, and 28 through 33.

PHOTOLYSIS RATES: The photolysis reactions appearing in the McRae and Seinfeld (1983) mechanism are reactions 20, 21, 22, 24, 35, and 51. The rates for these steps were taken from McRae et al. (1982a). They represent averages over daylight hours for Los Angeles, California.

3.7.2 NO to NO_2 Conversion Results

In each of the three test cases, the McRae and Seinfeld mechanism predicts significantly more NO to NO_2 conversions than does the master mechanism. In addition, the number of conversions predicted by this mechanism falls somewhere in the middle of the values predicted by the other lumped mechanisms. Examining Tables 4 to 6 shows that the predicted higher reactivity, relative to the master mechanism, occurs in each of the organic classes. The McRae and Seinfeld mechanism uses molar-weighted averaging based on initial concentrations to establish the lumped rate constants. From our analysis of the Demerjian mechanism, we are aware that this technique can lead to an overestimate of the total number of NO to NO_2 conversions. However, we expect that assigning each hydrocarbon its individual rate constant will only cause a small change in the predictions of this mechanism, similar in magnitude to the changes observed with the Demerjian mechanism. If we modify the McRae and Seinfeld mechanism to eliminate the molar-weighted averaging, we find that the total number of NO to NO_2 conversions predicted using initial condition set 1 is reduced from 813 ppb to 783 ppb, accounting for only a small percentage of the observed discrepancy from the predictions of the master mechanism.

Examining the counter species results for the McRae and Seinfeld mechanism more closely shows that the created carbonyl compounds are responsible for a large number of NO to NO_2 conversions. This is not unexpected since the lumped group RCHO is used to represent a wide variety of species. However, we also notice that the McRae and Seinfeld mechanism employs a large photolysis rate for these carbonyls. For example, the photolysis rate for RCHO used in this mechanism, $k_{RCHO} = 4.28 \times 10^{-3}\ k_{NO_2}$ is based on the upper limit reported by Demerjian et al. (1980) for acetaldehyde. This rate is $\sim$17 times faster than the currently accepted rate of $2.6 \times 10^{-4}\ k_{NO_2}$ (Horowitz and Calvert, 1982). The formaldehyde photolysis rates used by McRae and Seinfeld are also higher than the most recent values. Since the predictions of lumped mechanisms are particularly sensitive to these aldehyde photolysis rates, we expect that the predictions of this mechanism will change significantly if these photolysis rates are updated.

The counter species results obtained with a modified McRae and Seinfeld mechanism, having updated carbonyl photolysis rates and initial condition set 1, are given in Table 10. Also shown are the results for the original McRae and Seinfeld mechanism, and those for the master mechanism. Updating the aldehyde photolysis rates has an enormous effect on the performance of the McRae and Seinfeld mechanism. The total number of NO to NO_2 conversions has been reduced from 812 ppb to 426 ppb. This modified McRae and Seinfeld mechanism actually predicts fewer NO to NO_2 conversions than the master mechanism. These results illustrate the problems that can occur when rate constants are updated in lumped mechanisms. Including the updated photolysis rates renders the predictions of this mechanism

TABLE 10

Result of Updating the Aldehyde Photolysis Rates in the McRae and Seinfeld (1983) Mechanism

Results apply with Initial Condition Set 1
($[RHC]_o/[NO_x]_o = 7.14$)

	NO TO NO_2 CONVERSIONS (ppb)		
ORGANIC CLASS	MASTER MECHANISM	ORIGINAL MCRAE AND SEINFELD	MODIFIED MCRAE AND SEINFELD
Aromatics	185	253	112
Alkanes	157	260	105
Alkenes	181	202	140
Aldehydes and Ketones	68	97	69
TOTAL	591	812	426

useless until its performance has been thoroughly reevaluated. On the other hand, using a mechanism with an aldehyde photolysis rate constant 17 times larger than its currently recommended value is not very appealing, in spite of the fact that this out of date version has been tested with smog chamber data.

Another problem with the McRae and Seinfeld mechanism arises from its simplified treatment of aromatic chemistry. Little was known regarding aromatic hydrocarbon photooxidation at the time this mechanism was formulated. Incorporating a few additional species, such as methyl glyoxal, into a new treatment of aromatic chemistry should improve its performance.

One possible aromatic reaction mechanism for the McRae and Seinfeld mechanism is:

$$\begin{array}{lll}
\mathrm{ARO} + \mathrm{OH} \xrightarrow{1} 0.25\ \mathrm{HO_2\cdot} + 0.75\ \mathrm{ADD} & & k_1 = 2.76\mathrm{x}10^4\ \mathrm{ppm}^{-1}\text{-}\mathrm{min}^{-1} \\
\mathrm{ADD} + \mathrm{NO} \xrightarrow{2} \mathrm{NO_2} + \mathrm{HO_2\cdot} + \mathrm{MGLY} & & k_2 = 1.04\mathrm{x}10^4\ \mathrm{ppm}^{-1}\text{-}\mathrm{min}^{-1} \\
\mathrm{MGLY} + h\nu \xrightarrow{3} 0.65\ \mathrm{RCO_3} + 0.35\ \mathrm{RO_2} & & k_3 = 0.019\ k_{\mathrm{NO_2}} \\
\qquad + \mathrm{HO_2\cdot} + 1.35\ \mathrm{CO} & & \\
\mathrm{MGLY} + \mathrm{OH} \xrightarrow{4} \mathrm{RCO_3} + \mathrm{CO} & & k_4 = 2.5\mathrm{x}10^4\ \mathrm{ppm}^{-1}\text{-}\mathrm{min}^{-1}
\end{array}$$

This mechanism ignores many of the features of aromatic hydrocarbon photooxidation such as OH-abstraction pathways, cresol and dimethyl phenol formation, and the formation of conjugated-γ-dicarbonyls. However, it does provide a more up-to-date description of aromatic chemistry than does the current McRae and Seinfeld treatment, at the expense of only one additional non-steady-state species.

The results of substituting the above reaction sequence into the McRae and Seinfeld mechanism, along with the updated aldehyde photolysis rates discussed earlier, are shown in Table 11. The total number of NO to NO_2 conversions is increased from 426 ppb (see Table 11) to 514 ppb. This is much closer to the 591 ppb predicted by the master mechanism. Of course, we are not suggesting that the above reactions be adopted, as is, into the McRae and Seinfeld mechanism. We are merely pointing out that the current treatment of aromatic chemistry is not very representative of actual aromatic chemistry.

3.7.3 Possible Modifications to the McRae and Seinfeld (1982) Mechanism

In future versions of this mechanism, our major recommendations would include revising the out-of-date aldehyde photolysis rates, and developing a new treatment of aromatic chemistry. An improved treatment of aromatic chemistry will probably result in the addition of one or two new non-steady-state species.

3.8 The Penner and Walton (1982) Mechanism

3.8.1 Description of the Mechanism

The Penner and Walton (1982) mechanism as used in this study is shown in Table A.10 of the Appendix. Two changes have been made from the mechanism shown in Table 12 of Part I. First, the photolysis rates used in this mechanism were calculated using detailed tabulations furnished by

TABLE 11

Result of Replacing the Aromatic Reaction and Updating the Aldehyde Photolysis Rates in the McRae and Seinfeld (1983) Mechanism

These Results were Obtained Using Initial Condition Set 1.
($[RHC]_o/[NO_x]_o = 7.14$)

ORGANIC CLASS	NO TO NO_2 CONVERSIONS (ppb) MASTER MECHANISM	 ORIGINAL MCRAE AND SEINFELD	 MODIFIED MCRAE AND SEINFELD
Aromatics	185	253	139
Alkanes	157	260	158
Alkenes	181	202	139
Aldehydes and Ketones	68	97	78
TOTAL	591	812	514

Joyce Penner. These rates represent averages over a zenith angle range of 30 to 60 degrees as was described earlier for the Atkinson et al. (1982) and Demerjian (1982) mechanisms. Second, the two wall loss terms, reactions 62 and 71, have been removed.

Before discussing the counter species results, we first present a brief discussion of reactivity weighting, a concept that is unique to the Penner and Walton mechanism. Reactivity weighting is used in the Penner and Walton mechanism to determine the initial conditions for a given simulation. This method is roughly equivalent to the molar weighting of individual rate constants that is used in the Demerjian and McRae and Seinfeld mechanisms. The technique works as follows. First, a representative species for each class of hydrocarbons is chosen. For example, propene is the representative alkene and n-butane is the representative alkane. Next, the reactions involving lumped groups are assigned rates that are equal to the rate for the reaction of the representative species of that group. For instance, the rate assigned for the alkane plus OH reaction (HC2+OH) is equal to the rate of the n-butane plus OH reaction. To take into account differences in reactivity among the members of a class, the initial concentration of each organic is weighted by its reaction rate relative to that of the representative species. Consider initial condition set 1 which contains initially 15 ppb of propane, 190 ppb of n-butane, and 110 ppb of 2,3-dimethylbutane. Since n-butane is the representative alkane, the initial conditions specified with the Penner and Walton mechanism become:

$$[\text{propane}]_o = \frac{15\, k_{\text{propane + OH}}}{k_{\text{n-butane + OH}}} \qquad [\text{butane}]_o = 190$$

$$[\text{2,3-dimethylbutane}]_o = \frac{110\, k_{\text{2,3-dimethylbutane + OH}}}{k_{\text{n-butane + OH}}}$$

In order to calculate the initial conditions, the individual OH rate constants for each hydrocarbon comprising the class are needed. Joyce Penner indicated to us that she wanted the most up-to-date rate constants used in these calculations. Thus, the rate constants recommended by Atkinson and Lloyd (1983), which are employed in the master mechanism, were used in these calculations. However, the rate constants for the representative hydrocarbons that appear in the mechanism are those furnished to us by Joyce Penner. These rate constants are close to those recommended by Atkinson and Lloyd (1983).

3.8.2 NO to NO_2 Conversion Results

The performance of the Penner and Walton mechanism varies between the three test cases considered in this study. With initial conditions sets 1 and 2 ($[RHC]_o/[NO_x]_o = 7.14$ and 28.6, respectively), the Penner and Walton mechanism predicts significantly more NO to NO_2 conversions than does the master mechanism. However, with initial condition set 3 ($[RHC]_o/[NO_x]_o = 1.79$), there is excellent agreement between these two mechanisms. One reason for this behavior is the reactivity weighting of initial conditions used in the Penner and Walton mechanism. We will discuss the reactivity weighting technique in detail later in this section.

Examining Tables 4 to 6 shows that the greatest discrepancy between the master mechanism and the Penner and Walton mechanism occurs with the alkenes. Since the alkenes are a major source of aldehydes, (HC4), we suspect that out-of-date aldehyde photolysis rates used in the Penner and Walton mechanism may be responsible for a large portion of this discrepancy. In addition, the methyl glyoxal photolysis rate used in this mechanism is a factor of approximately 2.5 times larger than the recently measured rate (Plum et al., 1983). The results of incorporating these changes into the Penner and Walton mechanism are shown in Table 12. The predicted total number of NO to NO_2 conversions in case 1 has been drastically reduced from 846 ppb to 540 ppb. This is actually ∿50 ppb fewer NO to NO_2 conversions than predicted by the master mechanism. The Penner and Walton mechanism now agrees very well with the master mechanism for case 2, but predicts many fewer NO to NO_2 conversions in case 3. Thus, we once again see the importance of the radical producing photolysis steps. Also, it is important to note that even though the total number of conversions predicted by the Penner and Walton mechanism agrees very well with the master mechanism in case 2, the numbers for each hydrocarbon class differ substantially. This is a cause for concern, since changing the initial hydrocarbon distributions could result in drastically different performance relative to the master mechanism.

The Penner and Walton mechanism, like the Demerjian mechanism, does not separate ethene from the higher olefins. Earlier, we noted that this led the Demerjian mechanism to overpredict the number of NO to NO_2 conversions attributable to the alkenes. One might expect that a similar effect is taking place with the Penner and Walton mechanism. However, when the Penner and Walton mechanism is modified so that ethene is treated separately, the predicted number of NO to NO_2 conversions is virtually unchanged. The

TABLE 12

Results Obtained by Updating the Methyl Glyoxal and Aldehyde Photolysis Rates in the Penner and Walton (1982) Mechanism

ORGANIC CLASS	NO TO NO_2 CONVERSIONS (ppb)		
	MASTER MECHANISM	ORIGINAL PENNER AND WALTON	MODIFIED PENNER AND WALTON
INITIAL CONDITION SET 1 ($[RHC]_o/[NO_x]_o$ = 7.14):			
Aromatics	185	217	135
Alkanes	157	218	112
Alkenes	181	327	230
Aldehydes and Ketones	68	84	70
TOTAL	591	846	540
INITIAL CONDITION SET 2 ($[RHC]_o/[NO_x]_o$ = 28.6):			
Aromatics	175	188	147
Alkanes	197	179	148
Alkenes	232	349	300
Aldehydes and Ketones	60	70	55
TOTAL	664	786	650
INITIAL CONDITION SET 3 ($[RHC]_o/[NO_x]_o$ = 1.79):			
Aromatics	69	53	30
Alkanes	41	32	20
Alkenes	65	89	54
Aldehydes and Ketones	34	43	24
TOTAL	209	217	128

major effect of this modification is to increase slightly the number of conversions attributable to ethene.

The different behavior of these two mechanisms arises because of the different methods used to obtain the lumped rate constants. The Demerjian mechanism uses molar-weighted averaging of the individual rate constants. The Penner and Walton mechanism solves this problem indirectly by using the OH reactivity technique discussed earlier. This technique has several advantages over the molar weighting method used by Demerjian and McRae and Seinfeld. First, as we discussed earlier, the molar-weighting calculations lead to lumped rate constants that are too large for most of the simulation. Reactivity weighting does not lead to this problem. Secondly, reactivity weighting has the advantage of not requiring a new set of reaction rates each time the initial hydrocarbon distribution, or emission inventory, is changed.

One problem with this technique arises when large ozone concentrations are achieved. In this case, a significant fraction of the total alkene loss rate occurs through reaction with ozone. Since the initial alkene concentrations are determined using relative OH-reactivities, alkene decay may not be accurately represented in this situation. However, our tests indicate that this is not a serious problem. Nevertheless, there is an additional, and potentially more critical problem with the reactivity weighting technique. It is this potential problem that is reponsible for the change in performance of the Penner and Walton mechanism as the $[RHC]_o/[NO_x]_o$ ratio changes. This problem is best illustrated with an extreme example.

Let us assume that there are three hydrocarbons that we wish to group into a single lumped class. Each hydrocarbon is present in about the same concentration, say 5 ppb. Also assume that the OH-reaction rates of these three hydrocarbons are 0.1, 10, and 1000 in consistent units. Finally, assume that species 2 is the representative species for this lumped group. If we apply the reactivity weighting technique of Penner and Walton to this situation, we arrive at the following initial conditions:

Species	k_{OH}	actual initial concentration	reactivity weighted initial concentration
1	0.1	5	0.05
2	10	5	5
3	1000	5	500

The total initial concentration of this lumped group used in the Penner and Walton mechanism is 505.05 ppb, as opposed to the 15 ppb which would be used in an explicit mechanism. Thus, the potential for converting NO to NO_2 is much greater when reactivity weighting is used. Of course, species 3 is assigned a rate constant that is 100 times slower than its explicit rate, and the number of NO to NO_2 conversions is ultimately limited by NO_x availability. However, in cases where sufficient NO_x is present, and the opportunity exists for large amounts of primary hydrocarbon removal, this technique will over-predict the total number of NO to NO_2 conversions.

The above example is an extreme case, but the same effects occur in the test cases used in this study. Based on the above reasoning, we would expect that as we change from initial condition set 3 to initial condition set 1, the Penner and Walton mechanism would predict more NO to NO_2 conversions relative to the master mechanism. Examination of Tables 4 to 6, and Table 12 shows this to be the case. This same effect occurs as we change from initial condition set 3 to initial condition set 2, except that the disappearance of NO_x early in case 2 limits the number of conversions. Another way to illustrate this point is to modify the Penner and Walton mechanism by treating ethene and 2-butene explicitly. As expected, one finds that the number of conversions attributed to ethene increases, while those due to 2-butene decreases. However, the increase in the number of conversions attributable to 2-butene is seven times as large as the decrease in conversions due to ethene (for initial condition set 1). Since the conversions due to propene remain about the same, the total number of conversions due to the alkenes is much greater when reactivity weighting is applied.

3.8.3 Possible Modifications to the Penner and Walton (1982) Mechanism

Thus, we conclude that updating the aldehyde and methyl glyoxal photolysis rates renders the Penner and Walton mechanism very unreactive as compared to both the master mechanism and the other lumped mechanisms. However, the reactivity weighting of initial conditions (which can be considered a part of this mechanism) can result in large increases in the overall reactivity of the system. Thus, depending on the conditions, the actual predicted reactivity may or may not end up being in agreement with the other lumped mechanisms. Since reactivity weighting has such an important effect on the performance of this mechanism, we will not give any further suggestions for changes in the chemistry. We instead suggest that a thorough study of the reactivity weighting technique be carried out.

3.9 The Dodge (1977) Mechanism

3.9.1 Description of the Mechanism

Table A.12 of the Appendix contains a listing of the Dodge (1977) mechanism as used in this study. There are no changes from the mechanism shown in Table 6 of Part I (McRae et al. (1983)). The photolysis rates used in this mechanism are based on Demerjian et al. (1980).

Before discussing the results for the Dodge mechanism, we note that this mechanism does not rely on the use of a detailed initial hydrocarbon distribution such as the one used in this study. Instead, the total reactive hydrocarbon concentration is calculated and then represented as 75 percent n-butane and 25 percent propene. The only organics contained in the Dodge reaction mechanism are these two hydrocarbons plus four aldehydes. Thus, each of the organics in initial condition sets 1 through 3 are represented in this mechanism by n-butane, propene, formaldehyde, and acetaldehyde.

3.9.2 NO to NO_2 Conversion Results

In each of the three test cases, the Dodge (1977) mechanism predicts more NO to NO_2 conversions than does the master mechanism. This mechanism also generally predicts more conversions than do the other lumped mechanisms. However, as pointed out in Section 3.3, the relationship between NO to NO_2 conversions and O_3 concentration in the Dodge (1977) mechanism is much different from that in the other lumped mechanisms. For example, in case 2, the Dodge (1977) mechanism predicts 40 ppb more of NO to NO_2 conversions than does the master mechanism. However, in this same case the Dodge (1977) mechanism predicts 115 ppb less ozone. Thus the counter species results, which were so useful when comparing the other lumped mechanisms, are not as meaningful when examining the Dodge (1977) mechanism.

Since the Dodge (1977) mechanism was formulated several years ago, it contains many out of date rate constants. Updating these rate constants would, without doubt, significantly change the predictions of this mechanism. As an example, when the reactions involving PAN in the Dodge (1977) mechanism are updated, the maximum O_3 concentration obtained with initial condition set 1 is reduced from 470 ppb to 280 ppb. Thus, it is clear that these old rate constants cannot be updated without a complete reevaluation of the entire mechanism.

Figures 4, 5, and 6 show that the Dodge (1977) mechanism, relative to the other mechanisms, derives a much higher percentage of its NO to NO_2 conversions from the alkanes. Since the initial hydrocarbon distributions used here contain a majority of alkanes, they give rise to the majority of the conversions predicted by the Dodge (1977) mechanism.

The results in Figures 4, 5, and 6 also show that the Dodge (1977) mechanism does a fair job of predicting the number of NO to NO_2 conversions attributable to the aromatics. This is true in spite of the fact that aromatic hydrocarbons are not included in the mechanism. Our current knowledge of atmospheric aromatic hydrocarbon chemistry indicates that the number of NO to NO_2 conversions due to the aromatics falls somewhere in between those for the alkanes and alkenes. Since the Dodge (1977) mechanism splits the total hydrocarbon measurements on a mass basis into 75 percent n-butane and 25 percent propene, it is not unreasonable to expect that this mechanism is capable of adequately representing aromatic chemistry.

In summary, we find it difficult to compare the Dodge (1977) mechanism to the other lumped mechanisms. This difficulty arises because the counter species results for this mechanism cannot be compared to those for the other mechanisms, and because so much of the chemistry in the Dodge (1977) mechanism is out of date. We would be hesitant to recommend use of this mechanism in its current form because of the many out of date rate constants. At the same time, an updated version cannot be used until the entire mechanism has been reevaluated. Whether or not the effort involved in developing and testing an updated version of this mechanism is worthwhile is questionable, since there currently exist mechanisms of similar nature, such as that of Atkinson et al. (1982), that contain updated chemistry.

3.10 Discussion of Results

In this chapter we have presented a quantitative analysis of six lumped reaction mechanisms for photochemical smog. There are several important points that should be considered when interpreting the results of this analysis.

First, even though the master mechanism is fairly detailed and represents our current understanding of the most important gas phase reactions occurring in the atmosphere, the state of the art of atmospheric chemistry is not good enough for the master mechanism to be assumed correct. Therefore, one cannot judge the accuracy of a lumped mechanism by how close its predictions lie to those of the master mechanism. The usefulness of the master mechanism is that it provides a common grounds to which the lumped mechanism can be compared. Its purpose therefore is not to judge the adequacy of the lumped mechanisms.

Second, we reiterate that all chamber dependent reactions were removed from the mechanisms before they were analyzed. As discussed in section 2.6, there is a great deal of disagreement over the magnitude of unknown chamber radical sources. Differences in the amount of "reactivity" predicted by the various mechanisms will continue to exist until the chamber radical source issue is resolved.

Third, it is important to remember that each of the lumped mechanisms has been tested against smog chamber data, and, to a certain extent, the parameters and reactions in the mechanism reflect values chosen within the bounds of uncertainty that produce the best match of predicted and observed concentrations. Thus, changes in certain rate constants or reaction steps in a mechanism (such as those we have suggested) will require a complete reanalysis of the entire mechanism with respect to experimental chamber data in order to maintain the original degree of agreement.

Finally, remember that in choosing a mechanism one must consider not only how well the mechanism performs, but, if the mechanism is to be used in a full-scale atmospheric model, how many non-steady-state species it contains (McRae et al., 1983). The number of non-steady-state species is important because of computing time limitations.

3.11 Conclusions

In this chapter we have presented a quantitative analysis of the six lumped mechanisms under consideration in our study. The counter species analysis technique has been used to identify the key areas that lead to different predicted O_3 levels under identical initial conditions. Based on the results of our analysis, we have highlighted possible changes for each mechanism. It is clear that the predictions of these mechanisms will be in much closer agreement with each other if these modifications are adopted. We have not attempted to determine a "best" mechanism from among these six. Instead, we have identified why the predictions of each mechanism are so different, and have described changes that we believe will help to eliminate these discrepancies.

It is interesting to summarize this section by modifying each mechanism as per our suggestions, and once again performing a counter species analysis. The modifications that we have suggested for each mechanism are listed in Table 13. In each case, these modifications were made in order to either

TABLE 13

Summary of our Possible Modifications for all but the Dodge (1977) Mechanism

These Modifications are Used to Obtain the Results
Shown in Table 14

MECHANISM	MODIFICATIONS (AS DESCRIBED IN CHAPTER 3)
Atkinson et al. (1982) (see Section 3.4.2)	1) 25 percent aromatic nitrate formation removed 2) Photolysis rates of methyl glyoxal, formaldehyde and acetaldehyde updated 3) Products of methylglyoxal photolysis changed from $MGLY + hv \longrightarrow CH_3C(O)O_2 + CO + HO_2$ to $MGLY + hv \longrightarrow 0.65CH_3C(O)O_2 + 0.35CH_3O_2 + 1.35CO + HO_2$
Killus and Whitten (1982) (see Section 3.5.2)	1) Photolysis rates for the lumped groups DCRB and HCHO updated 2) Atkinson et al. (1982) treatment of APRC reactions substituted in place of existing, first order reactions 3) Correct mistake in product stoichiometric coefficients for the radical producing photolysis pathway from the aldehydes. Adjust parameter "a" from 0.33 to 0.75. Choose $k_f = k_a = 1.5k_b = 10k_c$ as opposed to $k_f = k_a = k_b = 2k_c$ 4) Treat acetone as unreactive
Demerjian (1982) (see Section 3.6.2)	1) Separate ethene from the remaining alkenes 2) Treat acetone as unreactive
McRae and Seinfeld (1983) (see Section 3.7.2)	1) Update aldehyde photolysis rates 2) Substitute simple, but improved treatment of aromatic chemistry
Penner and Walton (1982) (see Section 3.8.2)	1) Update methyl glyoxal and aldehyde photolysis rates

(1) up-date an out-of-date component, or (2) "improve" the treatment of certain reactions. We have not included any possible changes for the Dodge (1977) mechanism in Table 13.

The counter species results for the modified mechanisms are shown in Table 14. Also shown in this table are the total number of NO to NO_2 conversions predicted by the original mechanisms. These same results are shown graphically in Figures 10, 11, and 12. In addition, Figures 13, 14, and 15 show the amount of O_3 predicted by the original and modified mechanisms. We see that in nearly every case, the predictions of the modified mechanisms for both NO to NO_2 conversions and O_3 yield are in much better agreement with those of the master mechanism. This is true for each of the three sets of initial conditions. Just as important, we see that with only two exceptions, the lumped mechanisms now agree quite closely with each other. Thus, adopting the few modifications shown in Table 13 has eliminated most of the discrepancies between the predictions of these five mechanisms.

TABLE 14

Comparison of the Counter Species Results for the Original and Modified (in parenthesis) Versions of 5 Lumped Mechanisms

The Changes Made in Each of the Mechanisms are Shown in Table 13.

		NO TO NO2 CONVERSIONS (ppb)				
ORGANIC CLASS	MASTER	ATKINSON ET AL.	KILLUS AND WHITTEN	DEMERJIAN	MC RAE AND SEINFELD	PENNER AND WALTON
		INITIAL CONDITION SET 1 ($[RHC]_o/[NO_x]_o = 7.14$)				
Aromatics	185	157(146)	201(314)	199(239)	139(253)	135(217)
Alkanes	157	159(180)	187(321)	174(239)	158(260)	110(218)
Alkenes	181	160(191)	146(221)	248(346)	139(202)	227(327)
Aldehydes & Ketones	68	60 (74)	64(148)	71 (98)	78 (97)	60 (84)
TOTAL	591	536(591)	598(1007)	692(922)	514(812)	532(846)
		INITIAL CONDITION SET 2 ($[RHC]_o/[NO_x]_o = 28.6$)				
Aromatics	175	162(142)	183(246)	246(231)	171(224)	147(188)
Alkanes	197	201(207)	217(223)	229(216)	226(230)	148(179)
Alkenes	232	220(229)	162(175)	358(474)	198(243)	299(349)
Aldehydes & Ketones	60	59 (64)	64(115)	73 (90)	67 (92)	54 (70)
TOTAL	664	642(642)	626(759)	906(1011)	662(789)	648(786)
		INITIAL CONDITION SET 3 ($[RHC]_o/[NO_x]_o = 1.79$)				
Aromatics	69	68 (68)	82(133)	55 (59)	53 (95)	30 (53)
Alkanes	41	46 (54)	55 (88)	40 (44)	66 (76)	20 (32)
Alkenes	65	62 (74)	56 (95)	85(120)	41 (96)	53 (89)
Aldehydes & Ketones	34	30 (40)	32 (85)	33 (39)	34 (62)	24 (43)
TOTAL	209	206(236)	225(401)	213(262)	194(329)	127(217)

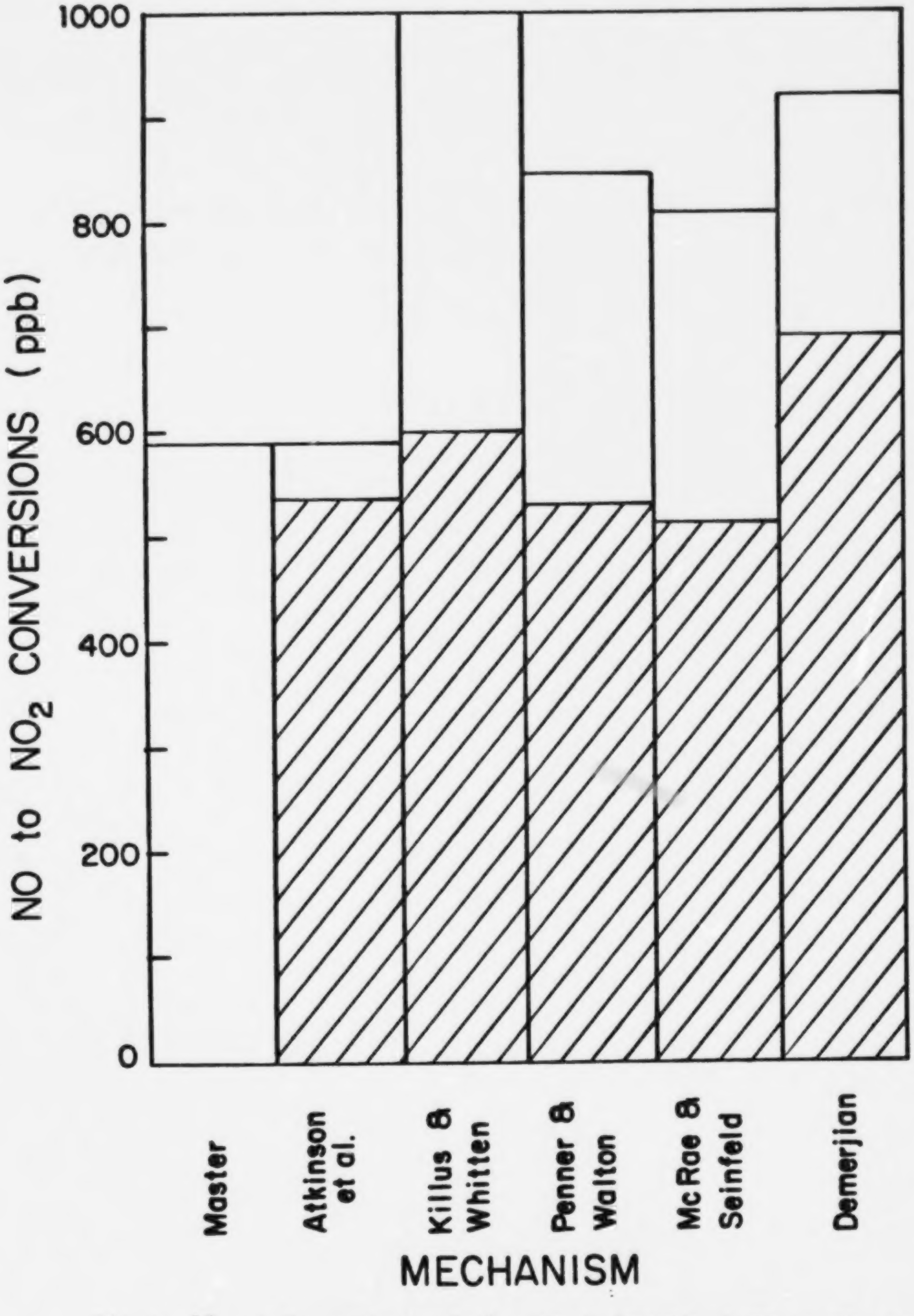

Figure 10. A Comparison of the Total Amount of NO to NO$_2$ Conversions Predicted by the Original (unshaded) and Modified (shaded) Versions of Five Lumped Mechanisms Using Initial Condition Set 1 ($[RHC]_o/[NO_x]_o = 7.14$).

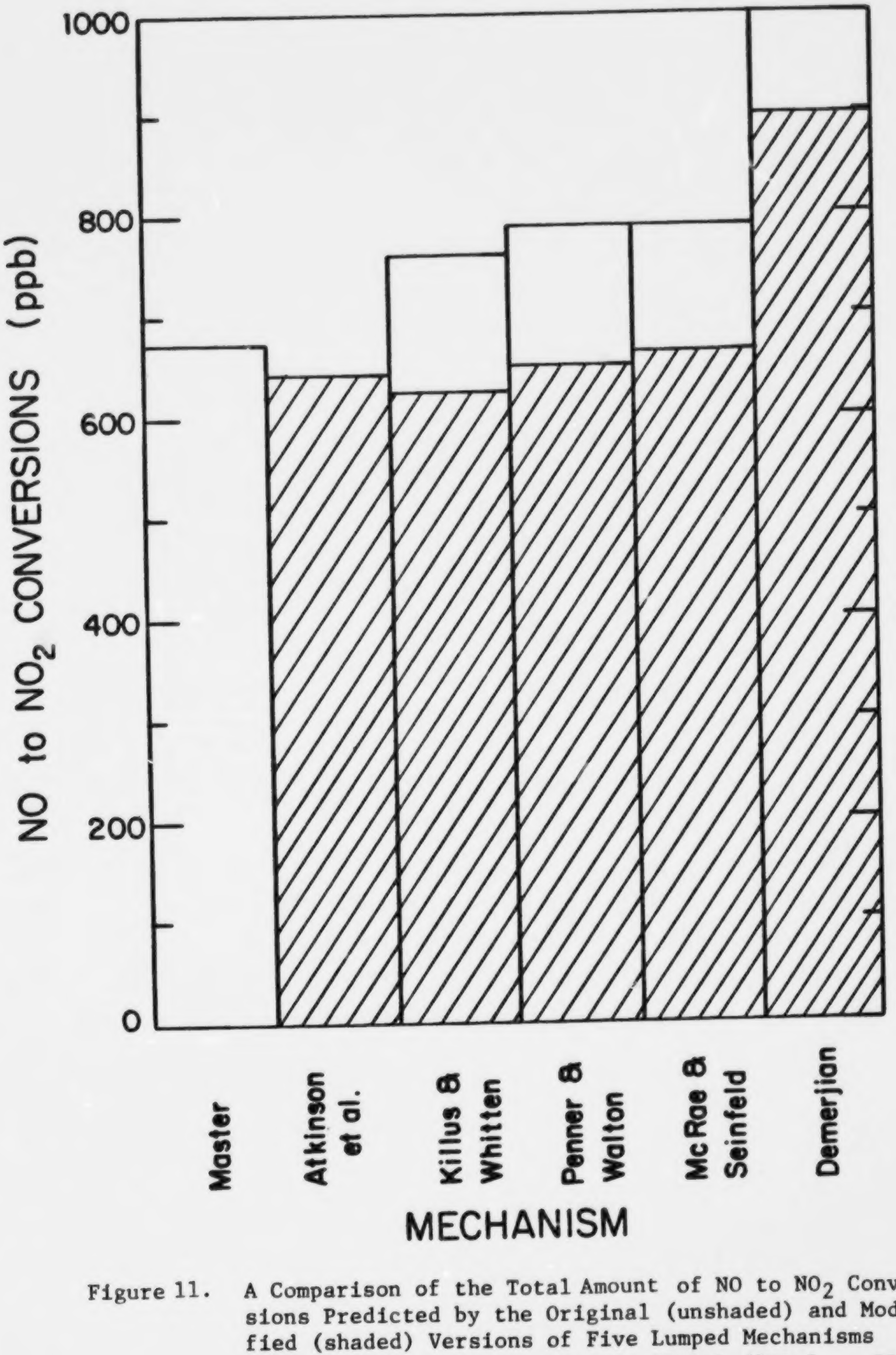

Figure 11. A Comparison of the Total Amount of NO to NO_2 Conversions Predicted by the Original (unshaded) and Modified (shaded) Versions of Five Lumped Mechanisms Using Initial Condition Set 2 ($[RHC]_o/[NO_x]_o$ = 28.6).

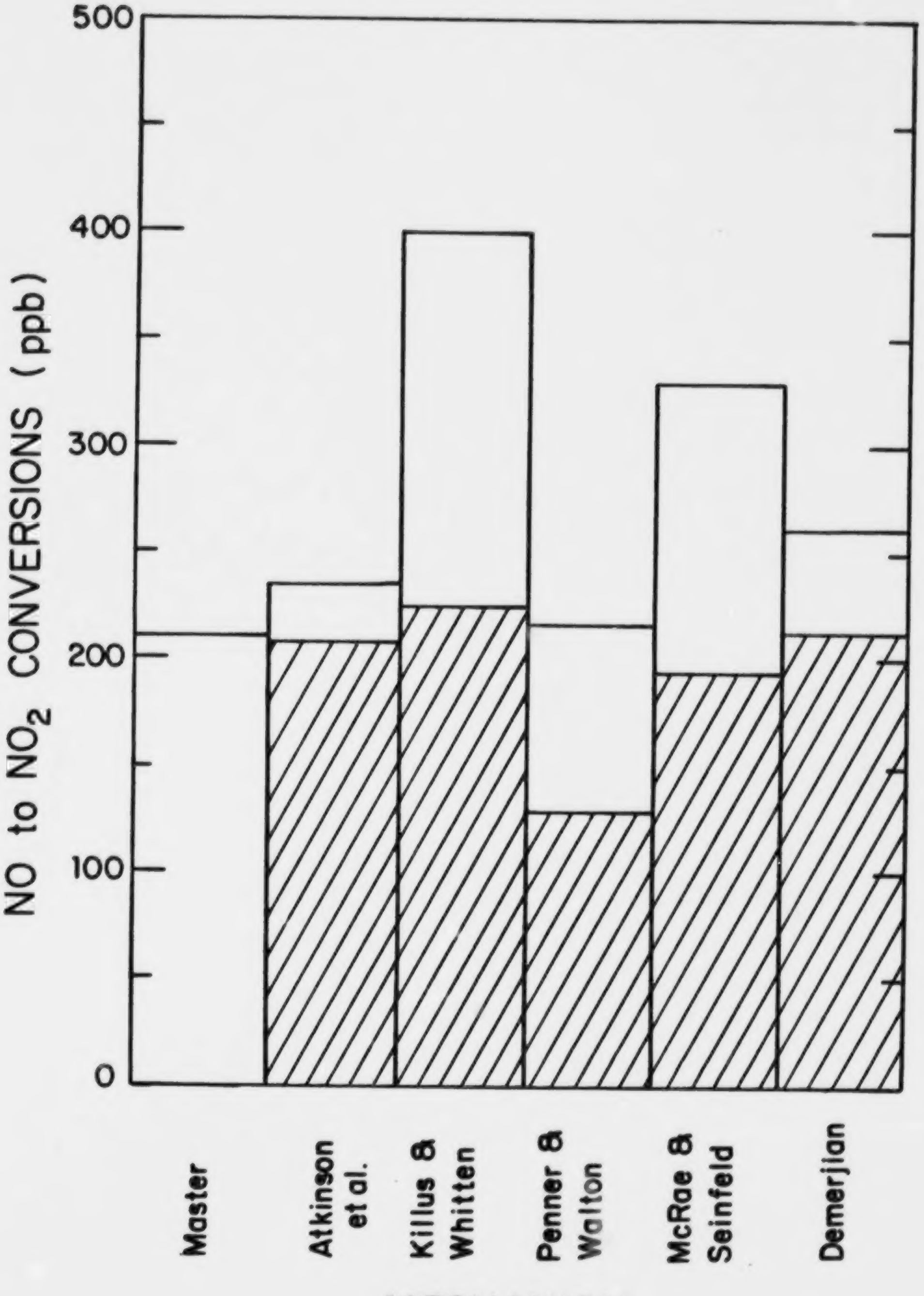

Figure 12. A Comparison of the Total Amount of NO to NO_2 Conversions Predicted by the Original (unshaded) and Modified (shaded) Versions of Five Lumped Mechanisms Using Initial Condition Set 3 ($[RHC]_o/[NO_x]_o = 1.79$).

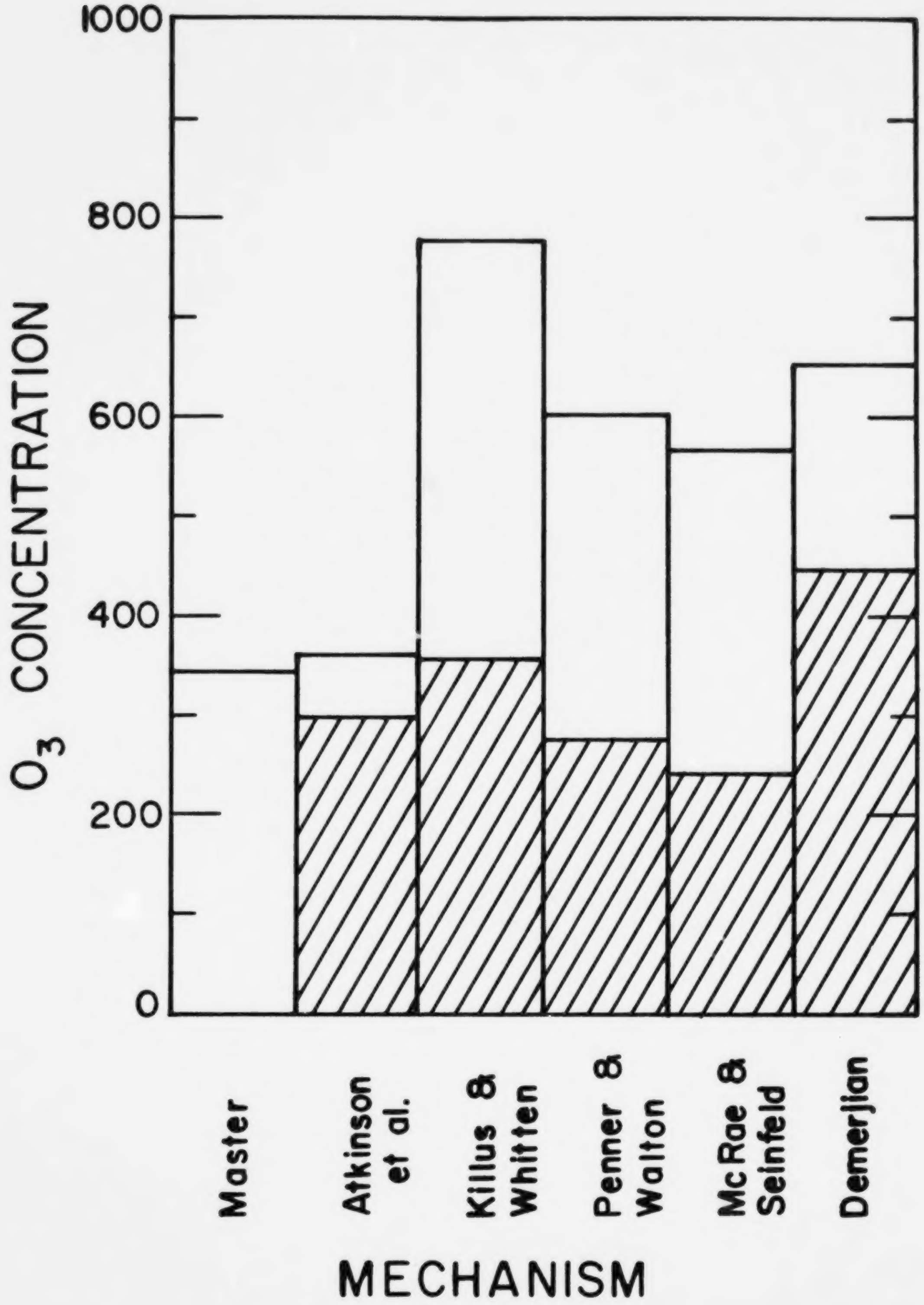

Figure 13. A Comparison of the O_3 Yield After 360 minutes of Simulation Predicted by the Original (unshaded) and Modified (shaded) Versions of Five Lumped Mechanisms Using Initial Condition Set 1.

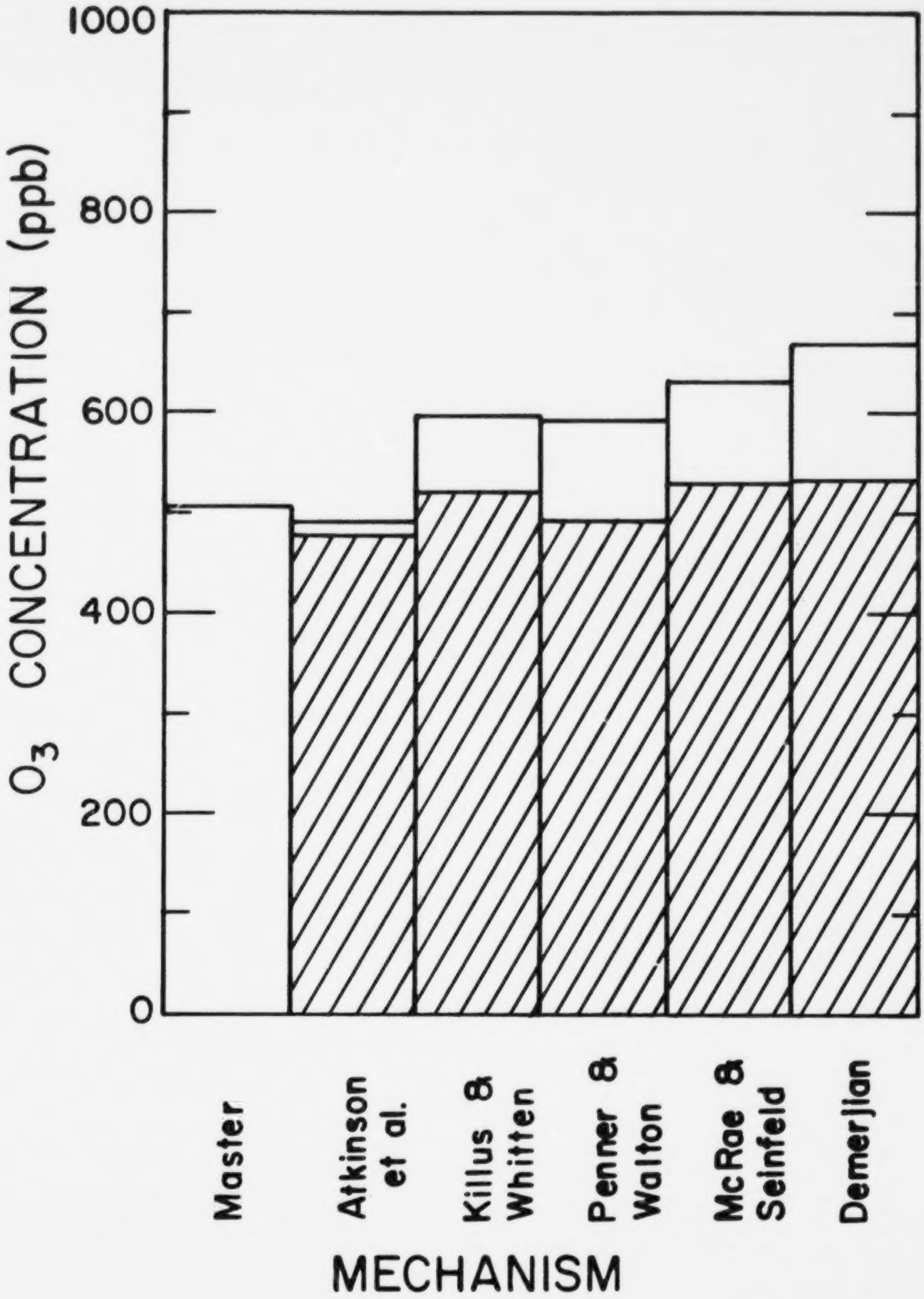

Figure 14. A Comparison of the O_3 Yield After 150 Minutes of Simulation Predicted by the Original (Unshaded) and Modified (shaded) Versions of Five Lumped Mechanisms Using Initial Condition Set 2.

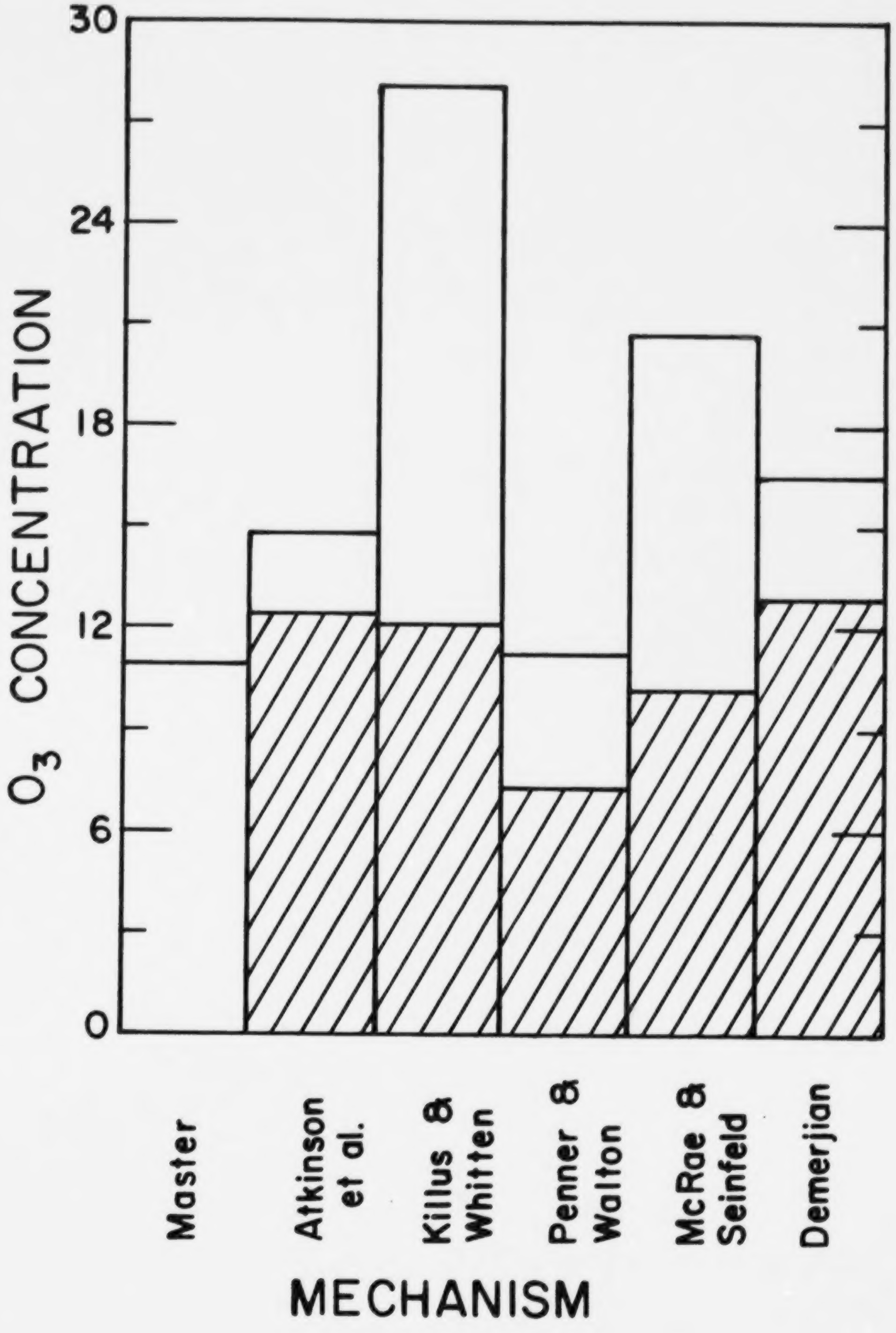

Figure 15. A Comparison of the O_3 Yield After 360 Minutes of Simulation Predicted by the Original (Unshaded) and Modified (shaded) Versions of Five Lumped Mechanisms Using Initial Condition Set 3.

CHAPTER 4

CONCLUSIONS AND RECOMMENDATIONS

In this report we have presented a quantitative analysis of six lumped mechanisms describing photochemical smog. At the outset of this study, our goal was to determine why these mechanisms, under identical conditions, give rise to widely different predictions of peak O_3 levels. We have come a long way toward achieving this goal. Based on the results of this analysis, we have identified specific areas in each mechanism that are most responsible for the observed discrepancies in O_3 predictions. For each mechanism, several recommendations have been made that are aimed at eliminating these discrepancies (Table 13). Some of these recommendations amount merely to updating rate constants, while others involve developing completely new reaction sequences. When the lumped mechanisms are modified to include our suggestions, their predictions are in much closer agreement. Of course, changes such as those that we have suggested should not be adopted until the performance of the entire mechanism is reevaluated.

Several recommendations for future work are apparent upon completing this study. These would include recommending that:

- future work be directed at several important areas of atmospheric chemistry where our knowledge is lacking. Perhaps the most critical area needing improvement concerns the mechanism of aromatic ring opening. The products formed when the aromatic-OH-O_2 adduct cleaves are unknown. This aspect of the mechanism must be eluciated before any faith can be placed in the predictions of photochemical smog mechanisms. The photolysis products of the important α-dicarbonyls such as methyl glyoxal also represents a critical area of uncertainty in aromatic chemistry.

- much greater resources be devoted to the determination of the fundamental mechanism leading to chamber radical sources. It is an unfortunate fact that mechanisms cannot be unambiguously evaluated using chamber data or compared to each other until the radical source issue is resolved. It now appears that the only way to resolve this controversy is to determine the mechanism which gives rise to this radical source.
- the counter species analysis technique be used by each investigator when future versions of these mechanisms are developed. We have only applied this analysis to a single primary hydrocarbon distribution, at 3 RHC to NO_x ratios. Individual investigators should make use of counter species analysis to test their mechanisms with a variety of initial hydrocarbon distributions and RHC to NO_x ratios.
- future work in evaluating these lumped mechanisms include an analysis of the methods for establishing initial conditions when detailed hydrocarbon composition profiles are not available. The emission control requirements predicted by these lumped mechanisms should be evaluated under real world conditions of continuous pollutant emissions, continuous dilution, and in the presence of background pollutants. Problems of this type will be addressed in Part III of this study.
- that a significant effort be devoted toward measuring the composition and amounts of organics emitted into urban environments. Without this information, the uncertainties involved in specifying input data could nullify any improvements in the reaction mechanisms themselves.

REFERENCES

Atkinson, R. and Lloyd, A.C.(1984), "Evaluation of Kinetic and Mechanistic Data for Modeling of Photochemical Smog," J. Phys. Chem. Ref. Data, 13 (2), in press.

Atkinson, R., Darnall, K.R., Lloyd, A.C., Winer, A.M. and Pitts, J.N. Jr. (1979), "Kinetics and Mechanisms of the Reaction of the Hydroxyl Radical with Organic Compounds in the Gas Phase," Advances in Photochemistry, 11, 375-488.

Atkinson, R., Carter, W.P.L., Darnall, K.R., Winer, A.M., and Pitts, J.N. Jr. (1980), "A Smog Chamber and Modeling Study of the Gas Phase NO_x-Air Photooxidation of Toluene and the Cresols," International Journal of Chemical Kinetics, 12, 779-837.

Atkinson, R., Lloyd, A.C. and Winges, L. (1982), "An Updated Chemical Mechanism for Hydrocarbons/NO_x/SO_2 Photooxidations Suitable for Inclusion in Atmospheric Simulation Models," Atmospheric Environment, 16, 1341-1355.

Baulch, D.L., Cox, R.A., Crutzen, P.J., Hampson, R.F., Kerr, J.A., Troe, J. and Watson, R.T. (1982), "Evaluated Kinetic and Photochemical Data for Atmospheric Chemistry: Supplement 1. CODATA Task Group on Chemical Kinetics," J. Physical and Chemical Reference Data, 11, 327-496.

Calvert, J.G., Su, F., Bottenheim, J.W. and Strausz, O.P. (1978), "Mechanism of the Homogeneous Oxidation of Sulfur Dioxide in the Troposphere," Atmospheric Environment, 12, 197-226.

Carter, W.P.L., Winer, A.M. and Pitts, J.N., Jr. (1982a) "Effect of Kinetic Mechanisms and Hydrocarbon Composition on Oxidant-Precursor Relationships Predicted by the EKMA Isopleth Technique," Atmospheric Environment 16, 113-120.

Carter, W.P.L., Atkinson, R., Winer, A.M. and Pitts, J.N. Jr., (1982b) "Experimental Investigation of Chamber-Dependent Radical Sources," International Journal of Chemical Kinetics, 14, 1071-1103.

Demerjian, K.L., Schere, K.L. and Peterson, J.T. (1980), "Theoretical Estimates of Actinic (Spherically Integrated) Flux and Photolytic Rate Constants of Atmospheric Species in the Lower Troposphere," Advances in Environmental Science and Technology, 10, 369-459.

Demerjian, K.L. (1982), "Personal Communication."

DeMore, W.B., Watson, R.T., Howard, C.J., Golden, D.M., Molina, M.J., Hampson, R.F., Kurylo, M. and Ravishankara, A.R. (1982), Chemical Kinetics and Photochemical Data for Use in Stratospheric Modeling, Jet Propulsion Laboratory Publication 82-57, California Institue of Technology, Pasadena, California.

Dodge, M.C. (1977), "Combined Use of Modeling Techniques and Smog Chamber Data to Derive Ozone -Precursor Relationships," U.S. Environmental Protection Agency Report, EPA-600/3-77-001a, 881-889.

Durbin, P.A., Hecht, T.A. and Whitten, G.Z. (1975), "Mathematical Modeling of Simulated Photochemical Smog," U.S. Environmental Protection Agency Report, EPA-650/4-75-026.

Falls, A.H. and Seinfeld, J.H. (1978), "Continued Development of a Kinetic Mechanism for Photochemical Smog," Environmental Science and Technology, 12, 1398-1406.

Falls, A.H., McRae, G.J. and Seinfeld, J.H. (1979), "Sensitivity and Uncertainty of Reaction Mechanisms for Photochemical Air Pollution," Int. J. Chemical Kinetics, 11, 1137-1162.

Gelinas, R.J., Dickerson, R.P. and Grant, K.E. (1974), Solar Flux and Photodissociation Calculations for LLL Atmospheric Physics Programs, Lawrence Livermore Laboratory Report UCRL-74944 Rev. 1, Lawrence Livermore National Laboratory, University of California, Livermore, California

Gelinas, R.J. and Skewes-Cox, P.D. (1975), "Tropospheric-Photochemical Mechanisms," J. Physical Chemistry, 81, 2468-2479.

Graedel, T.E. (1977), "Functional Group Analysis of Large Chemical Kinetic Systems," J. Physical Chemistry, 81, 2372-2374.

Horowitz, A. and Calvert, J.G. (1982), "Wavelength Dependence of the Primary Processes in Acetaldehyde Photolysis," J. Physical Chemistry, 86, 3105-3114.

Jeffries, H.E., Sexton, K.G. and Salmi, C.N. (1981), Effects of Chemistry and Meteorology on Ozone Control Calculations Using Simple Trajectory Models and the EKMA Procedure, Final Report to the U.S. Environmental Protection Agency Under Contract No. 68-02-3523, School of Public Health, University of North Carolina, Chapel Hill, North Carolina, 373 pp.

Killus, J.P. and Whitten, G.Z. (1982a), A New Carbon-Bond Mechanism for Air Quality Modeling, U.S. Environmental Protection Agency Report No. EPA-600/3-82-041.

Killus, J.P. and Whitten, G.Z. (1983), Effects of Photochemical Kinetic Mechanisms on Oxidant Model Predictions, U.S. Environmental Protection Agency Report No. EPA-600/3-83-111.

Leone, J.A. and Seinfeld, J.H. (1983a) "Analysis of the Characteristic of Complex Chemical Reaction Mechanisms - Application to Photochemical Smog Chemistry," Environmental Science & Technology (in press).

Leone, J.A. and Seinfeld, J.H. (1983b), "An Updated Chemical Mechanism for the Atmospheric Photooxidation of Toluene," *International Journal of Chemical Kinetics* (in press).

Luther, F.M. and Gelinas, R.J. (1976), "Effects of Molecular Multiple Scattering and Surface Albedo on Atmospheric Photodissociation Rates," *J. Geophysical Research*, *81*, 1125-1132.

MacCracken, M.C. and Sauter, G.C. eds. (1975), "Development of an Air Pollution Model for the San Francisco Bay Area," Final Report to the National Science Foundation, Lawrence Livermore Report UCRL-51920, 1169 pp.

McRae, G.J., Goodin, W.R. and Seinfeld, J.H. (1982a), *Mathematical Modeling of Photochemical Air Pollution*, California Institute of Technology, Environmental Quality Laboratory Report No. 18.

McRae, G.J., Goodin, W.R. and Seinfeld, J.H. (1982b), "Development of a Second-Generation Mathematical Model for Urban Air Pollution I. Model Formulation," *Atmospheric Environment*, *16*, 679-696.

McRae, G.J. and Seinfeld, J.H. (1983), "Development of a Second-Generation Mathematical Model for Urban Pollution II: Model Performance Evaluation," *Atmospheric Environment*, *17*, 501-523.

McRae, G.J., Leone, J.A. and Seinfeld, J.H. (1983) *Evaluation of Chemical Reaction Mechanisms for Photochemical Smog - Part I. Mechanism Description and Documentation*, U.S. Environmental Protection Agency Report No. EPA-600/3-83-086.

Penner, J.E. and Walton, J.J. (1982) *Air Quality Model Update,* Lawrence Livermore Laboratory Report UCID - 19300, Lawrence Livermore National Laboratory, University of California, Livermore, California, 55 pp.

Pitts, J.N., Winer, A.M., Darnall, K.R. et al. (1976), *Chemical Consequences of Air Quality Standards and of Control Implementation Programs: Roles of Hydrocarbons, Oxides of Nitrogen, and Aged Smog in the Production of Photochemical Oxidant*, Final Report to the California Air Resources Board under Contract Number 4-212, Statewide Air Pollution Research Center, University of California Riverside, California, 444 pp.

Pitts, J.N., Jr., Darnall , K., Carter, W.P.L., Winer, A.M. and Atkinson, R. (1979), *Mechanisms of Photochemical Reactions in Urban Air - Final Report,* U.S. Environmental Protection Agency Report No. EPA-600/3-79-110.

Plum, C.N., Sanhueza, E., Atkinson, R., Carter, W.P.L. and Pitts, J.N. (1983), "OH Radical Rate Constants and Photolysis Rates of Alpha-Dicarbonyls," *Environmental Science and Technology*, (in press).

Schere, K.L. (1983), "Personal Communcation - Letter dated 14 January."

Whitten, G.Z., Hogo, H. and Killus, J.P. (1980a), "The Carbon-Bond Mechanism: A Condensed Kinetic Mechanism for Photochemical Smog," Environmental Science and Technology, 14, 690-700.

Whitten, G.A., Hogo, H. and Killus, J.P. (1980b), Modeling of Simulated Photochemical Smog with Kinetic Mechanisms: Volume 1, U.S. Environmental Protection Agency Report No. EPA-600/3-80-028a, Prepared by Systems Applications Inc., San Rafael, California, 362 pp.

Whitten, G.Z. (1981) Comments at U.S. Environmental Protection Agency Workshop on the Empirical Kinetic Modeling Approach, December 15-16, Research Triangle Park, NC

Whitten, G.Z. (1983) Personal Communication.

APPENDIX

Table A.1. "Master" Reaction Mechanism

Reaction[1]	Rate Constant[2]	Activation Energy (K)	Note
Inorganic Reactions:			
1) $NO_2 + h\nu \rightarrow NO + O(^3P)$	*	-	
2) $O(^3P) + O_2 \rightarrow O_3$	2.6×10^1	-5.1×10^2	
3) $O_3 + NO \rightarrow NO_2 + O_2$	2.7×10^1	1.5×10^3	
4) $O(^3P) + NO_2 \rightarrow NO + O_2$	1.4×10^4	-	
5) $O_3 + NO_2 \rightarrow NO_3 + O_2$	4.7×10^{-2}	2.45×10^3	
6) $NO_3 + NO \rightarrow 2NO_2$	3.0×10^4	-	
7) $HO_2 + NO_2 \rightarrow HO_2NO_2$	1.6×10^3	-	
8) $NO_2 + OH \rightarrow HNO_3$	1.6×10^4	-	
9) $O_3 + OH \rightarrow HO_2 + O_2$	9.9×10^1	9.7×10^2	
10) $O_3 + HO_2 \rightarrow OH + 2O_2$	3.0×10^0	5.8×10^2	
11) $HO_2NO_2 \rightarrow HO_2 + NO_2$	5.1×10^0	1.042×10^4	
12) $HO_2 + NO \rightarrow NO_2 + OH$	1.2×10^4	-2.4×10^2	
13) $HO_2 + HO_2 \rightarrow H_2O + O_2$	3.9×10^3	-1.2×10^3	
14) $HO_2 + HO_2 + H_2O \rightarrow H_2O_2 + O_2 + H_2O$	2.2×10^{-1}	-5.8×10^3	
15) $O_3 + h\nu \rightarrow O(^3P) + O_2$	$6.5 \times 10^{-2}\ k_{NO_2}$	-	1
16) $O_3 + h\nu \rightarrow O(^1D) + O_2$	$2.8 \times 10^{-3}\ k_{NO_2}$	-	1
17) $O(^1D) + O_2 \rightarrow O(^3P) + O_2$	4.3×10^4	-	
18) $O(^1D) + H_2O \rightarrow 2OH$	3.2×10^5	-	
19) $NO + OH \rightarrow HONO$	9.7×10^3	-	
20) $HONO + h\nu \rightarrow NO + OH$	$1.8 \times 10^{-1}\ k_{NO_2}$	-	1
21) $NO + NO + O_2 \rightarrow 2NO_2$	7.2×10^{-10}	-5.3×10^2	
22) $NO_3 + NO_2 \rightarrow NO + NO_2 + O_2$	5.9×10^{-1}	1.23×10^3	

Table A.1 (continued)

Reaction	Rate Constant	Activation Energy (K)	Note
23) $NO_3 + NO_2 \rightarrow N_2O_5$	1.6×10^3	-	
24) $N_2O_5 \rightarrow NO_2 + NO_3$	3.1×10^0	1.108×10^4	
25) $N_2O_5 + H_2O \rightarrow 2HNO_3$	0.0	-	
26) $H_2O_2 + OH \rightarrow HO_2 + H_2O$	2.5×10^3	-	
27) $H_2O_2 + h\nu \rightarrow 2OH$	$8.4\times10^{-4}\ k_{NO_2}$	-	
28) $CO + OH \xrightarrow{O_2} HO_2 + CO_2$	4.0×10^2	-	
29) $NO_3 + h\nu \rightarrow 0.3NO + 0.7NO_2$ $+ 0.7O(^3P)$	$1.55\times10^1\ k_{NO_2}$	-	
Aldehyde Reactions and PAN Formation:			
30) $CH_3CHO + h\nu \xrightarrow{2O_2} CH_3O_2\cdot + HO_2 + CO$	$2.58\times10^{-4}\ k_{NO_2}$	-	1
31) $CH_3CHO + OH \xrightarrow{O_2} CH_3C(O)O_2\cdot + H_2O$	2.4×10^4	-2.6×10^2	
32) $CH_3O_2\cdot + NO \rightarrow NO_2 + CH_3O\cdot$	1.1×10^4	-	
33) $CH_3O\cdot + O_2 \rightarrow HCHO + NO_2$	2.1×10^0	1.35×10^3	
34) $CH_3O\cdot + NO_2 \rightarrow CH_3ONO_2$	2.2×10^4	-	
35) $CH_3O_2\cdot + HO_2 \rightarrow CH_3OOH + O_2$	9.2×10^3	-1.3×10^3	
36) $CH_3C(O)O_2\cdot + NO \xrightarrow{2O_2} NO_2 + CH_3O_2\cdot$ $+ NO_2 + CO_2$	1.1×10^4	-	
37) $CH_3C(O)O_2\cdot + NO_2 \rightarrow PAN$	6.9×10^3	-	
38) $CH_3C(O)O_2\cdot + HO_2 \rightarrow CH_3C(O)O_2H + O_2$	4.4×10^3	-	
39) $PAN \rightarrow CH_3C(O)O_2\cdot + NO_2$	2.2×10^{-2}	1.354×10^4	
40) $HCHO + h\nu \rightarrow H_2 + CO$	$3.3\times10^{-3}\ k_{NO_2}$	-	1
41) $HCHO + h\nu \xrightarrow{2O_2} 2HO_2 + CO$	$2.35\times10^{-3}\ k_{NO_2}$	-	1

Table A.1 (continued)

Reaction[1]	Rate Constant[2]	Activation Energy (K)	Note
42) $HCHO + OH \xrightarrow{O_2} HO_2 + CO + H_2O$	1.6×10^4	-	
α-Dicarbonyl Chemistry:			
43) $CH_3C(O)CHO + OH \xrightarrow{O_2} CH_3C(O)O_2\cdot + CO + H_2O$	2.5×10^4	-	
44) $CH_3C(O)CHO + h\nu \xrightarrow{2O_2} CH_3C(O)O_2\cdot + HO_2 + CO$	$1.3\times10^{-2}\ k_{NO_2}$	-	
45) $CH_3C(O)CHO + h\nu \xrightarrow{2O_2} CH_3O_2\cdot + HO_2 + 2CO$	$6.0\times10^{-3}\ k_{NO_2}$	-	
46) $(CHO)_2 + OH \xrightarrow{O_2} HO_2 + 2CO + H_2O$	1.7×10^4	-	
47) $(CHO)_2 + h\nu \rightarrow 0.13HCHO + 0.87H_2 + 1.87CO$	$8.0\times10^{-3}\ k_{NO_2}$	-	
Toluene Abstraction Pathway:			
48) $C_6H_5\text{-}CH_3 + OH \xrightarrow{O_2} C_6H_5\text{-}CH_2O_2\cdot + H_2O$	7.5×10^2	-	
49) $C_6H_5\text{-}CH_2O_2\cdot + NO \rightarrow NO_2 + C_6H_5\text{-}CH_2O\cdot$	9.0×10^3	-	
50) $C_6H_5\text{-}CH_2O_2\cdot + NO \rightarrow C_6H_5\text{-}CH_2ONO_2$	1.0×10^3	-	
51) $C_6H_5\text{-}CH_2O\cdot + O_2 \rightarrow C_6H_5\text{-}CHO + HO_2$	1.0×10^1	6.9×10^2	
52) $C_6H_5\text{-}CH_2O\cdot + NO_2 \rightarrow C_6H_5\text{-}CH_2ONO_2$	1.9×10^4	-	
53) $C_6H_5\text{-}CHO + h\nu \rightarrow$ stable products	1.6×10^{-3}	-	
54) $C_6H_5\text{-}CHO + OH \xrightarrow{O_2} C_6H_5\text{-}C(O)O_2\cdot + H_2O$	1.9×10^4	-	
55) $C_6H_5\text{-}C(O)O_2\cdot + NO \xrightarrow{O_2} NO_2 + C_6H_5\text{-}O_2\cdot + CO_2$	1.0×10^4	-	

Table A.1 (continued)

Reaction[1]	Rate[2] Constant	Activation Energy (K)	Note
56) $C_6H_5\text{-}C(O)O_2\cdot + NO_2 \rightarrow C_6H_5\text{-}C(O)O_2NO_2$	6.9×10^3	-	
57) $C_6H_5\text{-}C(O)O_2NO_2 \rightarrow C_6H_5\text{-}C(O)O_2\cdot + NO_2$	9.6×10^{-3}	1.304×10^4	
58) $C_6H_5\text{-}O_2\cdot + NO \rightarrow NO_2 + C_6H_5\text{-}O\cdot$	9.0×10^3	-	
59) $C_6H_5\text{-}O_2\cdot + NO_2 \rightarrow NO_3 + C_6H_5\text{-}O\cdot$	1.0×10^4	-	
60) $C_6H_5\text{-}O\cdot + NO_2 \rightarrow$ 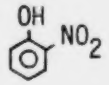	2.2×10^4	-	
61) 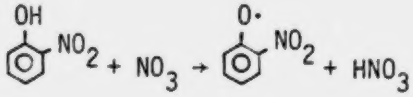	3.0×10^3	-	
62) 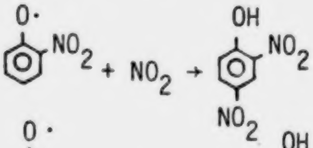	2.2×10^4	-	
63) 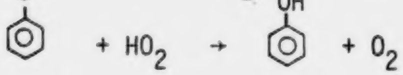	7.4×10^3	-	
Toluene Addition Pathway:			
64) 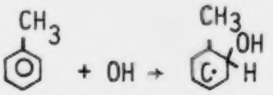	8.7×10^3	-	
65) 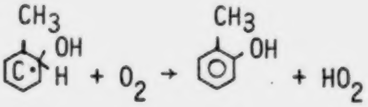	1.0×10^1	6.9×10^2	
66) 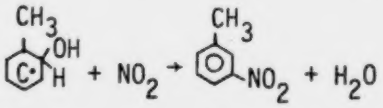	4.4×10^4	-	
67) 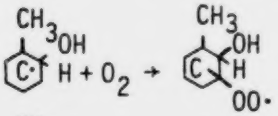	4.9×10^1	-	
68) 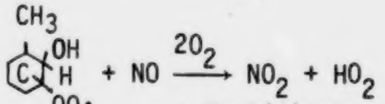 $+ CH_3C(O)CHO + CH(O)CH{=}CHCHO$	1.0×10^4	-	

Table A.1 (continued)

Reaction[1]	Rate Constant[2]	Activation Energy (K)	Note
Toluene addition path (continued)			
69) 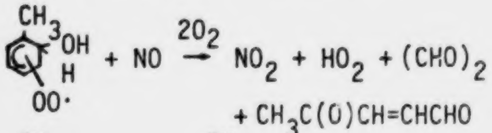	0.0	-	
70) 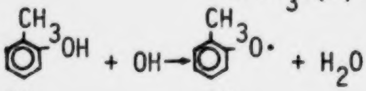	4.9×10^{3}	9.0×10^{2}	
71) 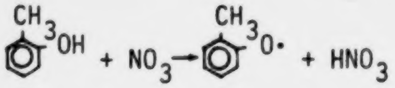	1.5×10^{4}	-	
72) 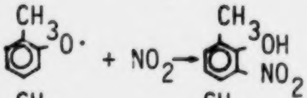	2.2×10^{4}	-	
73) 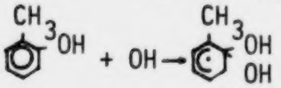	5.6×10^{4}	-	
74) 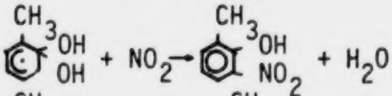	4.4×10^{4}	-	
75) 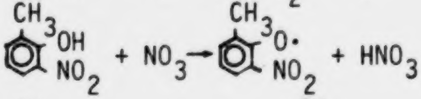	1.5×10^{4}	-	
76) 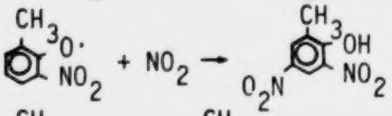	2.2×10^{4}	-	
77) 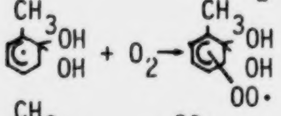	4.9×10^{1}	-	
78) 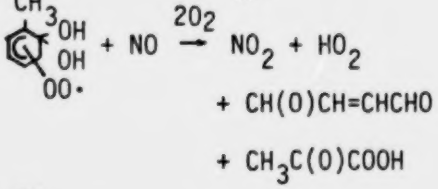	1.0×10^{4}	-	
79) 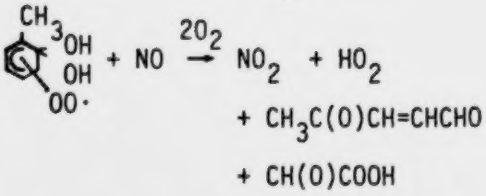	0.0	-	

Table A.1 (continued)

Reaction[1]	Rate Constant[2]	Activation Energy(K)	Note
80) $CH(O)COOH + OH \rightarrow HO_2 + H_2O + CO$	2.2×10^{4}	-	
81) $CH_3C(O)COOH + h\nu \rightarrow CH_3CHO + CO_2$	$1.4\times10^{-2}\ k_{NO_2}$	-	
Conjugated γ-dicarbonyl chemistry			
82) $HC(O)CH{=}CHCHO + OH \xrightarrow{O_2} HC(O)CH{=}CHC(O)O_2\cdot + H_2O$	4.4×10^{4}	-	
83) $HC(O)CH{=}CHC(O)O_2\cdot{+}NO \xrightarrow{O_2} NO_2{+}CO_2{+}HC(O)CH{=}CHO_2\cdot$	1.0×10^{4}	-	
84) $HC(O)CH{=}CHO_2\cdot{+}NO \xrightarrow{O_2} NO_2{+}HC(O)CH(O_2\cdot)CHO$	1.0×10^{4}	-	
85) $HC(O)CH(O_2\cdot)CHO{+}NO \rightarrow HC(O)CH(ONO_2)CHO$	4.0×10^{2}	-	
86) $HC(O)CH{=}CHC(O)O_2\cdot{+}NO_2 \rightarrow HC(O)CH{=}CHCO_3NO_2$	6.9×10^{3}	-	
87) $HC(O)CH{=}CHCO_3NO_2 \rightarrow HC(O)CH{=}CHC(O)O_2\cdot{+}NO_2$	2.2×10^{-2}	-	
88) $HC(O)CH(O_2\cdot)CHO{+}NO \xrightarrow{O_2} (CHO)_2{+}HO_2{+}NO_2{+}CO$	1.0×10^{4}	-	
89) $HC(O)CH{=}CHO_2\cdot{+}NO \rightarrow HC(O)CH{=}CHONO_2$	4.0×10^{2}	-	
90) $HC(O)CH{=}CHO_2\cdot{+}NO_2 \xrightarrow{O_2} HC(O)CH(O_2\cdot)CHO{+}NO_3$	1.0×10^{4}	-	
91) $CH_3C(O)CH{=}CHCHO + OH \xrightarrow{O_2} H_2O{+}CH_3C(O)CH{=}CHC(O)O_2\cdot$	2.2×10^{4}	-	
92) $CH_3C(O)CH{=}CHCHO{+}OH \xrightarrow{O_2} CH_3C(O)CH(OH)C(O_2\cdot)HCHO$	7.4×10^{3}	-	
93) $CH_3C(O)CH(OH)C(O_2\cdot)HCHO{+}NO \xrightarrow{O_2} NO_2{+}HO_2$ $+CH_3C(O)CHO{+}(CHO)_2$	1.0×10^{4}	-	
94) $CH_3C(O)CH{=}CHC(O)O_2\cdot{+}NO \xrightarrow{O_2} NO_2{+}CO_2$ $+CH_3C(O)CH{=}CHO_2\cdot$	1.0×10^{4}	-	
95) $CH_3C(O)CH{=}CHO_2\cdot{+}NO \xrightarrow{O_2} NO_2{+}CH_3C(O)CH(O_2\cdot)CHO$	1.0×10^{4}	-	
96) $CH_3C(O)CH(O_2\cdot)CHO{+}NO \rightarrow CH_3C(O)CH(ONO_2)CHO$	8.0×10^{6}	-	
97) $CH_3C(O)CH{=}CHC(O)O_2\cdot{+}NO \rightarrow CH_3C(O)CH{=}CHCO_3NO_2$	6.9×10^{3}	-	
98) $CH_3C(O)CH{=}CHCO_3NO_2 \rightarrow CH_3C(O)CH{=}CHC(O)O_2\cdot{+}NO_2$	2.2×10^{-2}	-	
99) $CH_3C(O)CH(O_2\cdot)CHO{+}NO \xrightarrow{O_2} NO_2{+}CH_3C(O)O_2\cdot{+}(CHO)_2$	5.0×10^{3}	-	

Table A.1 (continued)

Reaction	Rate Constant	Activation Energy(K)	Note
Conjugated γ-dicarbonyl chemistry (continued)			
100) $CH_3C(O)CH(O_2\cdot)CHO+NO \xrightarrow{O_2} NO_2+HO_2+CH_3C(O)CHO+CO$	5.0×10^3	-	
101) $CH_3C(O)CH{=}CHO_2\cdot+NO \rightarrow CH_3C(O)CH{=}CHONO_2$	8.0×10^2	-	
102) $CH_3C(O)CH{=}CHO_2\cdot+NO_2 \xrightarrow{O_2} NO_3+CH_3C(O)CH(O_2\cdot)CHO$	1.0×10^4	-	
m-Xylene chemistry:			
103) 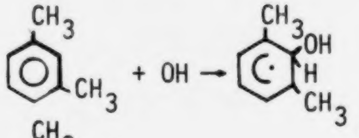	3.4×10^4	-	2
104) 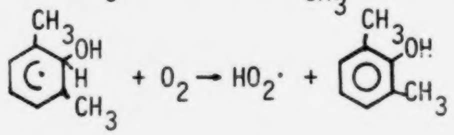	1.0×10^2	6.9×10^2	
105) 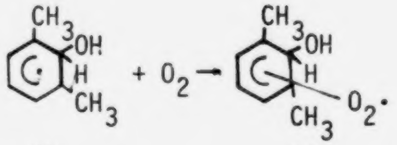	4.7×10^1	-	
106) 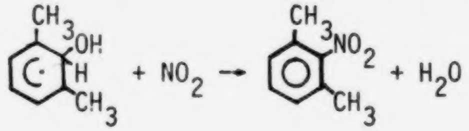	4.4×10^4	-	
107) 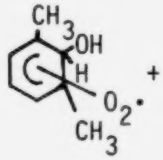 $+ NO \rightarrow NO_2 + HO_2\cdot + CH_3C(O)CHO$ $+ 0.5\ CH_3C(O)CH{=}CHCHO$ $+ 0.5\ CH(O)CH{=}C(CH_3)CHO$	1.0×10^4	-	3
108) 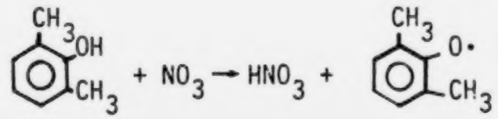	2.2×10^4	-	
109) 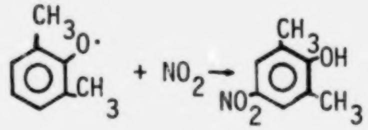	2.2×10^4	-	

Table A.1 (continued)

Reaction	Rate Constant	Activation Energy(K)	Note
m-Xylene chemistry (continued)			
110) 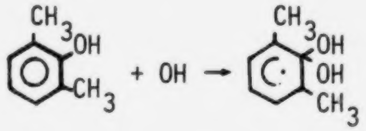 CH3 OH CH3 + OH → CH3 OH OH CH3	$1.1x10^5$	-	
111) 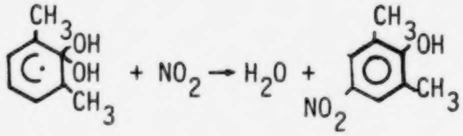 CH3 OH OH CH3 + NO2 → H2O + CH3 OH CH3 NO2	$4.4x10^4$	-	
112) 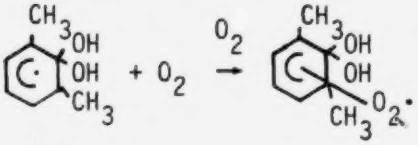 CH3 OH OH CH3 + O2 O2 → CH3 OH OH CH3 O2·	$4.7x10^1$	-	
113) 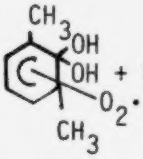 CH3 OH OH O2· CH3 $+ NO \rightarrow NO_2 + HO_2 + CH_3COCOOH$ $+ 0.5\ CH_3COCH{=}CHCHO$ $+ 0.5\ CHOCH{=}C(CH_3)CHO$	$1.0x10^4$	-	3
114) 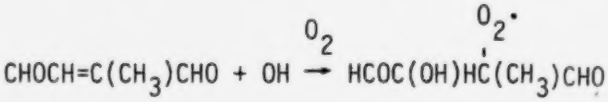 $CHOCH{=}C(CH_3)CHO + OH \xrightarrow{O_2} HCOC(OH)H\overset{O_2\cdot}{C}(CH_3)CHO$	$7.4x10^3$	-	
115) 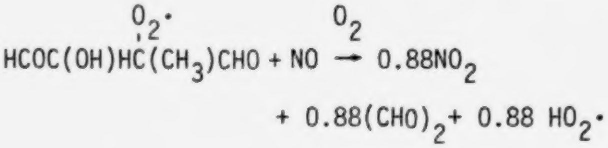 $HCOC(OH)H\overset{O_2\cdot}{C}(CH_3)CHO + NO \xrightarrow{O_2} 0.88NO_2$ $+ 0.88(CHO)_2 + 0.88\ HO_2\cdot$	$1.0x10^4$	-	4
116) 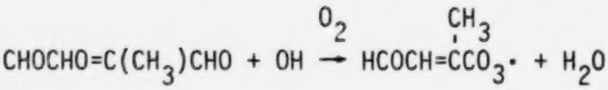 $CHOCHO{=}C(CH_3)CHO + OH \xrightarrow{O_2} HCOCH{=}\overset{CH_3}{C}CO_3\cdot + H_2O$	$4.4x10^4$		
117) 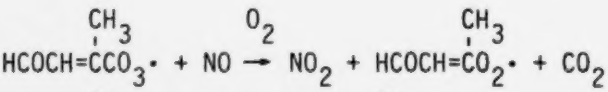 $HCOCH{=}\overset{CH_3}{C}CO_3\cdot + NO \xrightarrow{O_2} NO_2 + HCOCH{=}\overset{CH_3}{C}O_2\cdot + CO_2$			
118) 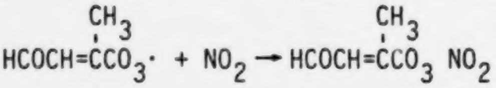 $HCOCH{=}\overset{CH_3}{C}CO_3\cdot + NO_2 \rightarrow HCOCH{=}\overset{CH_3}{C}CO_3\ NO_2$	$6.9x10^3$	-	
119) 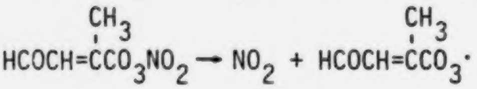 $HCOCH{=}\overset{CH_3}{C}CO_3NO_2 \rightarrow NO_2 + HCOCH{=}\overset{CH_3}{C}CO_3\cdot$	$2.2x10^{-2}$	$1.354x10^4$	

Table A.1 (continued)

Reaction	Rate Constant	Activation Energy(K)	Note
m-Xylene chemistry (continued)			
120) 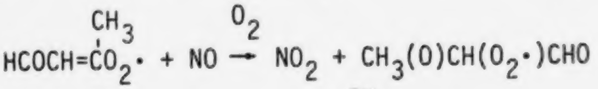 $HCOCH{=}\overset{CH_3}{C}O_2\cdot + NO \xrightarrow{O_2} NO_2 + CH_3(O)CH(O_2\cdot)CHO$	1.0×10^{4}	-	
121) 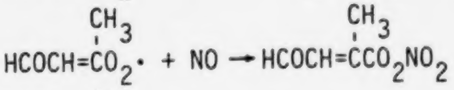 $HCOCH{=}\overset{CH_3}{C}O_2\cdot + NO \rightarrow HCOCH{=}\overset{CH_3}{C}CO_2NO_2$	8.0×10^{2}	-	
122) 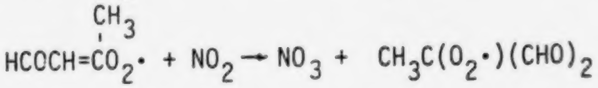 $HCOCH{=}\overset{CH_3}{C}O_2\cdot + NO_2 \rightarrow NO_3 + CH_3C(O_2\cdot)(CHO)_2$	1×10^{4}	-	
123) $CH_3C(O_2\cdot)(CHO)_2 + NO \rightarrow CH_3C(ONO_2)(CHO)_2$	8.0×10^{2}	-	
124) $CH_3C(O_2\cdot)(CHO)_2 + NO \xrightarrow{O_2} 0.75\ HO_2\cdot + 0.75\ CO$ $+ 0.75\ CH_3COCHO$ $+ 0.25\ (CHO)_2$ $+ 0.25\ CH_3C(O)O_2\cdot$ $+ NO_2$	1×10^{4}	-	
Ethene chemistry:			
125) $CH_2{=}CH_2 + OH \xrightarrow{O_2} HOCH_2CH_2O_2\cdot$	1.2×10^{4}	-3.82×10^{2}	
126) $HOCH_2CH_2O_2\cdot + NO \rightarrow NO_2 + HOCH_2CH_2O\cdot$	1×10^{4}		
127) $HOCH_2CH_2O\cdot \rightarrow HCHO + \cdot CH_2OH$	5.6×10^{6}		
128) $HOCH_2CH_2O\cdot + O_2 \rightarrow HOCH_2CHO + HO_2\cdot$	1.0×10^{1}	6.9×10^{2}	5
129) $\cdot CH_2OH + O_2 \rightarrow HCHO + HO_2\cdot$	$k_5{=}3\times10^{3}$		
130) $CH_2{=}CH_2 + O_3 \xrightarrow{O_2} HCHO + 0.4\ \dot{C}H_2O\dot{O} + 0.18\ CO_2$ $+ 0.42CO + 0.12\ H_2 + 0.42\ H_2O$ $+ 0.12\ HO_2\cdot$	2.5×10^{-3}	2.56×10^{3}	

Table A.1 (continued)

Reaction	Rate Constant	Activation Energy(K)	Note
Propene chemistry:			
131) 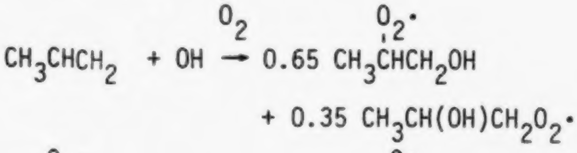 $CH_3CHCH_2 + OH \xrightarrow{O_2} 0.65\ CH_3\overset{O_2\cdot}{C}HCH_2OH$ $+ 0.35\ CH_3CH(OH)CH_2O_2\cdot$	$3.7x10^4$	$-5.37x10^2$	
132) 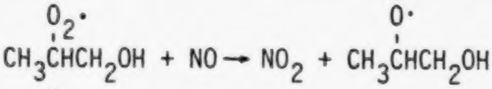 $CH_3\overset{O_2\cdot}{C}HCH_2OH + NO \rightarrow NO_2 + CH_3\overset{O\cdot}{C}HCH_2OH$	$1x10^4$	-	
133) 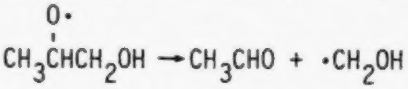 $CH_3\overset{O\cdot}{C}HCH_2OH \rightarrow CH_3CHO + \cdot CH_2OH$	$1x10^5$	-	
134) $CH_3CH(OH)CH_2O\cdot \rightarrow HCHO + CH_3\dot{C}HOH$	$1x10^2$	-	
135) 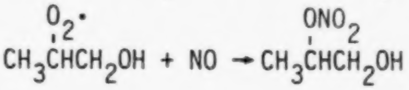 $CH_3\overset{O_2\cdot}{C}HCH_2OH + NO \rightarrow CH_3\overset{ONO_2}{C}HCH_2OH$	$4.0x10^2$	-	
136) $CH_3CH(OH)CH_2O_2\cdot + NO \rightarrow NO_2 + CH_3CH(OH)CH_2O\cdot$	$1x10^4$	-	
137) $CH_3CH(OH)CH_2O_2\cdot + NO \rightarrow CH_3CH(OH)CH_2ONO_2$	400	-	
138) $CH_3\dot{C}HOH + O_2 \rightarrow HO_2\cdot + CH_3CHO$	$3x10^3$	-	
139) $CH_3CHCH_2 + O_3 \rightarrow 0.5\ CH_3CHO + 0.2\ CH_3\dot{C}HO\dot{O}$ $+ 0.06\ CH_4 + 0.27\ CO_2$ $+ 0.33\ CO + 0.20\ HO_2\cdot$ $+ 0.1\ OH + 0.22\ CH_3O_2\cdot$ $+ 0.03\ CH_3O\cdot + 0.2\ \dot{C}H_2O\dot{O}$ $+ 0.06\ H_2 + 0.21\ H_2O$	$1.6x10^{-2}$	$1.897x10^3$	
tr-2-butene chemistry:			
140) 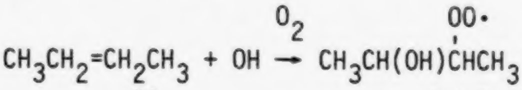 $CH_3CH_2{=}CH_2CH_3 + OH \xrightarrow{O_2} CH_3CH(OH)\overset{OO\cdot}{C}HCH_3$	$1.0x10^5$	$-5.42x10^2$	
141) 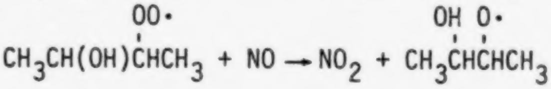 $CH_3CH(OH)\overset{OO\cdot}{C}HCH_3 + NO \rightarrow NO_2 + CH_3\overset{OH}{C}H\overset{O\cdot}{C}HCH_3$	$1.0x10^4$	-	

Table A.1 (continued)

Reaction	Rate Constant	Activation Energy(K)	Note
tr-2-butene chemistry (continued)			
142) 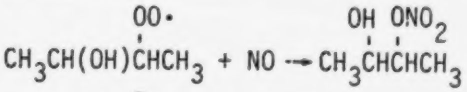 $CH_3CH(OH)\overset{OO\cdot}{C}HCH_3 + NO \rightarrow CH_3\overset{OH}{C}H\overset{ONO_2}{C}HCH_3$	8.0×10^{2}	-	
143) 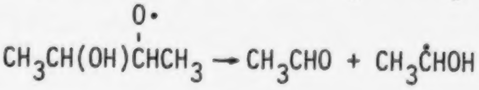 $CH_3CH(OH)\overset{O\cdot}{C}HCH_3 \rightarrow CH_3CHO + CH_3\dot{C}HOH$	1.0×10^{4}	-	
144) $CH_3CH_2{=}CH_2CH_3 + O_3 \rightarrow CH_3CHO + 0.4\ CH_3\dot{C}HO\dot{O}$ $+ 0.12\ CH_4 + 0.36\ CO_2$ $+ 0.24\ CO + 0.29\ HO_2\cdot$ $+ 0.19\ OH + 0.05\ CH_3O\cdot$ $+ 0.43\ CH_3O_2\cdot$	2.7×10^{-1}	1.051×10^{3}	
145) $\dot{C}H_2O\dot{O} + NO \rightarrow NO_2 + HCHO$	1.0×10^{4}	-	
146) $\dot{C}H_2O\dot{O} + NO_2 \rightarrow NO_3 + HCHO$	1.0×10^{3}	-	
147) $\dot{C}H_2O\dot{O} + H_2O \rightarrow HCOOH + H_2O$	6.0×10^{-3}	-	
148) $CH_3\dot{C}HO\dot{O} + NO \rightarrow NO_2 + CH_3CHO$	1.0×10^{4}	-	
149) $CH_3\dot{C}HO\dot{O} + NO_2 \rightarrow NO_3 + CH_3CHO$	1.0×10^{3}	-	
150) $CH_3\dot{C}HO\dot{O} + H_2O \rightarrow CH_3COOH + H_2O$	6.0×10^{-3}	-	
Propane chemistry:			
151) 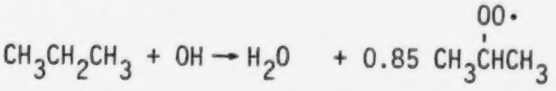 $CH_3CH_2CH_3 + OH \rightarrow H_2O + 0.85\ CH_3\overset{OO\cdot}{C}HCH_3$ $+ 0.15\ CH_3CH_2CH_2O_2\cdot$	2.3E3	6.8×10^{2}	
152) 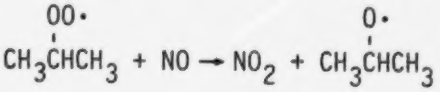 $CH_3\overset{OO\cdot}{C}HCH_3 + NO \rightarrow NO_2 + CH_3\overset{O\cdot}{C}HCH_3$	1.1×10^{4}	-	
153) $CH_3CH_2CH_2O_2\cdot + NO \rightarrow NO_2 + CH_3CH_2CHO\cdot$	1.1×10^{4}	-	

Table A.1 (continued)

Reaction	Rate Constant	Activation Energy(K)	Note
Propane chemistry (continued)			
154) 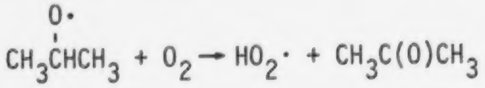 $CH_3\overset{O\cdot}{C}HCH_3 + O_2 \rightarrow HO_2\cdot + CH_3C(O)CH_3$	4.4×10^1	-	
155) $CH_3CH_2CH_2O\cdot + O_2 \rightarrow HO_2\cdot + CH_3CH_2CHO$	1.0×10^2	6.9×10^2	
n-Butane chemistry:			
156) 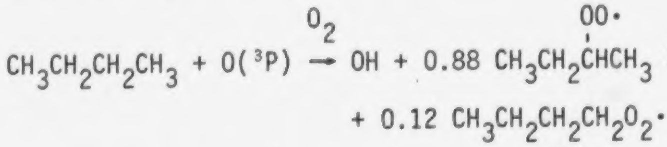 $CH_3CH_2CH_2CH_3 + O(^3P) \xrightarrow{O_2} OH + 0.88\ CH_3CH_2\overset{OO\cdot}{C}HCH_3 + 0.12\ CH_3CH_2CH_2CH_2O_2\cdot$	3.3×10^1	2.099×10^3	
157) 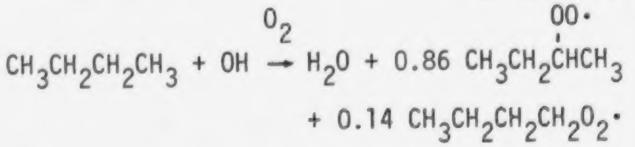 $CH_3CH_2CH_2CH_3 + OH \xrightarrow{O_2} H_2O + 0.86\ CH_3CH_2\overset{OO\cdot}{C}HCH_3 + 0.14\ CH_3CH_2CH_2CH_2O_2\cdot$	3.8×10^3	5.59×10^2	
158) $CH_3CH_2CH_2CH_2O_2\cdot + NO \rightarrow CH_3CH_2CH_2CH_2O\cdot + NO_2$	1.0×10^4	-	
159) $CH_3CH_2CH_2CH_2O_2\cdot + NO \rightarrow CH_3CH_2CH_2CH_2ONO_2$	8.0×10^2	8.0×10^2	
160) $CH_3CH_2CH_2CH_2O\cdot + O_2 \rightarrow HO_2\cdot + CH_3CH_2CH_2CHO$	1.0×10^1	6.90×10^2	
161) $CH_3CH_2CH_2CH_2O\cdot \xrightarrow{O_2} \cdot OOCH_2CH_2CH_2CH_2OH$	7.2×10^6	4.200×10^3	
162) $\cdot OOCH_2CH_2CH_2CH_2OH + NO \rightarrow NO_2 + \cdot OCH_2CH_2CH_2CH_2OH$	1.0×10^4	-	
163) $\cdot OOCH_2CH_2CH_2CH_2OH + NO \rightarrow O_2NOCH_2CH_2CH_2CH_2OH$	8.0×10^2	-	
164) $\cdot OCH_2CH_2CH_2CH_2OH \rightarrow HOCH_2CH_2CH_2\dot{C}HOH$	3.6×10^7	-	6
165) $HOCH_2CH_2CH_2\dot{C}HOH + O_2 \rightarrow HO_2\cdot + OHCH_2CH_2CH_2CHO$	1.0×10^1	6.90×10^2	
166) 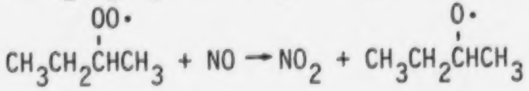 $CH_3CH_2\overset{OO\cdot}{C}HCH_3 + NO \rightarrow NO_2 + CH_3CH_2\overset{O\cdot}{C}HCH_3$	1.0×10^4	-	

Table A.1 (continued)

	Reaction	Rate Constant	Activation Energy(K)	Note
	n-Butane chemistry (continued)			
167)	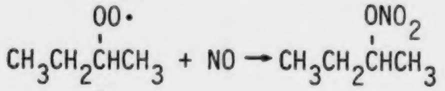 $CH_3CH_2\overset{OO\cdot}{C}HCH_3 + NO \rightarrow CH_3CH_2\overset{ONO_2}{C}HCH_3$	8.0×10^2	-	
168)	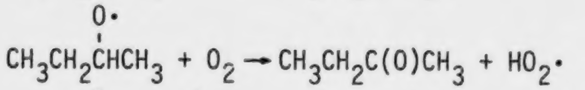 $CH_3CH_2\overset{O\cdot}{C}HCH_3 + O_2 \rightarrow CH_3CH_2C(O)CH_3 + HO_2\cdot$	4.4×10^1	-	
169)	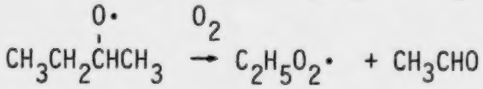 $CH_3CH_2\overset{O\cdot}{C}HCH_3 \xrightarrow{O_2} C_2H_5O_2\cdot + CH_3CHO$	4.0×10^6	7.0×10^3	
170)	$C_2H_5O_2\cdot + NO \rightarrow C_2H_5O\cdot + NO_2$	1.1×10^4	-	
171)	$C_2H_5O\cdot + NO_2 \rightarrow C_2H_5ONO_2$	2.2×10^4	-	
172)	$C_2H_5O\cdot + NO \rightarrow C_2H_5ONO$	4.4×10^4	-	
173)	$C_2H_5O\cdot + O_2 \rightarrow CH_3CHO + HO_2\cdot$	1.0×10^1	6.90×10^2	
	2,3-dimethyl butane chemistry:			
174)	$(CH_3)_2CHCH(CH_3)_2 + O(^3P) \rightarrow (CH_3)_2CHC(O_2\cdot)(CH_3)_2 + OH$	3.1×10^2	1.250×10^3	
175)	$(CH_3)_2CHCH(CH_3)_2 + OH \rightarrow 0.14(CH_3)_2CHCH(CH_3)CH_2O_2\cdot$ $+ 0.86\ (CH_3)_2CHC(O_2\cdot)(CH_3)_2$	9.3×10^3	-	
176)	$(CH_3)_2CHCH(CH_3)CH_2O_2\cdot + NO \rightarrow 0.9\ NO_2$ $+ 0.9\ (CH_3)_2CHCH(CH_3)CH_2O\cdot$ $+ 0.1\ (CH_3)_2CHCH(CH_3)CH_2ONO_2$	1.0×10^4	-	
177)	$(CH_3)_2CHCH(CH_3)CH_2O\cdot + O_2 \rightarrow HO_2\cdot + (CH_3)_2CHCH(CH_3)CHO$	1.0×10^1	6.90×10^2	
178)	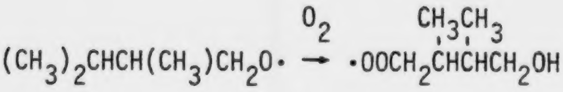 $(CH_3)_2CHCH(CH_3)CH_2O\cdot \xrightarrow{O_2} \cdot OOCH_2\overset{CH_3}{C}H\overset{CH_3}{C}HCH_2OH$	1.4×10^7	4.20×10^3	

Table A.1 (continued)

Reaction	Rate Constant	Activation Energy(K)	Note
2,3-dimethyl butane chemistry (continued)			
179) 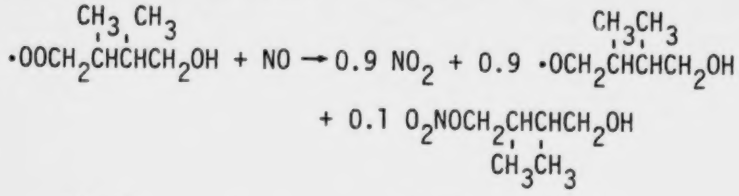 $\cdot OOCH_2\overset{CH_3}{C}H\overset{CH_3}{C}HCH_2OH + NO \rightarrow 0.9\,NO_2 + 0.9\,\cdot OCH_2\overset{CH_3}{C}H\overset{CH_3}{C}HCH_2OH + 0.1\,O_2NOCH_2\underset{CH_3}{C}H\underset{CH_3}{C}HCH_2OH$	$1.0\text{x}10^4$	-	
180) 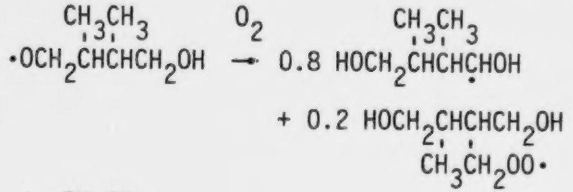 $\cdot OCH_2\overset{CH_3}{C}H\overset{CH_3}{C}HCH_2OH \xrightarrow{O_2} 0.8\,HOCH_2\overset{CH_3}{C}H\overset{CH_3}{C}H\underset{\cdot}{C}HOH + 0.2\,HOCH_2\underset{CH_3}{C}H\underset{CH_2OO\cdot}{C}HCH_2OH$	$1.4\text{x}10^7$	$4.200\text{x}10^3$	
181) 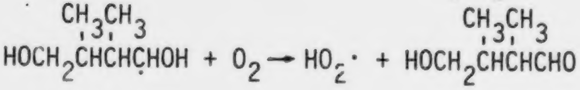 $HOCH_2\overset{CH_3}{C}H\overset{CH_3}{C}H\underset{\cdot}{C}HOH + O_2 \rightarrow HO_2\cdot + HOCH_2\overset{CH_3}{C}H\overset{CH_3}{C}HCHO$	$1.0\text{x}10^1$	$6.90\text{x}10^2$	
182) 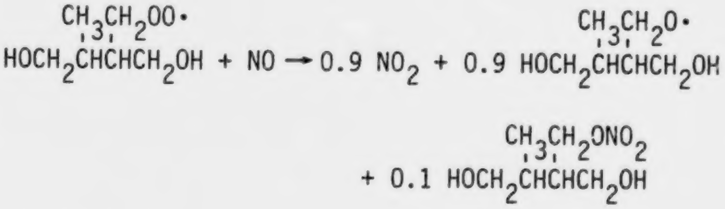 $HOCH_2\overset{CH_3}{C}H\overset{CH_2OO\cdot}{C}HCH_2OH + NO \rightarrow 0.9\,NO_2 + 0.9\,HOCH_2\overset{CH_3}{C}H\overset{CH_2O\cdot}{C}HCH_2OH + 0.1\,HOCH_2\overset{CH_3}{C}H\overset{CH_2ONO_2}{C}HCH_2OH$	$1.0\text{x}10^4$	-	
183) 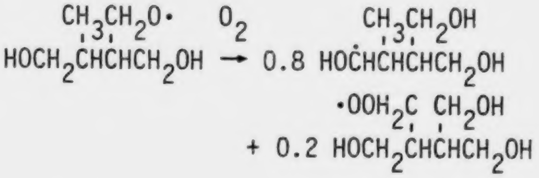 $HOCH_2\overset{CH_3}{C}H\overset{CH_2O\cdot}{C}HCH_2OH \xrightarrow{O_2} 0.8\,HO\dot{C}H\overset{CH_3}{C}H\overset{CH_2OH}{C}HCH_2OH + 0.2\,HOCH_2\overset{\cdot OOH_2C}{C}H\overset{CH_2OH}{C}HCH_2OH$	$1.4\text{x}10^7$	$4.200\text{x}10^3$	
184) 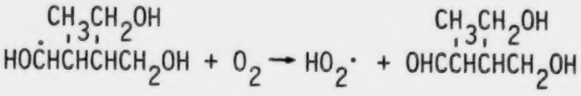 $HO\dot{C}H\overset{CH_3}{C}H\overset{CH_2OH}{C}HCH_2OH + O_2 \rightarrow HO_2\cdot + OHC\overset{CH_3}{C}H\overset{CH_2OH}{C}HCH_2OH$	$1.0\text{x}10^1$	$6.90\text{x}10^2$	
185) 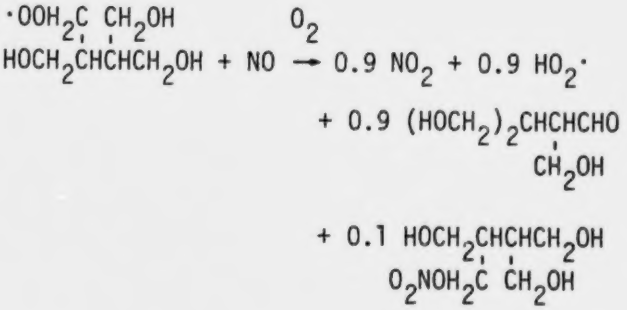 $HOCH_2\overset{\cdot OOH_2C}{C}H\overset{CH_2OH}{C}HCH_2OH + NO \xrightarrow{O_2} 0.9\,NO_2 + 0.9\,HO_2\cdot + 0.9\,(HOCH_2)_2CH\underset{CH_2OH}{C}HCHO + 0.1\,HOCH_2\underset{O_2NOH_2C}{C}H\underset{CH_2OH}{C}HCH_2OH$	$1.0\text{x}10^4$	-	

Table A.1 (continued)

Reaction	Rate Constant	Activation Energy	Note
2,3-dimethyl butane chemistry (continued)			
186) $(CH_3)_2CHC(O_2\cdot)(CH_3)_2 + NO \rightarrow 0.9\ NO_2$ $+ 0.9\ (CH_3)_2CHC(O\cdot)(CH_3)_2$ $+ 0.9\ (CH_3)_2CHC(ONO_2)(CH_3)_2$	$1.0x10^4$	-	
187) $(CH_3)_2CHC(O\cdot)(CH_3)_2 \xrightarrow{O_2} CH_3C(O)CH_3 + CH_3CH(O_2\cdot)CH_3$	$3.0x10^7$	$6.440x10^3$	
188) $CH_3CH(O_2\cdot)CH_3 + NO \rightarrow CH_3CH(ONO_2)CH_3$	$4.0x10^2$	-	
189) $CH_3CH(O_2\cdot)CH_3 + NO \rightarrow NO_2 + CH_3CH(O\cdot)CH_3$	$1.0x10^4$	-	
190) $CH_3CH(O\cdot)CH_3 + O_2 \rightarrow CH_3C(O)CH_3 + HO_2\cdot$	$4.4x10^1$	-	
Propionaldehyde chemistry:			
191) $C_2H_5CHO + OH \xrightarrow{O_2} H_2O + C_2H_5CO_3\cdot$	$2.8x10^4$	$-2.5x10^2$	
192) $C_2H_5CHO + NO_3 \xrightarrow{O_2} HNO_3 + C_2H_5CO_3\cdot$	$2.2x10^0$	-	
193) $C_2H_5CHO + h\nu \xrightarrow{O_2} C_2H_5O_2\cdot + HO_2\cdot + CO$	$8.4x10^{-4}k_{NO_2}$	-	
194) $C_2H_5CO_3\cdot + NO_2 \rightarrow C_2H_5CO_3NO_2$	$6.9x10^3$	-	
195) $C_2H_5CO_3\cdot + NO \xrightarrow{O_2} C_2H_5O_2\cdot + NO_2 + CO$	$1.1x10^4$	-	
196) $C_2H_5CO_3NO_2 \rightarrow C_2H_5CO_3\cdot + NO_2$	$2.2x10^{-2}$	$1.354x10^4$	
Butyraldehyde chemistry:			
197) $C_3H_7CHO + OH \xrightarrow{O_2} H_2O + C_3H_7CO_3\cdot$	$3.7x10^4$	-	
198) $C_3H_7CHO + NO_3 \xrightarrow{O_2} HNO_3 + C_3H_7CO_3\cdot$	$2.2x10^0$	-	

Table A.1 (continued)

Reaction	Rate Constant	Activation Energy	Note
Butyraldehyde chemistry (continued)			
199) $C_3H_7CHO + h\nu \xrightarrow{O_2} C_3H_7O_2\cdot + HO_2\cdot + CO$	$8.4\times10^{-4}k_{NO_2}$	-	
200) $C_3H_7CO_3\cdot + NO_2 \rightarrow C_3H_7CO_3NO_2$	6.9×10^{3}	-	
201) $C_3H_7CO_3\cdot + NO \xrightarrow{O_2} NO_2 + CO_2 + C_3H_7O_2\cdot$	1.1×10^{4}	-	
202) $C_3H_7CO_3NO_2 \rightarrow C_3H_7CO_3\cdot + NO_2$	2.2×10^{-2}	1.354×10^{4}	
203) $C_3H_7O_2\cdot + NO \rightarrow NO_2 + C_3H_7O\cdot$	1.1×10^{4}	-	
204) $C_3H_7O\cdot + NO \rightarrow C_3H_7ONO$	4.4×10^{4}	-	
205) $C_3H_7O\cdot + NO_2 \rightarrow C_3H_7ONO_2$	2.2×10^{4}	-	
206) $C_3H_7O\cdot + O_2 \rightarrow HO_2\cdot + C_2H_5CHO$	1.0×10^{1}	6.90×10^{2}	
Acetone chemistry:			
207) $CH_3C(O)CH_3 + OH \xrightarrow{O_2} H_2O + CH_3C(O)CH_2O_2\cdot$	4.1×10^{2}	1.230×10^{3}	
208) $CH_3C(O)CH_3 + h\nu \xrightarrow{O_2} CH_3CO_3\cdot + CH_3O_2\cdot$	$1.7\times10^{-4}k_{NO_2}$		
209) $CH_3C(O)CH_2O_2\cdot + NO \rightarrow CH_3C(O)CH_2O\cdot + NO_2$	1.0×10^{4}	-	
210) $CH_3C(O)CH_2O_2\cdot + NO \rightarrow CH_3C(O)CH_2ONO_2$	4.0×10^{2}	-	
211) $CH_3C(O)CH_2O\cdot + O_2 \rightarrow HO_2\cdot + CH_3C(O)CHO$	1.0×10^{1}	6.9×10^{2}	

Table A.1 (continued)

	Reaction	Rate Constant	Activation Energy	Note
MEK chemistry:				
212)	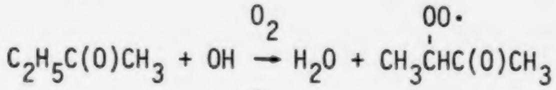 $C_2H_5C(O)CH_3 + OH \xrightarrow{O_2} H_2O + CH_3\overset{OO\cdot}{C}HC(O)CH_3$	8.1×10^2	-	
213)	$C_2H_5C(O)CH_3 + h\nu \xrightarrow{O_2} CH_3CO_3\cdot + C_2H_5O_2\cdot$	$1.7\times10^{-3}k_{NO_2}$	-	
214)	$C_2H_5C(O)CH_3 + OH \rightarrow H_2O + C_2H_5C(O)CH_2\cdot$	4.9×10^2	-	7
215)	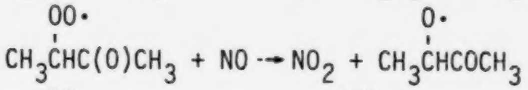 $CH_3\overset{OO\cdot}{C}HC(O)CH_3 + NO \rightarrow NO_2 + CH_3\overset{O\cdot}{C}HCOCH_3$	1.0×10^4	-	
216)	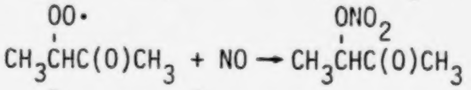 $CH_3\overset{OO\cdot}{C}HC(O)CH_3 + NO \rightarrow CH_3\overset{ONO_2}{C}HC(O)CH_3$	8.0×10^2	-	
217)	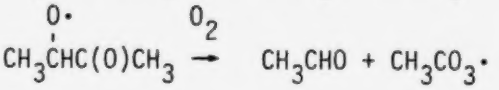 $CH_3\overset{O\cdot}{C}HC(O)CH_3 \xrightarrow{O_2} CH_3CHO + CH_3CO_3\cdot$	7.8×10^6	6.440×10^3	

* See Table 4

[1] Only one isomer is shown, even when many are possible.

[2] 298K, ppm-min units

Notes:

(1) These photolysis rates represent averages over zenith angles ranging from 30 to 60 degrees.

(2) Abstraction pathway neglected.

(3) 50/50 split of the two γ-dicarbonyls is assumed.

(4) 12 percent nitrate formation assumed.

(5) Reactions of glycolaldehyde are ignored.

(6) Hydroxy substituted aldehydes are assumed to react the same as un-substituted aldehydes.

(7) Reactions of the $C_2H_5C(O)CH_2\cdot$ species are neglected.

TABLE A.2

The Atkinson et al. (1982) Reaction Mechanism as Used in this Study[a]

REACTION	NUMBER	RATE CONSTANT[c]			KEY
		A	B	C	
NO2 + HV --> NO + O3	(01)	d	0	0.	2
NO + O3 --> NO2 + O2	(02)	1.0E+6	-1	1450.	1
O3 + H2O + HV --> 2 OH + O2	(03)	2.3E-8	1	0.	3
OH + NO --> HONO	(04)	8.7E+8	-2	0.	1
OH + NO2 --> HNO3	(05)	1.5E+9	-2	0.	1
HONO + HV --> OH + NO	(06)	0.17	1	0.	3
HO2 + NO --> OH + NO2	(07)	3.7E+6	-1	0.	1
HO2 + NO2 --> HNO4	(08)	1.5E+8	-2	0.	1
HNO4 --> HO2 + NO2	(09)	7.8E+15	0	10420.	1
HO2 + HO2 --> H2O2 + O2	(10)	3.4E+4	-1	-1100.	1
HO2 + HO2 + H2O --> H2O2 + O2	(11)	5.8E-5	-2	-5800.	1
H2O2 + HV --> 2 OH	(12)	7.1E-4	1	0.	3
OH + CO --> HO2	(13)	1.3E+5	-1	0.	1
NO2 + O3 --> NO3	(14)	5.3E+4	-1	2450.	1
NO + NO3 --> 2 NO2	(15)	8.4E+6	-1	0.	1
NO2 + NO3 --> N2O5	(16)	3.1E+7	-1	1100.	1
N2O5 --> NO2 + NO3	(17)	3.5E+18	0	12280.	1
N2O5 + H2O --> 2 HNO3	(18)	0.	-1	0.	1
NO3 + HV --> 0.3 NO + 0.7 NO2 + 0.7 O3	(19)	15.5	1	0.	3
OH + O3 --> HO2	(20)	7.0E+5	-1	940.	1
HO2 + O3 --> OH	(21)	4.8E+3	-1	580.	1
HCHO + HV --> 2 HO2 + CO	(22)	3.1E-3	1	0.	3
HCHO + HV --> CO + H2	(23)	3.0E-3	1	0.	3
OH + HCHO --> HO2 + CO	(24)	4.4E+6	-1	0.	1
ALD2 + HV --> MPOX + HO2 + CO	(25)	6.0E-4	1	0.	3
OH + ALD2 --> ACOX	(26)	3.0E+6	-1	-250.	1
ACOX + NO2 --> PAN	(26)	2.1E+6	-1	0.	1
PAN --> ACOX + NO2	(28)	1.2E+18	0	13543.	1
ACOX + NO --> NO2 + MPOX	(29)	3.1E+6	-1	0.	1
MPOX + NO --> HCHO + HO2 + NO2	(30)	3.1E+6	-1	0.	1
OH + PRPA --> PO2	(31)	6.6E+6	-1	680.	1
PO2 + NO --> HO2 + NO2 + ACET	(32)	3.1E+6	-1	0.	1
OH + ALKA --> AO2	(33)	6.6E+6	-1	400.	1
AO2 + NO --> 1.7 NO2 + 0.9 HO2 + 0.15 HCHO + 0.3 ALD2 + 0.1 RCHO + 0.30 ACET + 0.45 MEK - 0.8 NO	(34)	3.1E+6	-1	0.	1
OH + RCHO --> RCO3	(35)	9.2E+6	-1	0.	1
RCO3 + NO2 --> PPN	(36)	2.1E+6	-1	0.	1
PPN --> RCO3 + NO2	(37)	1.2E+18	0	13543.	1
RCO3 + NO --> ETO2 + NO2	(38)	3.1E+6	-1	0.	1
ETO2 + NO --> ALD2 + HO2 + NO2	(39)	3.1E+6	-1	0.	1
RCHO + HV --> ETO2 + CO + HO2	(40)	8.4E-4	1	0.	3
OH + MEK --> XO2	(41)	4.4E+6	-1	330.	1

TABLE A.2 (Continued)

		RATE CONSTANT[c]			
REACTION	NUMBER	A	B	C	KEY
XO2 + NO --> NO2 + ALD2 + ACOX	(42)	3.1E+6	-1	0.	1
MEK + HV --> ACOX + ETO2	(43)	1.7E-3	1	0.	3
ACET + HV --> ACOX + MPOX	(44)	1.7E-4	1	0.	3
OH + ETHE --> NO2 + HO2 + 2.0 HCHO - 1.0 NO	(45)	9.7E+5	-1	-380.	1
OH + PRPE --> NO2 + HO2 + 1.0 HCHO + 1.0 ALD2 - 1.0 NO	(46)	1.8E+6	-1	-540.	1
OH + BUTE --> 0.9 NO2 + 0.9 HO2 + 1.8 ALD2 - 1.0 NO	(47)	5.0E+6	-1	-540.	1
O3 + ETHE --> HCHO + 0.4 CHO2 + 0.4 CO + 0.12 HO2	(48)	4.2E+3	-1	2560.	1
O3 + PRPE --> 0.5 HCHO + 0.5 ALD2 + 0.2 CHO2 + 0.2 CD + 0.3 CO + 0.2 HO2 + 0.1 OH + 0.2 MPOX	(49)	3.1E+3	-1	1900.	1
O3 + BUTE --> ALD2 + 0.40 CD + 0.3 HO2 + 0.2 OH + 0.45 MPOX + 0.2 CO	(50)	3.3E+3	-1	1050.	1
CHO2 + NO --> HCHO + NO2	(51)	3.1E+6	-1	0.	1
CHO2 + NO2 --> HCHO + NO3	(52)	3.1E+5	-1	0.	1
CHO2 + H2O --> PROD	(53)	1.5E+0	-1	0.	1
CD + NO --> ALD2 + NO2	(54)	3.1E+6	-1	0.	1
CD + NO2 --> ALD2 + NO3	(55)	3.1E+5	-1	0.	1
CD + H2O --> PROD	(56)	1.5E+0	-1	0.	1
OH + BENZ --> 0.25 CRES + 0.25 HO2 + 0.75 ADD	(57)	5.3E+5	-1	0.	1
OH + TOLU --> 0.15 ARO2 + 0.20 CRES + 0.65 ADD + 0.20 HO2	(58)	2.7E+6	-1	0.	1
OH + XYEN --> 0.25 CRES + 0.25 HO2 + 0.75 ADD	(59)	1.0E+7	-1	0.	1
ADD + NO --> 0.75 NO2 + 0.75 HO2 + 0.75 DIAL + 0.75 MGLY	(60)	3.1E+6	-1	0.	1
OH + DIAL --> EL	(61)	1.3E+7	-1	0.	1
EL + NO2 --> ENO2	(62)	2.1E+6	-1	0.	1
ENO2 --> EL + NO2	(63)	1.2E+18	0	13543.	1
EL + NO --> 3 NO2 - 2 NO + B03*HO2+B03*GLY + B04*ACOX + B04*MGLY + B03*CO[b]	(64)	3.1E+6	-1	0.	1
OH + GLY --> HO2 + CO	(65)	8.8E+6	-1	0.	1
GLY + HV --> HCHO + CO	(66)	1.E-10	1	0.	3
OH + MGLY --> ACOX + CO	(67)	6.6E+6	-1	0.	1
MGLY + HV --> ACOX + HO2 + CO	(68)	0.15	1	0.	3
OH + CRES --> ADD2	(69)	1.9E+7	-1	0.	1
ADD2 + NO --> 0.75 NO2 + 0.75 HO2 + 0.75 DIAL	(70)	3.1E+6	-1	0.	1
NO3 + CRES --> HNO3 + PHEN	(71)	6.6E+6	-1	0.	1
PHEN + NO2 --> PRODN	(72)	6.6E+6	-1	0.	1
ARO2 + NO --> 0.75 NO2 + 0.75 HO2 + 0.75 ACHO	(73)	3.1E+6	-1	0.	1
ACHO + HV --> PROD	(74)	4.5E-3	1	0.	3
ACHO + OH --> ARC3	(75)	5.7E+6	-1	0.	1
ARC3 + NO2 --> PBZN	(76)	2.1E+6	-1	0.	1

TABLE A.2 (Continued)

REACTION					RATE CONSTANT[c]			
				NUMBER	A	B	C	KEY
PBZN	-->	ARC3	+ NO2	(77)	1.0E+17	0	13025.	1
ARC3 + NO	-->	PHO2	+ NO2	(78)	3.1E+6	-1	0.	1
PHO2 + NO	-->	PHEN	+ NO2	(79)	3.1E+6	-1	0.	1

Footnotes for Table A.2

(a) Mechanism documentation: Atkinson et al.(1979, 1982), Carter et al.(1979) A computer tape containing the reaction mechanism was obtained from F. Lurmann, Environmental Research and Technology, Inc., Westlake Village, California, on 8 July 1982. The original mechanism has been slightly modified for use in our study (see Section 3.4.1).

(b) See Section 3.4.1 for values of these coefficients.

(c) Reaction rate constants are of the form $k = A * TEMP^B * \exp(-C/TEMP)$ with units in terms of the ppm-min system. The explanation for the key is given in Table A.14.

(d) See Table 3.

TABLE A.3

Species Used in the Atkinson et al. (1982) Reaction Mechanism

NUMBER	CODE	SPECIES NAME
1	ACET	Acetone
2	ACHO	Benzaldehyde
3	ACOX	CH_3CO_3
4	ADD	OH-Aromatic-O_2 adducts
5	ADD2	OH-Aromatic-O_2 adducts
6	ALD2	Acetaldehyde
7	ALKA	>C3 alkanes
8	AO2	Alkyl peroxy radical
9	ARO2	Aromatic peroxy radical
10	ARC3	Peroxy benzoyl
11	BENZ	Benzene
12	BUTE	>C3 alkenes
13	CD	CH_3CHOO
14	CHO2	CH_2O_2
15	CO	Carbon monoxide
15	CONE	Wall source term for OH
17	CRES	Cresol
18	DIAL	Conjugated gamma dicarbonyls
19	EL	Radical formed from DIAL
20	ENO2	PAN analog from α-dicarbonyls
21	ETHE	Ethylene
22	ETO2	$C_2H_5O_2$
23	GLY	Glyoxal
24	HCHO	Formaldehyde
25	HNO3	Nitric acid
26	HNO4	Pernitric acid
27	HONO	Nitrous acid
28	HO2	Hydroperoxyl radical
29	H2O	Water vapor
30	H2O2	Hydrogen peroxide
31	MEK	Methylethylketone
32	MGLY	Methylglyoxal
33	MPOX	Methyl peroxy radical (CH_3O_2)
34	NO	Nitric oxide
35	NO2	Nitrogen dioxide
36	NO3	Nitrogen trioxide
37	N2O5	Nitrogen pentoxide
38	OH	Hydroxyl radical
39	O3	Ozone
40	PAN	Peroxyacetyl nitrate
41	PBZN	Peroxy Benzoyl nitrate
42	PHEN	Phenoxy Radical
43	PHO2	$C_6H_5O_2$ Radical
44	PO2	Propoxy Radical

TABLE A.3 (Continued)

NUMBER	CODE	SPECIES NAME
45	PPN	Higher PANS
46	PRPA	Propane
47	PRPE	Propylene
48	RCHO	C3-C5 aldehydes
49	RCO3	Acylperoxy
50	TOLU	Toluene
51	XO2	Peroxy radical
52	XYEN	>C7 aromatics

TABLE A.4

The Killus and Whitten (1982a) Reaction Mechanism as Used in this Study[a]

REACTION	NUMBER	RATE CONSTANT[b] A	B	C	KEY
NO2 + HV --> NO + O	(1)	c	0	0.	2
O --> O3	(2)	4.40E+6	0	0.	1
NO + O3 --> NO2 + O2	(3)	3.45E+3	0	1450.	1
NO2 + O3 --> NO3 + O2	(4)	1.79E+2	0	2450.	1
NO2 + O --> NO + O2	(5)	1.34E+4	0	0.	1
O3 + OH --> HO2 + O2	(6)	2.87E+1	0	1000.	1
O3 + HO2 --> OH + 2 O2	(7)	4.01E+2	0	1525.	1
OH + NO2 --> HNO3	(8)	1.60E+4	0	0.	1
OH + CO --> HO2	(9)	4.40E+2	0	0.	1
NO + NO --> 2 NO2	(10)	1.50E-4	0	0.	1
NO + NO3 --> 2 NO2	(11)	2.80E+4	0	0.	1
NO3 + NO2 + H2O --> 2 HNO3	(12)	5.56E-19	0	-10600.	1
NO + HO2 --> NO2 + OH	(13)	1.20E+4	0	0.	1
HO2 HO2 --> H2O2 + O2	(14)	1.50E+4	0	0.	1
X + PAR -->	(15)	1.00E+5	0	0.	1
OH + PAR --> MEO2 + H2O	(16)	8.51E+3	0	560.	1
O + OLE --> MEO2 + ACO3 + X	(17)	8.04E+3	0	325.	1
O + OLE --> CARB + PAR	(18)	8.04E+3	0	325.	1
OH + OLE --> RAO2	(19)	6.04E+3	0	-540.	1
O3 + OLE --> CARB + CRIG	(20)	4.70	0	1900.	1
O3 + OLE --> CARB + MCRG + X	(21)	4.70	0	1900.	1
O + ETH --> MEO2 + HO2 + CO	(22)	8.79E+3	0	800.	1
O + ETH --> CARB + PAR	(23)	8.79E+3	0	800.	1
OH + ETH --> RBO2	(24)	3.33E+3	0	-382.	1
O3 + ETH --> CARB + CRIG	(25)	1.29E+1	0	2560.	1
NO + ACO3 --> NO2 + MEO2 + CO2	(26)	1.04E+4	0	0.	1
NO + RBO2 --> NO2 + 2 CARB + HO2	(27)	1.20E+4	0	0.	1
NO + RAO2 --> NO2 + 2 CARB + HO2	(28)	1.20E+4	0	0.	1
NO + MEO2 --> NO2 + CARB + MEO2 + X	(29)	3.80E+3	0	0.	1
NO + MEO2 --> NO2 + CARB + HO2	(30)	7.70E+3	0	0.	1
NO + MEO2 --> NRAT	(31)	5.00E+2	0	0.	1
O3 + RBO2 --> 2 CARB + HO2 + O2	(32)	5.00	0	0.	1
O3 + RAO2 --> 2 CARB + HO2 + O2	(33)	2.00E+2	0	0.	1
OH + CARB --> CRO2 + X	(34)	5.00E+2	0	0.	1
OH + CARB --> HO2 + CO	(35)	7.00E+3	0	0.	1
OH + CARB --> ACO3 + X	(36)	6.00E+3	0	0.	1
CARB + HV --> CO + H2	(37)	1.0E-3	1	0.	3
CARB + HV --> 1.333 HO2 + CO + 0.667 MEO2 + 0.667 X	(38)	2.0E-3	1	0.	3
ACO3 + NO2 --> PAN	(39)	7.00E+3	0	0.	1
PAN --> ACO3 + NO2	(40)	1.04E+18	0	13500.	1
ACO3 + HO2 --> PRD1	(41)	1.50E+4	0	0.	1
MEO2 + HO2 --> PRD2	(42)	9.00E+3	0	0.	1
NO + CRIG --> NO2 + CARB	(43)	1.20E+4	0	0.	1

TABLE A.4 (Continued)

REACTION		RATE CONSTANT^{b}			
	NUMBER	A	B	C	KEY
NO2 + CRIG --> NO3 + CARB	(44)	8.00E+3	0	0.	1
CARB + CRIG --> OZD	(45)	2.00E+3	0	0.	1
NO + MCRG --> NO2 + CARB	(46)	1.20E+4	0	0.	1
NO2 + MCRG --> NO3 + CARB + PAR	(47)	8.00E+3	0	0.	1
CARB + MCRG --> OZD	(48)	2.00E+3	0	0.	1
CRIG --> CO + H2O	(49)	6.70E+2	0	0.	1
CRIG --> PRD3	(50)	2.40E+2	0	0.	1
CRIG --> 2 HO2 + CO2	(51)	9.00E+1	0	0.	1
MCRG --> PRD4	(52)	1.50E+2	0	0.	1
MCRG --> MEO2 + OH + CO	(53)	3.40E+2	0	0.	1
MCRG --> MEO2 + HO2 + CO2	(54)	4.25E+2	0	0.	1
MCRG --> 2 HO2 + CARB + CO	(55)	8.50E+1	0	0.	1
ARO + OH --> RARO + H2O	(56)	5.99E+4	0	600.	1
ARO + OH --> OPEN + HO2	(57)	5.55E+4	0	400.	1
RARO + NO --> NO2 + PHEN + HO2	(58)	4.00E+3	0	0.	1
OPEN + NO --> NO2 + DCRB + X + APRC	(59)	6.00E+3	0	0.	1
APRC --> DCRB + CARB + CO + X	(60)	1.00E+4	0	0.	1
APRC --> 2 CARB + 2 CO	(61)	1.00E+4	0	0.	1
PHEN + NO3 --> PHO + HNO3	(62)	5.00E+3	0	0.	1
PHO + NO2 --> NPHN	(63)	4.00E+3	0	0.	1
PHO + HO2 --> PHEN	(64)	5.00E+4	0	0.	1
OPEN + O3 --> DCRB + APRC + X	(65)	4.00E+1	0	0.	1
PHEN + OH --> HO2 + APRC + PAR + CARB	(66)	3.00E+4	0	0.	1
DCRB + HV --> HO2 + 0.5 ACO3 + 1.5 CO + 0.5 MEO2	(67)	4.0E-2	1	0.	3
PHEN + OH --> PHO	(68)	1.00E+4	0	0.	1
CRO2 + NO --> NO2 + CARB + ACO3 + X	(69)	1.20E+4	0	0.	1
DCRB + OH --> ACO3 + CO	(70)	7.00E+3	0	0.	1
HONO + HV --> OH + NO	(71)	1.80E-1	1	0.	3
NO + OH --> HONO	(72)	9.77E+3	0	0.	1
O3 + HV --> O1D	(73)	1.00E-3	1	0.	3
O1D --> O	(74)	4.44E+10	0	0.	1
O1D + H2O --> 2 OH	(75)	3.40E+5	0	0.	1

Footnotes for Table A.4

(a) Mechanism documentation: Killus and Whitten (1982a) and Whitten et al. (1980a,b). The reaction mechanism was coded from Table 3 of Killus and Whitten (1982a) with the photolysis rates and wall terms obtained from a computer listing supplied by J.P. Killus on 25 August 1982. Reactions 26, 48, 54, 60, 69 and 70 have been corrected to maintain the overall carbon balance. The original mechanism has been slightly modified to adapt it for use in our study. See Section 3.5.1 for details.

(b) Reaction rate constants are of the form $k = A * TEMP^{B} * \exp(-C/TEMP)$ with units in terms of the ppm-min system. The explanation for the key is given in Table A.14.

(c) See Table 3.

TABLE A.5

Species Used in the Killus and Whitten (1982a) Reaction Mechanism

NUMBER	CODE[a]	SPECIES NAME
1	ACO3 (2)	Peroxyacyl radical (Two-carbon surrogate for RCO3)
2	APRC (4)	Free radical
3	ARO (6)	Reactive aromatic rings
4	CO (1)	Carbon monoxide
5	CO2 (1)	Carbon dioxide
6	CRIG (1)	Criegee intermediate
7	CRO2 (2)	Peroxy radical
8	DCRB (3)	Highly photolytic alpha-dicarbonyl compounds including methyl glyoxal and biacetyl
9	ETH (2)	Slow double bonds that are almost exclusively ethylene
10	CARB (1)	Carbonyl compounds such as aldehydes and ketones
11	HNO3	Nitric acid
12	HONO	Nitrous acid
13	HO2	Hydroperoxy radical
14	H2	Hydrogen
15	H2O	Water vapor
16	H2O2	Hydrogen peroxide
17	MCRG (2)	Criegee intermediate
18	MEO2 (1)	Peroxy radical (one-carbon surrogate for RO2)
19	NO	Nitric oxide
20	NO2	Nitrogen dioxide
21	NO3	Nitrogen trioxide (nitrate radical)
22	NPHN (6)	Nitrophenol
23	NRAT (1)	Nitrate
24	OLE (2)	Relatively reactive double-bonded carbon molecules
25	O	Atomic oxygen O(3P)
26	OH	Hydroxyl radical
27	OPEN (6)	Bicyclic peroxy radical
28	O1D	Atomic oxygen O(1D)
29	O2	Molecular oxygen
30	O3	Ozone
31	OZD (2)	Ozonide
32	OZON (1)	Ozonide
33	PAN (2)	Peroxyacetyl nitrate
34	PAR (1)	Single-bonded carbon atoms whose principal constituent are paraffinic carbon molecules
35	PHEN (6)	Phenol

TABLE A.5 (Continued)

NUMBER	CODE	SPECIES NAME
35	PHO (6)	C_6H_5O Radical
36	RAO2 (2)	Peroxy radical
37	RARO (6)	Peroxy radical
38	RBO2 (2)	Peroxy radical
39	WNO3	Wall loss of NO_x species
40	X (-1)	Species introduced to maintain Carbon balance

Footnotes for Table A.5

(a) The values in brackets are the species carbon numbers

TABLE A.6

The Demerjian (1982) Reaction Mechanism as Used in this Study[a]

REACTION	NUMBER	RATE CONSTANT[b] A	B	C	KEY
NO2 + HV --> NO + O	(01)	c	0	0.	2
O2 + O + M --> O3 + M	(02)	3.90E-6	0	-510.	1
O3 + NO --> NO2 + O2	(03)	3.40E+3	0	1450.	1
O3 + NO2 --> NO3 + O2	(04)	1.77E+2	0	2450.	1
O3 + HV --> O1D + O2	(05)	2.77E-3	1	0.	3
O1D + M --> O + M	(06)	6.68E+4	0	0.	1
O1D + H2O --> 2 OH	(07)	4.14E+5	0	0.	1
NO3 + NO --> 2 NO2	(08)	2.96E+4	0	0.	1
NO3 + NO2 --> N2O5	(09)	1.36E+16	-4.6	0.	1
N2O5 --> NO3 + NO2	(10)	1.30E+16	0	9700.	1
N2O5 + H2O --> 2 HNO3	(11)	1.92E-5	0	0.	1
HONO + HV --> HO + NO	(12)	1.80E-1	1	0.	3
HO + CO --> HO2 + CO2	(13)	4.10E+2	0	0.	1
HO2 + NO2 --> HONO + O2	(14)	4.40E+0	0	0.	1
HO2 + NO --> HO + NO2	(15)	6.36E+3	0	-200.	1
HO2 + NO2 + M --> HO4N + M	(16)	2.63E-3	0	0.	1
HO4N --> HO2 + NO2	(17)	5.21E+15	0	10420.	1
HO + HONO --> NO2 + H2O	(18)	9.75E+3	0	0.	1
HO + NO2 + M --> HNO3 + M	(19)	1.54E-2	0	0.	1
HO + NO + M --> HONO + M	(20)	7.39E-3	0	0.	1
HO + HNO3 --> H2O + NO3	(21)	1.26E+2	0	0.	1
HO2 + O3 --> HO + 2 O2	(22)	2.07E+1	0	600.	1
HO + O3 --> HO2 + O2	(23)	2.81E+3	0	1000.	1
HO2 + HO2 --> H2O2 + O2	(24)	3.40E+3	0	0.	1
H2O2 + HV --> 2 HO	(25)	8.37E-4	1	0.	3
HC1 + O --> RO2 + HC3 + HO2	(26)	1.20E+4	0	0.	1
HC1 + O3 --> RO2 + HC3 + HO2	(27)	7.90E-2	0	0.	1
HC1 + HO --> RO2 + HC3	(28)	4.50E+4	0	0.	1
HC2 + HO --> RO2	(29)	5.10E+3	0	0.	1
HC3 + HV --> 0.5 RO2 + 1.5 HO2 + CO	(30)	1.60E-3	1	0.	3
HC3 + HO --> 0.3 R1O2 + 0.7 HO2 + 0.7 CO	(31)	1.95E+4	0	0.	1
RO2 + NO --> RO + NO2	(32)	1.10E+4	0	0.	1
RO + O2 --> HC3 + HO2	(33)	7.39E+2	0	2000.	1
R1O2 + NO2 --> PAN	(34)	2.07E+3	0	0.	1
PAN --> R1O2 + NO2	(35)	4.77E+16	0	12516.	1
RO + NO2 --> RNO3	(36)	1.00E+2	0	0.	1
RO2 + O3 --> RO + 2 O2	(37)	2.00E+0	0	0.	1
R1O2 + NO --> RO2 + NO2	(38)	4.00E+3	0	0.	1
HC4 + HO --> R2O2 + 2 HC3 + CO	(39)	2.70E+4	0	0.	1
R2O2 + NO --> R2O + NO2	(40)	1.10E+4	0	0.	1
R2O + O2 --> HC3 + HO2 + 2 CO	(41)	8.87E-1	0	0.	1
R2O2 + O3 --> R2O + 2 O2	(42)	2.00E+0	0	0.	1

TABLE A.6 (Continued)

		RATE CONSTANT[b]			
REACTION	**NUMBER**	**A**	**B**	**C**	**KEY**
R1O2 + O3 --> RO2 + 2 O2	(43)	2.00E+0	0	0.	1
HC3 + HV --> CO	(44)	2.0E-3	1	0.	3
HC1 + O3 --> COOH + HC3	(45)	8.80E-3	0	0.	1

Footnotes for Table A.6

(a) Mechanism Documentation: Demerjian (1982) and Schere (1983) A computer tape containing the reaction mechanism was obtained from K. Schere, U.S. Environmental Protection Agency, Research Triangle Park, North Carolina, on 16 June 1982. The original mechanism has been modified to adapt it for use in our study. See section 3.6.1 for details.

(b) Reaction rate constants are of the form $k = A * TEMP^{B} * \exp(-C/TEMP)$ with units in terms of the ppm-min system. The explanation for the key is given in Table A.14.

(c) See Table 3.

TABLE A.7

Species Used in the Demerjian (1982) Reaction Mechanism

NUMBER	CODE	SPECIES NAME
1	CO	Carbon monoxide
2	COOH	Criegee intermediate
3	CO2	Carbon dioxide
4	HC1	Olefins including C2H4
5	HC2	Alkanes (excluding methane)
6	HC3	Aldehydes
7	HC4	Aromatics
8	HNO3	Nitric acid
9	HO	Hydroxyl radical
10	HO4N	Pernitric acid
11	HONO	Nitrous acid
12	HO2	Hydroperoxyl radical
13	H2O	Water vapor
14	H2O2	Hydrogen peroxide
15	M	Third body for deactivation
16	NO	Nitric oxide
17	NO2	Nitrogen dioxide
18	NO3	Nitrogen trioxide (nitrate radical)
19	N2O5	Nitrogen pentoxide
20	O	Atomic oxygen
21	O1D	Singlet D oxygen
22	O2	Molecular oxygen
23	O3	Ozone
24	PAN	Peroxacetylnitrate
25	RNO3	Alkyl nitrate
26	RO	Alkoxyl radical
27	RO2	Alkylperoxy radical
28	R1O2	Peroxyacyl radical
29	R2O	Alkoxy radical
30	R2O2	Peroxy radical

TABLE A.8

The McRae and Seinfeld (1983) Reaction Mechanism as Used in this Study[a]

REACTION[b]	NUMBER	RATE CONSTANT[c]			KEY
		A	B	C	
NO2 + HV --> NO + O3P	(1)	h	0	0.	2
O3P + O2 + M --> O3 + M	(2)	0.346	-2	-510.	1
O3 + NO --> NO2 + O2	(3)	9.24E+05	-1	1450.	1
NO2 + O3P --> NO + O2	(4)	3.99E+06	-1	0.	1
NO + O3P --> NO2	(5)	1.67E+05	-1	-584.	1
NO2 + O3P --> NO3	(6)	1.07E+06	-1	0.	1
O3 + NO2 --> NO3 + O2	(7)	5.19E+04	-1	2450.	1
NO3 + NO --> 2NO2	(8)	8.05E+06	-1	0.	1
NO + OH --> HONO	(9)	5.07E+06	-1	0.	1
HONO + HV --> OH + NO	(10)	1.86E-01	1	0.	3
HO2 + NO2 --> HONO + O2	(11)	1.73E+01	-1	-1006.	1
HONO + OH --> NO2 + H2O	(12)	2.91E+06	-1	0.	1
NO2 + HO2 --> HO2NO2	(13)	1.73E+04	-1	-1006.	1
HO2NO2 --> HO2 + NO2	(14)	1.80E+15	0	9950.	1
HO2 + NO --> NO2 + OH	(15)	3.58E+06	-1	0.	1
RO2 + NO --> NO2 + RO	(16)	3.58E+06	-1	0.	1
RCO3 + NO --> NO2 + RO2 + CO2	(17)	1.13E+06	-1	0.	1
NO2 + OH --> HONO2	(18)	4.53E+06	-1	0.	1
CO + OH --> HO2 + CO2	(19)	1.31E+05	-1	0.	1
O3 + HV --> O3P + O2	(20)	6.84E-02	1	0.	3
HCHO + HV --> 2 HO2 + CO	(21)	4.81E-03	1	0.	3
HCHO + HV --> H2 + CO	(22)	8.73E-03	1	0.	3
HCHO + OH --> HO2 + H2O + CO	(23)	4.14E+06	-1	0.	1
RCHO + HV --> RO2 + HO2 + CO	(24)	4.28E-03	1	0.	3
RCHO + OH --> RCO3	(25)	2.75E+04	0	0.	1
C2H4 + OH --> RO2	(26)	1.16E+04	0	0.	1
C2H4 + O3P --> RO2 + HO2	(27)	1.22E+03	0	0.	1
OLE + OH --> RO2	(28)	8.19E+04	0	0.	1
OLE + O3P --> RO2 + RCO3	(29)	2.44E+04	0	0.	1
OLE + O3 --> A01*RCHO + A02*HCHO + A03*HO2 + A04*RO2 + A05*OH + A06*RO	(30)	1.79E-01	0	0.	1
ALK + OH --> RO2	(31)	5.83E+03	0	0.	1
ALK + O3P --> RO2 + OH	(32)	1.58E+02	0	0.	1
ARO + OH --> RO2 + RCHO	(33)	2.76E+04	0	0.	1
RO --> B01*HO2 + B02*HCHO + B03*RCHO + B04*RO2	(34)	2.0E+05	0	0.	1
RONO + HV --> NO + RO	(35)	2.2E-01	1	0.	3
RO + NO --> RONO	(36)	4.38E+06	-1	0.	1
RO + NO2 --> RONO2	(37)	2.19E+06	-1	0.	1
RO + NO2 --> RCHO + HONO	(38)	6.39E+02	0	0.	1
NO2 + RO2 --> RO2NO2	(39)	1.64E+06	-1	0.	1
NO2 + RO2 --> RCHO + HONO2	(40)	1.64E+03	-1	0.	1
RO2NO2 --> NO2 + RO2	(41)	1.80E+15	0	9950.	1

TABLE A.8 (Continued)

REACTION[b]	NUMBER	RATE CONSTANT[c] A	B	C	KEY
RCO3 + NO2 --> PAN	(42)	6.17E+05	-1	0.	1
PAN --> RCO3 + NO2	(43)	4.77E+16	0	12516.	1
NO2 + NO3 --> N205	(44)	2.20E+06	-1	0.	1
N205 --> NO2 + NO3	(45)	3.44E+016	0	10600.	1
H20 + N205 --> 2 HONO2	(46)	4.47E-03	-1	0.	1
03 + OH --> HO2 + 02	(47)	6.62E+05	-1	1000.	1
03 + HO2 --> OH + 2 02	(48)	4.85E+03	-1	580.	1
03 --> WALL	(49)	0.	0	0.	1
HO2 + HO2 --> H2O2 + 02	(50)	7.45E+03	0	0.	1
H2O2 + HV --> 2 OH	(51)	2.89E-03	1	0.	3
RO2 + RO2 --> 2 RO	(52)	2.04E+04	-1	-223.	1

Footnotes for Table A.8

(a) Mechanism documentation: Falls and Seinfeld (1978) Falls et al. (1979), McRae et al. (1982b) and McRae and Seinfeld (1983). (15 November 1982) The original mechanism has been slightly modified to adapt it for our study. See Section 3.7.1 for details.

(b) In two reactions (30,34) the product stoichiometry varies as a function concentration. The functional forms for the coefficients A01 - A06 and B01-B04 are given by:

A01 = 0.5 A02 = 0.5 A03 = 0.304
A04 = 0.306 A05 = 0.136 A06 = 0.034

and

B01 = 1.0 B02 = 0.5 B03 = 0.5
B04 = (1-B01) = 0.0

(c) Reaction rate constants are of the form $k = A * TEMP^{b} * \exp(-C/TEMP)$ with units in terms of the ppm-mim system. The key is explained in Table A.14.

(d) $k_{37}/(k_{37} + k_{38}) = 0.92$ for CH_3, $k_{38} = 0.087\ k_{37}$

(e) Rate constants for reactions 39 and 40 are based on the assumption that $k_{16}/(k_{39} + k_{40}) = 2.2$.

(f) Rate constant for reaction 18 determined from

$$1.477x10^{15}x10^{-(11.6T/(17.4+T))}SQRT(280/T)$$

Footnotes for Table A.8 (Continued)

(g) Rate constant for reaction 50 determined from

$$k_{50} = \frac{3.4\text{x}10^{4}}{T}\exp(1100/T) + \frac{5.8\text{x}10^{-5}}{T^{2}}\exp(5800/T)[H_2O]$$

at 298 °K, $[H_2O = 15500$ ppm$]$ $k_{50} = 7.45\text{x}10^{3}$

(h) See Table 3.

TABLE A.9

Species Used in the McRae and Seinfeld (1983) Reaction Mechanism

NUMBER	CODE	SPECIES NAME
1	ALK	Alkanes (excluding CH4)
2	ARO	Aromatics
3	CO	Carbon monoxide
4	CO2	Carbon dioxide
5	ETH	Ethylene (C2H4)
6	HCHO	Formaldehyde
7	HNO2	Nitrous acid
8	HNO3	Nitric acid
9	HNO4	Pernitric acid
10	HO2	Hydroperoxyl radical
11	H2	Hydrogen
12	H2O	Water vapor
13	H2O2	Hydrogen peroxide
14	M	Third body for collisional deactivation
15	NO	Nitric oxide
16	NO2	Nitrogen dioxide
17	NO3	Nitrogen trioxide
18	N2O5	Dinitrogen pentoxide
19	OLE	Olefins excluding ethylene
20	O	Atomic oxygen (O(3P))
21	OH	Hydroxyl radical
22	O2	Molecular oxygen
23	O3	Ozone
24	PAN	Peroxacetylnitrate
25	RCHO	Higher aldehydes
26	RCO3	Peroxyacyl radical
27	RO	Alkoxyl radical
28	RONO	Alkyl nitrite
29	RNO4	Peroxyalkyl nitrate
30	RO2	Alkylperoxy radical
31	RNO3	Alkyl nitrate
32	WALL	Wall loss term

TABLE A.10

The Penner and Walton (1982) Reaction Mechanism as Used in this Study[a]

REACTION							NUMBER	RATE CONSTANT[b] A	 B	 C	KEY
:											
:	Inorganic reactions (R1 - R23)										
:											
O	+ O2	+ M	-->	O3	+ M		(01)	3.90E-6	0	-510.	1
O3	+ NO		-->	NO2	+ O2		(02)	1.01E+6	-1	1450.	1
O	+ NO		-->	NO2			(03)	1.59E+7	-1.5	0.	1
O	+ NO2		-->	NO	+ O2		(04)	4.09E+6	-1	0.	1
O	+ NO2		-->	NO3			(05)	2.05E+8	-2	0.	1
O3	+ NO2		-->	NO3	+ O2		(06)	5.28E+4	-1	2450.	1
NO3	+ NO2		-->	N2O5			(07)	6.05E+4	-0.7	0.	1
		N2O5	-->	NO2	+ NO3		(08)	2.16E+18	-0.7	11180.	1
NO3	+ NO		-->	2 NO2			(09)	8.80E+6	-1	0.	1
N2O5	+ H2O		-->	2 HNO3[c]			(10)	1.32E-3	-1	0.	1
HO	+ NO2		-->	HNO3			(11)	8.67E+7	-1.5	0.	1
HO	+ NO		-->	HNO2			(12)	4.99E+7	-1.5	0.	1
HO	+ CO		-->	HO2			(13)	1.19E+5	-1	0.	1
HO2	+ NO		-->	HO	+ NO2		(14)	1.54E+6	-1	-250.	1
HNO2	+ HO		-->	NO2			(26)	2.90E+6	-1	0.	1
HO2	+ HO2		-->	H2O2	+ O2		(27)	3.70E+4	-1	-1250.	1
HO	+ HO2		-->	H2O	+ O2		(36)	3.52E+7	-1	0.	1
HO	+ H2O2		-->	HO2			(72)	7.04E+5	-1	0.	1
HO	+ HNO4		-->	H2O	+ NO2	+ O2	(93)	1.76E+6	-1	0.	1
		HNO4	-->	HO2	+ NO2		(84)	3.00E+16	0	10720.	1
HO2	+ NO2		-->	HNO4			(34)	6.23E+15	-5	0.	1
HO	+ O3		-->	HO2			(48)	7.04E+5	-1	940.	1
HO2	+ O3		-->	HO			(49)	4.84E+3	-1	580.	1
:											
:	Reactions of HC1 (Alkenes, isoprene and mono-terpenes)										
:											
HC1	+ HO		-->	RO2	+ HC4		(17)	1.76E+7	-1	120.	1
HC1	+ O3		-->	HO2	+ HC4		(16)	1.54E+3	-1	1900.	1
HC1	+ O3		-->	HC4			(47)	1.54E+3	-1	1900.	1
HC1	+ O		-->	RO2	+ RCO3		(15)	4.40E+6	-1	360.	1
HC1	+ NO3		-->	RO2	+ RNO3		(40)	4.40E+5	-1	1400.	1
:											
:	Reactions of HC2 (Alkanes)										
:											
HC2	+ HO		-->	RO2	+ H2O		(19)	2.20E+7	-1	900.	1
HC2	+ O		-->	RO2	+ HO		(18)	7.04E+6	-1	2000.	1
:											
:	Reactions of HC4 (Aldehydes and Ketones)										
:											
HC4	+ HO		-->	RCO3	+ H2O		(20)	3.52E+6	-1	0.	1
HC4	+ HO		-->	CO	+ HO2	+ H2O	(37)	3.43E+6	-1	150.	1
HC4	+ NO3		-->	RCO3	+ HNO3		(35)	1.32E+3	-1	200.	1

TABLE A.10 (Continued)

REACTION	NUMBER	RATE CONSTANT^b A	B	C	KEY
:					
: Reactions of HC3 (Aromatics)					
:					
HC3 + HO --> BRO2OHHH	(86)	1.76E+6	-1	0.	1
HC3 + HO --> HO2	(87)	1.06E+6	-1	0.	1
NO + BRO2OHHH --> HO2 + MGLY + NO2	(88)	8.80E+7	-1	0.	1
HO + MGLY --> H2O + RCO3 + CO	(91)	7.04E+6	-1	0.	1
:					
: Reactions of Organic Radicals					
:					
RCO3 + HO2 --> RO2H	(41)	2.64E+6	-1	0.	1
RCO3 + NO --> RO2 + NO2	(22)	1.13E+6	-1	0.	1
RCO3 + NO2 --> PAN	(23)	5.98E+5	-1	0.	1
PAN --> NO2 + RCO3	(43)	4.74E+16	0	12516.	1
RO2 + NO --> RO + NO2	(21)	3.08E+6	-1	0.	1
HO2 + RO2 --> RO2H + O2	(28)	1.19E+6	-1	0.	1
RO2 + RO2 --> 2 RO + O2	(29)	1.76E+5	-1	0.	1
RO2 + O3 --> RO + O2	(38)	4.84E+3	-1	580.	1
RO + O2 --> HO2 + HC4	(24)	2.20E+5	-1	2000.	1
RO + NO2 --> RNO3	(25)	4.40E+6	-1	0.	1
:					
: These terms are the Photolysis reaction steps (J1 - J12)					
:					
NO2 + HV --> NO + O	(51)	d	0	0.	2
O3 + HV --> O + O2	(58)	5.71E-2	1	0.	3
O3 + HV --> O2 + 2 HO	(59)	6.20E-4	1	0.	3
HNO2 + HV --> HO + NO	(52)	2.20E-2	1	0.	3
H2O2 + HV --> 2 HO	(53)	1.18E-3	1	0.	3
NO3 + HV --> NO2 + O	(57)	1.56E+1	1	0.	3
NO3 + HV --> NO + O2	(83)	1.90	1	0.	3
N2O5 + HV --> 2 NO2 + O	(60)	3.90E-6	1	0.	3
HC4 + HV --> CO	(42)	1.50E-3	1	0.	3
HC4 + HV --> CO + 2 HO2	(50)	1.20E-3	1	0.	3
HC4 + HV --> RO2 + HO2 + CO	(54)	1.20E-3	1	0.	3
MGLY + HV --> RCO3 + HO2 + CO	(90)	5.05E-2	1	0.	3

Footnotes for Table A.10

(a) Mechanism Documentation: Gelinas et al. (1974), Luther and Gelinas (1976), Gelinas and Skewes-Cox (1975), MacCracken and Sauter eds. (1975) and Penner and Walton (1982). A computer tape containing the reaction mechanism was obtained from J. Penner, Lawrence Livermore National Laboratory, Livermore, California, on 2 July 1982. Some minor modifications have been made to adapt this mechanism to our study. See Section 3.8.1 for details.

(b) Reaction rate constants are of the form $k = A * TEMP^B * \exp(-C/TEMP)$ with units in terms of the ppm-min system. Note that the values used in this table have been converted from the cgs system reported in Penner and Walton (1982). The key is explained in Table A.14.

(c) HNO_3, RNO_2, RNO_3, RO_2H, Wall, H_2O, M, and O_2 are not calculated in the PW mechanism.

(d) See Table 3.

TABLE A.11

Species Used in the Penner and Walton (1982) Reaction Mechanism

NUMBER	CODE	SPECIES NAME
1	BRO2OHHH	Oxygenated aromatic radical
2	CO	Carbon monoxide
3	HC1	Alkenes, isoprene and mono-terpenes
4	HC2	Alkanes
5	HC3	Aromatics
6	HC4	Aldehydes and ketones
7	HNO2	Nitrous acid
8	HNO3	Nitric acid
9	HNO4	Peroxy nitric acid
10	HO	Hydroxyl radical
11	HO2	Hydroperoxyl radical
12	H2O	Water vapor
13	H2O2	Hydrogen peroxide
14	M	Third body for deactivation
15	MGLY	Methylglyoxal
16	NO	Nitric Oxide
17	NO2	Nitrogen Dioxide
18	NO3	Nitrogen trioxide (nitrate radical)
19	N2O5	Dinitrogen pentoxide
20	O	Atomic oxygen
21	O2	Molecular oxygen
22	O3	Ozone
23	PAN	Peroxactyl nitrate
24	RCO3	Peroxyacyl radical
25	RNO2	Alkyl nitrite
26	RNO3	Alkyl nitrate
27	RO	Alkoxyl radical
28	RO2	Alkylperoxy radical
29	RO2H	Peroxide
30	WALL	Loss term

TABLE A.12

The Dodge (1977) Reaction Mechanism as Used in this Study[a]

REACTION	NUMBER	RATE CONSTANT[b] A	B	C	KEY
NO2 + HV --> NO + O	(1)	c	0	0.	2
O + O2 + M --> O3 + M	(2)	2.0E-5	0	0.	1
NO + O3 --> NO2	(3)	25.0	0	0.	1
O3 + NO2 --> NO3	(4)	0.045	0	0.	1
O + NO2 --> NO	(5)	1.3E+4	0	0.	1
NO + NO3 --> 2 NO2	(6)	1.3E+4	0	0.	1
NO3 + NO2 --> N2O5	(7)	5.6E+3	0	0.	1
N2O5 --> NO2 + NO3	(8)	22.0	0	0.	1
H2O + N2O5 --> 2 WHNO3	(9)	2.5E-6	0	0.	1
NO2 + NO + H2O --> 2 HONO	(10)	1.0E-9	0	0.	1
HONO + HONO --> NO + NO2	(11)	1.0E-3	0	0.	1
HONO + HV --> OH + NO	(12)	1.8E-1	1	0.	3
NO2 + OH --> HNO3	(13)	8.0E+3	0	0.	1
NO + OH --> HONO	(14)	3.0E+3	0	0.	1
NO + HO2 --> NO2 + OH	(15)	1.2E+3	0	0.	1
HO2 + HO2 --> HOOH + O2	(16)	8.4E+3	0	0.	1
HOOH + HV --> 2 OH	(17)	2.4E-3	1	0.	3
O3 + HV --> O1D	(18)	2.71E-3	1	0.	3
O3 + HV --> O	(19)	5.43E-3	1	0.	3
O1D + M --> O + M	(20)	8.7E+4	0	0.	1
O1D + H2O --> 2 OH	(21)	5.1E+5	0	0.	1
O3 + OH --> HO2 + O2	(22)	84.0	0	0.	1
HO2 + O3 --> OH	(23)	2.4	0	0.	1
OH + PROP --> ADD	(24)	2.5E+4	0	0.	1
NO + ADD --> X + NO2	(25)	1.0E+3	0	0.	1
ADD + ADD --> 2 X	(26)	1.2E+4	0	0.	1
MEO2 + ADD --> X + MEO	(27)	1.0E+3	0	0.	1
C2O2 + ADD --> X + C2O	(28)	1.0E+3	0	0.	1
C3O2 + ADD --> X + C3O	(29)	1.0E+3	0	0.	1
X --> HCHO + ALD2 + HO2	(30)	1.0E+5	0	0.	1
O3 + PROP --> OH + HO2 + ALD2	(31)	8.0E-3	0	0.	1
O3 + PROP --> OH + C2O3 + HCHO	(32)	8.0E-3	0	0.	1
OH + BUT --> SCO2	(33)	1.8E+3	0	0.	1
OH + BUT --> C4O2	(34)	1.8E+3	0	0.	1
C4O2 + NO --> NO2 + C4O	(35)	1.8E+3	0	0.	1
SCO2 + NO --> NO2 + SCO	(36)	1.8E+3	0	0.	1
C3O2 + NO --> NO2 + C3O	(37)	1.8E+3	0	0.	1
C2O2 + NO --> NO2 + C2O	(38)	1.8E+3	0	0.	1
MEO2 + NO --> NO2 + MEO	(39)	1.8E+3	0	0.	1
C4O --> HCHO + C3O2	(40)	7.5E+4	0	0.	1
SCO --> ALD2 + C2O2	(41)	1.0E+5	0	0.	1
C3O --> HCHO + C2O2	(42)	8.0E+3	0	0.	1

TABLE A.12 (Continued)

		RATE CONSTANT[b]			
REACTION	NUMBER	A	B	C	KEY
C20 --> HCHO + MEO2	(43)	4.0E+3	0	0.	1
C40 + O2 --> ALD4 + HO2	(44)	0.7	0	0.	1
SCO + O2 --> MEK + HO2	(45)	1.4	0	0.	1
C30 + O2 --> ALD3 + HO2	(46)	0.5	0	0.	1
C20 + O2 --> ALD2 + HO2	(47)	0.4	0	0.	1
MEO + O2 --> HCHO + HO2	(48)	0.4	0	0.	1
HCHO + HV --> PROD	(49)	8.57E-3	1	0.	3
HCHO + HV --> 2 HO2	(50)	2.85E-3	1	0.	3
OH + HCHO --> HO2 + CO	(51)	1.5E+4	0	0.	1
ALD2 + HV --> PROD	(52)	1.2E-5	1	0.	3
ALD2 + HV --> MEO2 + HO2	(53)	2.8E-5	1	0.	3
OH + ALD2 --> C203	(54)	1.5E+4	0	0.	1
ALD3 + HV --> PROD	(55)	1.71E-4	1	0.	3
ALD3 + HV --> C202 + HO2	(56)	7.14E-3	1	0.	3
OH + ALD3 --> C303	(57)	4.5E+4	0	0.	1
ALD4 + HV --> PROD	(58)	1.71E-4	1	0.	3
ALD4 + HV --> C302 + HO2	(59)	5.42E-3	1	0.	3
OH + ALD4 --> C403	(60)	4.5E+4	0	0.	1
C402 + ADD --> X + C40	(61)	1.0E+3	0	0.	1
SCO2 + ADD --> X + SCO	(62)	1.0E+3	0	0.	1
NO + C403 --> C302 + NO2	(63)	8.0E+2	0	0.	1
NO + C303 --> C203 + NO2	(64)	8.0E+2	0	0.	1
NO + C203 --> MEO2 + NO2	(65)	8.0E+2	0	0.	1
NO2 + C403 --> PAN	(66)	1.0E+2	0	0.	1
NO2 + C303 --> PAN	(67)	1.0E+2	0	0.	1
NO2 + C203 --> PAN	(68)	1.0E+2	0	0.	1
HO2 + C402 --> PROD	(69)	4.0E+3	0	0.	1
HO2 + C302 --> PROD	(70)	4.0E+3	0	0.	1
HO2 + SCO2 --> PROD	(71)	4.0E+3	0	0.	1
HO2 + C202 --> PROD	(72)	4.0E+3	0	0.	1
HO2 + MEO2 --> PROD	(73)	4.0E+3	0	0.	1
HO2 + C403 --> PROD	(74)	4.0E+3	0	0.	1
HO2 + C303 --> PROD	(75)	4.0E+3	0	0.	1
HO2 + C203 --> PROD	(76)	4.0E+3	0	0.	1

Footnotes for Table A.12

(a) Mechanism Documentation: Dodge (1977) and Durbin et al. (1975) The actual coding for the reactions and the rate constants were derived from the computer program: OZIPP - Isopleth Plotting Plotting Program obtained from H.L. Jeffries on 20 November 1982.

(b) Reaction rate constants are of the form $k = A * \mathrm{TEMP}^{B} * \exp(-C/\mathrm{TEMP})$ with units in terms of the ppm-min system. The key is explained in Table A.14.

(c) See Table 3.

TABLE A.13

Species Used in the Dodge (1977) Reaction Mechanism

NUMBER	CODE	SPECIES NAME
1	ADD	$CH_3CH(OH)CH_2OO$
2	ALD2	CH_3CHO
3	ALD3	CH_3CH_2CHO
4	ALD4	$CH_3CH_2CH_2CHO$
5	BUT	n-Butane (n-C_4H_{10})
6	C2O	CH_3CH_2O
7	C2O2	$CH_3CH_2O_2$
8	C2O3	$CH_3C(O)O_2$
9	C3O	$CH_3CH_2CH_2O$
10	C3O2	$CH_3CH_2CH_2O_2$
11	C3O3	$CH_3CH_2C(O)O_2$
12	C4O	$CH_3CH_2CH_2CH_2O$
13	C4O2	$CH_3CH_2CH_2CH_2O_2$
14	C4O3	$CH_3CH_2CH_2C(O)O_2$
15	HCHO	Formaldehyde
16	HNO3	Nitric acid
17	HONO	Nitrous acid
18	HO2	Hydroperoxyl radical
19	H2O	Water vapor
20	HOOH	Hydrogen peroxide
21	M	Third body
22	MEK	Methyl ethyl ketone
23	MEO	Methoxy radical
24	MEO2	Methyl peroxy radical
25	NO	Nitric oxide
26	NO2	Nitrogen dioxide
27	NO3	Nitrogen trioxide (nitrate radical)
28	N2O5	Nitrogen pentoxide
29	O	Atomic oxygen $O(^3P)$
30	OH	Hydroxyl radical
31	O1D	Singlet D oxygen
32	O2	Molecular oxygen
33	O3	Ozone
34	PAN	Peroxyacetyl nitrate
35	PROP	Propylene
36	SCO	$CH_3CH(O)CH_2CH_3$
37	SCO2	$CH_3CH(O_2)CH_2CH_3$
38	PROD	Stable products
39	X	$CH_3CH(OH)CH_2O$

TABLE A.14

KEY	RATE CONSTANT FORMAT
1	$k = A*TEMP^{B}*EXP(- C/T)$
2	Rate constant specified externally, this form is usually only used for photolysis steps.
3	Rate constant expressed as a proportion of another rate constant so that K = A*K(B) where B identifies the reaction number.

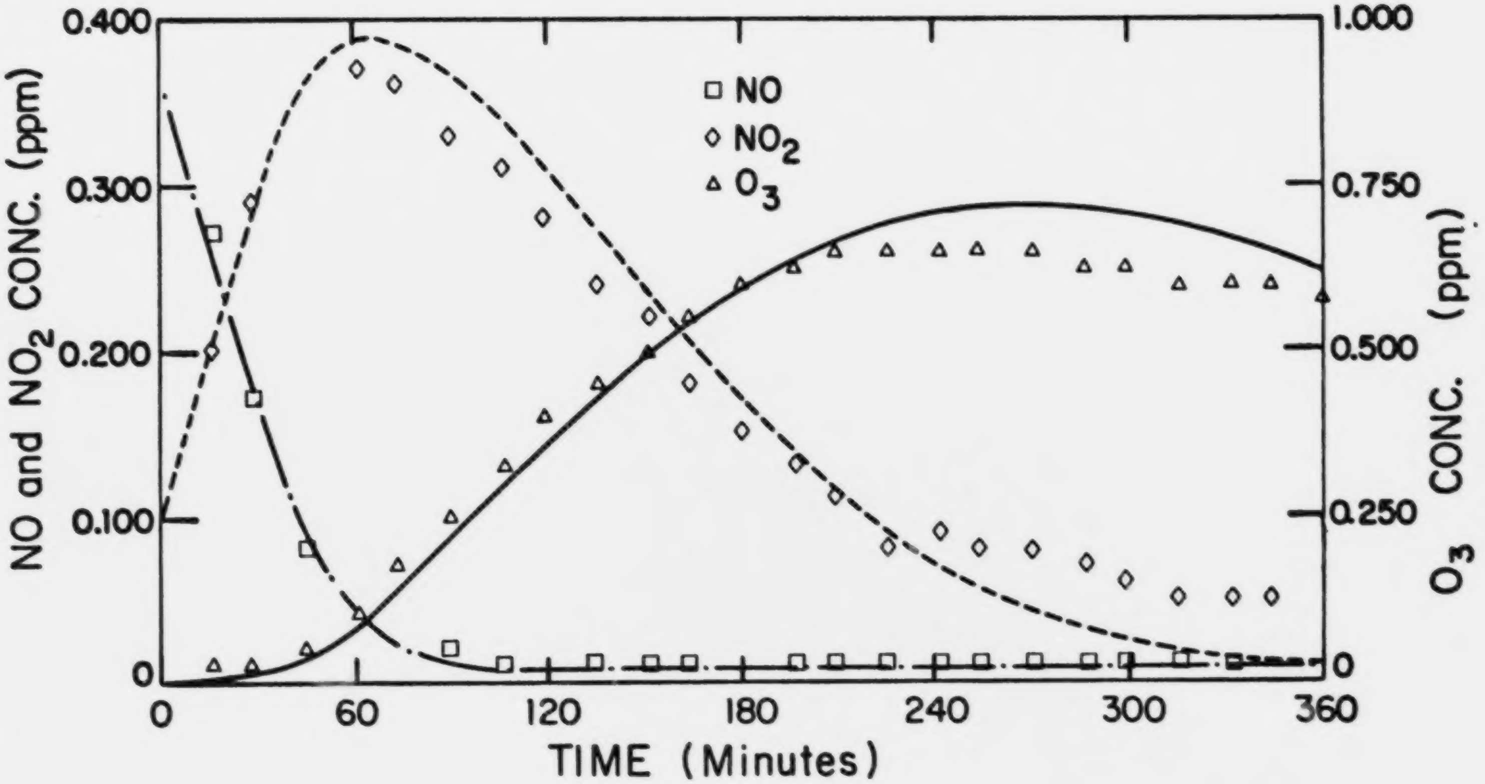

Figure Ala. Observed and Calculated Concentration-Time Profiles for 7-Hydrocarbon-NO$_x$ Experiment EC-237

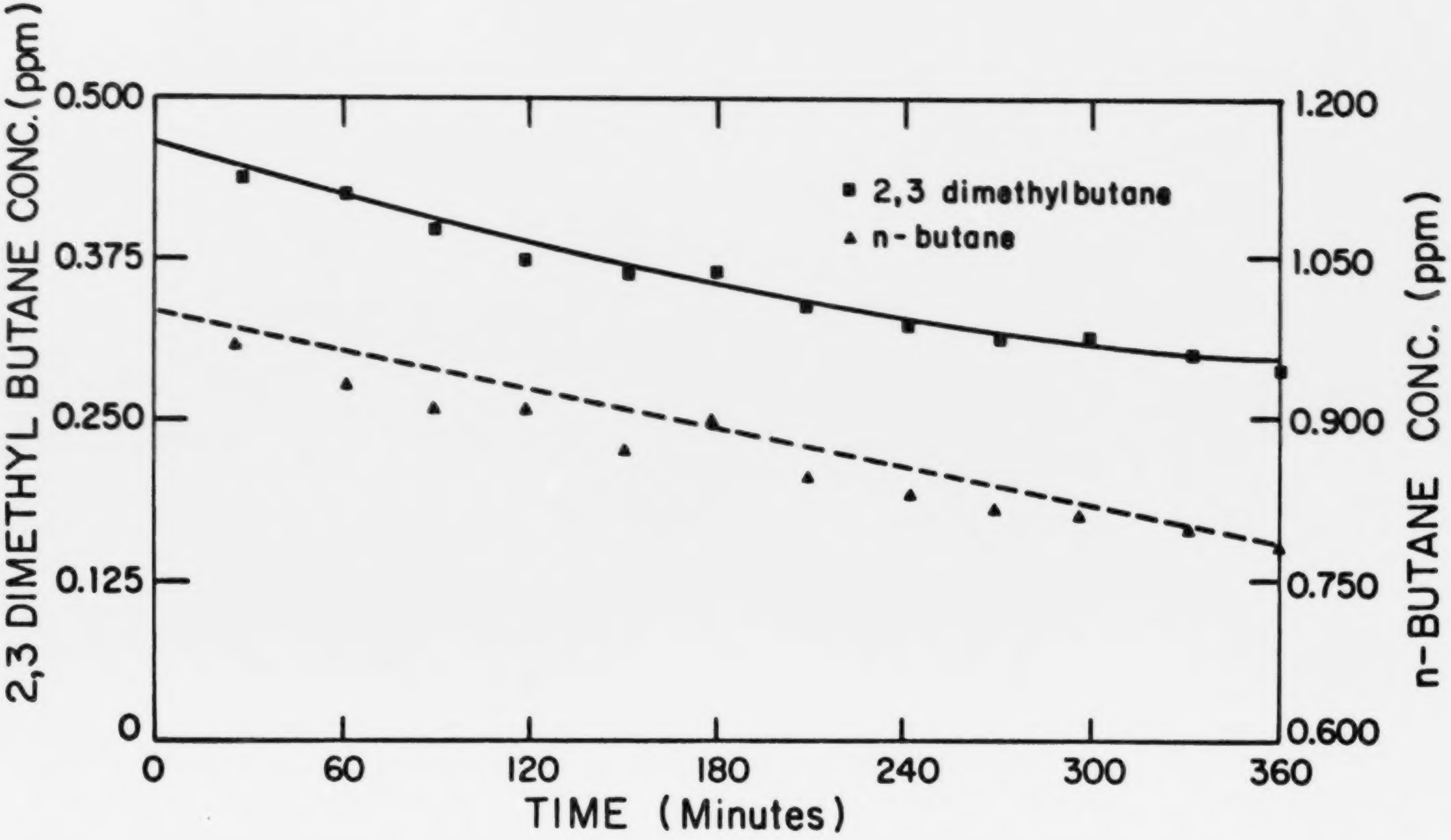

Figure A1b. Observed and Calculated Concentration-Time Profiles for 7-Hydrocarbon-NO_x Experiment EC-237

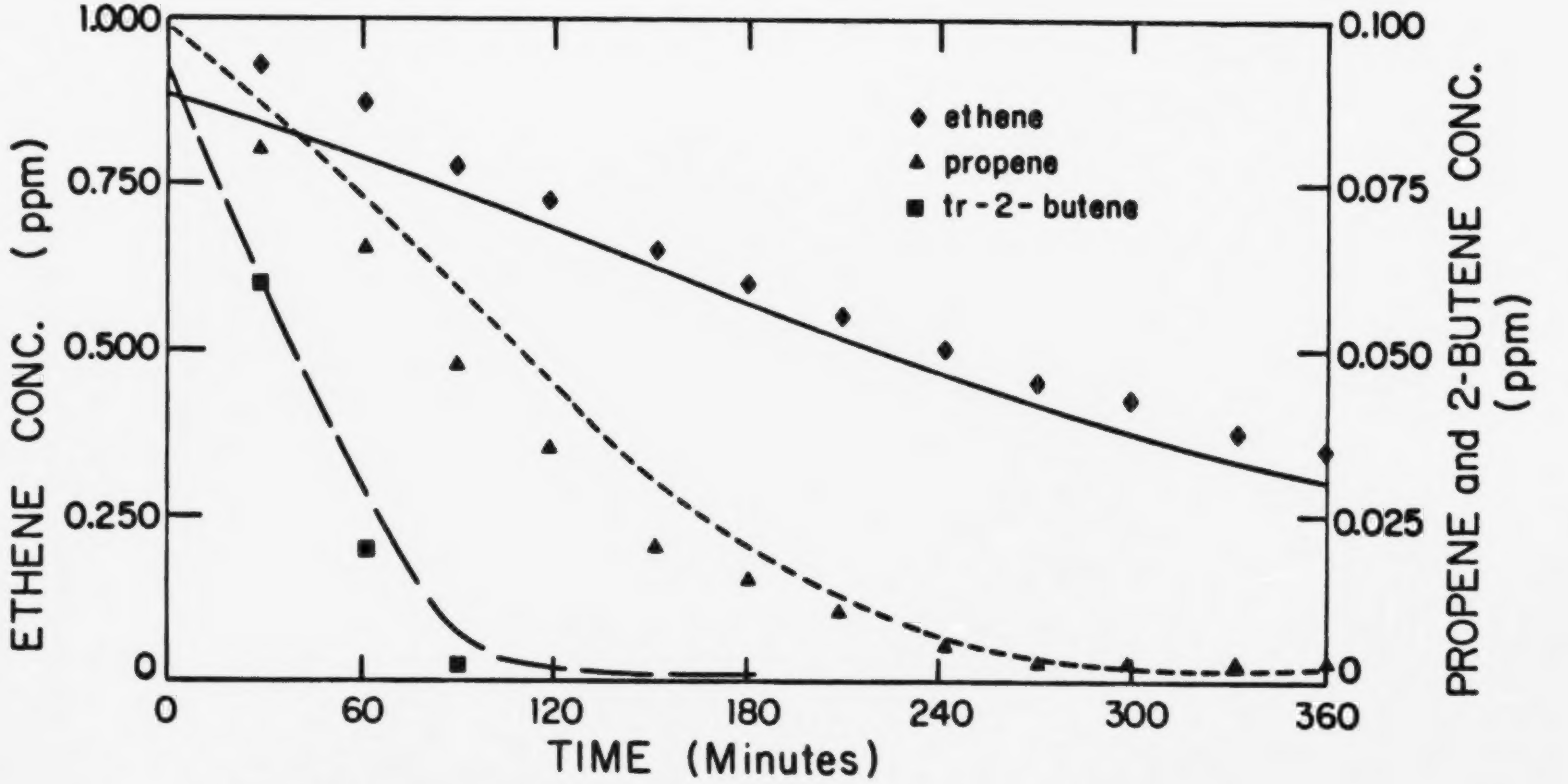

Figure A1c. Observed and Calculated Concentration-Time Profiles for 7-Hydrocarbon-NO_x Experiment EC-237

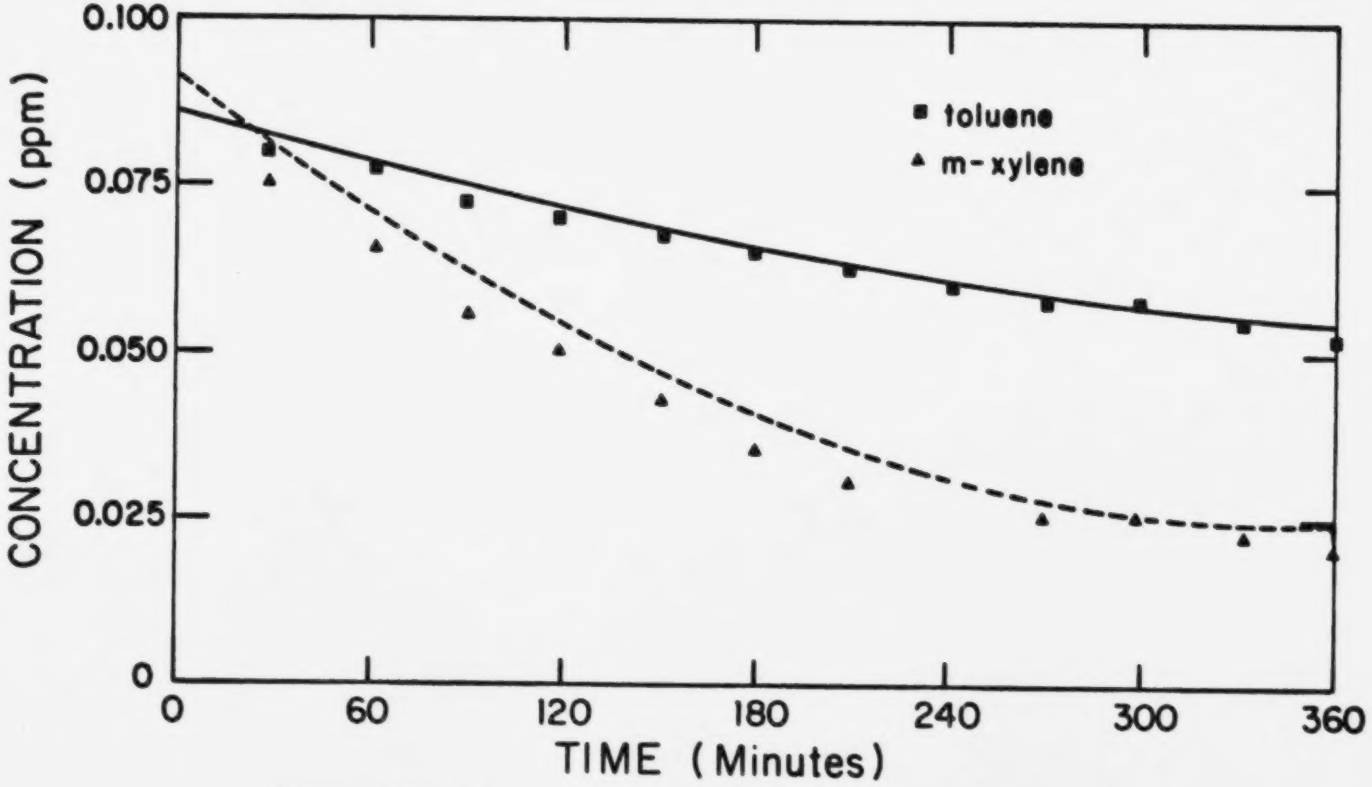

Figure Ald. Observed and Calculated Concentration-Time Profiles for 7-Hydrocarbon-NO_x Experiment-237

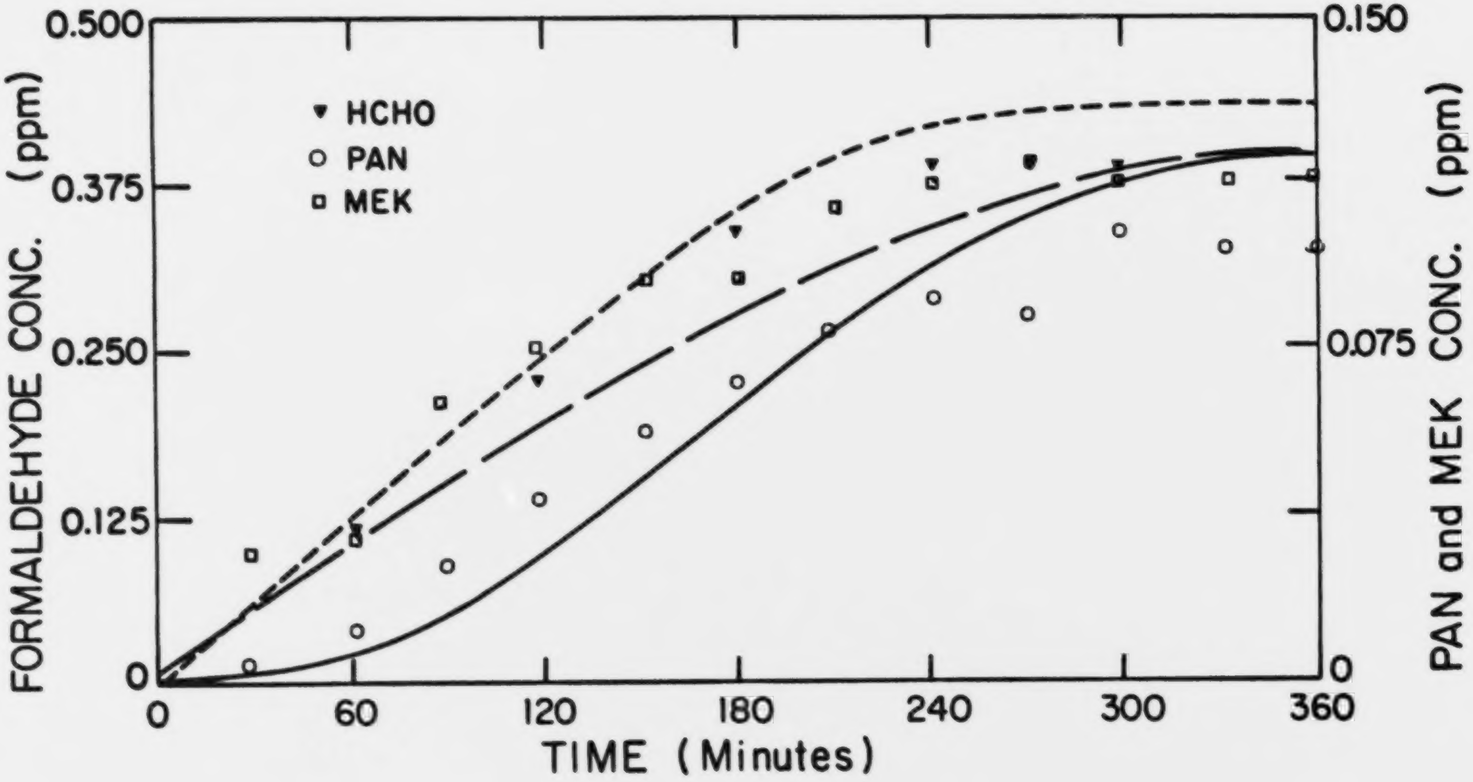

Figure A1e. Observed and Calculated Concentration-Time Profiles for 7-Hydrocarbon-NO_x Experiment EC-237

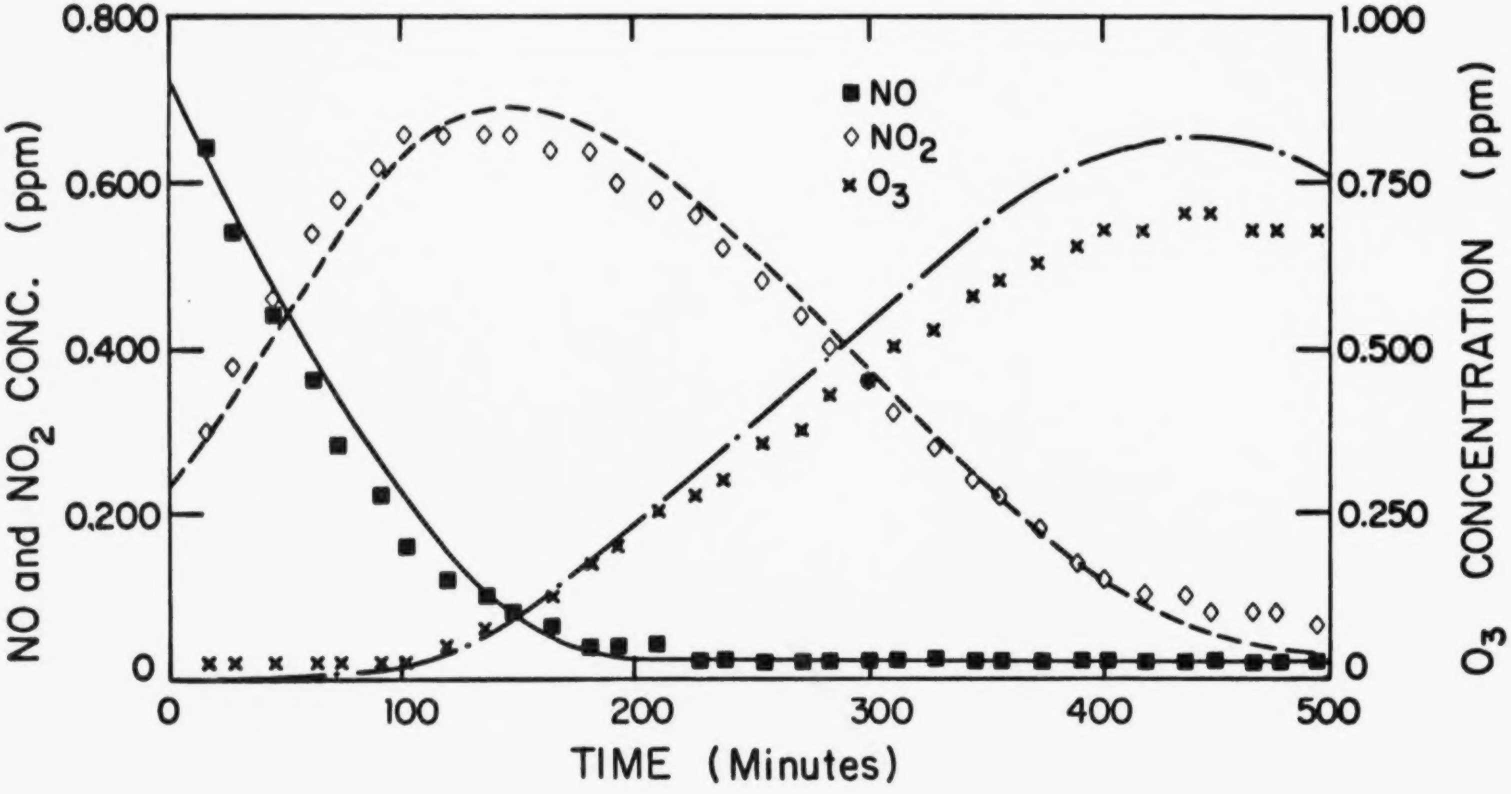

Figure A2a. Observed and Calculated Concentration-Time Profiles for 7-Hydrocarbon-NO_x Experiment EC-238

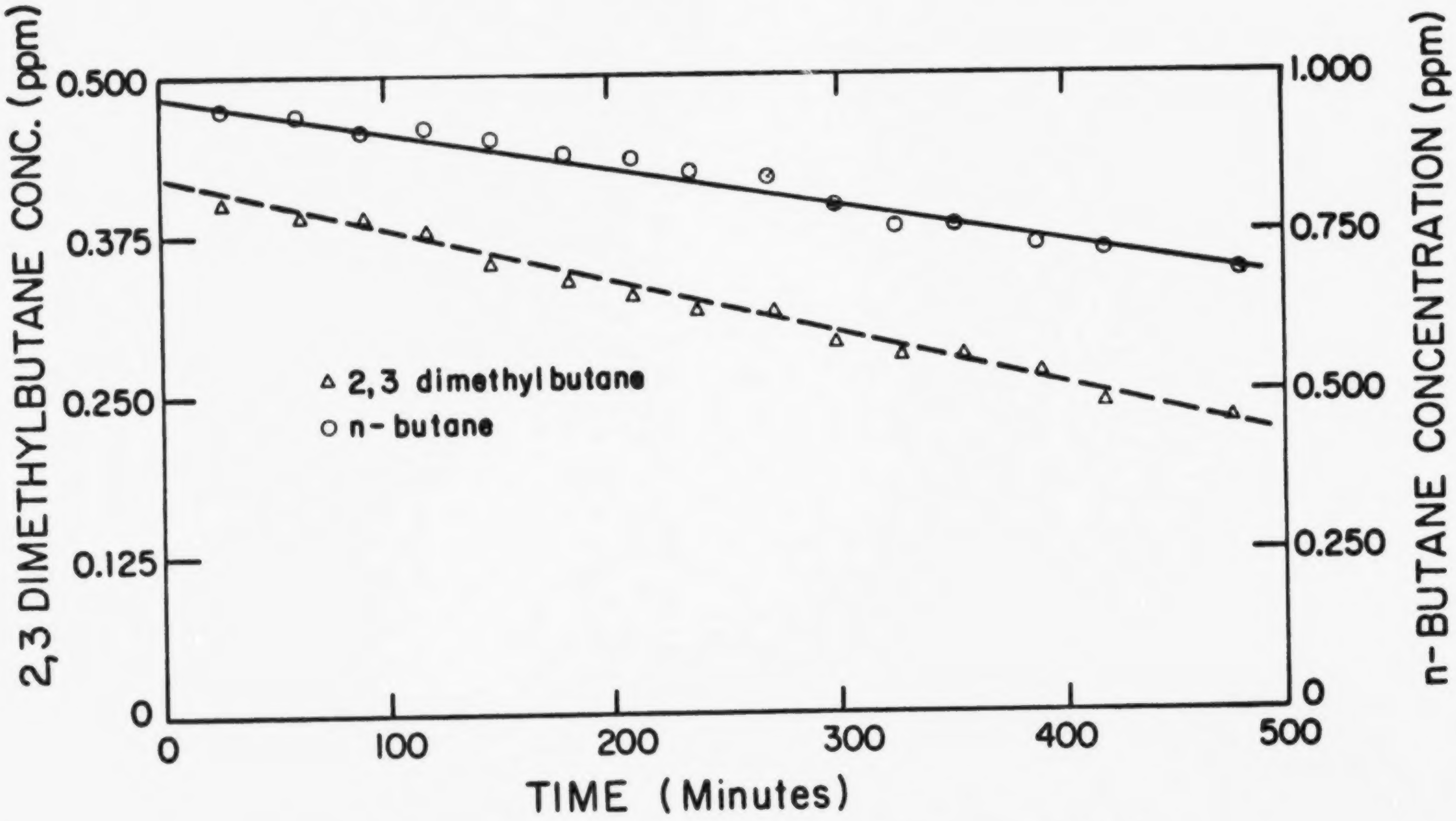

Figure A2b. Observed and Calculated Concentration-Time Profiles for 7-Hydrocarbon-NO_x Experiment EC-238

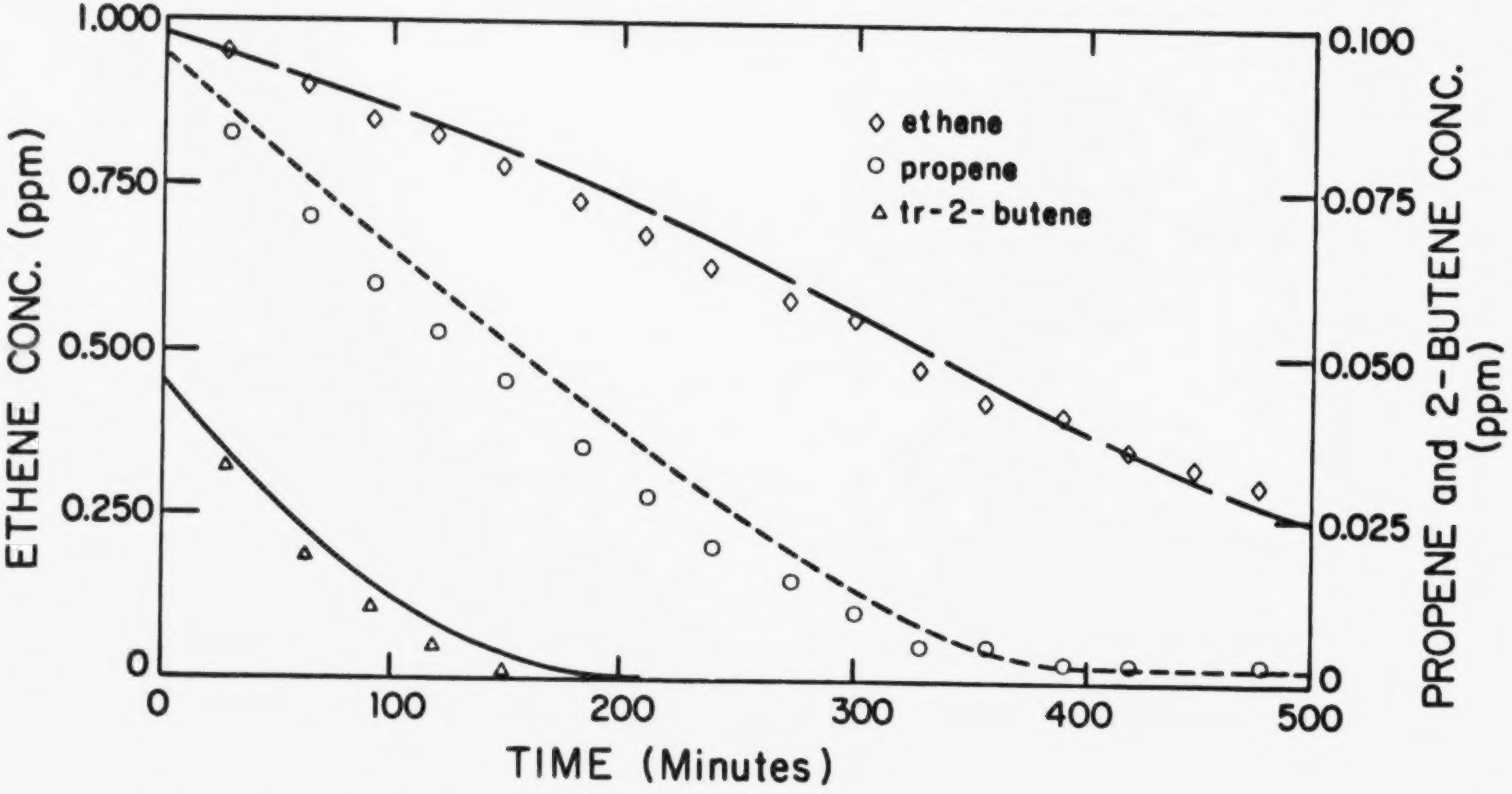

Figure A2c. Observed and Calculated Concentration-Time Profiles for 7-Hydrocarbon-NO_x Experiment EC-238

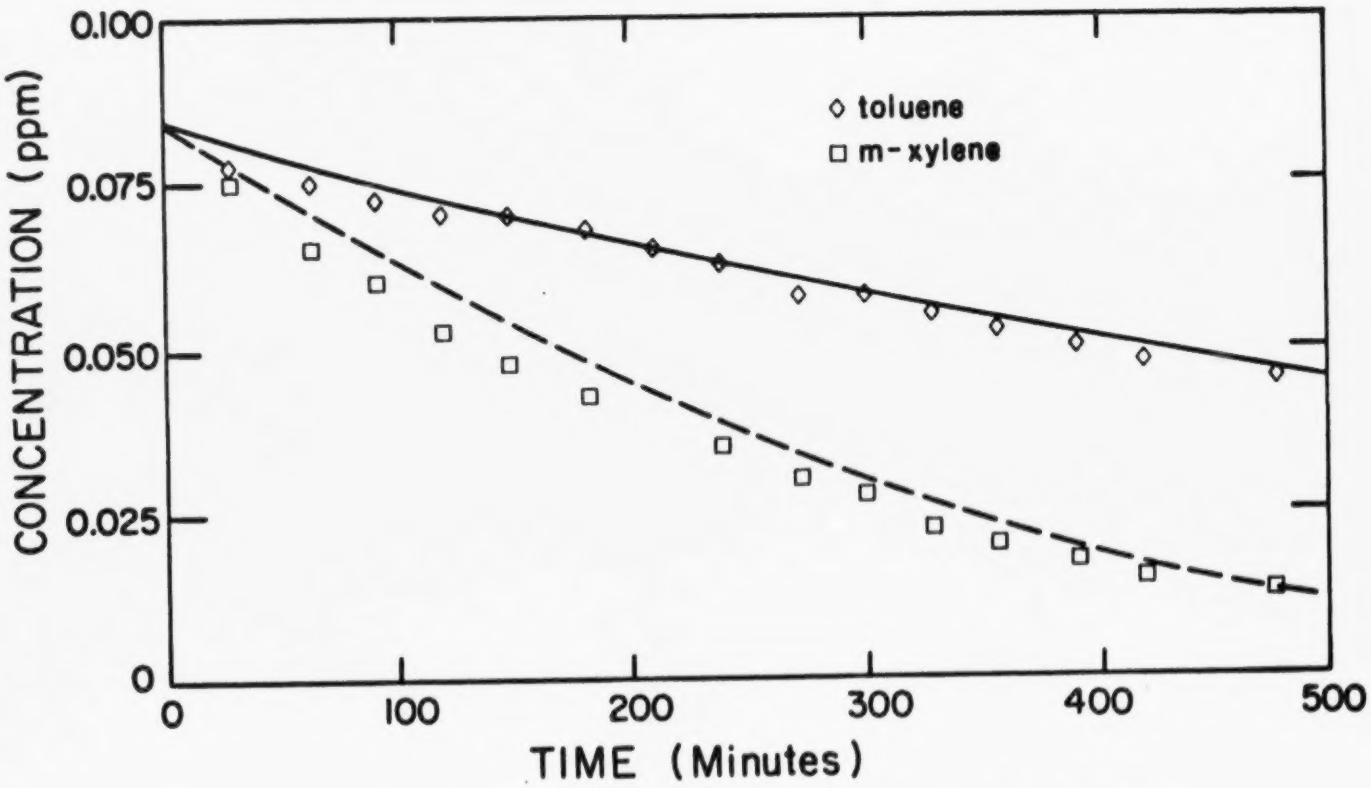

Figure A2d. Observed and Calculated Concentration-Time Profiles for 7-Hydrocarbon-NO_x Experiment EC-238

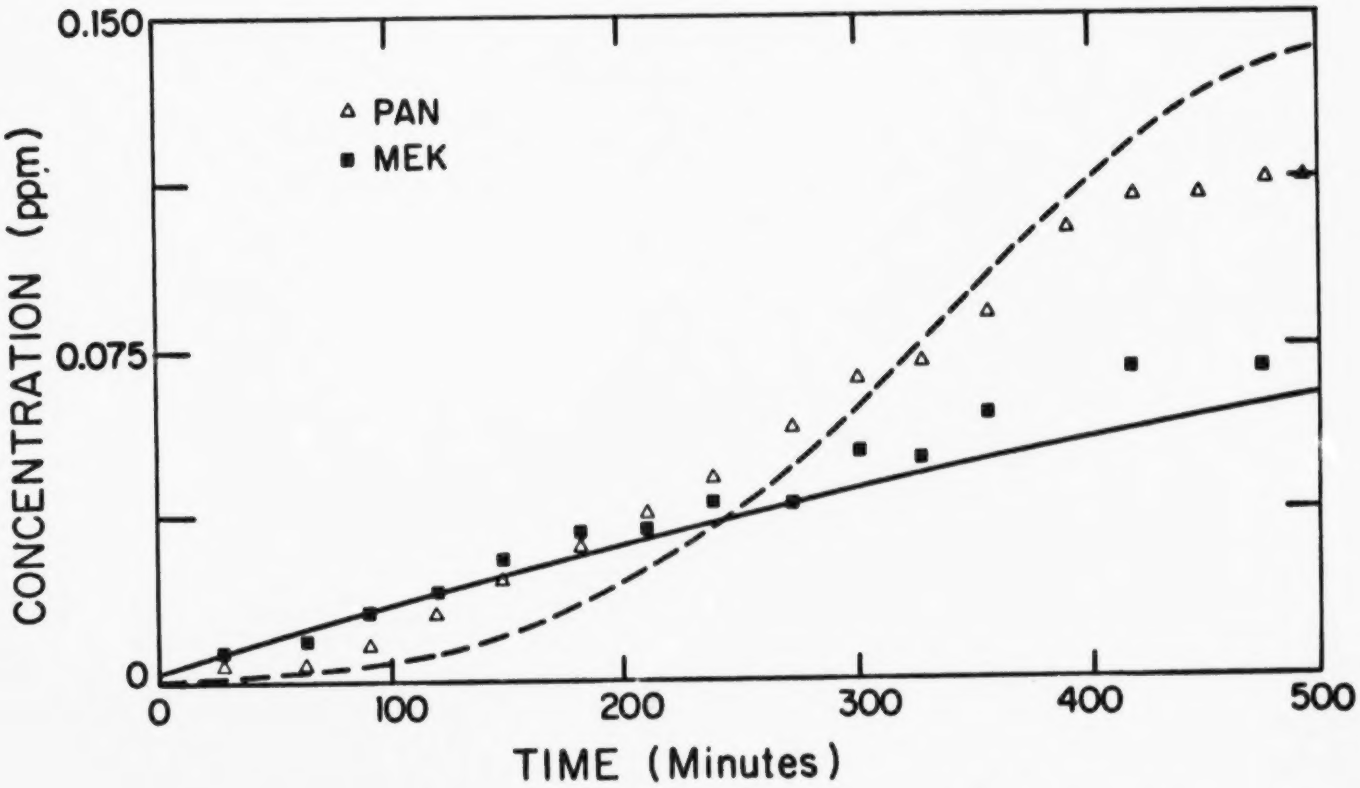

Figure A2e. Observed and Calculated Concentration-Time Profiles for 7-Hydrocarbon-NO_x Experiment EC-238

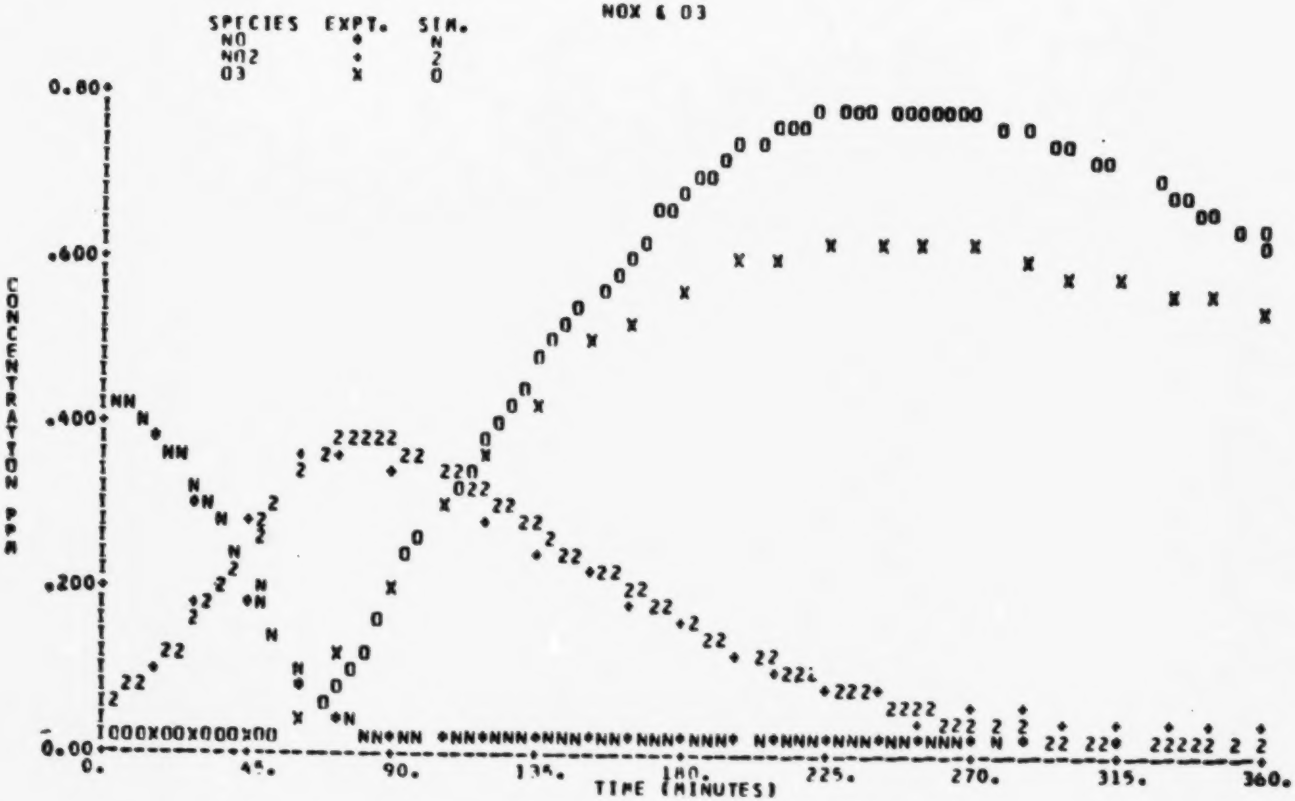

Figure A3a. Observed and Calculated Concentration-Time Profiles for 7-Hydrocarbon-NO_x Experiment EC-231

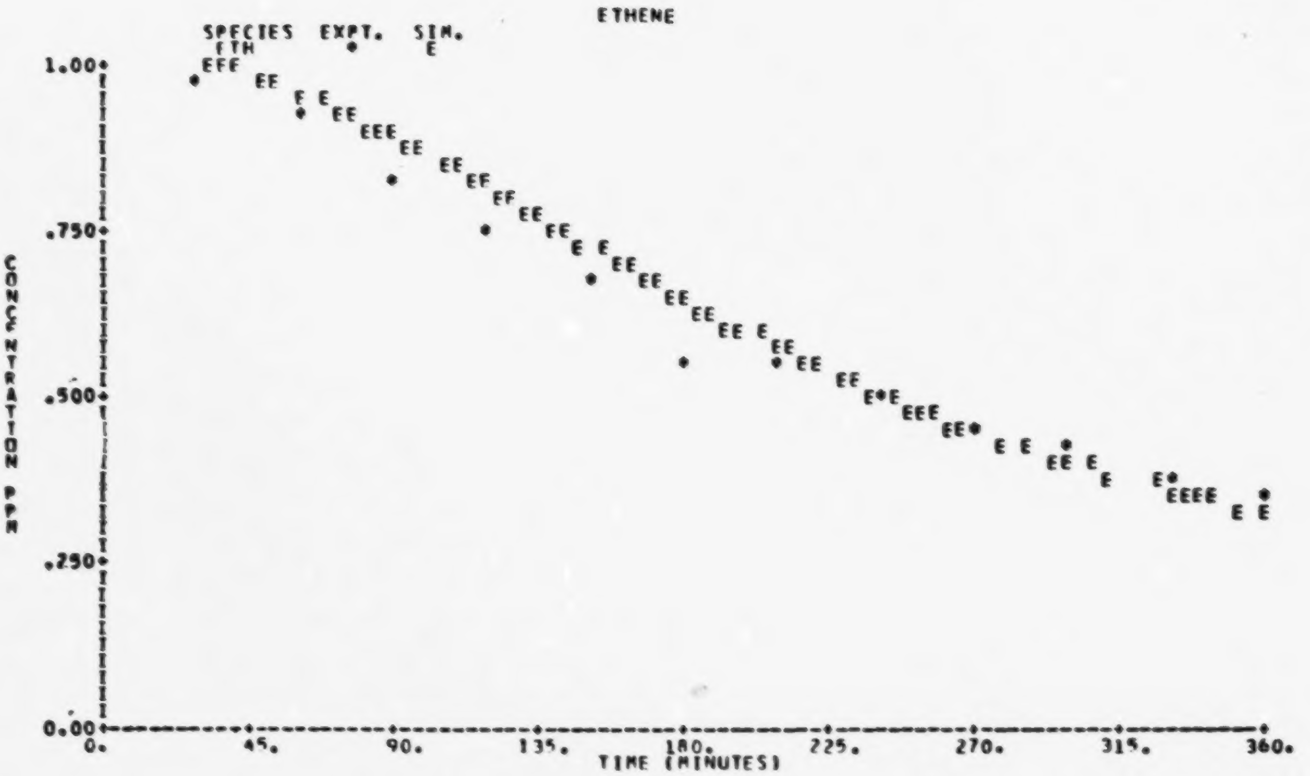

Figure A3b. Observed and Calculated Concentration-Time Profiles for 7-Hydrocarbon-NO_x Experiment EC-231

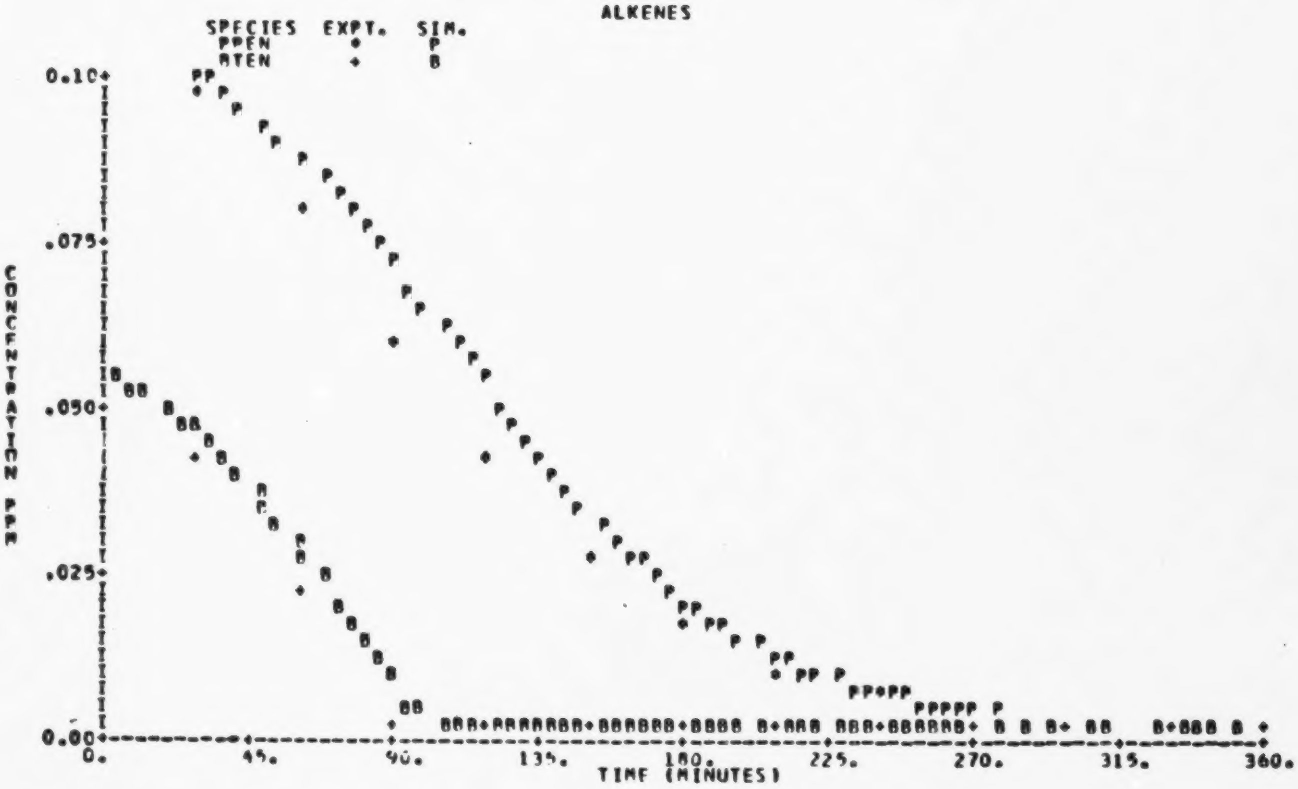

Figure A3c. Observed and Calculated Concentration-Time Profiles for 7-Hydrocarbon-NO_x Experiment EC-231

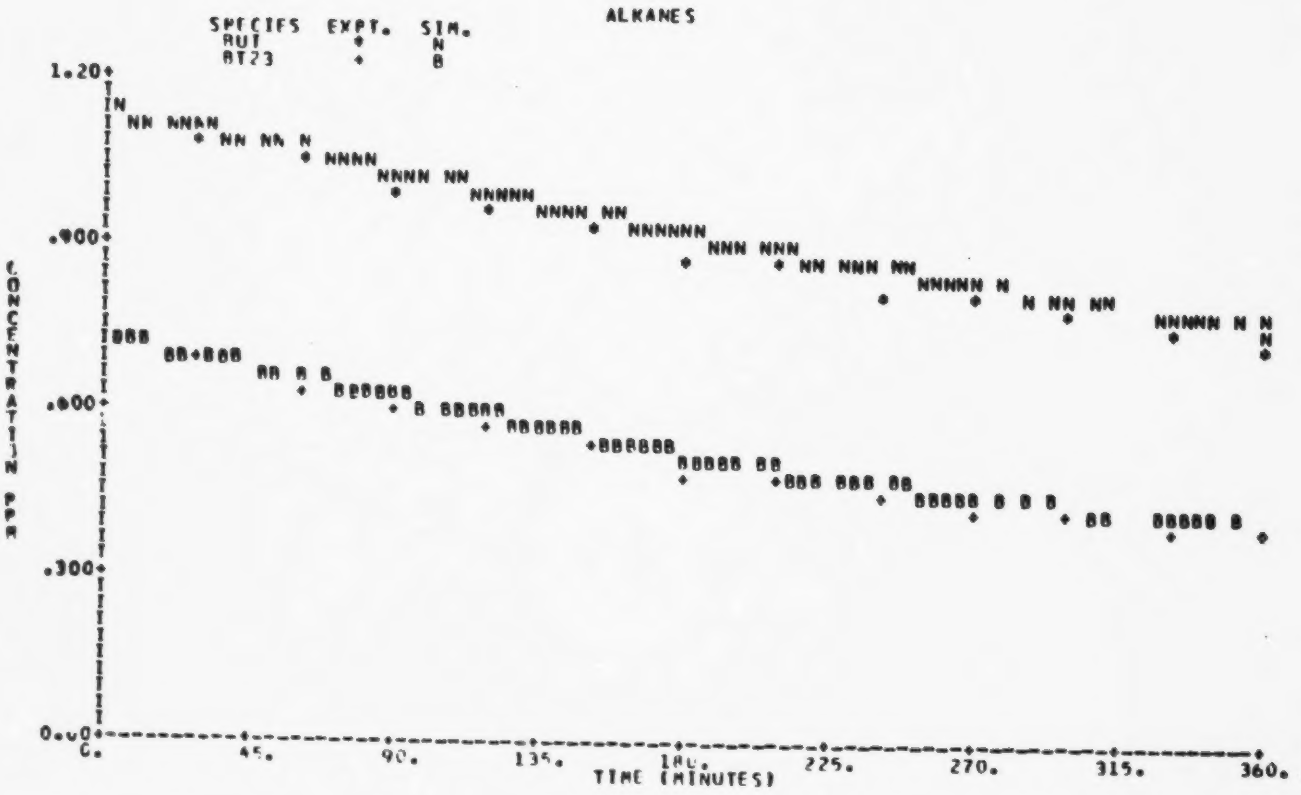

Figure A3d. Observed and Calculated Concentration-Time Profiles for 7-Hydrocarbon-NO_x Experiment EC-231

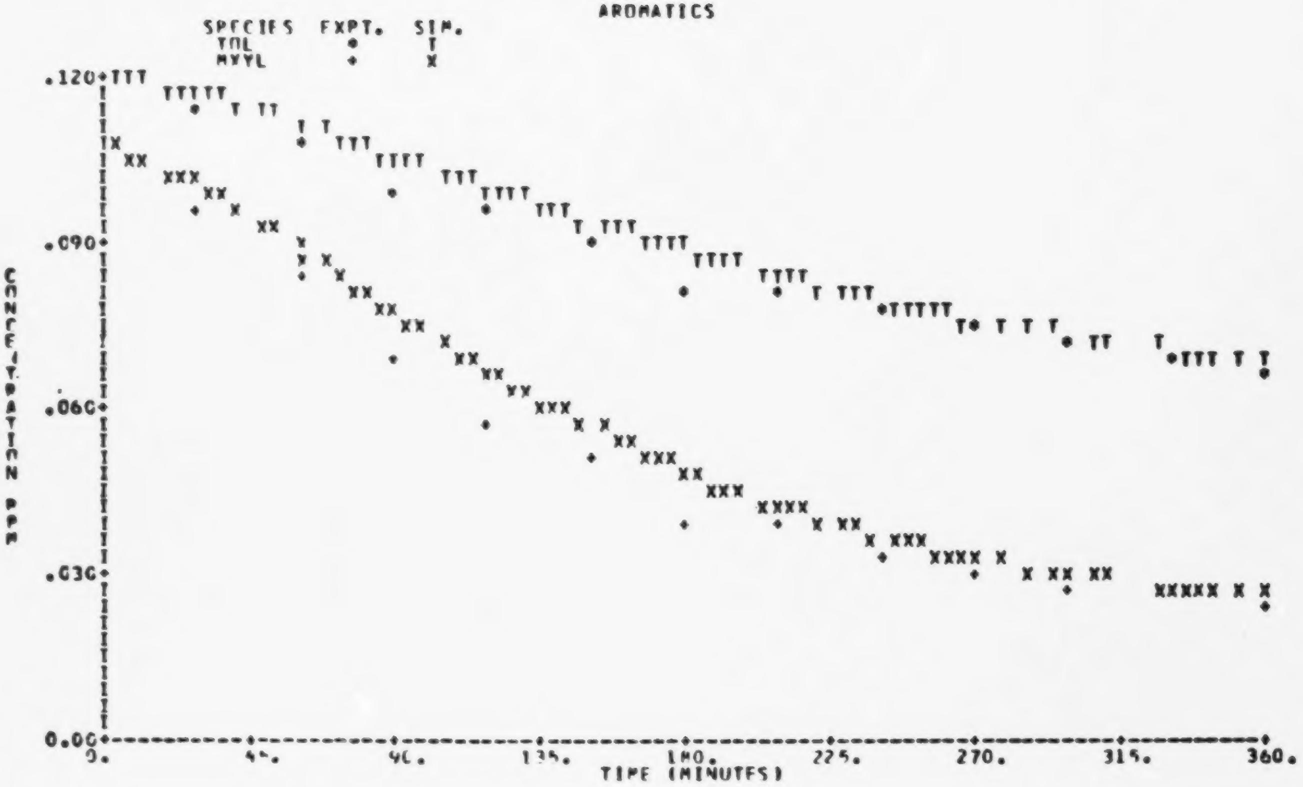

Figure A3e. Observed and Calculated Concentration-Time Profiles for 7-Hydrocarbon-NO_x Experiment EC-231

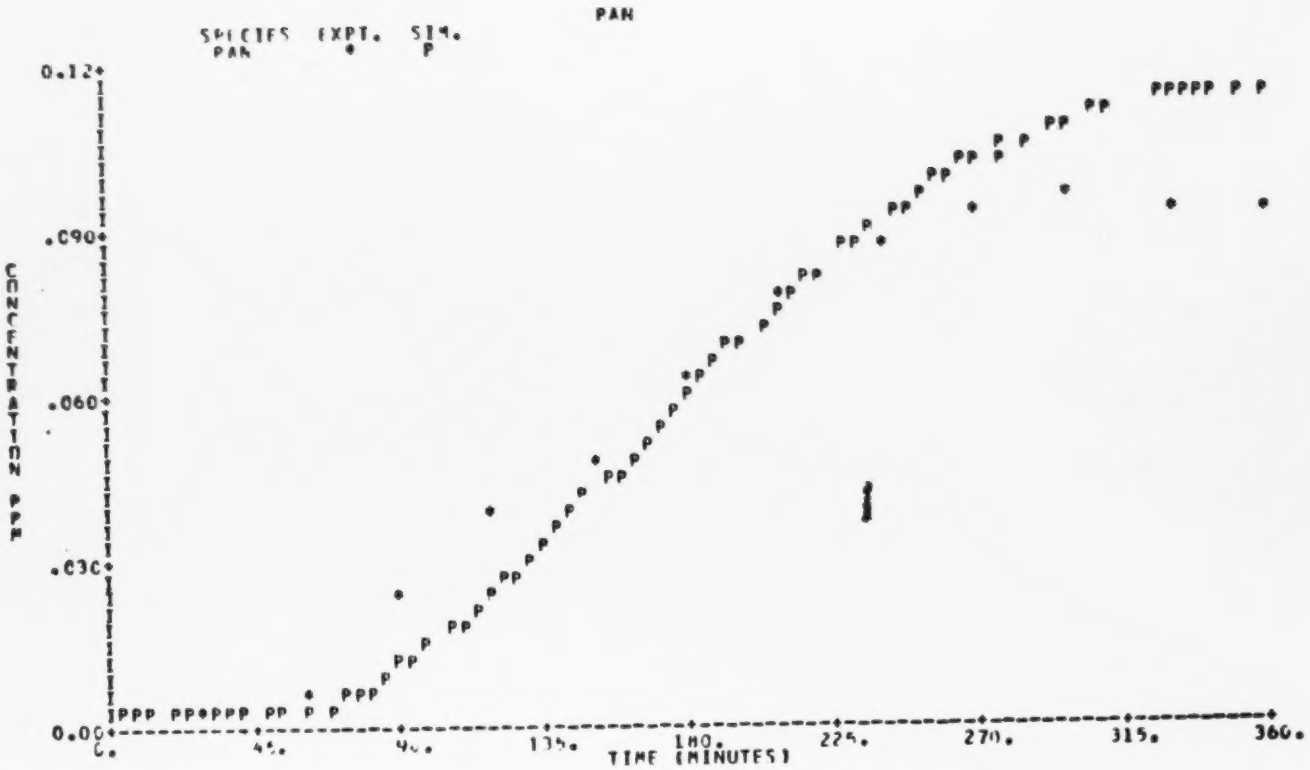

Figure A3f. Observed and Calculated Concentration-Time Profiles for 7-Hydrocarbon-NO_x Experiment EC-231

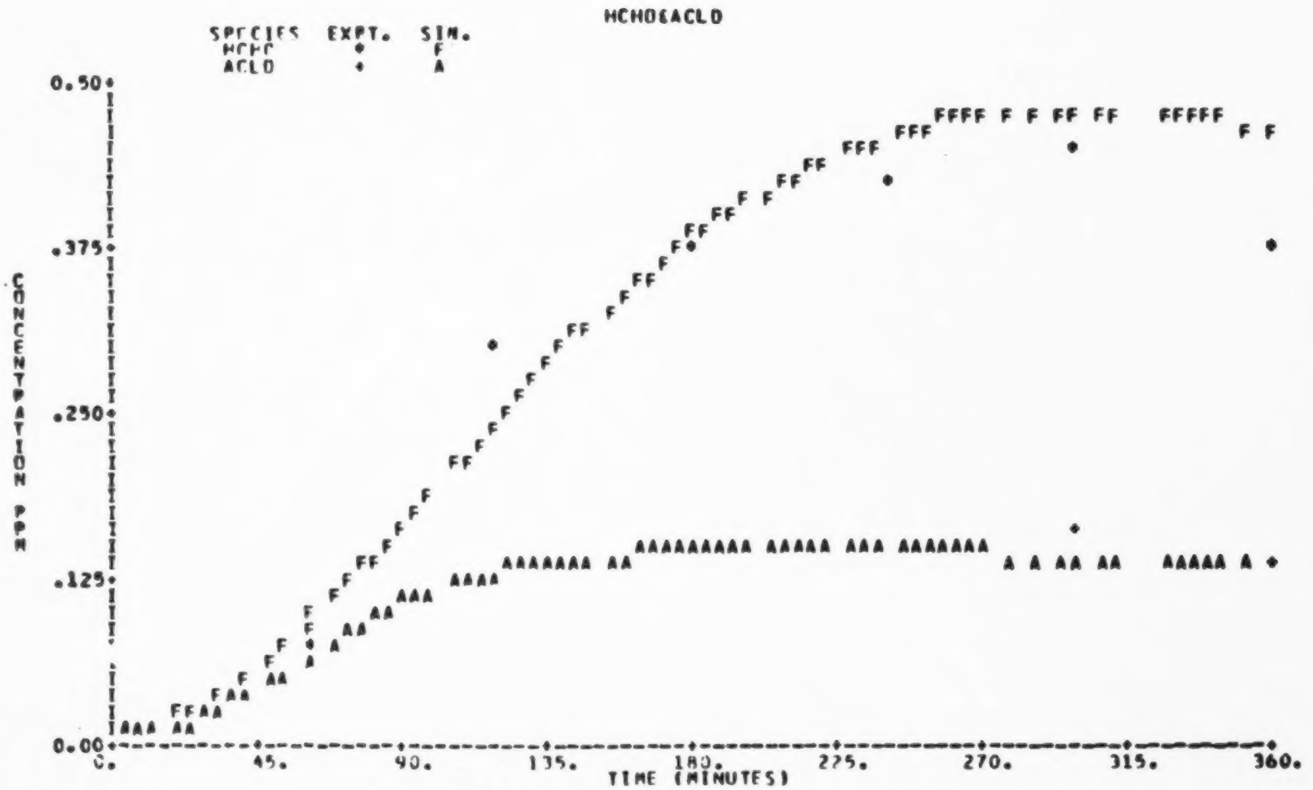

Figure A3g. Observed and Calculated Concentration-Time Profiles for 7-Hydrocarbon-NO_x Experiment EC-231

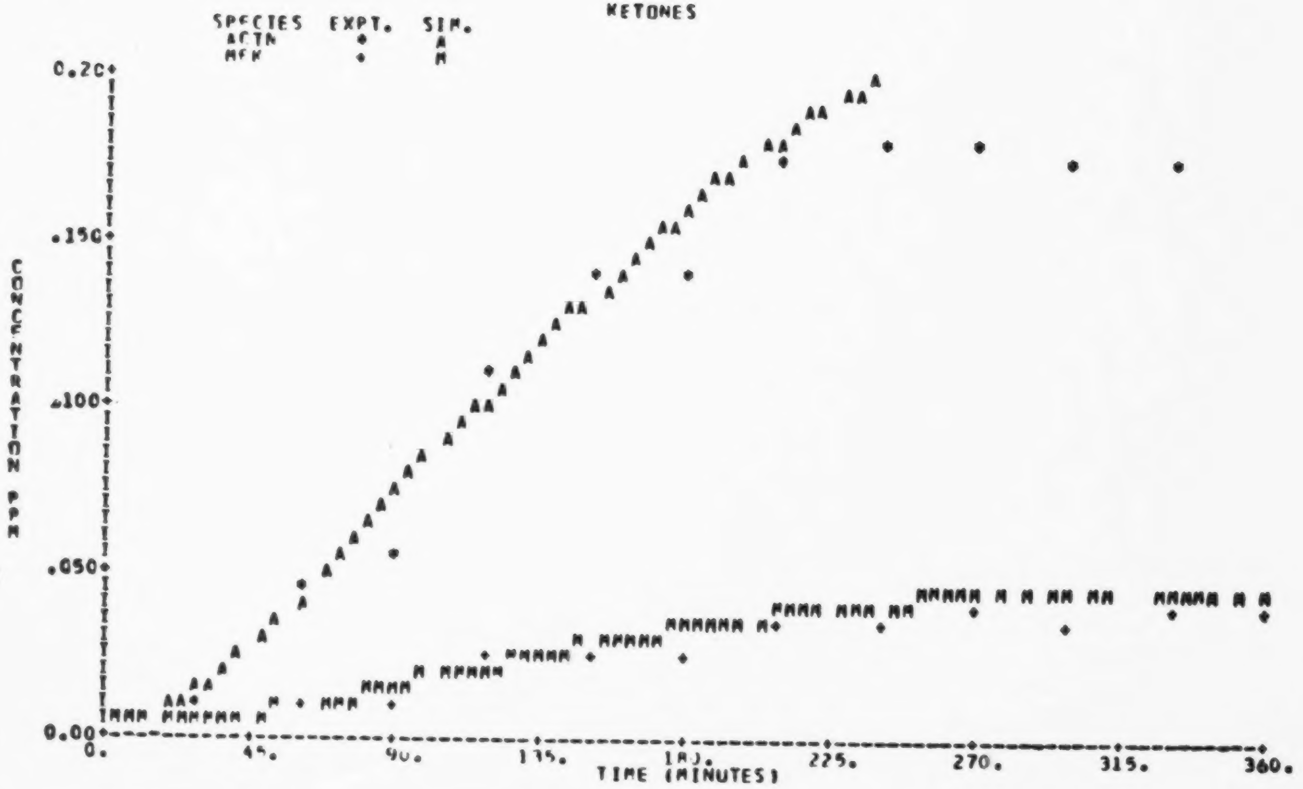

Figure A3h. Observed and Calculated Concentration-Time Profiles for 7-Hydrocarbon-NO_x Experiment EC-231

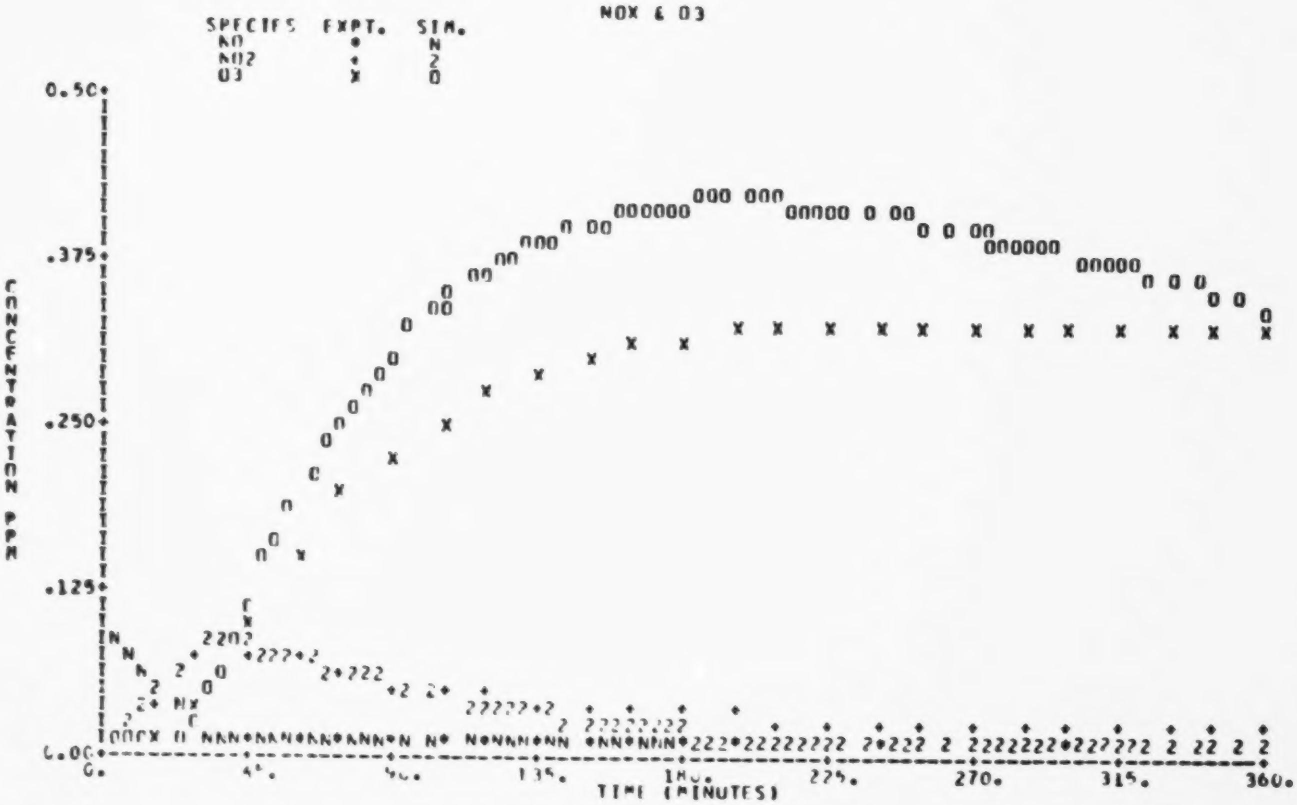

Figure A4a. Observed and Calculated Concentration-Time Profiles for 7-Hydrocarbon-NO_x Experiment EC-233.

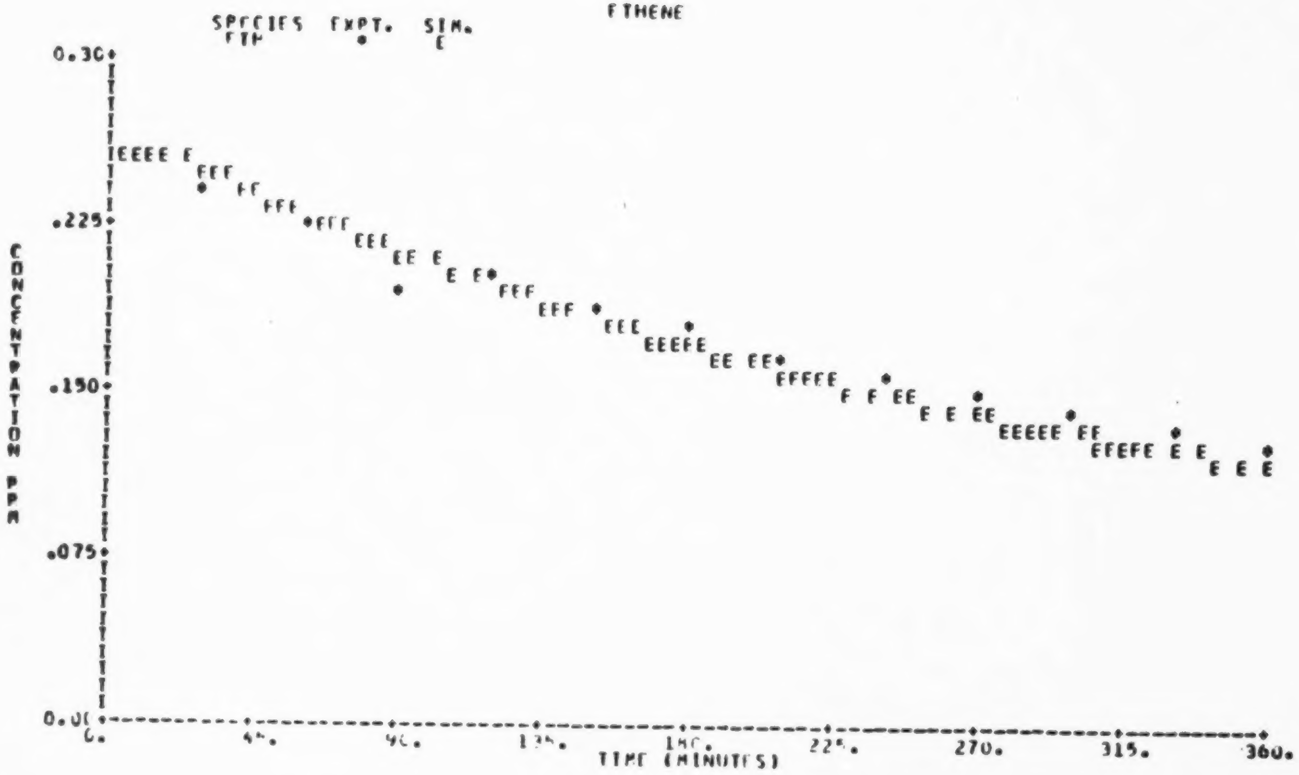

Figure A4b. Observed and Calculated Concentration-Time Profiles for 7-Hydrocarbon-NO_x Experiment EC-233.

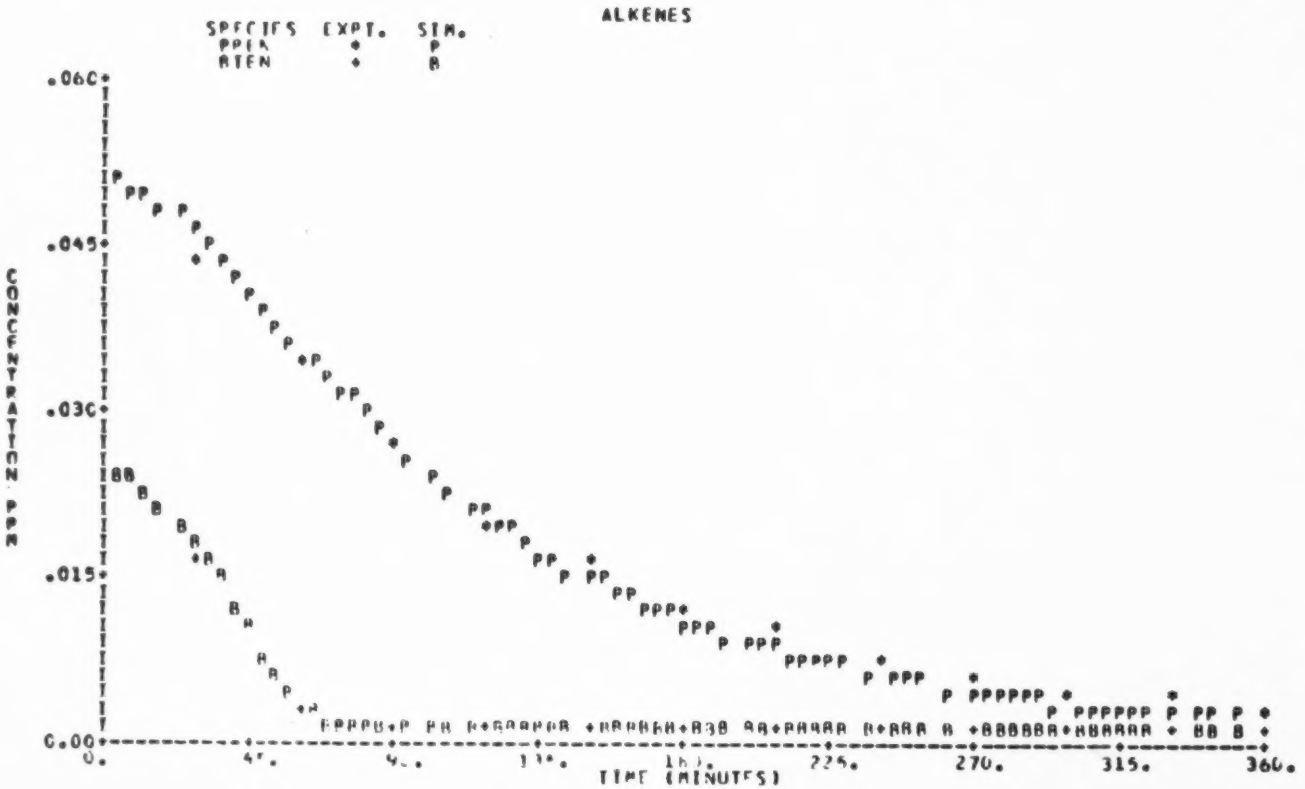

Figure A4c. Observed and Calculated Concentration-Time Profiles for 7-Hydrocarbon-NO_x Experiment EC-233.

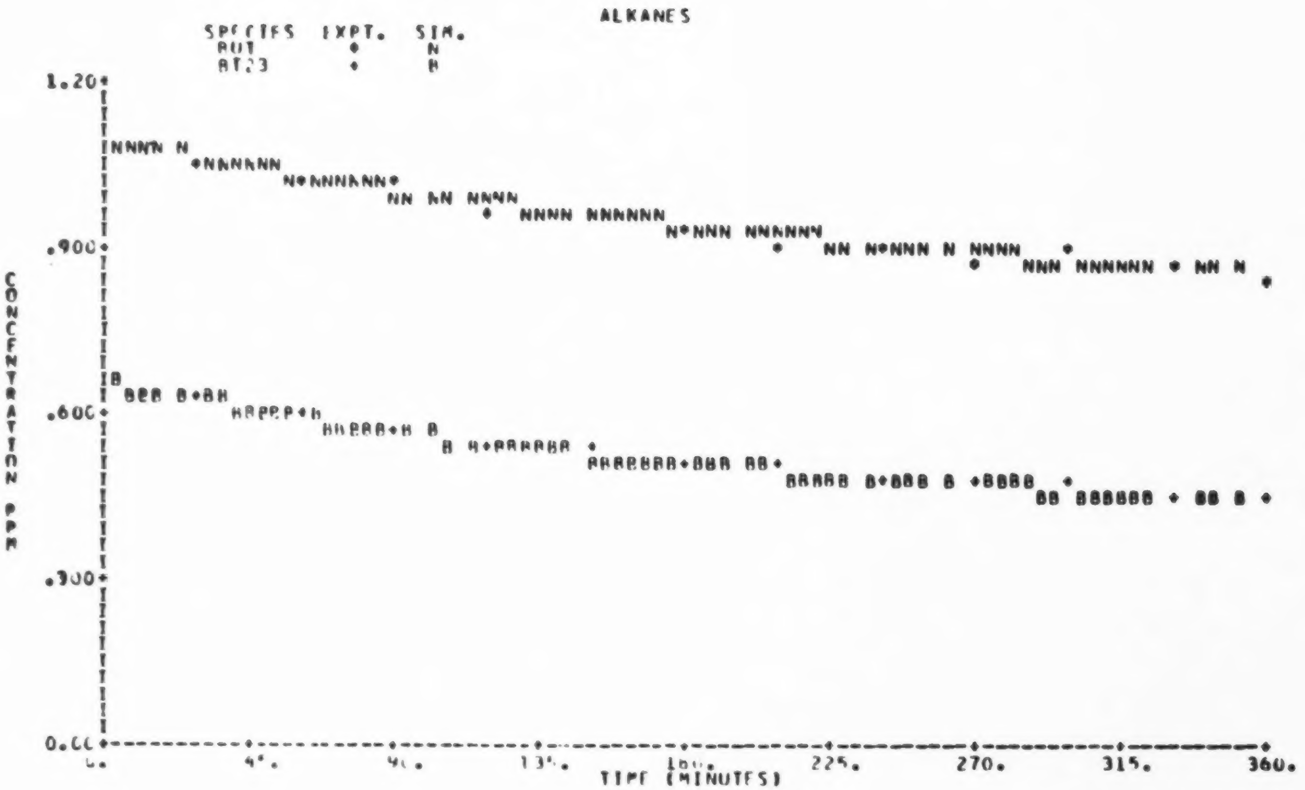

Figure A4d. Observed and Calculated Concentration-Time Profiles for 7-Hydrocarbon-NO_x Experiment EC-233.

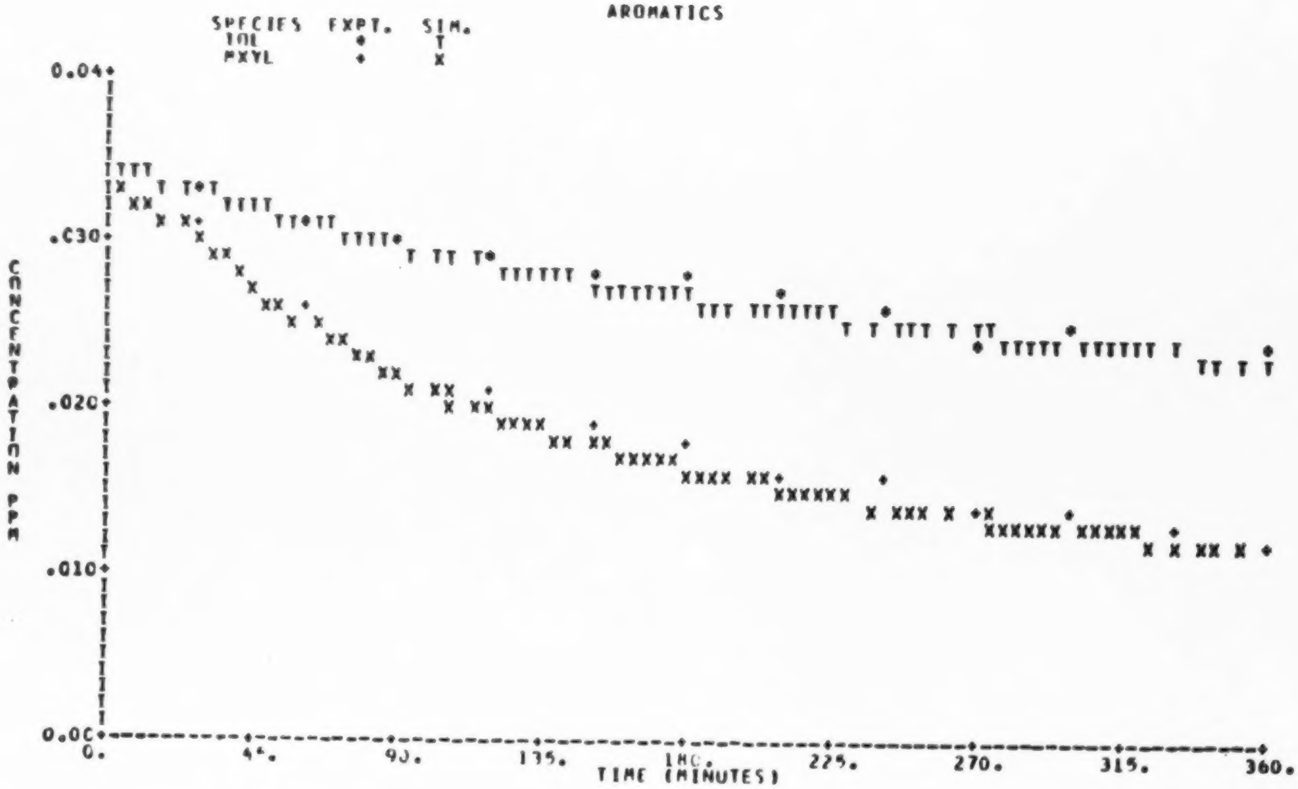

Figure A4e. Observed and Calculated Concentration-Time Profiles for 7-Hydrocarbon-NO_x Experiment EC-233.

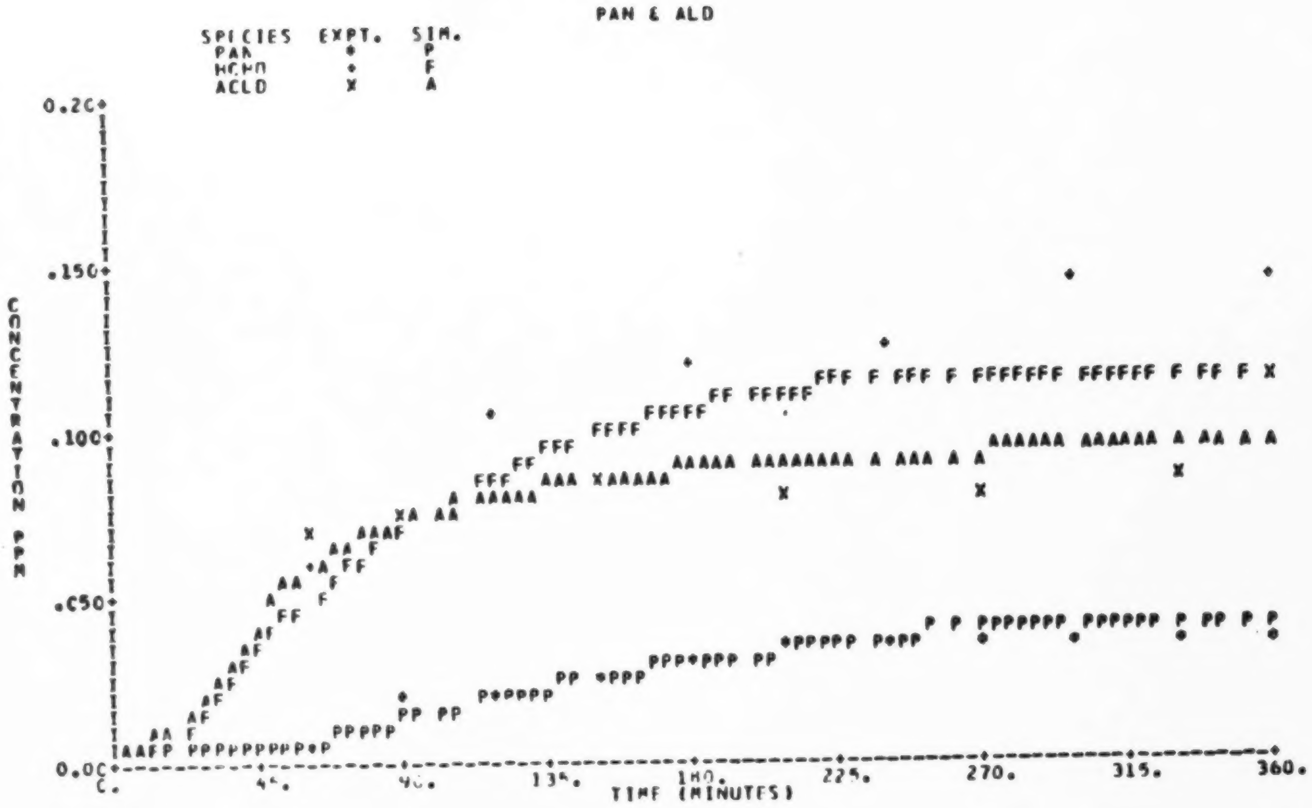

Figure A4f. Observed and Calculated Concentration-Time Profiles for 7-Hydrocarbon-NO_x Experiment EC-233.

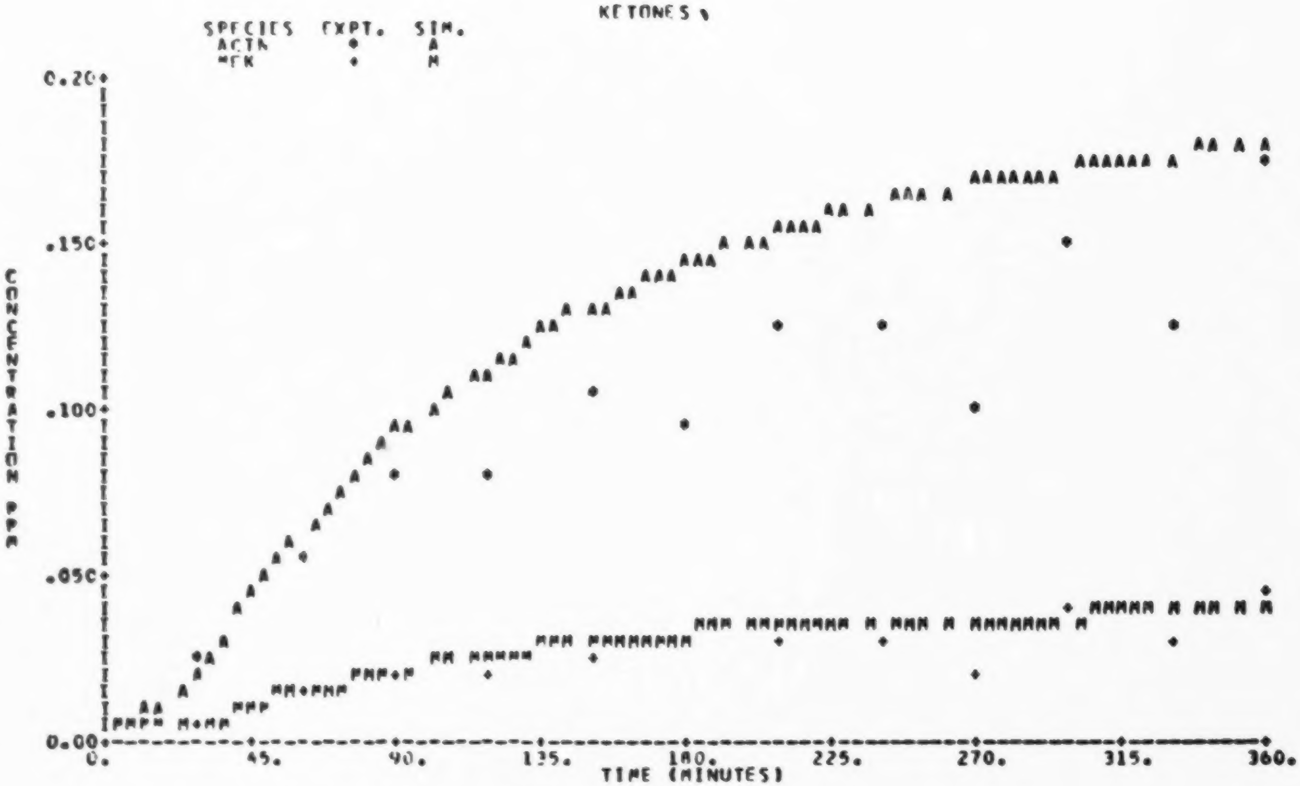

Figure A4g. Observed and Calculated Concentration-Time Profiles for 7-Hydrocarbon-NO_x Experiment EC-233.

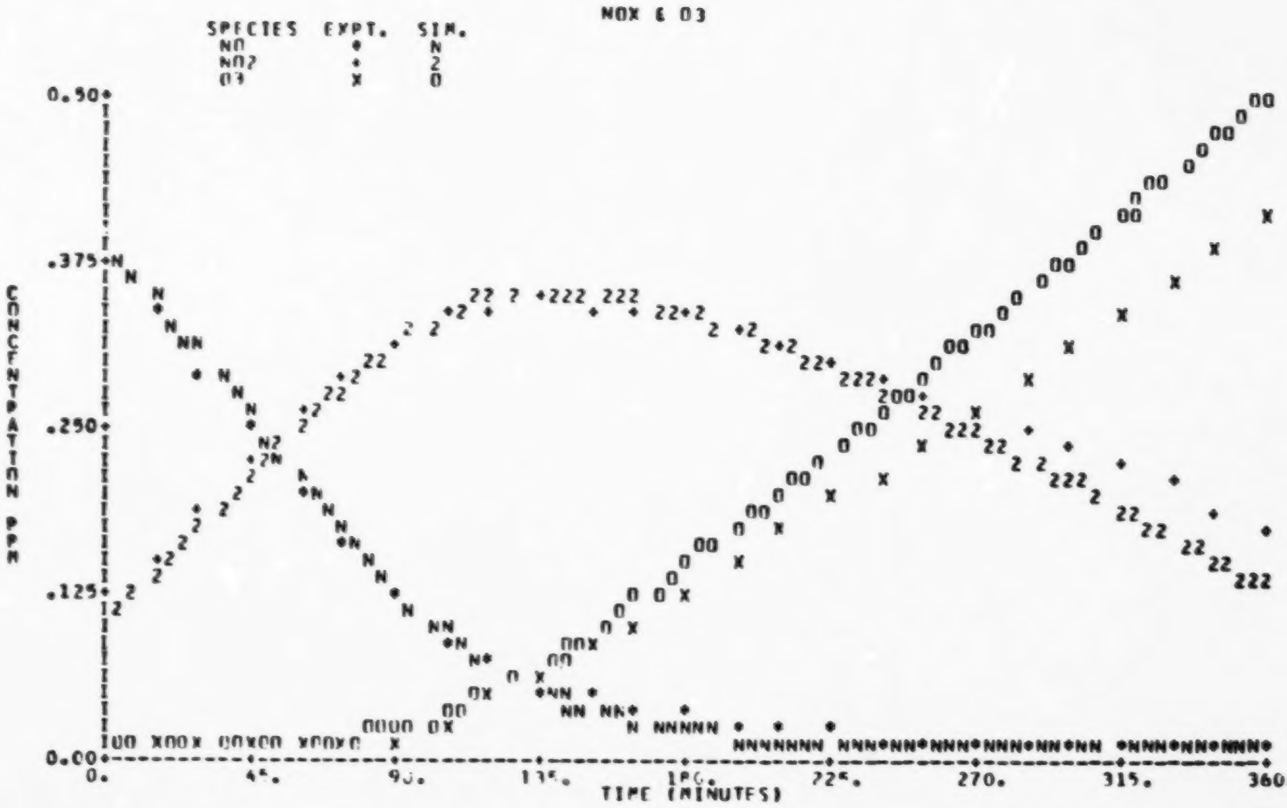

Figure A5a. Observed and Calculated Concentration-Time Profiles for 7-Hydrocarbon-NO_x Experiment EC-241.

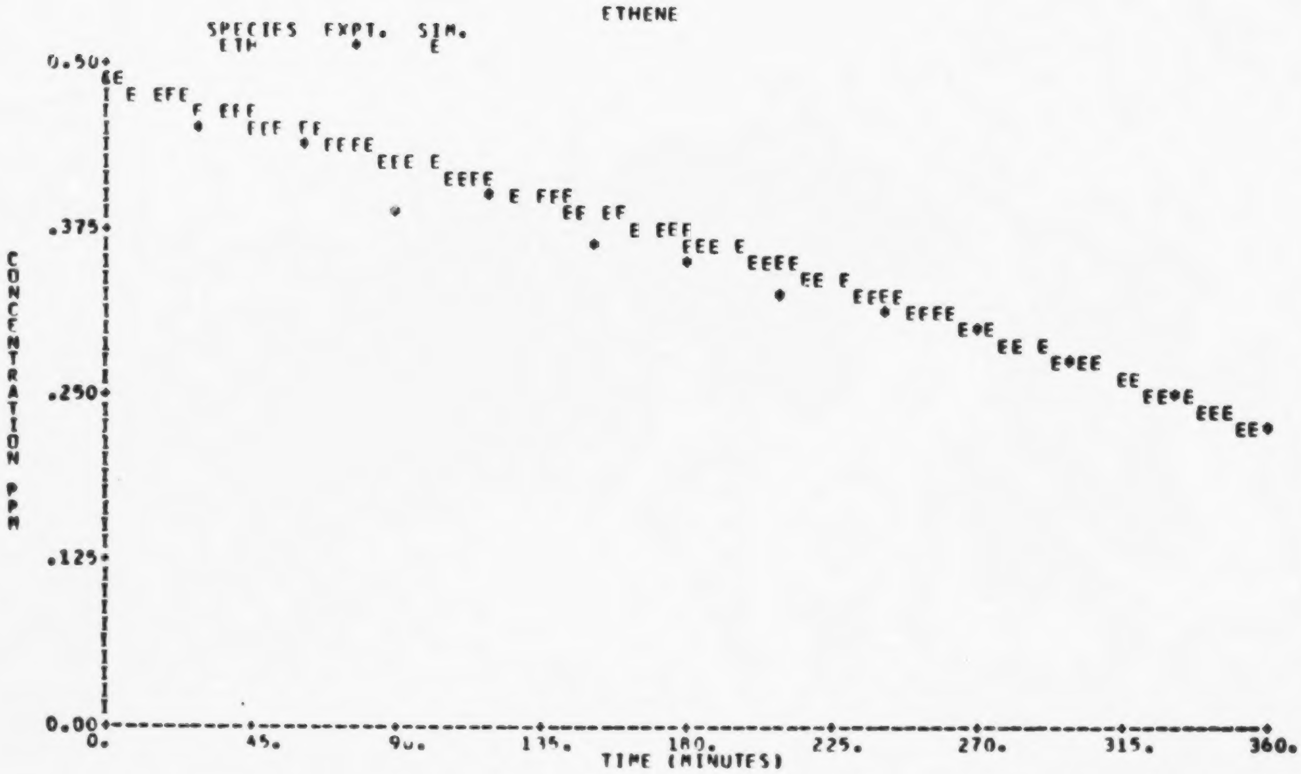

Figure A5b. Observed and Calculated Concentration-Time Profiles for 7-Hydrocarbon-NO_x Experiment EC-241.

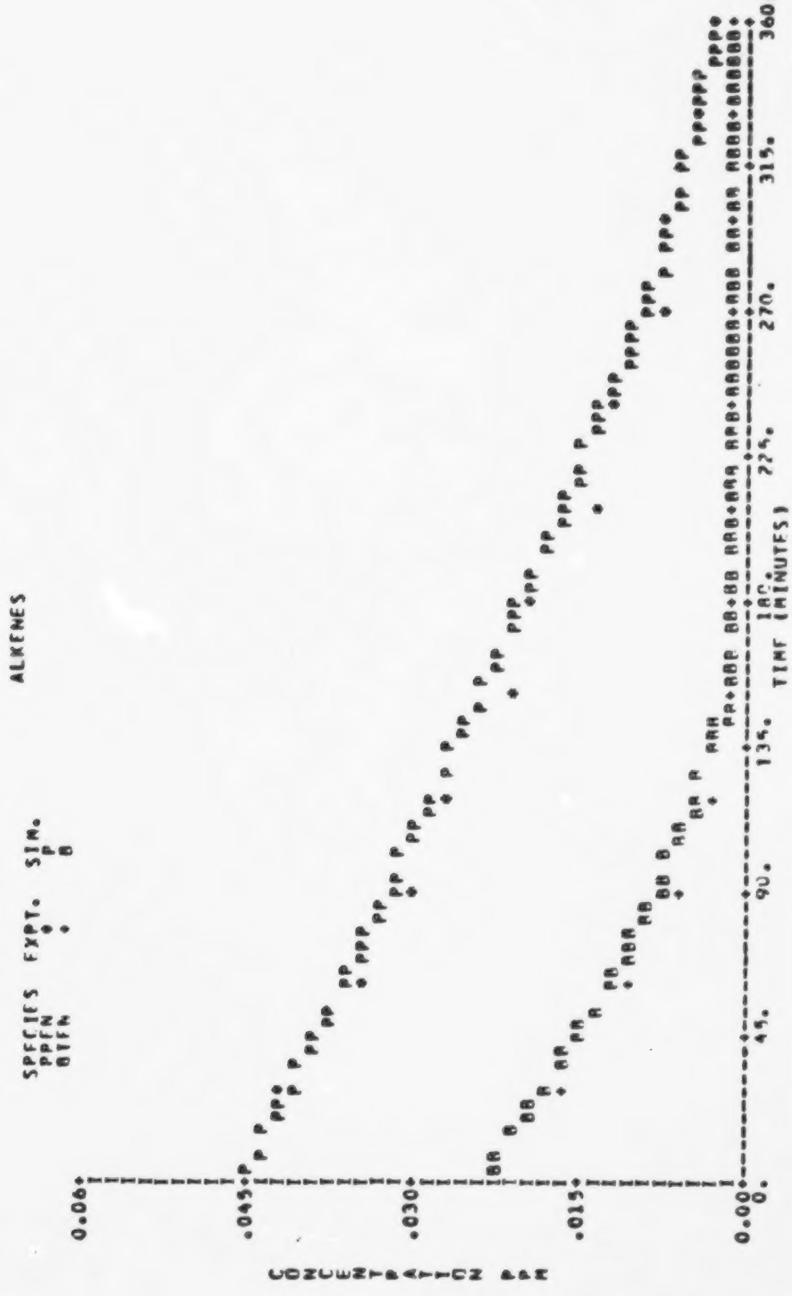

Figure A5c. Observed and Calculated Concentration-Time Profiles for 7-Hydrocarbon-NO_x Experiment EC-241.

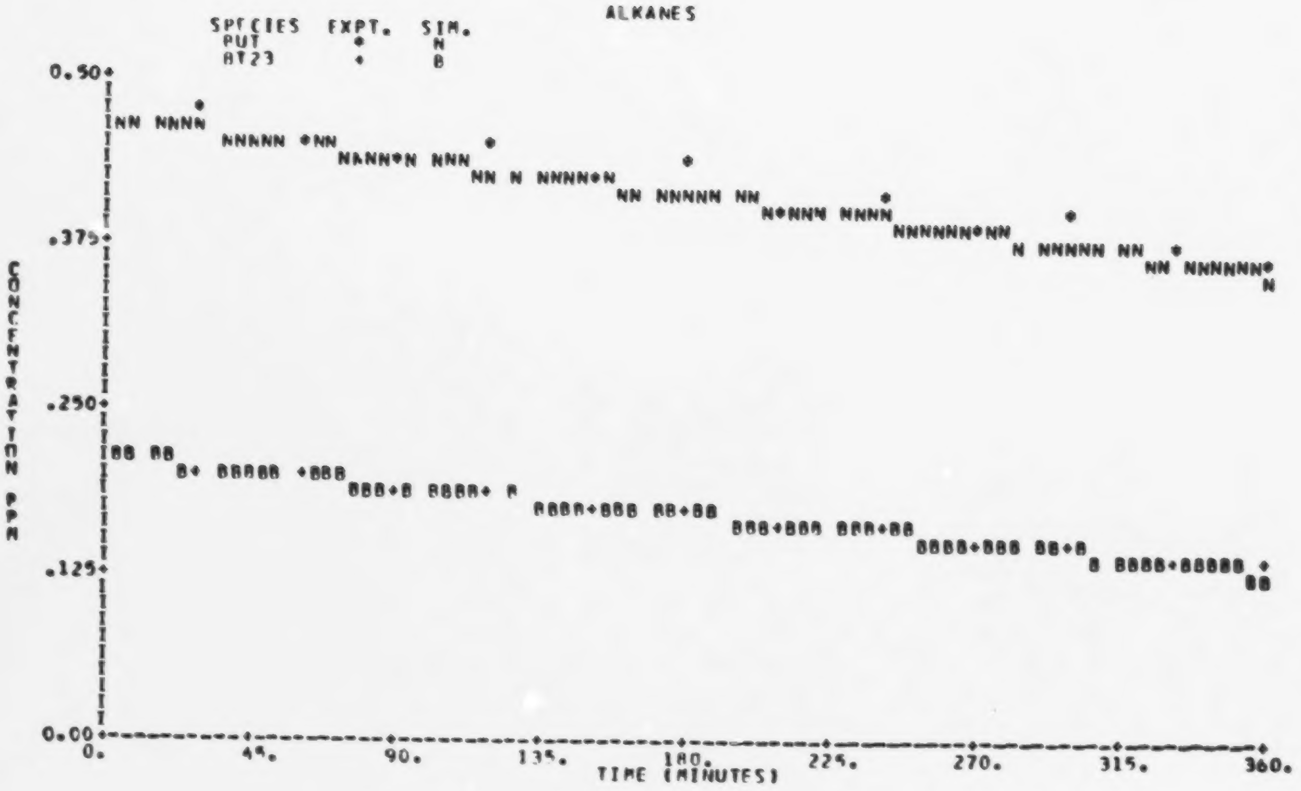

Figure A5d. Observed and Calculated Concentration-Time Profiles for 7-Hydrocarbon-NO_x Experiment EC-241.

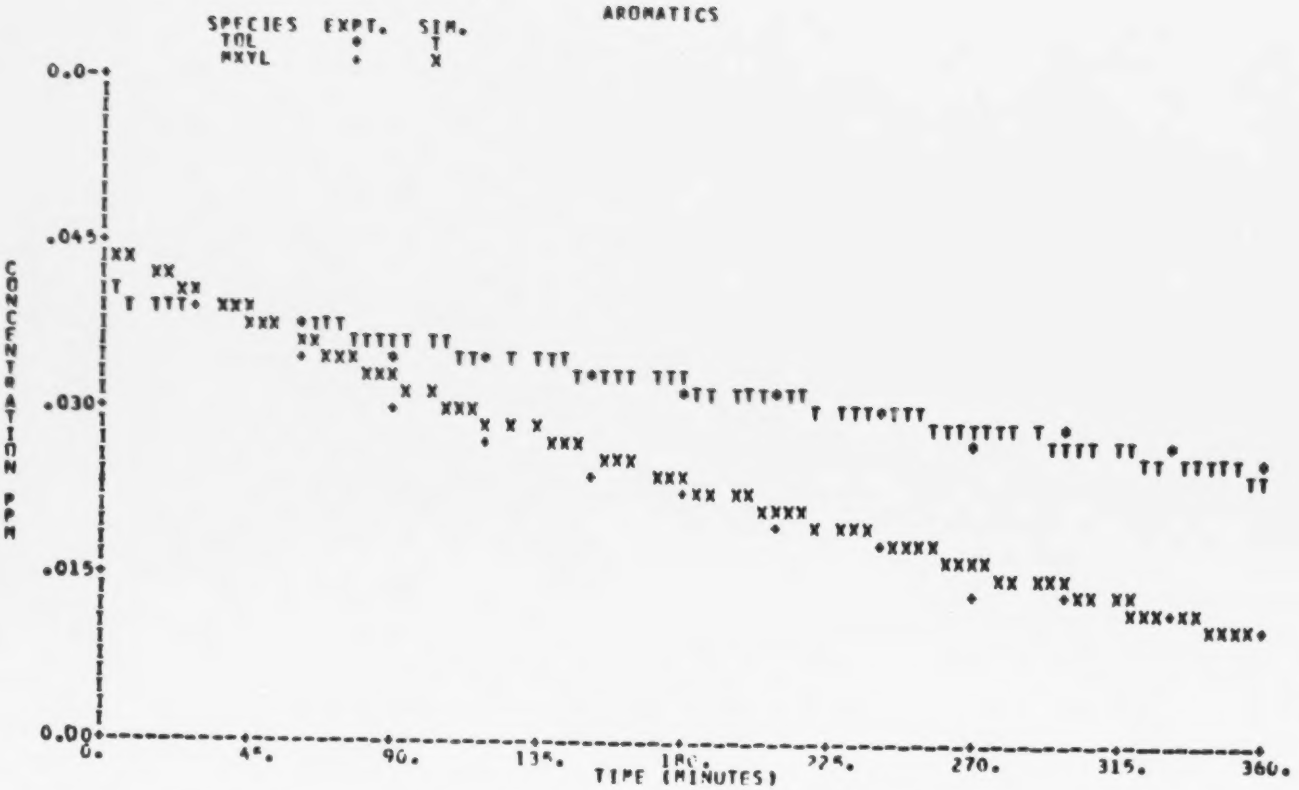

Figure A5e. Observed and Calculated Concentration-Time Profiles for 7-Hydrocarbon-NO_x Experiment EC-241.

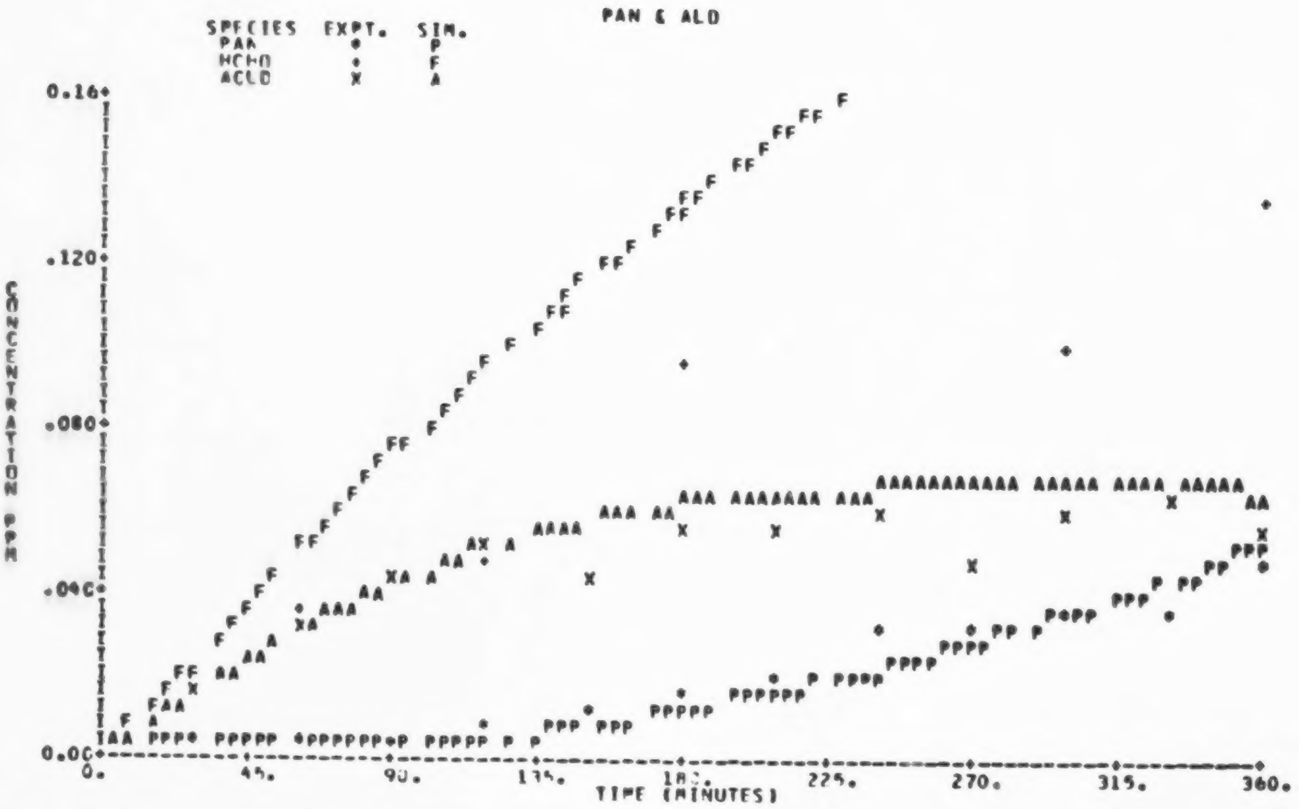

Figure A5f. Observed and Calculated Concentration-Time Profiles for 7-Hydrocarbon-NO_x Experiment EC-241.

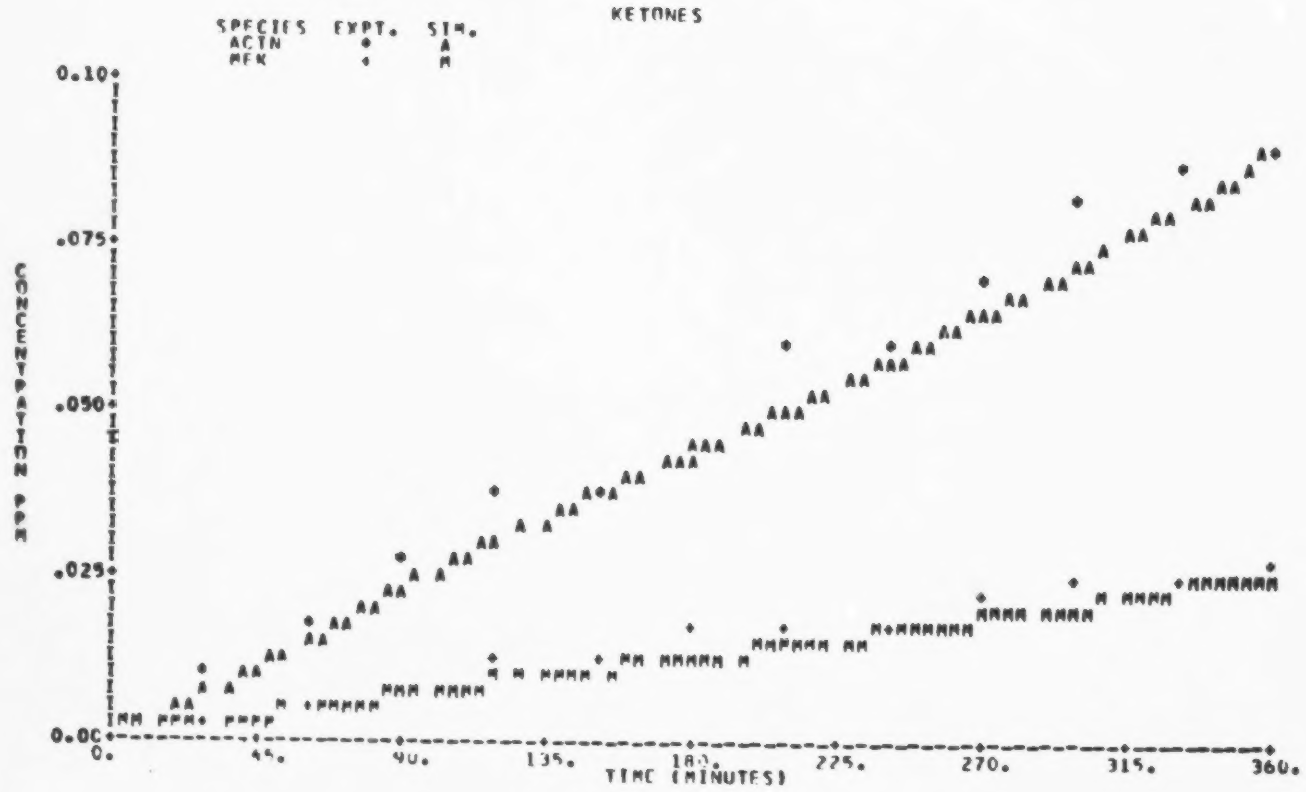

Figure A5g. Observed and Calculated Concentration-Time Profiles for 7-Hydrocarbon-NO_x Experiment EC-241.

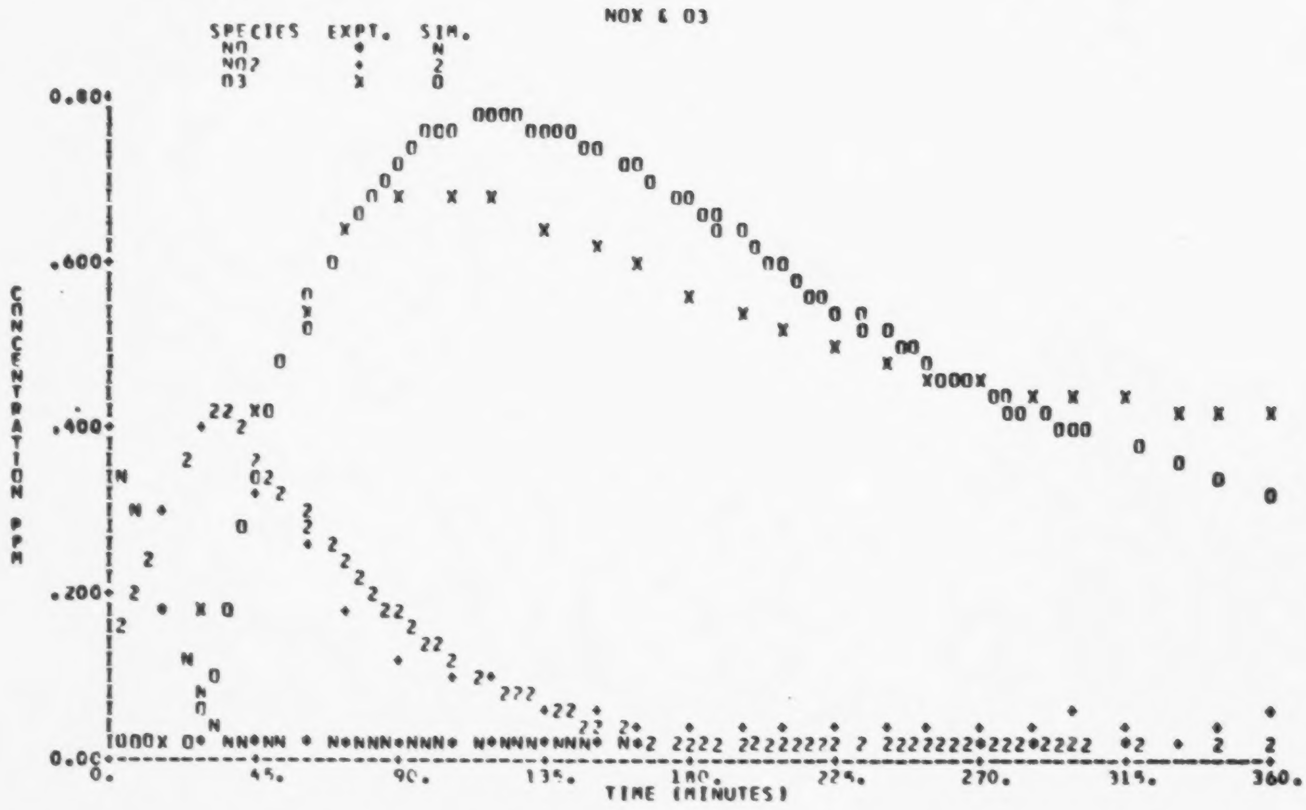

Figure A6a. Observed and Calculated Concentration-Time Profiles for 7-Hydrocarbon-NO_x Experiment EC-242.

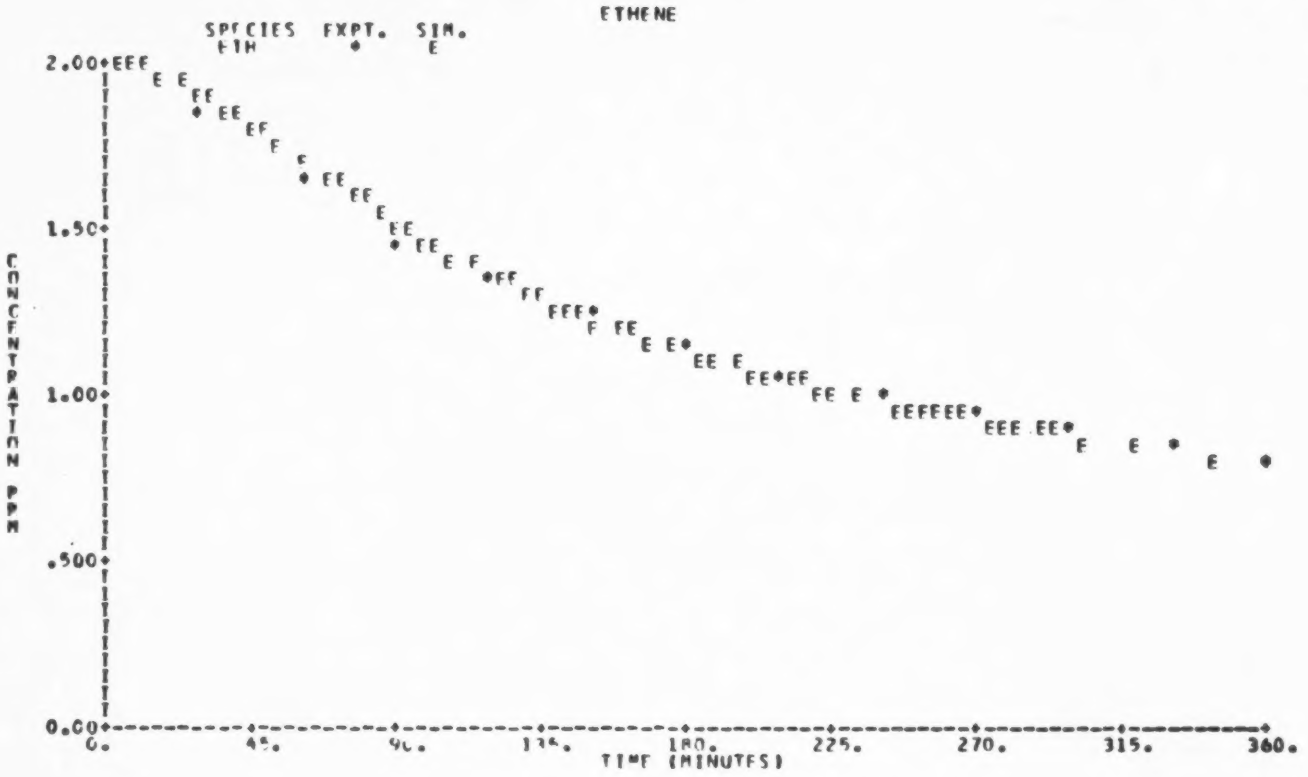

Figure A6b. Observed and Calculated Concentration-Time Profiles for 7-Hydrocarbon-NO_x Experiment EC-242.

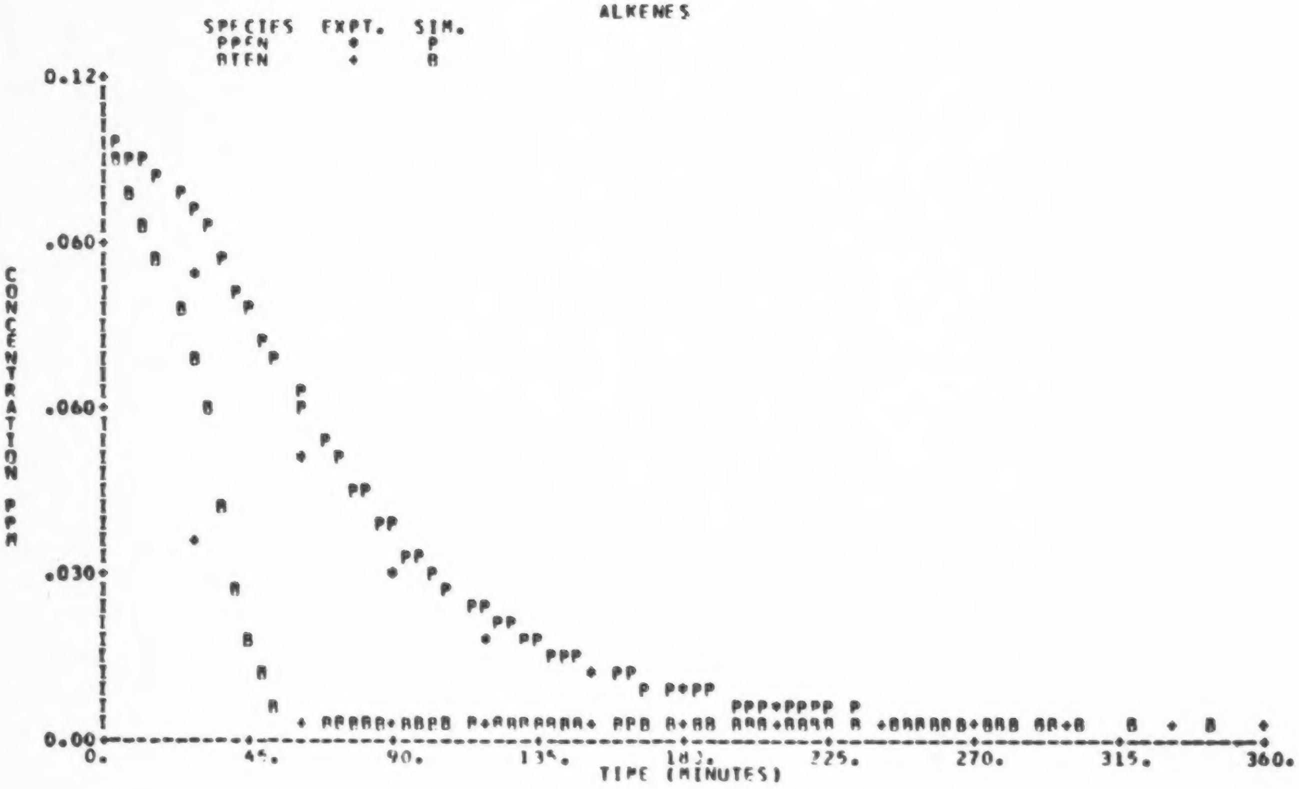

Figure A6c. Observed and Calculated Concentration-Time Profiles for 7-Hydrocarbon-NO_x Experiment EC-242.

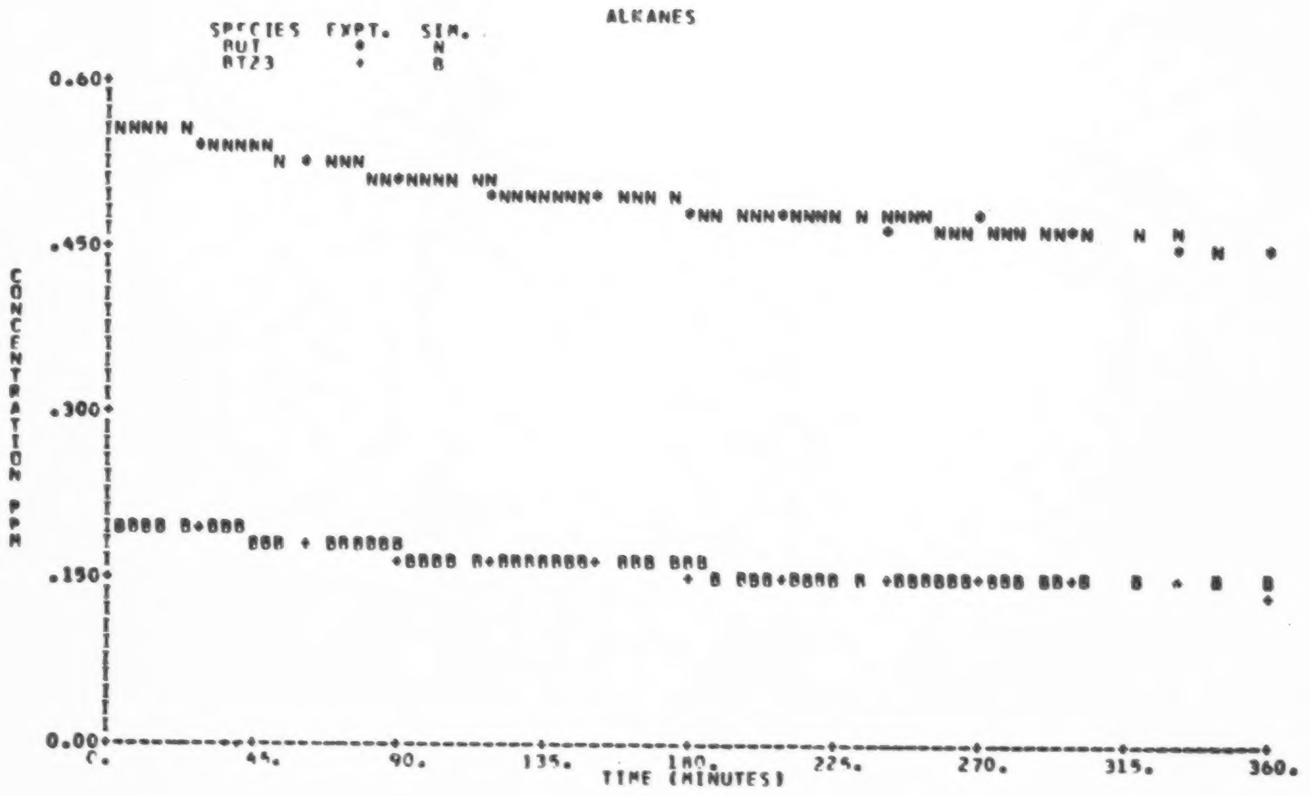

Figure A6d. Observed and Calculated Concentration-Time Profiles for 7-Hydrocarbon-NO_x Experiment EC-242.

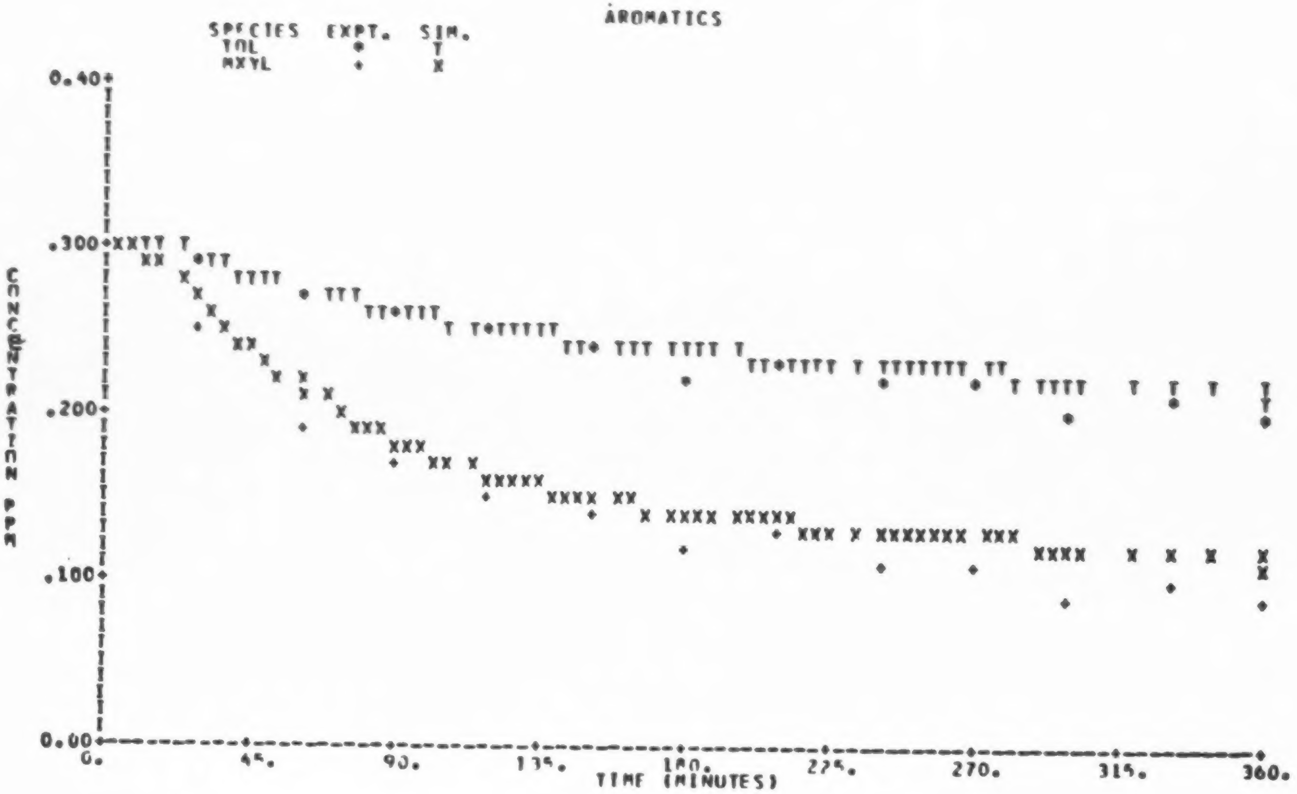

Figure A6e. Observed and Calculated Concentration-Time Profiles for 7-Hydrocarbon-NO_x Experiment EC-242.

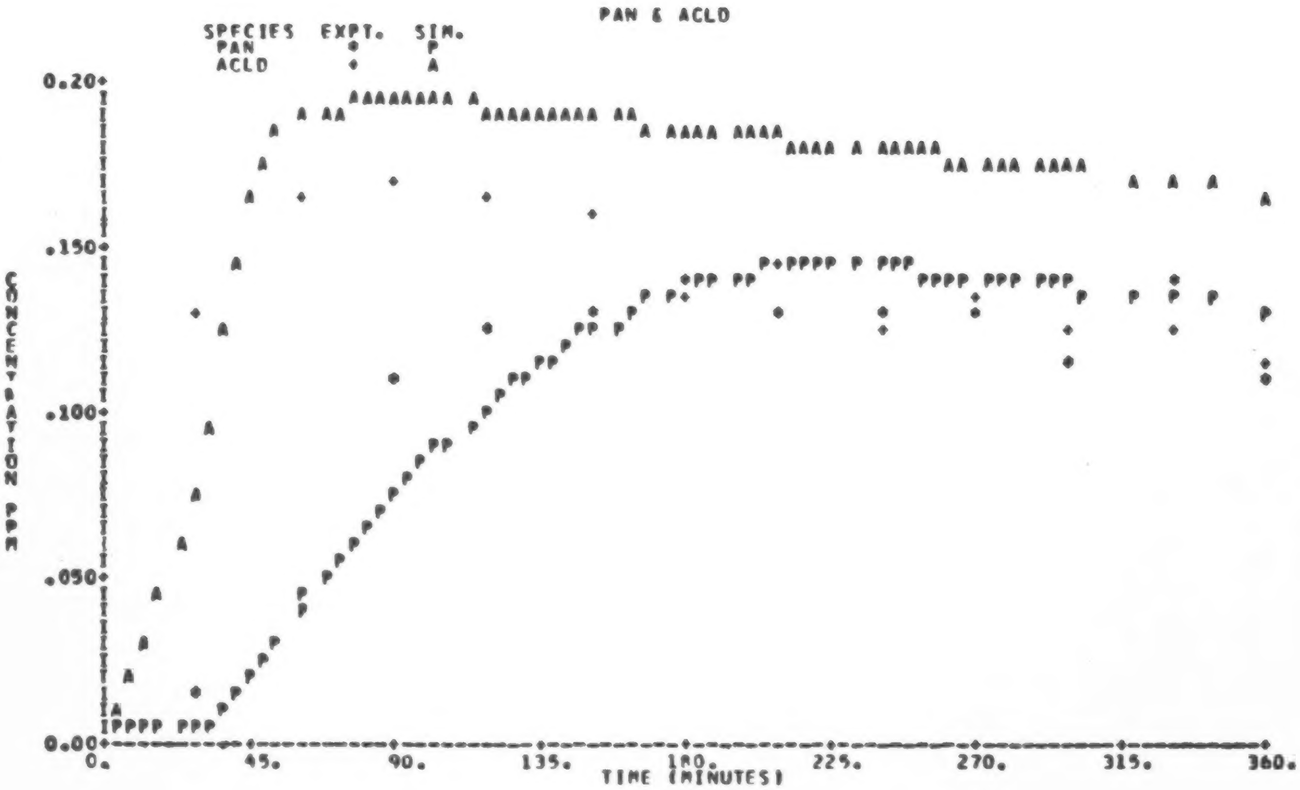

Figure A6f. Observed and Calculated Concentration-Time Profiles for 7-Hydrocarbon-NO_x Experiment EC-242.

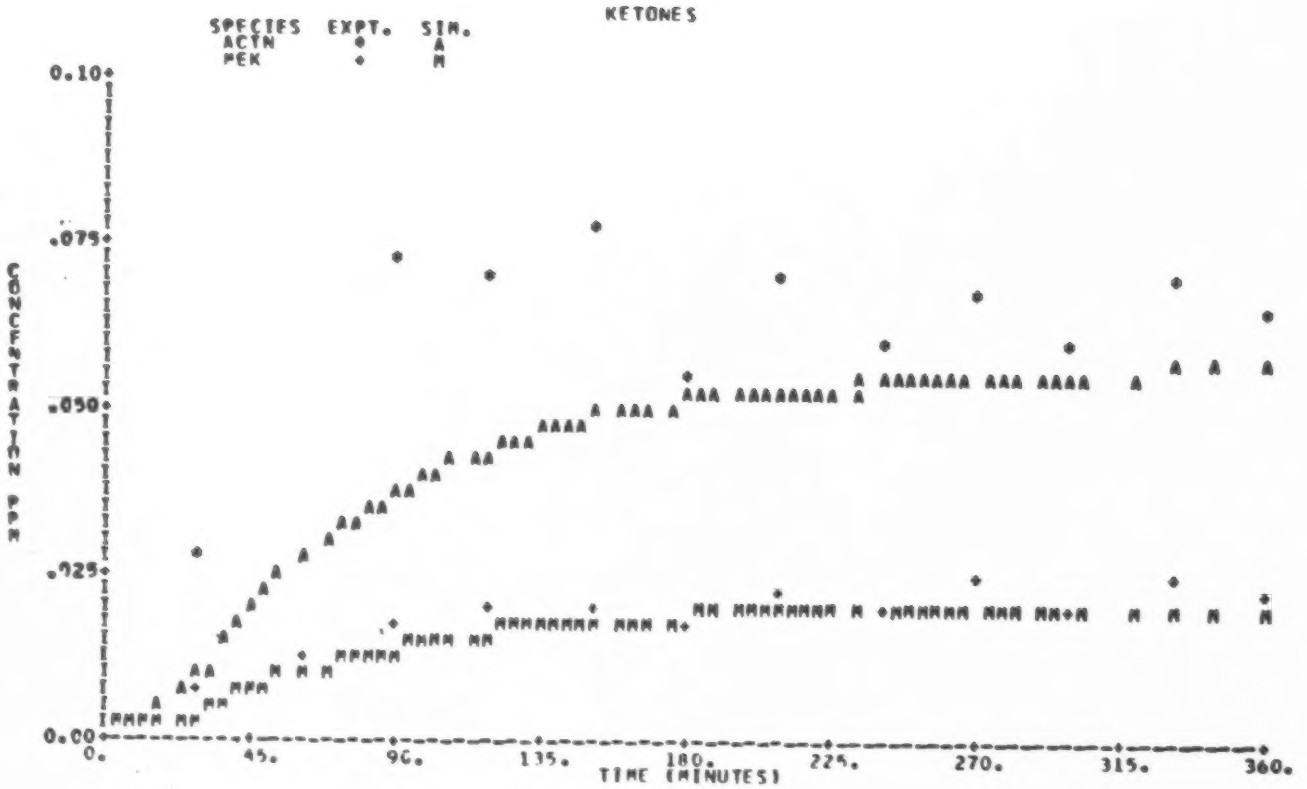

Figure A6g. Observed and Calculated Concentration-Time Profiles for 7-Hydrocarbon-NO_x Experiment EC-242.

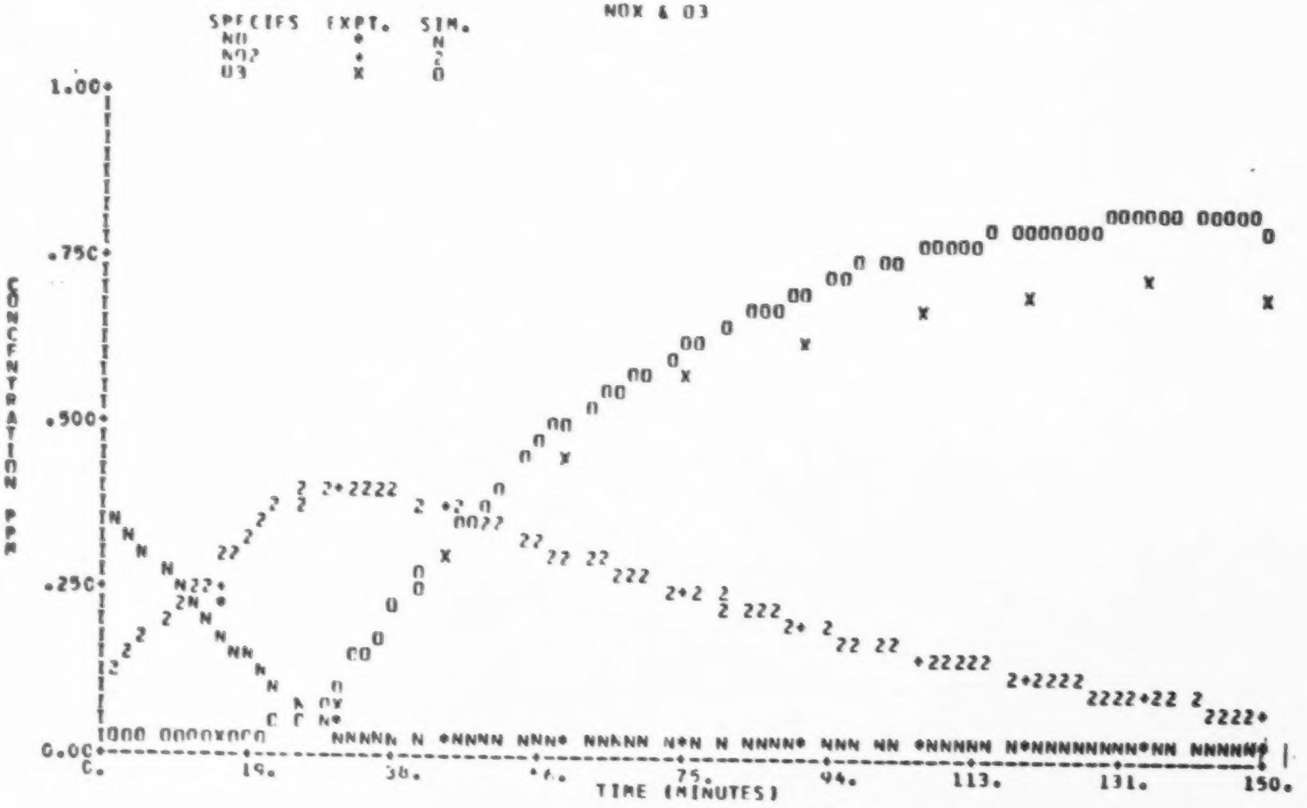

Figure A7a. Observed and Calculated Concentration-Time Profiles for 7-Hydrocarbon-NO_x Experiment EC-243.

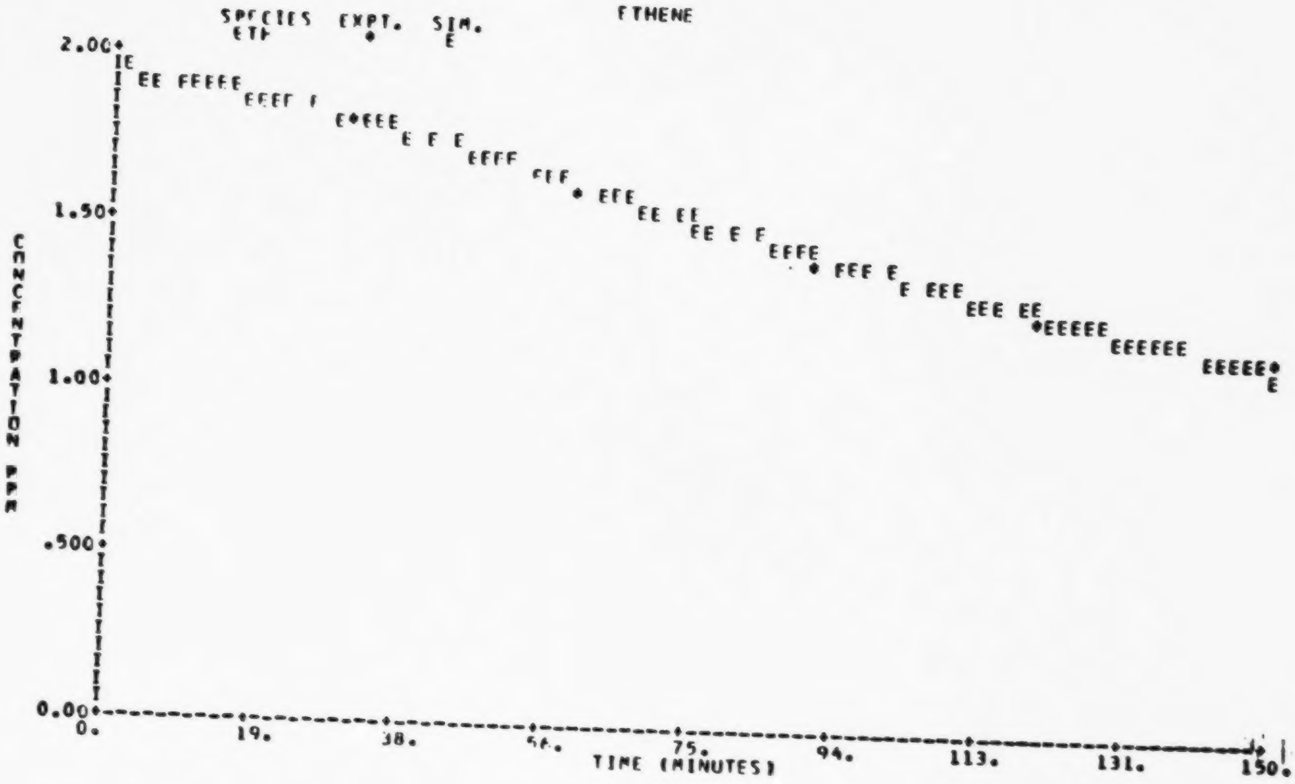

Figure A7b. Observed and Calculated Concentration-Time Profiles for 7-Hydrocarbon-NO_x Experiment EC-243.

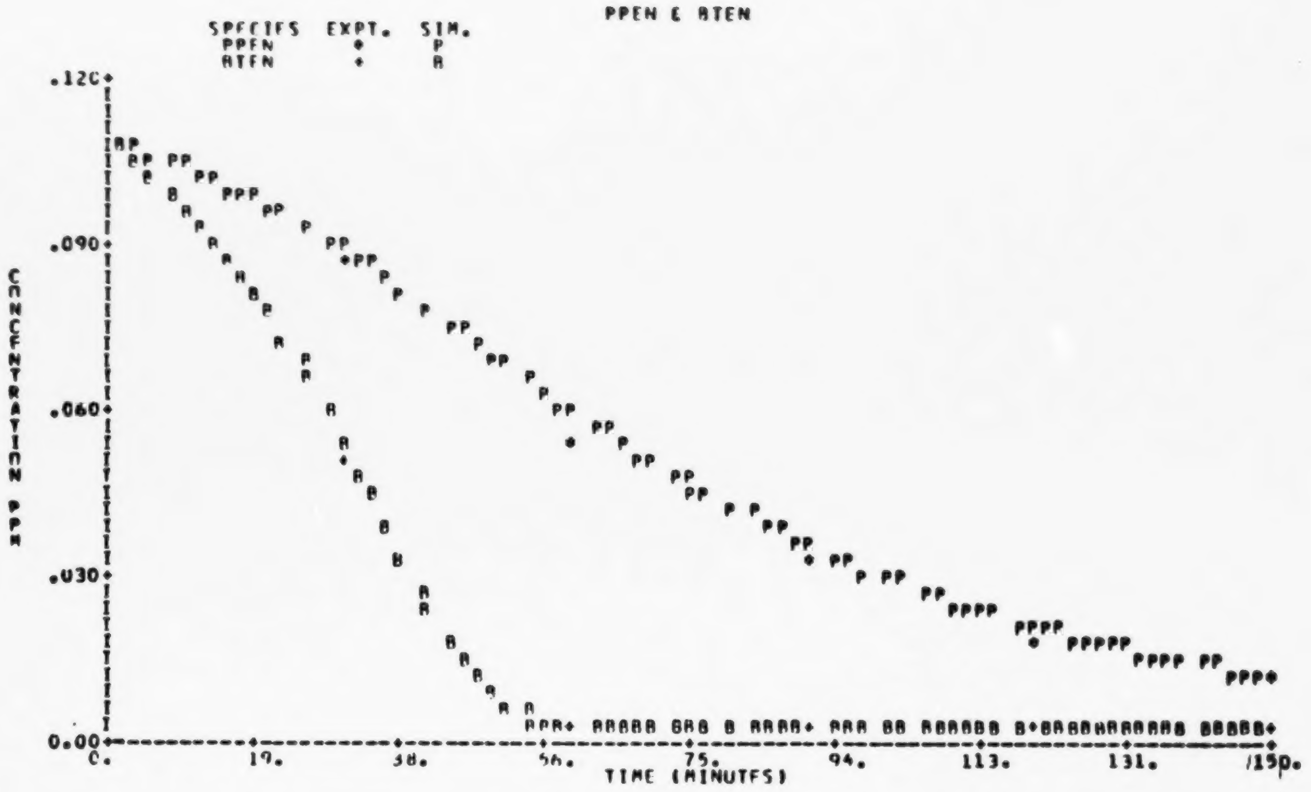

Figure A7c. Observed and Calculated Concentration-Time Profiles for 7-Hydrocarbon-NO_x Experiment EC-243.

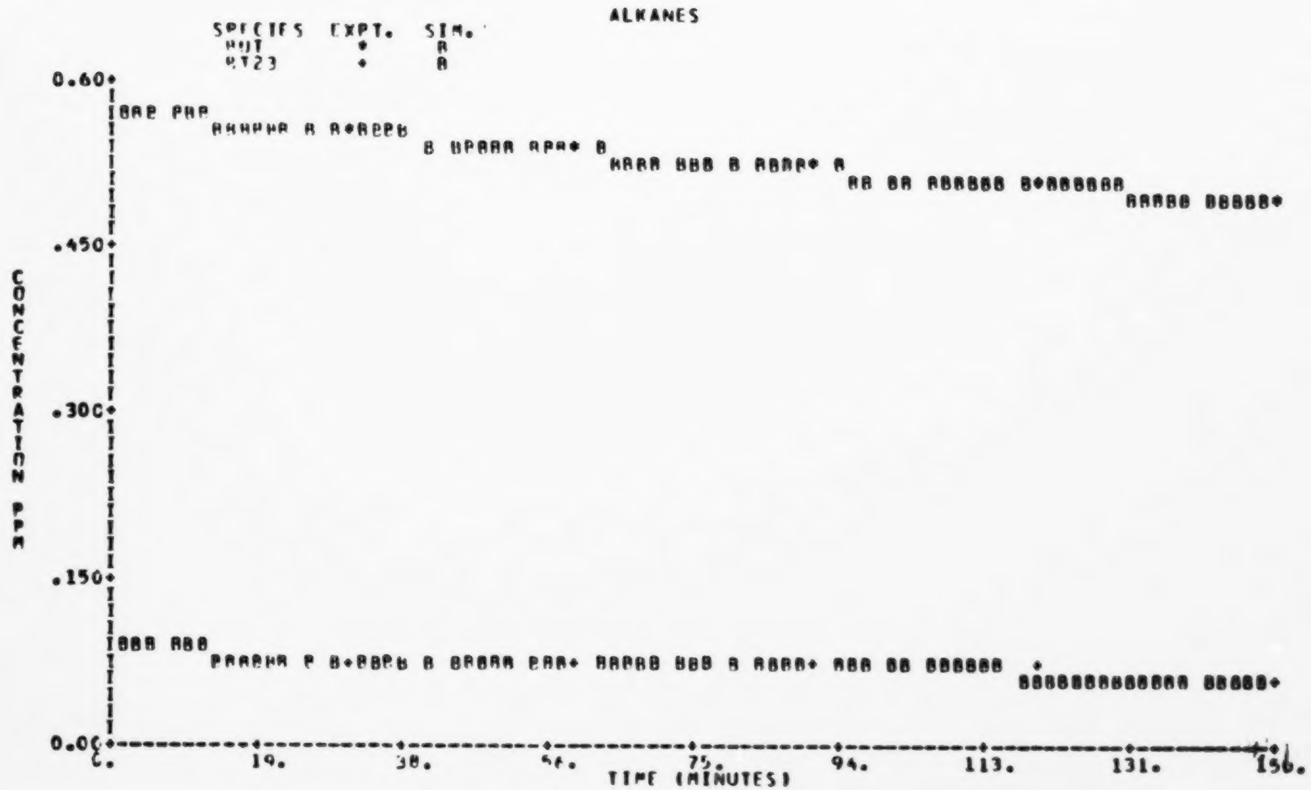

Figure A7d. Observed and Calculated Concentration-Time Profiles for 7-Hydrocarbon-NO_x Experiment EC-243.

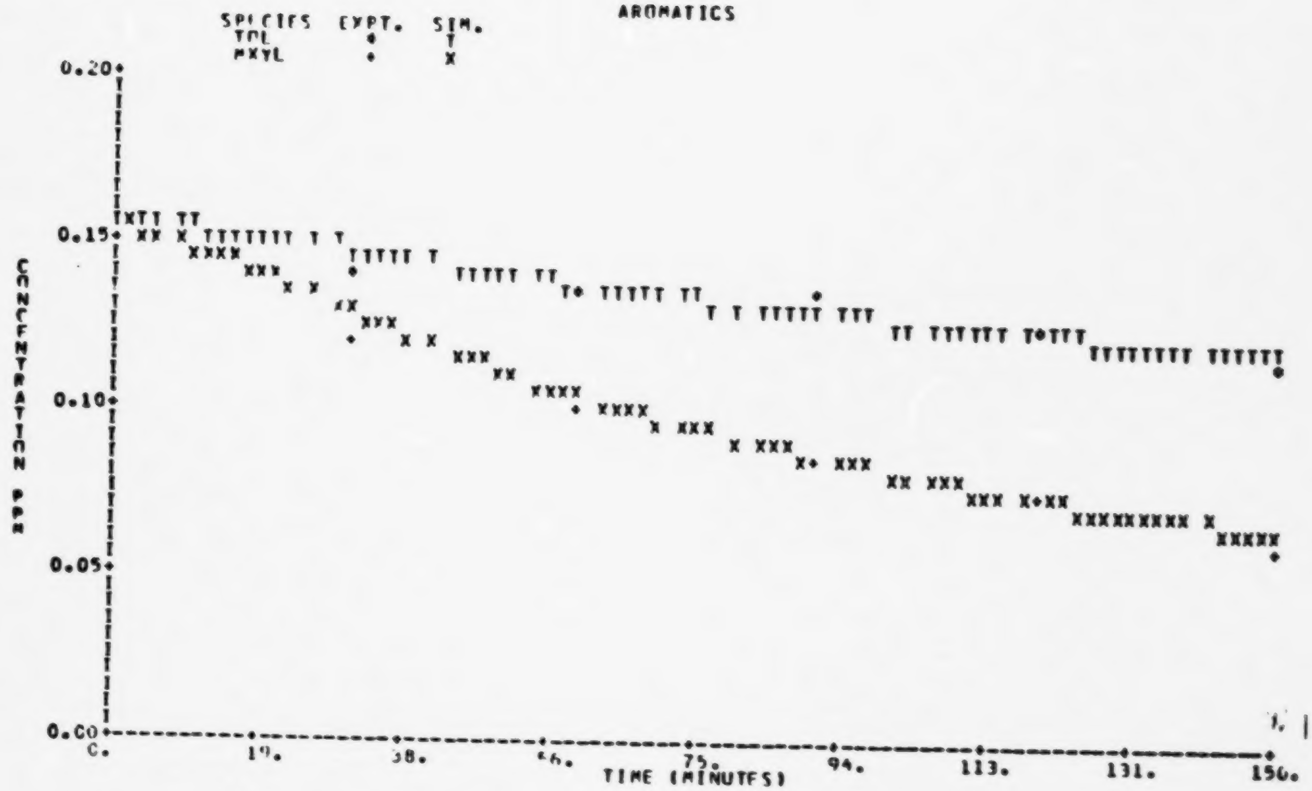

Figure A7e. Observed and Calculated Concentration-Time Profiles for 7-Hydrocarbon-NO_x Experiment EC-243.

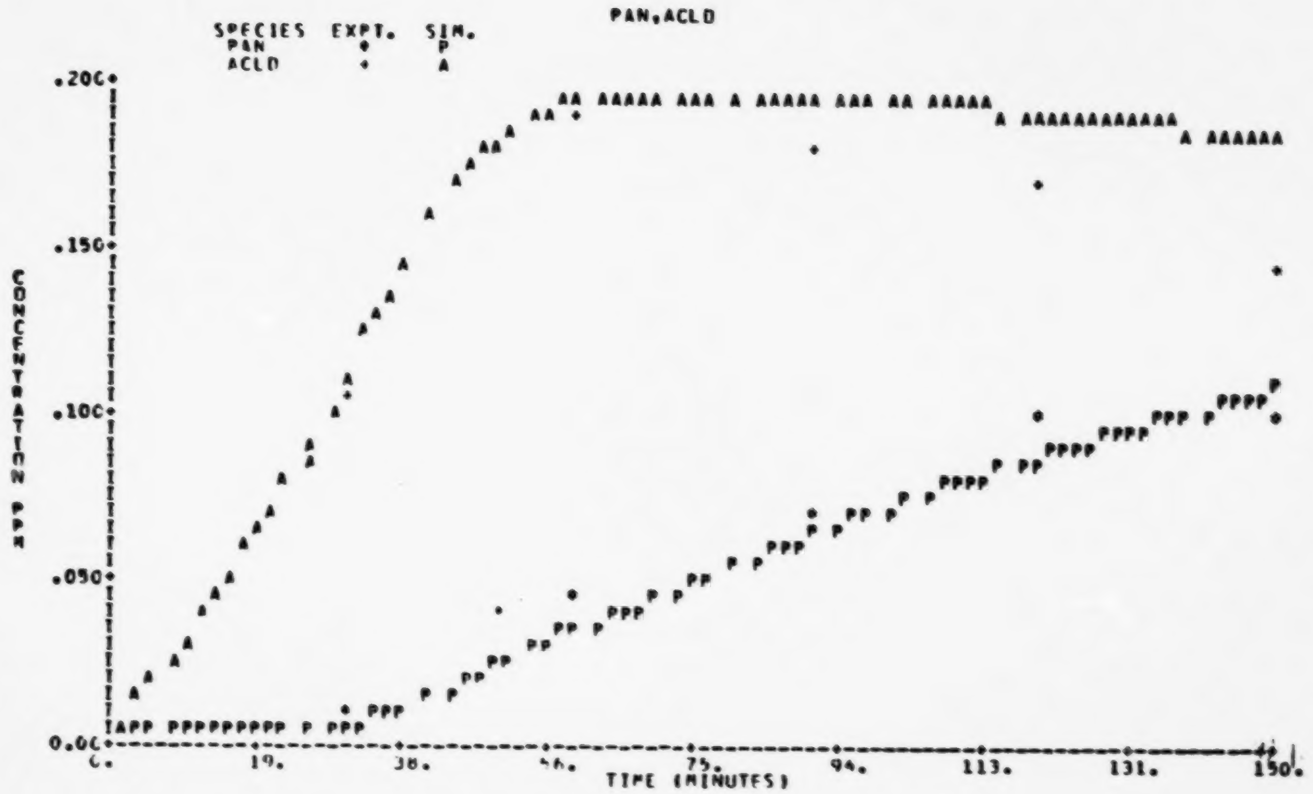

Figure A7f. Observed and Calculated Concentration-Time Profiles for 7-Hydrocarbon-NO_x Experiment EC-243.

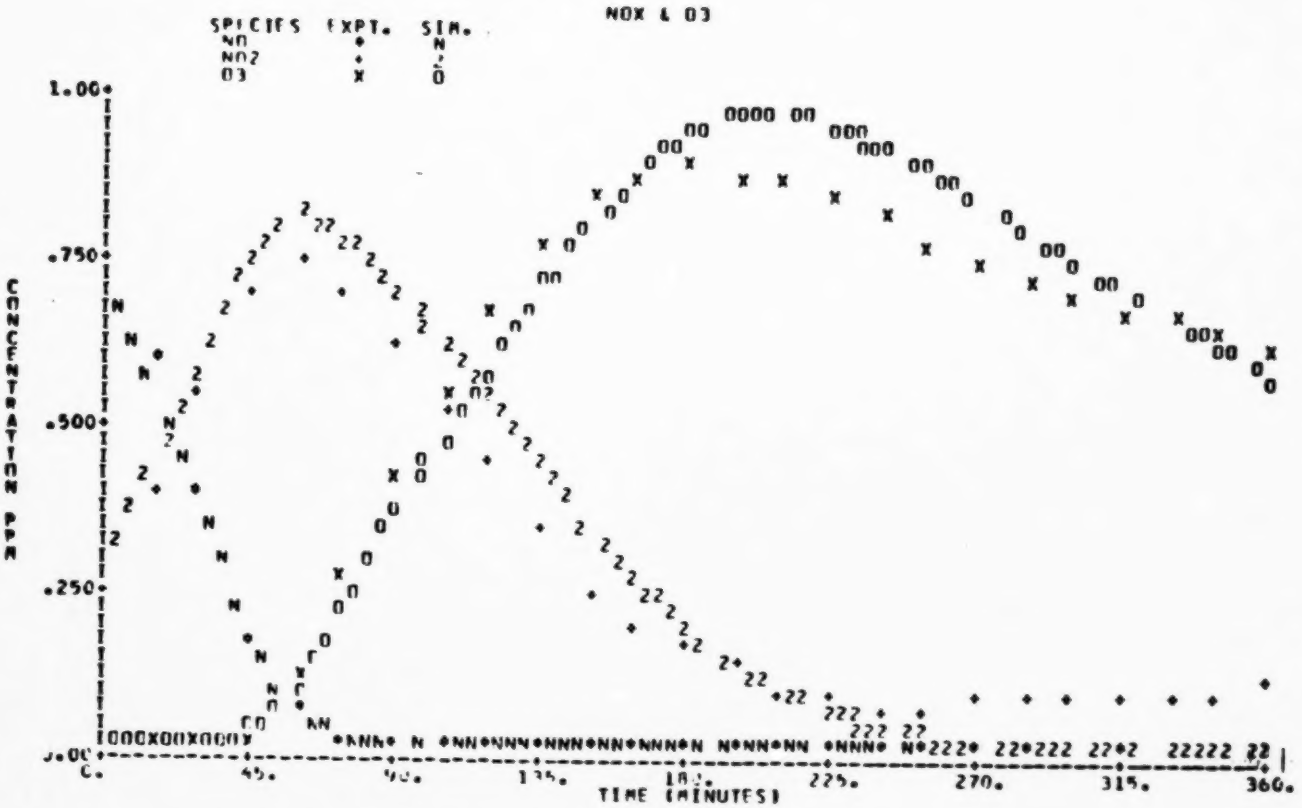

Figure A8a. Observed and Calculated Concentration-Time Profiles for 7-Hydrocarbon-NO_x Experiment EC-245.

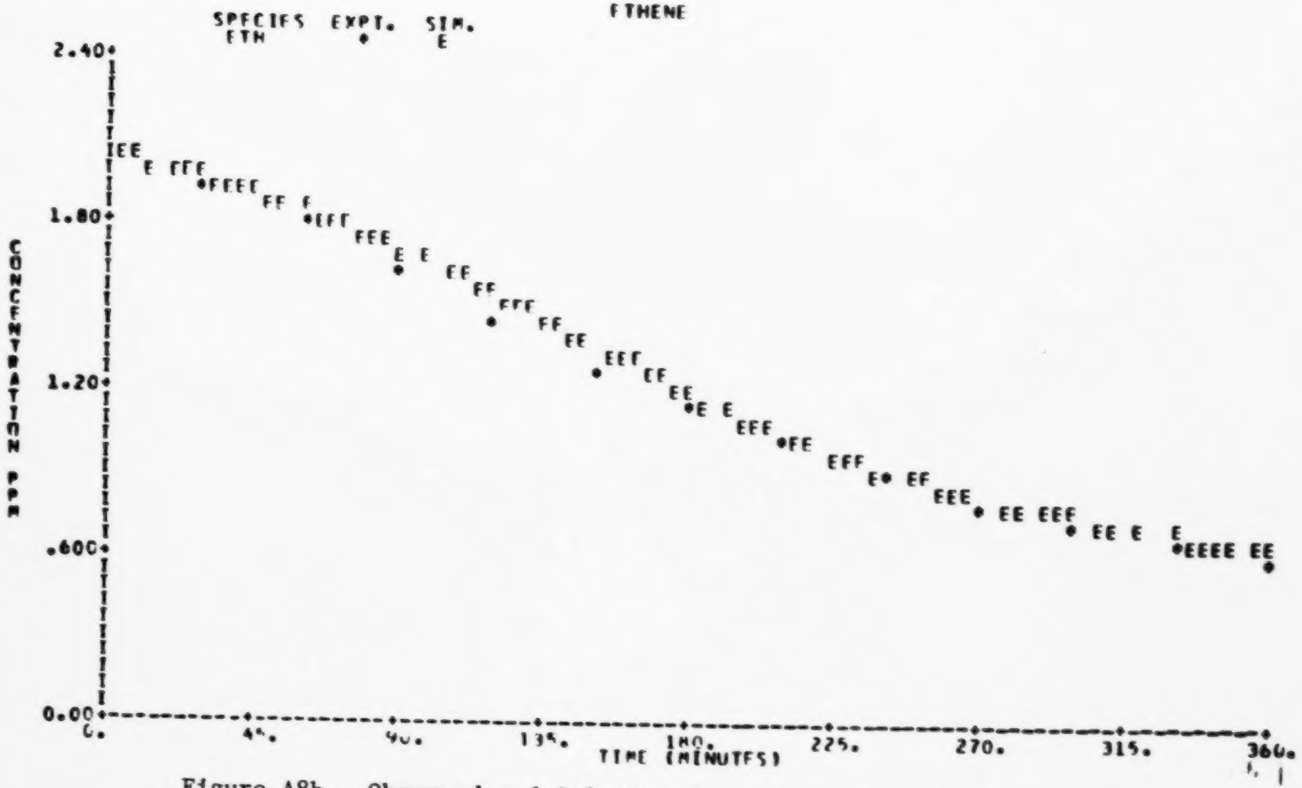

Figure A8b. Observed and Calculated Concentration-Time Profiles for 7-Hydrocarbon-NO_x Experiment EC-245.

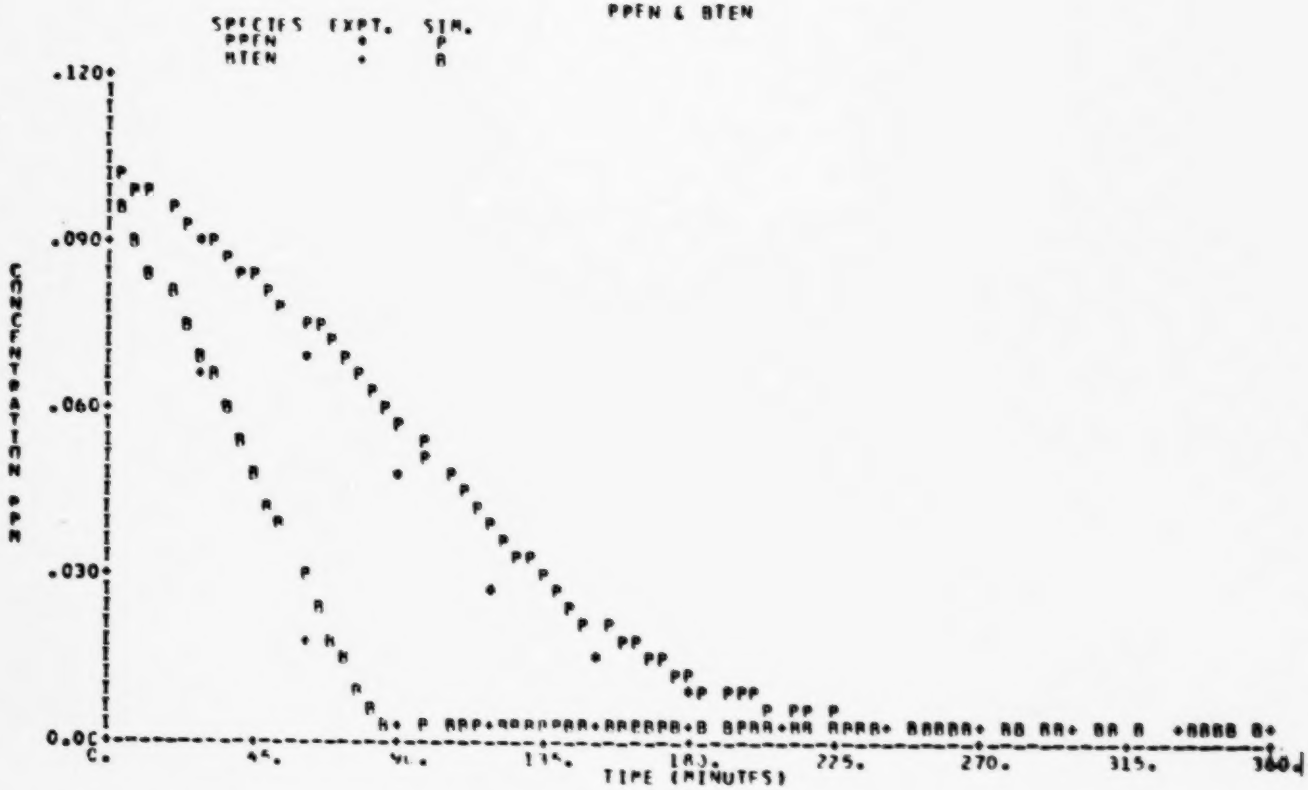

Figure A8c. Observed and Calculated Concentration-Time Profiles for 7-Hydrocarbon-NO_x Experiment EC-245.

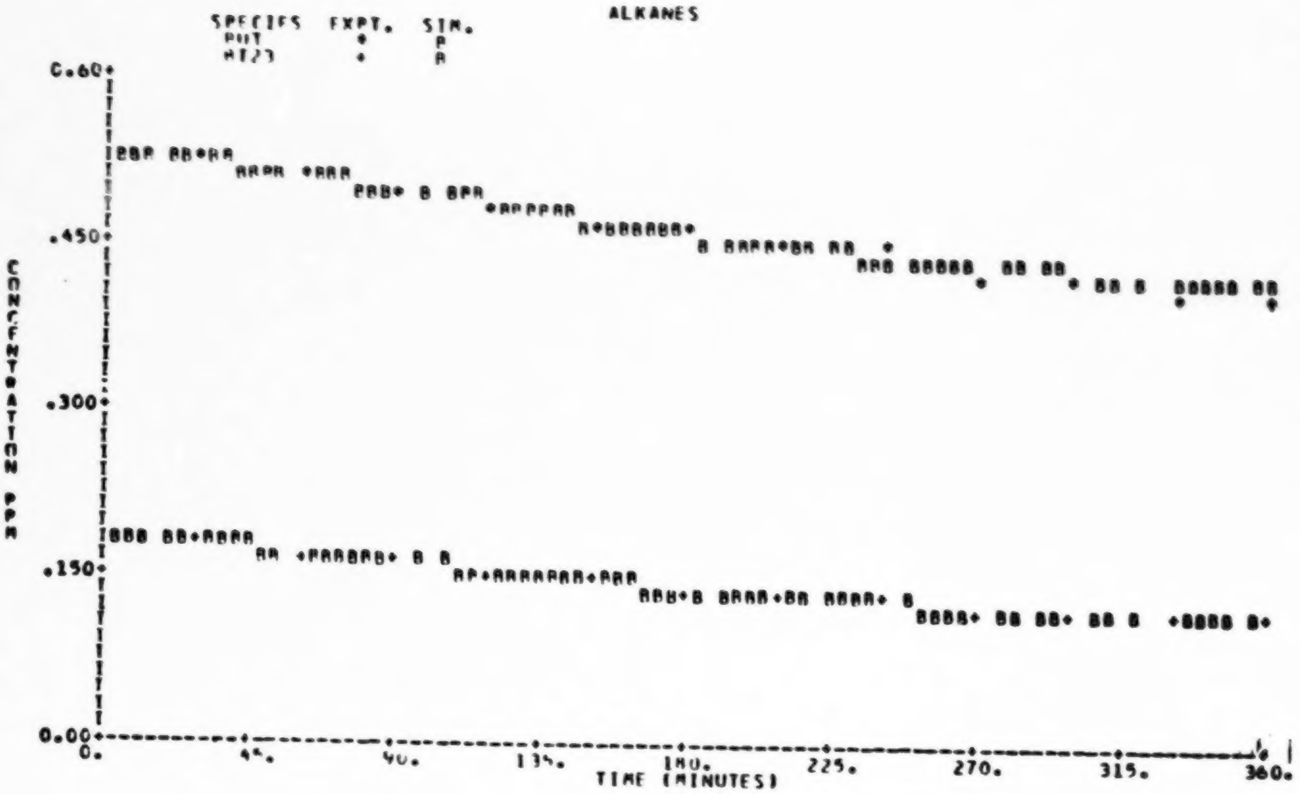

Figure A8d. Observed and Calculated Concentration-Time Profiles for 7-Hydrocarbon-NO_x Experiment EC-245.

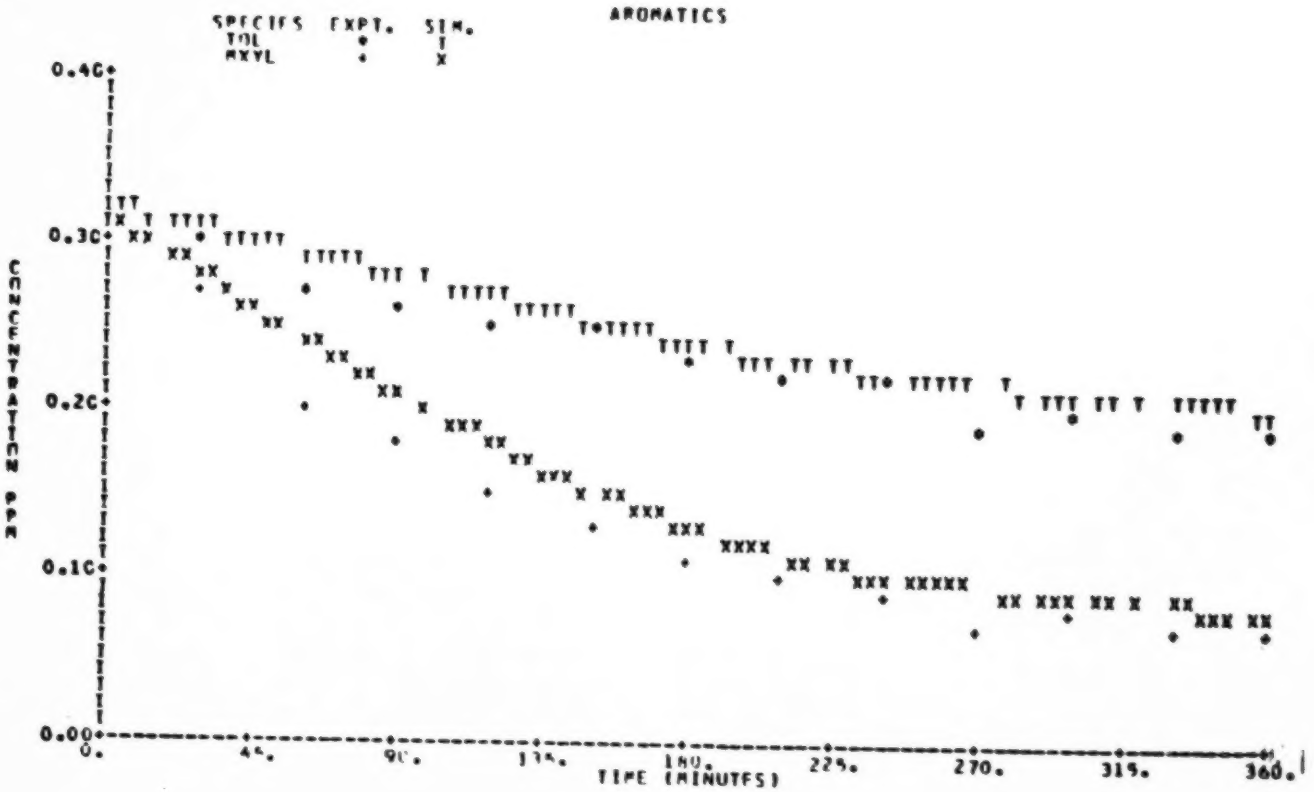

Figure A8e. Observed and Calculated Concentration-Time Profiles for 7-Hydrocarbon-NO_x Experiment EC-245.

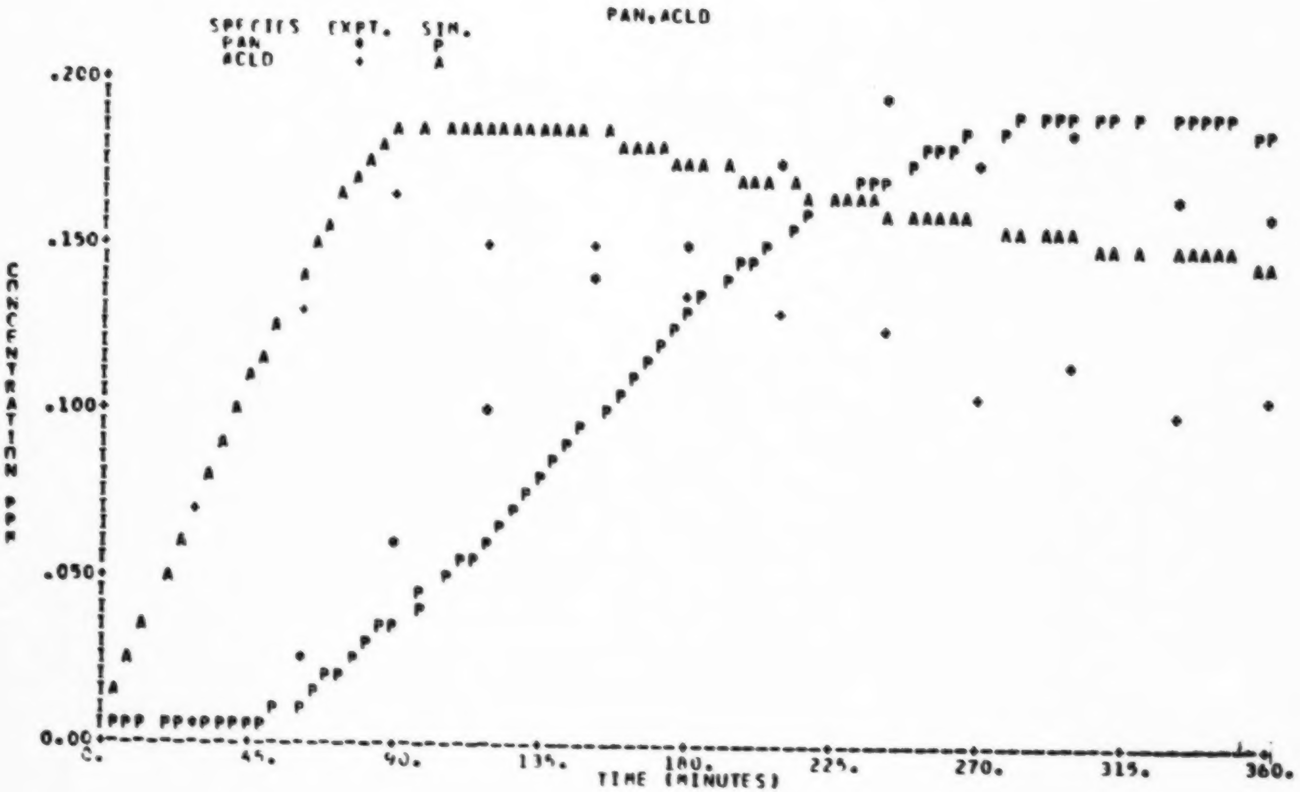

Figure A8f. Observed and Calculated Concentration-Time Profiles for 7-Hydrocarbon-NO_x Experiment EC-245.

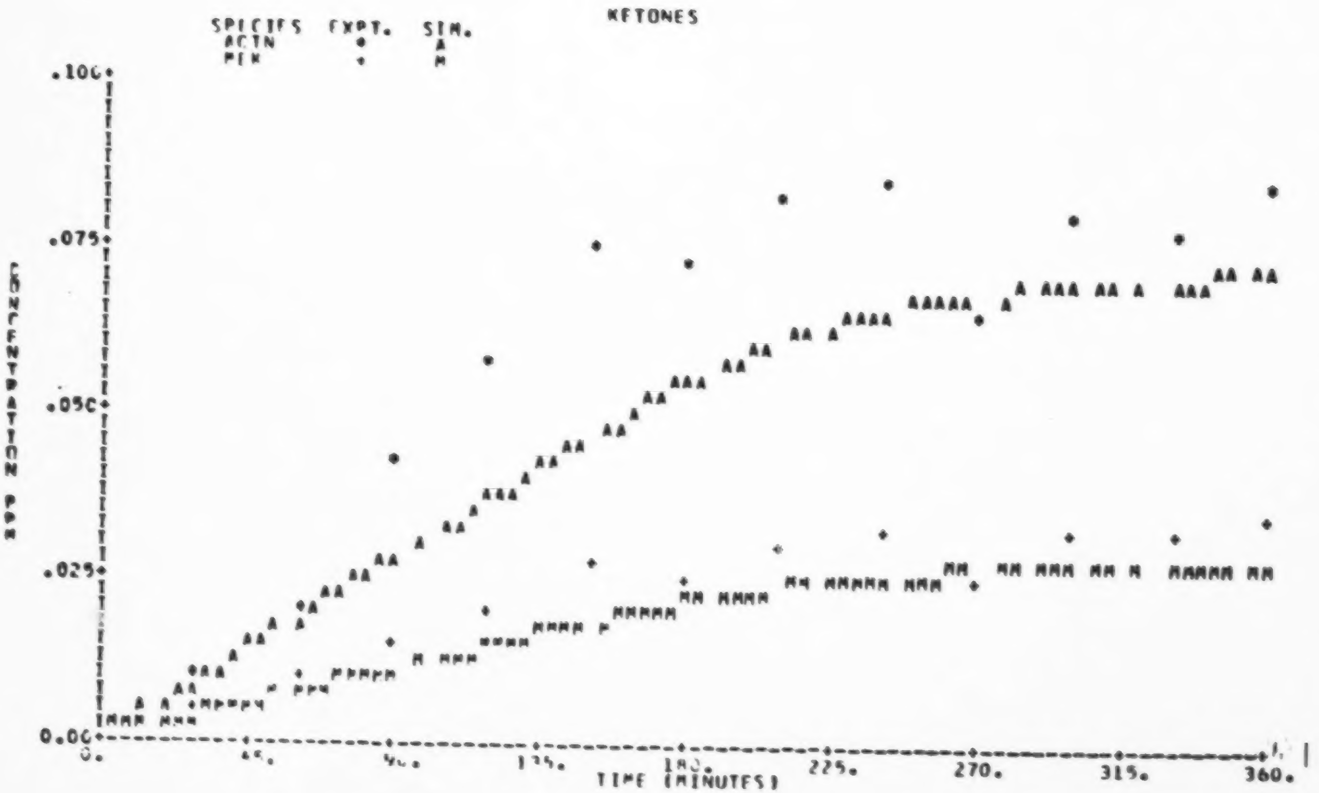

Figure A8g. Observed and Calculated Concentration-Time Profiles for 7-Hydrocarbon-NO_x Experiment EC-245.

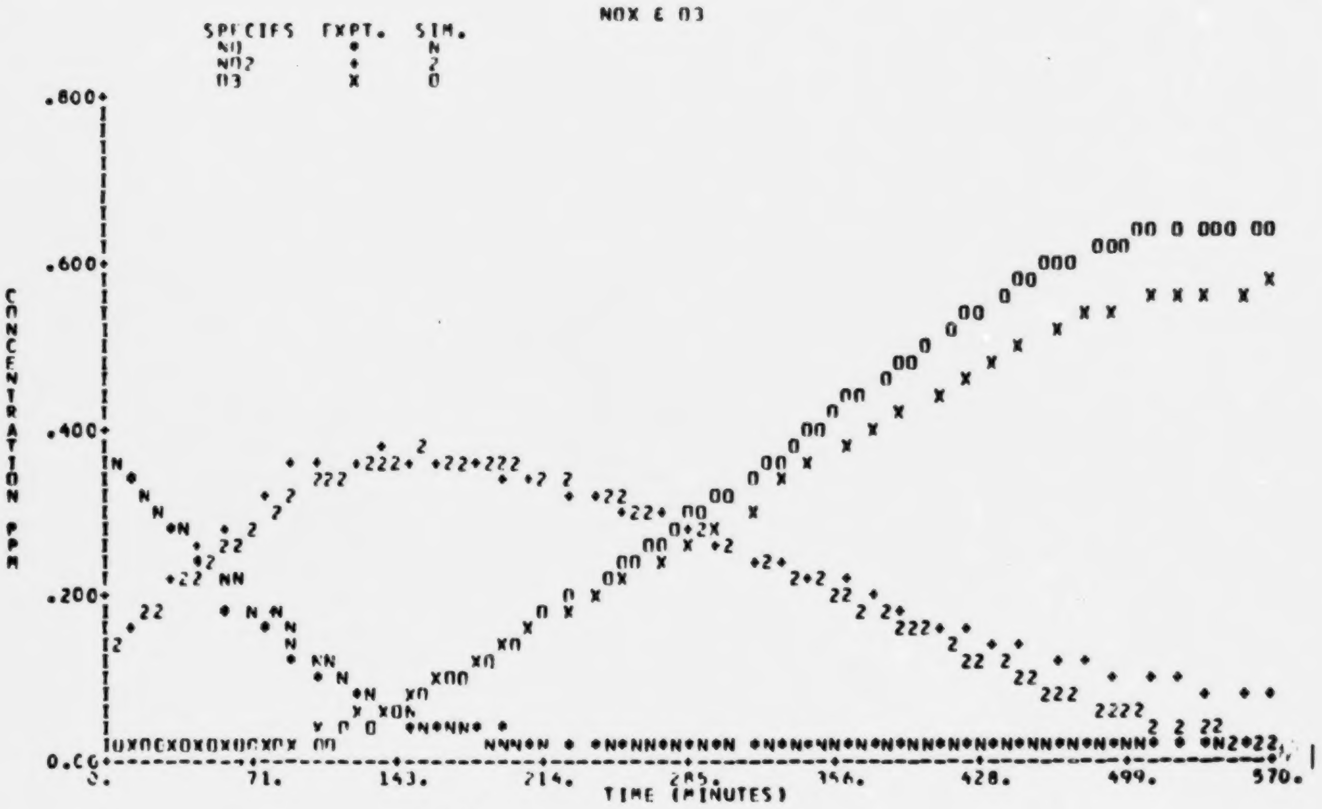

Figure A9a. Observed and Calculated Concentration-Time Profiles for 7-Hydrocarbon-NO_x Experiment EC-246.

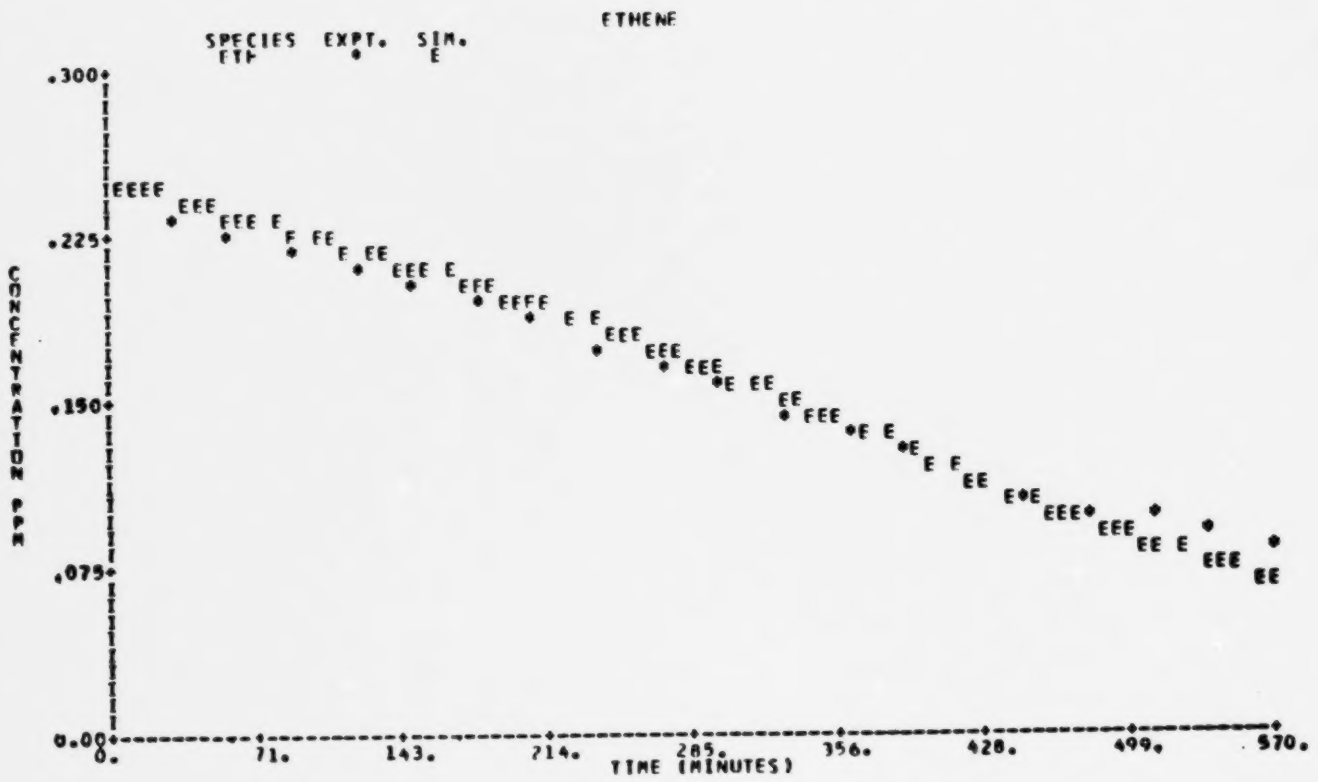

Figure A9b. Observed and Calculated Concentration-Time Profiles for 7-Hydrocarbon-NO_x Experiment EC-246.

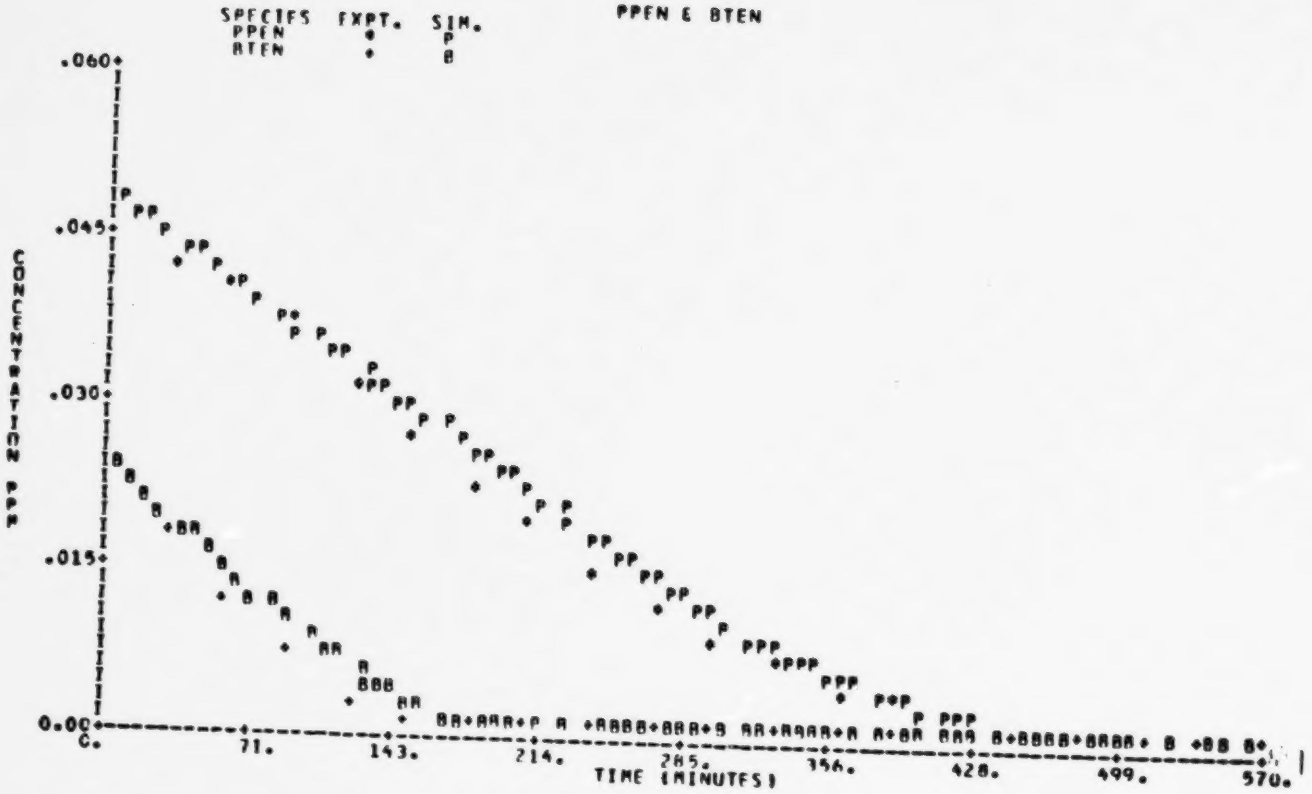

Figure A9c. Observed and Calculated Concentration-Time Profiles for 7-Hydrocarbon-NO_x Experiment EC-246.

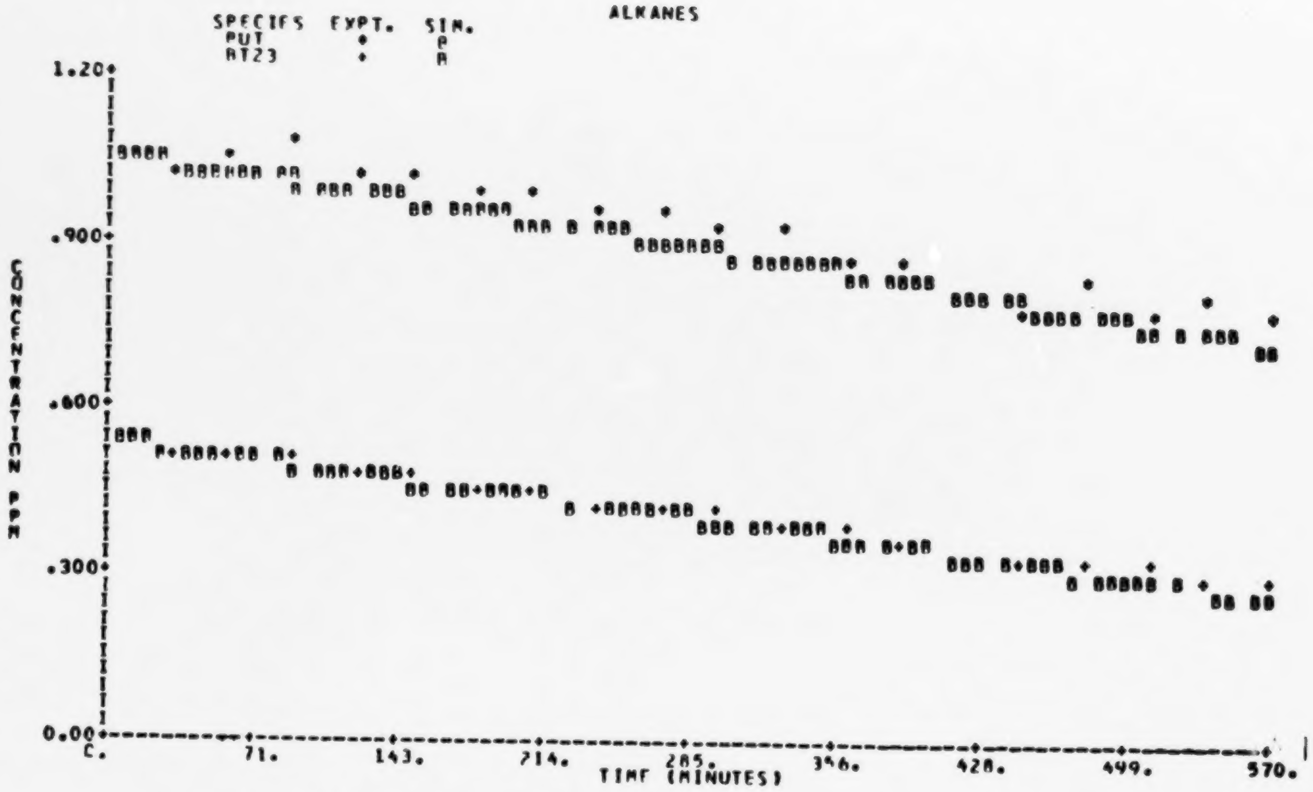

Figure A9d. Observed and Calculated Concentration-Time Profiles for 7-Hydrocarbon-NO_x Experiment EC-246.

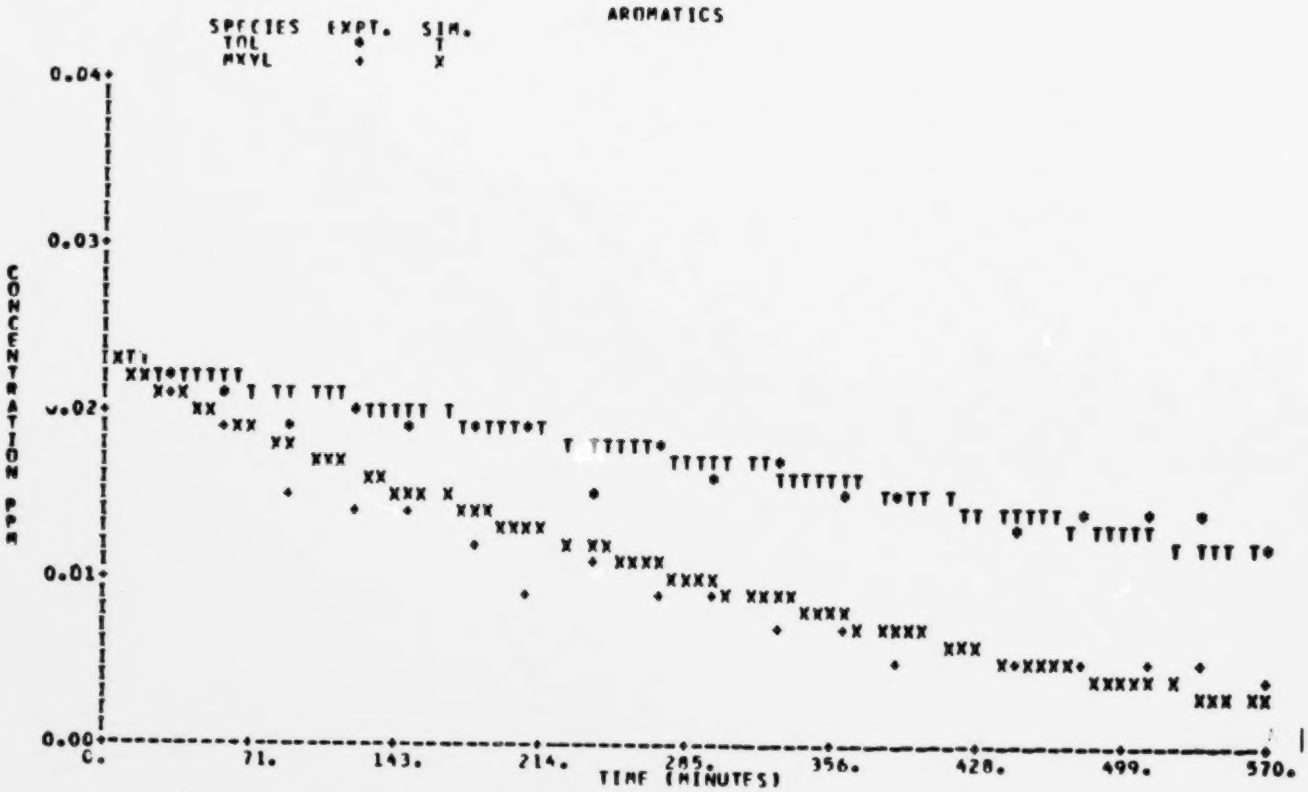

Figure A9e. Observed and Calculated Concentration-Time Profiles for 7-Hydrocarbon-NO_x Experiment EC-246.

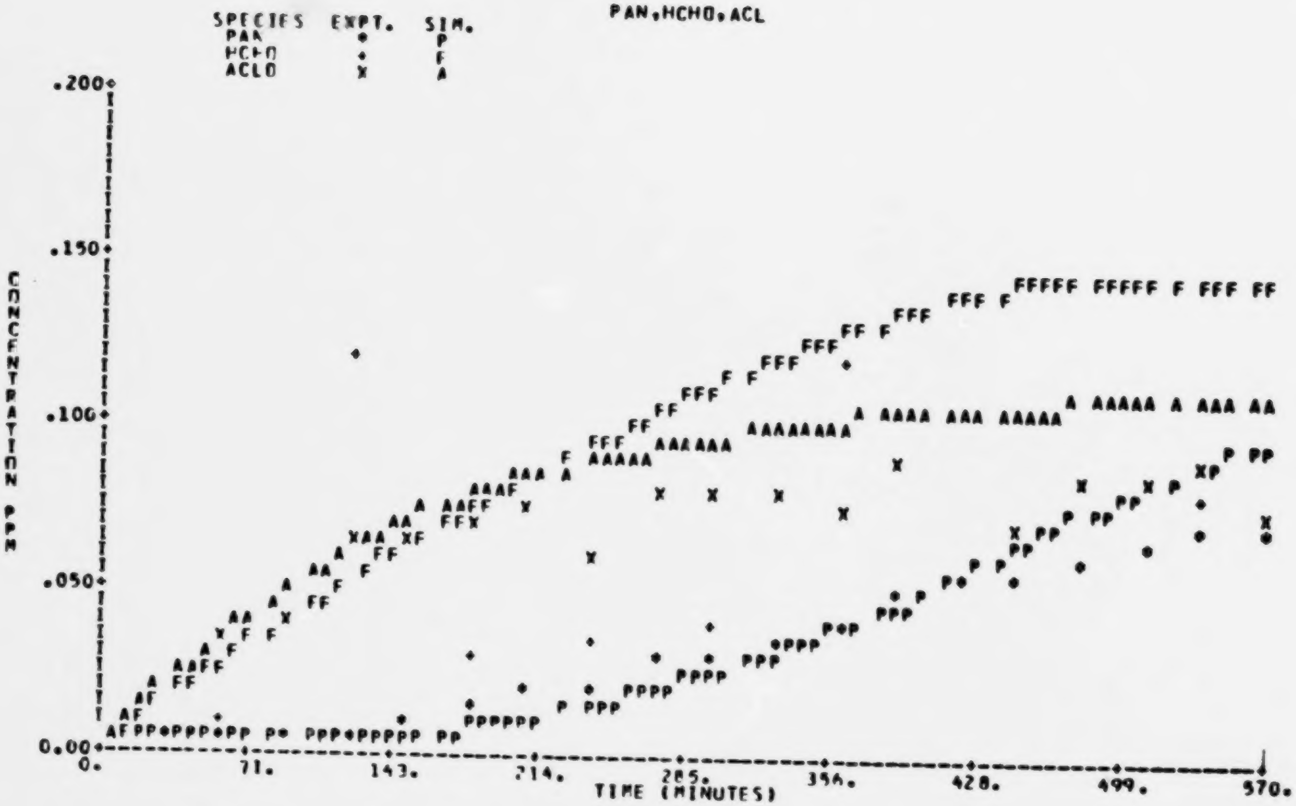

Figure A9f. Observed and Calculated Concentration-Time Profiles for 7-Hydrocarbon-NO_x Experiment EC-246.

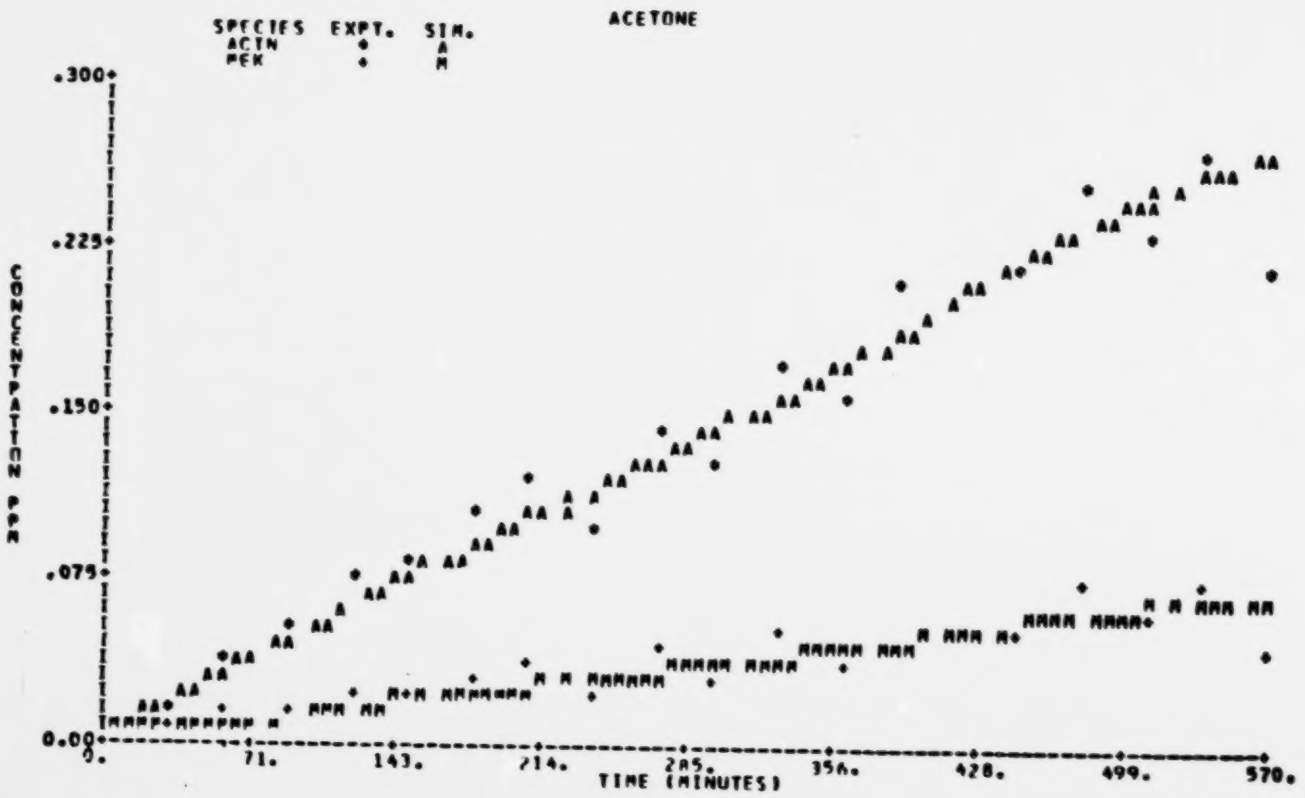

Figure A9g. Observed and Calculated Concentration-Time Profiles for 7-Hydrocarbon-NO_x Experiment EC-246.